

# **SANDIA REPORT**

SAND2016-2565

Unlimited Release

Printed March 2016

## **Analysis of SHDAS Platform Evaluation at PSRF**

B. John Merchant

Prepared by  
Sandia National Laboratories  
Albuquerque, New Mexico 87185 and Livermore, California 94550

Sandia National Laboratories is a multi-program laboratory managed and operated by Sandia Corporation, a wholly owned subsidiary of Lockheed Martin Corporation, for the U.S. Department of Energy's National Nuclear Security Administration under contract DE-AC04-94AL85000.

Approved for public release; further dissemination unlimited.



**Sandia National Laboratories**

Issued by Sandia National Laboratories, operated for the United States Department of Energy by Sandia Corporation.

**NOTICE:** This report was prepared as an account of work sponsored by an agency of the United States Government. Neither the United States Government, nor any agency thereof, nor any of their employees, nor any of their contractors, subcontractors, or their employees, make any warranty, express or implied, or assume any legal liability or responsibility for the accuracy, completeness, or usefulness of any information, apparatus, product, or process disclosed, or represent that its use would not infringe privately owned rights. Reference herein to any specific commercial product, process, or service by trade name, trademark, manufacturer, or otherwise, does not necessarily constitute or imply its endorsement, recommendation, or favoring by the United States Government, any agency thereof, or any of their contractors or subcontractors. The views and opinions expressed herein do not necessarily state or reflect those of the United States Government, any agency thereof, or any of their contractors.

Printed in the United States of America. This report has been reproduced directly from the best available copy.

Available to DOE and DOE contractors from

U.S. Department of Energy  
Office of Scientific and Technical Information  
P.O. Box 62  
Oak Ridge, TN 37831

Telephone: (865) 576-8401  
Facsimile: (865) 576-5728  
E-Mail: [reports@adonis.osti.gov](mailto:reports@adonis.osti.gov)  
Online ordering: <http://www.osti.gov/bridge>

Available to the public from

U.S. Department of Commerce  
National Technical Information Service  
5285 Port Royal Rd.  
Springfield, VA 22161

Telephone: (800) 553-6847  
Facsimile: (703) 605-6900  
E-Mail: [orders@ntis.fedworld.gov](mailto:orders@ntis.fedworld.gov)  
Online order: <http://www.ntis.gov/help/ordermethods.asp?loc=7-4-0#online>



SAND2016-2565  
Unlimited Release  
Printed March 2016

# **Analysis of SHDAS Platform Evaluation at PSRF**

B. John Merchant  
Ground-Based Monitoring R&E  
Sandia National Laboratories  
P.O. Box 5800  
Albuquerque, New Mexico 87185-MS0404

## **Abstract**

The Seismo-Hydroacoustic Data Acquisition System (SHDAS) is undergoing evaluation in preparation for its engineering, development, and deployment by the U.S. Navy as an ocean bottom seismic monitoring system. A prototype of the Underwater Platform has been deployed at the Pinedale Seismic Research Facility (PSRF) in Wyoming to determine how well it couples to the ground for the purpose of measuring ground motion. The evaluation was conducted during the summer of 2014 by the U.S. Navy, U.S. Air Force, RP Kromer Consulting, and other contractors. Sandia National Laboratories (SNL) was asked to analyze and interpret the collected data so as to comment on coupling of the Underwater Platform to the ground.

## **ACKNOWLEDGMENTS**

This work was funded by the United States Department of Defense. The evaluation data was collected by RP Kromer Consulting.

# CONTENTS

1	Introduction.....	13
2	Configuration.....	15
2.1	Seismic Background.....	17
2.1.1	Vertical.....	18
2.1.2	North.....	18
2.1.3	East.....	19
3	Results.....	21
3.1	Dry Testing.....	21
3.1.1	Transfer Function.....	22
3.1.2	Transfer Function – Wet Platform.....	29
3.2	Dry Platform Testing.....	33
3.2.1	Transfer Function.....	34
3.2.2	Geophone.....	41
3.2.3	Cross-Axis Coupling.....	48
3.3	Wet Platform Testing.....	52
3.3.1	Transfer Function.....	53
3.3.2	Geophone.....	65
3.3.3	Cross-Axis Coupling.....	71
3.4	Wet Seafloor Platform Testing.....	75
3.4.1	Transfer Function.....	76
3.4.2	Geophone.....	94
3.4.3	Cross-Axis Coupling.....	100
3.4.4	Bubble Test.....	105
3.5	Wet Seafloor Platform with Backfill Testing.....	109
3.5.1	Transfer Function.....	110
3.5.2	Cross-Axis Coupling.....	117
3.5.3	Bubble Test.....	122
3.5.4	Thumper Test.....	126
4	Summary.....	129
4.1	Transfer Function.....	129
4.2	Geophone.....	130
4.3	Cross-Axis Coupling.....	130
4.4	Bubble Tests.....	131
4.5	Thumper Test.....	131
	Appendix.....	132
	Nanometrics Trillium OBS Response.....	132
	Navy Geophone OBS Response.....	132
	References.....	133
	Distribution.....	134

## FIGURES

Figure 1 SHDAS Underwater Platform .....	13
Figure 2 Example Testing Diagram (RPKromer Consulting) .....	16
Figure 3 Background, Vertical Power Spectra .....	18
Figure 4 Background, Vertical Coherence .....	18
Figure 5 Background, North Power Spectra .....	18
Figure 6 Background, North Coherence .....	19
Figure 7 Background, East Power Spectra .....	19
Figure 8 Background, East Coherence .....	19
Figure 9 Dry Testing Diagram (RPKromer Consulting) .....	21
Figure 10 Dry Testing Waveforms .....	22
Figure 11 Dry Testing, Transfer Function, Vertical Waveforms .....	23
Figure 12 Dry Testing, Transfer Function, Vertical Power Spectra .....	23
Figure 13 Dry Testing, Transfer Function, Vertical Coherence .....	23
Figure 14 Dry Testing, Transfer Function, Vertical Incoherent Noise .....	24
Figure 15 Dry Testing, Transfer Function, Vertical Magnitude Response .....	24
Figure 16 Dry Testing, Transfer Function, Vertical Phase Response .....	24
Figure 17 Dry Testing, Transfer Function, North Waveforms .....	25
Figure 18 Dry Testing, Transfer Function, North Power Spectra .....	25
Figure 19 Dry Testing, Transfer Function, North Coherence .....	25
Figure 20 Dry Testing, Transfer Function, North Incoherent Noise .....	26
Figure 21 Dry Testing, Transfer Function, North Magnitude Response .....	26
Figure 22 Dry Testing, Transfer Function, North Phase Response .....	26
Figure 23 Dry Testing, Transfer Function, East Waveforms .....	27
Figure 24 Dry Testing, Transfer Function, East Power Spectra .....	27
Figure 25 Dry Testing, Transfer Function, East Coherence .....	27
Figure 26 Dry Testing, Transfer Function, East Incoherent Noise .....	28
Figure 27 Dry Testing, Transfer Function, East Magnitude Response .....	28
Figure 28 Dry Testing, Transfer Function, East Phase Response .....	28
Figure 29 Dry Testing, Transfer Function - Wet, Vertical Waveforms .....	30
Figure 30 Dry Testing, Transfer Function - Wet, Vertical Power Spectra .....	30
Figure 31 Dry Testing, Transfer Function - Wet, Vertical Coherence .....	30
Figure 32 Dry Testing, Transfer Function - Wet, North Waveforms .....	31
Figure 33 Dry Testing, Transfer Function - Wet, North Power Spectra .....	31
Figure 34 Dry Testing, Transfer Function - Wet, North Coherence .....	31
Figure 35 Dry Testing, Transfer Function - Wet, East Waveforms .....	32
Figure 36 Dry Testing, Transfer Function - Wet, East Power Spectra .....	32
Figure 37 Dry Testing, Transfer Function - Wet, East Coherence .....	32
Figure 38 Dry Platform Photo .....	33
Figure 39 Dry Platform Testing Diagram (RP Kromer Consulting) .....	33
Figure 40 Dry Platform Testing, Transfer Function, Vertical Waveforms .....	35
Figure 41 Dry Platform Testing, Transfer Function, Vertical Power Spectra .....	35
Figure 42 Dry Platform Testing, Transfer Function, Vertical Coherence .....	35
Figure 43 Dry Platform Testing, Transfer Function, Vertical Incoherent Noise .....	36
Figure 44 Dry Platform Testing, Transfer Function, Vertical Magnitude Response .....	36

Figure 45 Dry Platform Testing, Transfer Function, Vertical Phase Response .....	36
Figure 46 Dry Platform Testing, Transfer Function, North Waveforms .....	37
Figure 47 Dry Platform Testing, Transfer Function, North Power Spectra .....	37
Figure 48 Dry Platform Testing, Transfer Function, North Coherence .....	37
Figure 49 Dry Platform Testing, Transfer Function, North Incoherent Noise .....	38
Figure 50 Dry Platform Testing, Transfer Function, North Magnitude Response .....	38
Figure 51 Dry Platform Testing, Transfer Function, North Phase Response .....	38
Figure 52 Dry Platform Testing, Transfer Function, East Waveforms .....	39
Figure 53 Dry Platform Testing, Transfer Function, East Power Spectra .....	39
Figure 54 Dry Platform Testing, Transfer Function, East Coherence .....	39
Figure 55 Dry Platform Testing, Transfer Function, East Incoherent Noise .....	40
Figure 56 Dry Platform Testing, Transfer Function, East Magnitude Response .....	40
Figure 57 Dry Platform Testing, Transfer Function, East Phase Response .....	40
Figure 58 Dry Platform Testing, Geophone, Vertical Waveforms .....	42
Figure 59 Dry Platform Testing, Geophone, Vertical Power Spectra .....	42
Figure 60 Dry Platform Testing, Geophone, Vertical Coherence .....	42
Figure 61 Dry Platform Testing, Geophone, Vertical Incoherent Noise .....	43
Figure 62 Dry Platform Testing, Geophone, Vertical Magnitude Response .....	43
Figure 63 Dry Platform Testing, Geophone, Vertical Phase Response .....	43
Figure 64 Dry Platform Testing, Geophone, North Waveforms .....	44
Figure 65 Dry Platform Testing, Geophone, North Power Spectra .....	44
Figure 66 Dry Platform Testing, Geophone, North Coherence .....	44
Figure 67 Dry Platform Testing, Geophone, North Incoherent Noise .....	45
Figure 68 Dry Platform Testing, Geophone, North Magnitude Response .....	45
Figure 69 Dry Platform Testing, Geophone, North Phase Response .....	45
Figure 70 Dry Platform Testing, Geophone, East Waveforms .....	46
Figure 71 Dry Platform Testing, Geophone, East Power Spectra .....	46
Figure 72 Dry Platform Testing, Geophone, East Coherence .....	46
Figure 73 Dry Platform Testing, Geophone, East Incoherent Noise .....	47
Figure 74 Dry Platform Testing, Geophone, East Magnitude Response .....	47
Figure 75 Dry Platform Testing, Geophone, East Phase Response .....	47
Figure 76 Dry Platform, Cross-Axis Coupling, Reference Power Spectra .....	49
Figure 77 Dry Platform, Cross-Axis Coupling, Reference Coherence .....	49
Figure 78 Dry Platform, Cross-Axis Coupling, Trillium OBS Platform Power Spectra .....	50
Figure 79 Dry Platform, Cross-Axis Coupling, Trillium OBS Platform Coherence .....	50
Figure 80 Dry Platform, Cross-Axis Coupling, Navy OBS Platform Power Spectra .....	51
Figure 81 Dry Platform, Cross-Axis Coupling, Navy OBS Platform Coherence .....	51
Figure 82 Wet Platform Photo .....	52
Figure 83 Wet Platform Testing Diagram (RPKromer Consulting) .....	52
Figure 84 Wet Platform, Transfer Function, Low Frequency, Vertical Waveforms .....	53
Figure 85 Wet Platform, Transfer Function, Low Frequency, Vertical Power Spectra .....	53
Figure 86 Wet Platform, Transfer Function, Low Frequency, Vertical Coherence .....	54
Figure 87 Wet Platform, Transfer Function, Low Frequency, Vertical Incoherent Noise .....	54
Figure 88 Wet Platform, Transfer Function, Low Frequency, Vertical Magnitude Response .....	54
Figure 89 Wet Platform, Transfer Function, Low Frequency, Vertical Phase Response .....	54
Figure 90 Wet Platform, Transfer Function, Low Frequency, North Waveforms .....	55

Figure 91 Wet Platform, Transfer Function, Low Frequency, North Power Spectra.....	55
Figure 92 Wet Platform, Transfer Function, Low Frequency, North Coherence.....	55
Figure 93 Wet Platform, Transfer Function, Low Frequency, North Incoherent Noise.....	56
Figure 94 Wet Platform, Transfer Function, Low Frequency, North Magnitude Response.....	56
Figure 95 Wet Platform, Transfer Function, Low Frequency, North Phase Response.....	56
Figure 96 Wet Platform, Transfer Function, Low Frequency, East Waveforms.....	57
Figure 97 Wet Platform, Transfer Function, Low Frequency, East Power Spectra.....	57
Figure 98 Wet Platform, Transfer Function, Low Frequency, East Coherence.....	57
Figure 99 Wet Platform, Transfer Function, Low Frequency, East Incoherent Noise.....	58
Figure 100 Wet Platform, Transfer Function, Low Frequency, East Magnitude Response.....	58
Figure 101 Wet Platform, Transfer Function, Low Frequency, East Phase Response.....	58
Figure 102 Wet Platform, Transfer Function, High Frequency, Vertical Waveforms.....	59
Figure 103 Wet Platform, Transfer Function, High Frequency, Vertical Power Spectra.....	59
Figure 104 Wet Platform, Transfer Function, High Frequency, Vertical Coherence.....	59
Figure 105 Wet Platform, Transfer Function, High Frequency, Vertical Incoherent Noise.....	60
Figure 106 Wet Platform, Transfer Function, High Frequency, Vertical Magnitude Response.....	60
Figure 107 Wet Platform, Transfer Function, High Frequency, Vertical Phase Response.....	60
Figure 108 Wet Platform, Transfer Function, High Frequency, North Waveforms.....	61
Figure 109 Wet Platform, Transfer Function, High Frequency, North Power Spectra.....	61
Figure 110 Wet Platform, Transfer Function, High Frequency, North Coherence.....	61
Figure 111 Wet Platform, Transfer Function, High Frequency, North Incoherent Noise.....	62
Figure 112 Wet Platform, Transfer Function, High Frequency, North Magnitude Response.....	62
Figure 113 Wet Platform, Transfer Function, High Frequency, North Phase Response.....	62
Figure 114 Wet Platform, Transfer Function, High Frequency, East Waveforms.....	63
Figure 115 Wet Platform, Transfer Function, High Frequency, East Power Spectra.....	63
Figure 116 Wet Platform, Transfer Function, High Frequency, East Coherence.....	63
Figure 117 Wet Platform, Transfer Function, High Frequency, East Incoherent Noise.....	64
Figure 118 Wet Platform, Transfer Function, High Frequency, East Magnitude Response.....	64
Figure 119 Wet Platform, Transfer Function, High Frequency, East Phase Response.....	64
Figure 120 Wet Platform Testing, Geophone, Vertical Waveforms.....	65
Figure 121 Wet Platform Testing, Geophone, Vertical Power Spectra.....	65
Figure 122 Wet Platform Testing, Geophone, Vertical Coherence.....	66
Figure 123 Wet Platform Testing, Geophone, Vertical Incoherent Noise.....	66
Figure 124 Wet Platform Testing, Geophone, Vertical Magnitude Response.....	66
Figure 125 Wet Platform Testing, Geophone, Vertical Phase Response.....	66
Figure 126 Wet Platform Testing, Geophone, North Waveforms.....	67
Figure 127 Wet Platform Testing, Geophone, North Power Spectra.....	67
Figure 128 Wet Platform Testing, Geophone, North Coherence.....	67
Figure 129 Wet Platform Testing, Geophone, North Incoherent Noise.....	68
Figure 130 Wet Platform Testing, Geophone, North Magnitude Response.....	68
Figure 131 Wet Platform Testing, Geophone, North Phase Response.....	68
Figure 132 Wet Platform Testing, Geophone, East Waveforms.....	69
Figure 133 Wet Platform Testing, Geophone, East Power Spectra.....	69
Figure 134 Wet Platform Testing, Geophone, East Coherence.....	69
Figure 135 Wet Platform Testing, Geophone, East Incoherent Noise.....	70
Figure 136 Wet Platform Testing, Geophone, East Magnitude Response.....	70

Figure 137 Wet Platform Testing, Geophone, East Phase Response .....	70
Figure 138 Wet Platform, Cross-Axis Coupling, Reference Power Spectra .....	72
Figure 139 Wet Platform, Cross-Axis Coupling, Reference Coherence .....	72
Figure 140 Wet Platform, Cross-Axis Coupling, Trillium OBS Platform Power Spectra .....	73
Figure 141 Wet Platform, Cross-Axis Coupling, Trillium OBS Platform Coherence .....	73
Figure 142 Wet Platform, Cross-Axis Coupling, Navy OBS Platform Power Spectra .....	74
Figure 143 Wet Platform, Cross-Axis Coupling, Navy OBS Platform Coherence .....	74
Figure 144 Wet Seafloor Photo .....	75
Figure 145 Wet Seafloor Platform Testing Diagram (RPKromer Consulting) .....	75
Figure 146 Seafloor, Transfer Function, Low Frequency, Vertical Waveforms .....	76
Figure 147 Seafloor, Transfer Function, Low Frequency, Vertical Power Spectra .....	77
Figure 148 Seafloor, Transfer Function, Low Frequency, Vertical Coherence .....	77
Figure 149 Seafloor, Transfer Function, Low Frequency, Vertical Incoherent Noise .....	77
Figure 150 Seafloor, Transfer Function, Low Frequency, Vertical Magnitude Response .....	78
Figure 151 Seafloor, Transfer Function, Low Frequency, Vertical Phase Response .....	78
Figure 152 Seafloor, Transfer Function, Low Frequency, North Waveforms .....	79
Figure 153 Seafloor, Transfer Function, Low Frequency, North Power Spectra .....	79
Figure 154 Seafloor, Transfer Function, Low Frequency, North Coherence .....	80
Figure 155 Seafloor, Transfer Function, Low Frequency, North Incoherent Noise .....	80
Figure 156 Seafloor, Transfer Function, Low Frequency, North Magnitude Response .....	80
Figure 157 Seafloor, Transfer Function, Low Frequency, North Phase Response .....	81
Figure 158 Seafloor, Transfer Function, Low Frequency, East Waveforms .....	82
Figure 159 Seafloor, Transfer Function, Low Frequency, East Power Spectra .....	82
Figure 160 Seafloor, Transfer Function, Low Frequency, East Coherence .....	83
Figure 161 Seafloor, Transfer Function, Low Frequency, East Incoherent Noise .....	83
Figure 162 Seafloor, Transfer Function, Low Frequency, East Magnitude Response .....	83
Figure 163 Seafloor, Transfer Function, Low Frequency, East Phase Response .....	84
Figure 164 Seafloor, Transfer Function, High Frequency, Vertical Waveforms .....	85
Figure 165 Seafloor, Transfer Function, High Frequency, Vertical Power Spectra .....	85
Figure 166 Seafloor, Transfer Function, High Frequency, Vertical Coherence .....	86
Figure 167 Seafloor, Transfer Function, High Frequency, Vertical Incoherent Noise .....	86
Figure 168 Seafloor, Transfer Function, High Frequency, Vertical Magnitude Response .....	86
Figure 169 Seafloor, Transfer Function, High Frequency, Vertical Phase Response .....	87
Figure 170 Seafloor, Transfer Function, High Frequency, North Waveforms .....	88
Figure 171 Seafloor, Transfer Function, High Frequency, North Power Spectra .....	88
Figure 172 Seafloor, Transfer Function, High Frequency, North Coherence .....	89
Figure 173 Seafloor, Transfer Function, High Frequency, North Incoherent Noise .....	89
Figure 174 Seafloor, Transfer Function, High Frequency, North Magnitude Response .....	89
Figure 175 Seafloor, Transfer Function, High Frequency, North Phase Response .....	90
Figure 176 Seafloor, Transfer Function, High Frequency, East Waveforms .....	91
Figure 177 Seafloor, Transfer Function, High Frequency, East Power Spectra .....	91
Figure 178 Seafloor, Transfer Function, High Frequency, East Coherence .....	92
Figure 179 Seafloor, Transfer Function, High Frequency, East Incoherent Noise .....	92
Figure 180 Seafloor, Transfer Function, High Frequency, East Magnitude Response .....	92
Figure 181 Seafloor, Transfer Function, High Frequency, East Phase Response .....	93
Figure 182 Seafloor, Geophone, Vertical Waveforms .....	94

Figure 183 Seafloor, Geophone, Vertical Power Spectra .....	94
Figure 184 Seafloor, Geophone, Vertical Coherence .....	95
Figure 185 Seafloor, Geophone, Vertical Incoherent Noise .....	95
Figure 186 Seafloor, Geophone, Vertical Magnitude Response .....	95
Figure 187 Seafloor, Geophone, Vertical Phase Response .....	95
Figure 188 Seafloor, Geophone, North Waveforms .....	96
Figure 189 Seafloor, Geophone, North Power Spectra .....	96
Figure 190 Seafloor, Geophone, North Coherence .....	96
Figure 191 Seafloor, Geophone, North Incoherent Noise .....	97
Figure 192 Seafloor, Geophone, North Magnitude Response .....	97
Figure 193 Seafloor, Geophone, North Phase Response .....	97
Figure 194 Seafloor, Geophone, East Waveforms .....	98
Figure 195 Seafloor, Geophone, East Power Spectra .....	98
Figure 196 Seafloor, Geophone, East Coherence .....	98
Figure 197 Seafloor, Geophone, East Incoherent Noise .....	99
Figure 198 Seafloor, Geophone, East Magnitude Response .....	99
Figure 199 Seafloor, Geophone, East Phase Response .....	99
Figure 200 Seafloor, Cross-Axis Coupling, Reference Power Spectra .....	101
Figure 201 Seafloor, Cross-Axis Coupling, Reference Coherence .....	101
Figure 202 Seafloor, Cross-Axis Coupling, Seafloor Power Spectra .....	102
Figure 203 Seafloor, Cross-Axis Coupling, Seafloor Coherence .....	102
Figure 204 Seafloor, Cross-Axis Coupling, Trillium OBS Platform Power Spectra .....	103
Figure 205 Seafloor, Cross-Axis Coupling, Trillium OBS Platform Coherence .....	103
Figure 206 Seafloor, Cross-Axis Coupling, Navy OBS Platform Power Spectra .....	104
Figure 207 Seafloor, Cross-Axis Coupling, Navy OBS Platform Coherence .....	104
Figure 208 Seafloor, Bubble, Vertical Waveforms .....	106
Figure 209 Seafloor, Bubble, Vertical Power Spectra .....	106
Figure 210 Seafloor, Bubble, Vertical Coherence .....	106
Figure 211 Seafloor, Bubble, Vertical Magnitude Response .....	106
Figure 212 Seafloor, Bubble, North Waveforms .....	107
Figure 213 Seafloor, Bubble, North Power Spectra .....	107
Figure 214 Seafloor, Bubble, North Coherence .....	107
Figure 215 Seafloor, Bubble, North Magnitude Response .....	107
Figure 216 Seafloor, Bubble, East Waveforms .....	108
Figure 217 Seafloor, Bubble, East Power Spectra .....	108
Figure 218 Seafloor, Bubble, East Coherence .....	108
Figure 219 Seafloor, Bubble, East Magnitude Response .....	108
Figure 220 Wet Seafloor with Backfill Photo .....	109
Figure 221 Wet Seafloor Platform with Backfill Testing Diagram (RPKromer Consulting) .....	109
Figure 222 Backfill, Transfer Function, Vertical Waveforms .....	110
Figure 223 Backfill, Transfer Function, Vertical Power Spectra .....	110
Figure 224 Backfill, Transfer Function, Vertical Coherence .....	111
Figure 225 Backfill, Transfer Function, Vertical Incoherent Noise .....	111
Figure 226 Backfill, Transfer Function, Vertical Magnitude Response .....	111
Figure 227 Backfill, Transfer Function, Vertical Phase Response .....	111
Figure 228 Backfill, Transfer Function, North Waveforms .....	113

Figure 229 Backfill, Transfer Function, North Power Spectra.....	113
Figure 230 Backfill, Transfer Function, North Coherence.....	113
Figure 231 Backfill, Transfer Function, North Incoherent Noise.....	113
Figure 232 Backfill, Transfer Function, North Magnitude Response.....	114
Figure 233 Backfill, Transfer Function, North Phase Response.....	114
Figure 234 Backfill, Transfer Function, East Waveforms.....	115
Figure 235 Backfill, Transfer Function, East Power Spectra.....	115
Figure 236 Backfill, Transfer Function, East Coherence.....	115
Figure 237 Backfill, Transfer Function, East Incoherent Noise.....	116
Figure 238 Backfill, Transfer Function, East Magnitude Response.....	116
Figure 239 Backfill, Transfer Function, East Phase Response.....	116
Figure 240 Backfill Testing, Cross-Axis Coupling, Reference Power Spectra.....	118
Figure 241 Backfill Testing, Cross-Axis Coupling, Reference Coherence.....	118
Figure 242 Backfill Testing, Cross-Axis Coupling, Seafloor Power Spectra.....	119
Figure 243 Backfill Testing, Cross-Axis Coupling, Seafloor Coherence.....	119
Figure 244 Backfill Testing, Cross-Axis Coupling, Trillium OBS Platform Power Spectra.....	120
Figure 245 Backfill Testing, Cross-Axis Coupling, Trillium OBS Platform Coherence.....	120
Figure 246 Backfill Testing, Cross-Axis Coupling, Navy OBS Power Spectra.....	121
Figure 247 Backfill Testing, Cross-Axis Coupling, Navy OBS Coherence.....	121
Figure 248 Backfill, Bubble, Vertical Waveforms.....	123
Figure 249 Backfill, Bubble, Vertical Power Spectra.....	123
Figure 250 Backfill, Bubble, Vertical Coherence.....	123
Figure 251 Backfill, Bubble, Vertical Magnitude Response.....	123
Figure 252 Backfill, Bubble, North Waveforms.....	124
Figure 253 Backfill, Bubble, North Power Spectra.....	124
Figure 254 Backfill, Bubble, North Coherence.....	124
Figure 255 Backfill, Bubble, North Magnitude Response.....	124
Figure 256 Backfill, Bubble, East Waveforms.....	125
Figure 257 Backfill, Bubble, East Power Spectra.....	125
Figure 258 Backfill, Bubble, East Coherence.....	125
Figure 259 Backfill, Bubble, East Magnitude Response.....	125
Figure 260 Thumper Generator.....	126
Figure 261 Backfill, Thumper, Vertical Waveforms.....	127
Figure 262 Backfill, Thumper, North Waveforms.....	127
Figure 263 Backfill, Thumper, Single Thump East Waveforms.....	127

## NOMENCLATURE

dB	decibel
DOE	Department of Energy
OBS	Ocean Bottom Seismometer
SNL	Sandia National Laboratories
SNR	Signal to Noise Ratio
UP	Underwater Platform
PSRF	Pinedale Seismic Research Facility

# 1 INTRODUCTION

Evaluation of the SHDAS system at PSRF was performed to determine the performance characteristics of the Underwater Platform and how well it couples to the ground for the purpose of measuring ground motion.

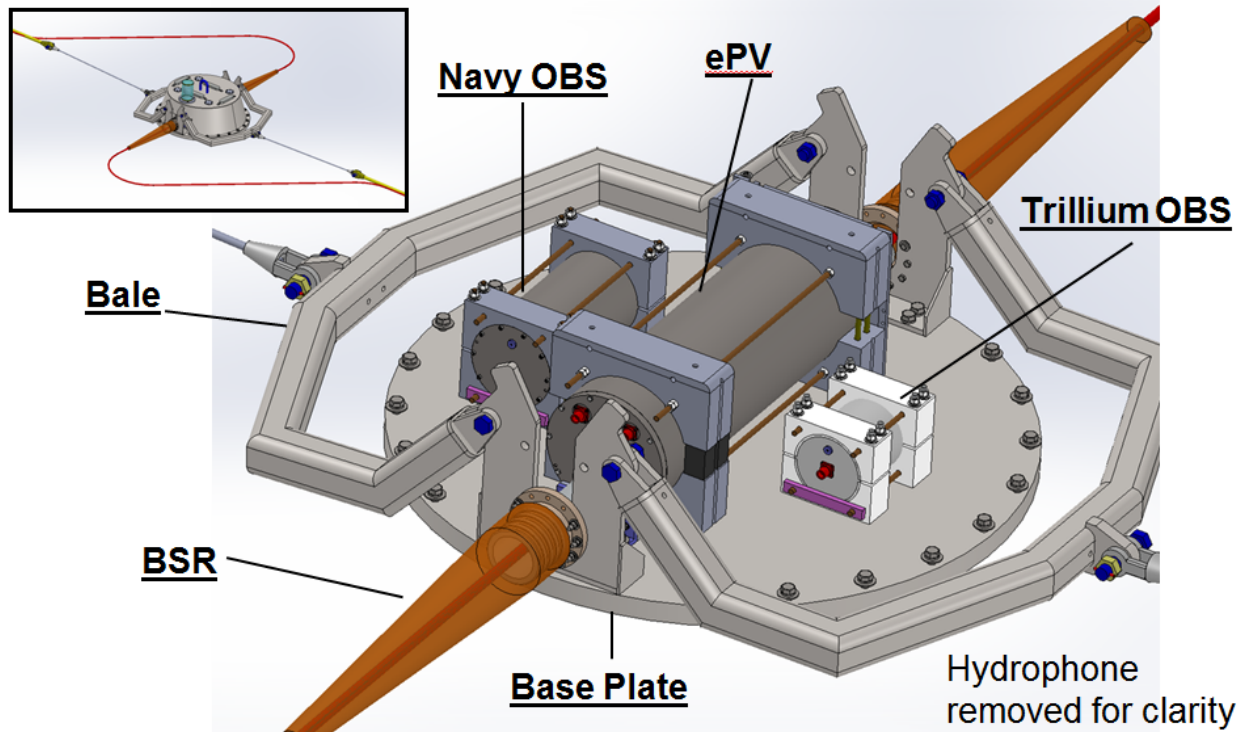


**Figure 1 SHDAS Underwater Platform**

The Underwater Platform, shown above, was placed in a Test Pool at the PSRF Remote Operating Facility (ROF). Conditions within the Test Pool were varied in order to evaluate the platform performance when directly coupled to the bottom of the concrete floor when dry, with the addition of water, with the addition of seafloor material between the platform and the floor, and the addition of backfill material.

The purpose of this evaluation is to comment on the performance impact of the Underwater Platform and not the seismometers themselves. The seismometer performance observed in each phase of the evaluation should only be considered in the context of how that performance has changed from one phase of the testing to the next. For each phase of the testing, analysis will be performed to evaluate:

- Transfer Function – the degree of coherence and sensor response characteristics of the various sensors relative to the reference sensor placed on the floor of the Test Pool. This analysis should be interpreted as encompassing the difference in coupling effects between the reference sensor and each of the other sensors in the test.

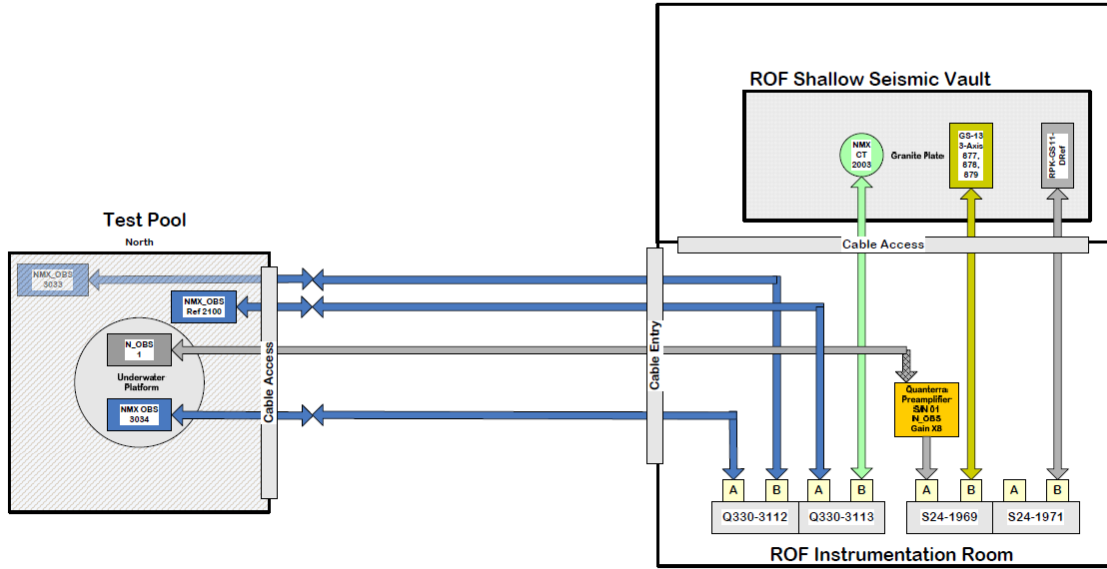
- Geophone – the degree of coherence and sensor response characteristics between the Trillium OBS and the Navy Geophone OBS both on the Underwater Platform. The purpose of this analysis is to determine whether the two seismometers are well coupled to one another on the Underwater Platform.
- Cross-Axis Coupling – the degree of coherence between each pair of axes (Z-N, Z-E, and N-E) on each seismometer. The coherence between the axes of a seismometer should be evaluated with regard to the changes from one testing phase and between the different seismometers in the test configuration. Changes in cross-axis coupling should be interpreted as being due to changes in the medium to which the sensors are coupled and not intrinsic changes in the sensors themselves.
- Bubble Tests – Bubbles were introduced into the water in the Test Pool during the last two phases of testing to simulate the presence of water noise and its effects.
- Thumper Tests – A ground thumper was employed during the final testing phase to observe the characteristics of a repeated ground motion source on the various seismometers in the test.

## 2 CONFIGURATION

The digitizers and seismometers used in the SHDAS PSRF platform evaluation were configured with the bitweights and seismometer connections as described below. Bitweights were measured by RPKromer Consulting prior to the start of the PSRF platform evaluation.

Manufacturer	Model	Serial Number	Application Bitweights	Seismometer	Sensitivity	Location
Geotech	Smart24R	1969	CH1: 51 nV/count CH2: 51 nV/count CH3: 51 nV/count CH4: 102 nV/count CH5: 102 nV/count CH6: 102 nV/count	Navy GS11-D OBS (Z) Navy GS11-D OBS (N/Y) Navy GS11-D OBS (E/X) Geotech GS13 V 858 (Z) Geotech GS13 H 877 (N/Y) Geotech GS13 H 879 (E/X)	1200 V/m/s 1200 V/m/s 1200 V/m/s 2000 V/m/s 2000 V/m/s 2000 V/m/s	Underwater Platform Underwater Platform Underwater Platform ROF Vault ROF Vault ROF Vault
Geotech	Smart24R	1971	CH1: 204 nV/count CH2: 204 nV/count CH3: 204 nV/count CH4: 102 nV/count CH5: 102 nV/count CH6: 102 nV/count	Terminated Terminated Terminated GS11-D (Z) GS11-D (N/Y) GS11-D (E/X)	N/A N/A N/A 1200 V/m/s 1200 V/m/s 1200 V/m/s	N/A N/A N/A ROF Vault ROF Vault ROF Vault
Quanterra	Q330	3112	CH1: 29.8 nV/count CH2: 29.8 nV/count CH3: 29.8 nV/count CH4: 29.8 nV/count CH5: 29.8 nV/count CH6: 29.8 nV/count	Nanometrics OBS 3034 (Z) Nanometrics OBS 3034 (N/Y) Nanometrics OBS 3034 (E/X) Nanometrics OBS 3033 (Z) Nanometrics OBS 3033 (N/Y) Nanometrics OBS 3033 (E/X)	750 V/m/s 750 V/m/s 750 V/m/s 750 V/m/s 750 V/m/s 750 V/m/s	Underwater Platform Underwater Platform Underwater Platform Test Pool Floor (Reference) Test Pool Floor (Reference) Test Pool Floor (Reference)
Quanterra	Q330	3113	CH1: 29.8 nV/count CH2: 29.8 nV/count CH3: 29.8 nV/count CH4: 29.8 nV/count CH5: 29.8 nV/count CH6: 29.8 nV/count	Nanometrics OBS 2100 (Z) Nanometrics OBS 2100 (N/Y) Nanometrics OBS 2100 (E/X) Nanometrics Trillium 2003 (Z) Nanometrics Trillium 2003 (N/Y) Nanometrics Trillium 2003 (E/X)	750 V/m/s 750 V/m/s 750 V/m/s 750 V/m/s 750 V/m/s 750 V/m/s	Seafloor Material Seafloor Material Seafloor Material ROF Vault ROF Vault ROF Vault

IV&V 5e Wet Platform Testing (simulated seafloor)  
Glass beads installed in Underwater Platform



PSRF SCE ML-6

September 15, 2014

**Figure 2 Example Testing Diagram (RPKromer Consulting)**

This evaluation makes use of the nominal response models provided by the manufacturers for the respective Nanometrics Trillium Seismometers and Navy Geophone Seismometer. It is recognized that the response characteristics of a given seismometer are expected to have some amount of deviation from this nominal. However, the evaluations performed of the underwater platform are intended to compare the relative change in performance from one set of test conditions to the next, in effect negating the impact of any slight deviations from the nominal response.

## 2.1 Seismic Background

The seismic background observed at the PSRF Test Pool and ROF must be evaluated in order to determine what will be needed in terms of a suitable seismic event in order to generate sufficient ground motion.

The data used for this evaluation of the PSRF background is taken from the Wet Testing phase in which both the reference Trillium OBS (#3033) and the Underwater Platform with Trillium OBS (#3034) are coupled directly to the bottom of the Test Pool. The Test Pool has been filled with water to help stabilize the temperature of the sensors.

The waveform data used for analysis was a 5 hour window of data on August 29, 2014 from 07:30 to 12:30 GMT. The power spectra and coherence for each of the Vertical, North, and East channels are shown below.

For each of the channels, the power spectra of the two seismometers and the relevant noise models (Navy OBS noise, New Low Noise Model, Q330 digitizer noise, and Trillium Compact OBS noise) are shown.

The self-noise of each seismometer, and any accompanying amplification electronics, will limit what can be observed in the signals that were collected. We observe that on the Trillium OBS's, there is significant SNR around the microseism, confirmed by the high values of coherence between approximately 0.1 and 0.6 Hz. Outside of that band around the microseism, the Trillium OBS's will require increased levels of ground motion in order to perform any analysis.

For comparisons involving the Navy OBS, which has significantly more noise at low frequencies as seen in the reference noise model, there is almost no signal above the estimated noise until well above 1 Hz.

Performing a comparison between the Trillium OBS and the Navy OBS will require increased ground motion across the entire frequency band due to the upper bound of the respective sensor noise models falling at or near the observed background.

### 2.1.1 Vertical

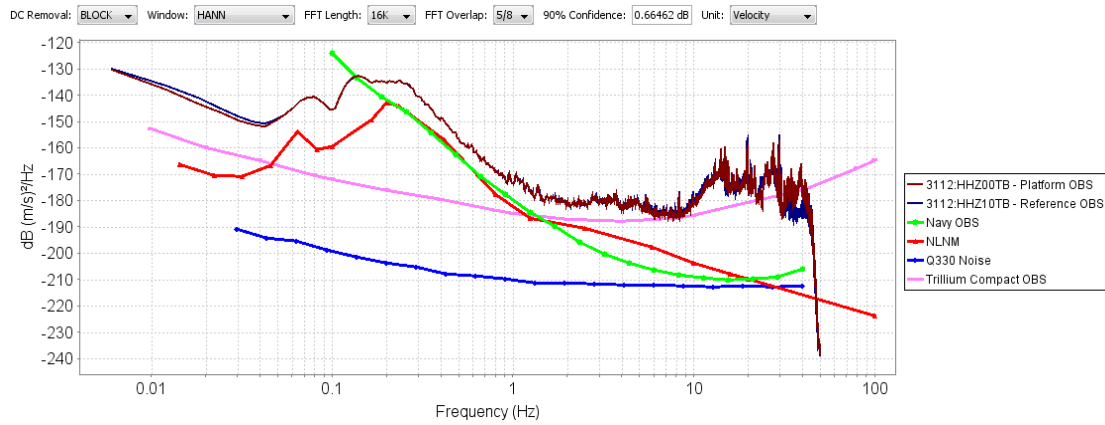


Figure 3 Background, Vertical Power Spectra

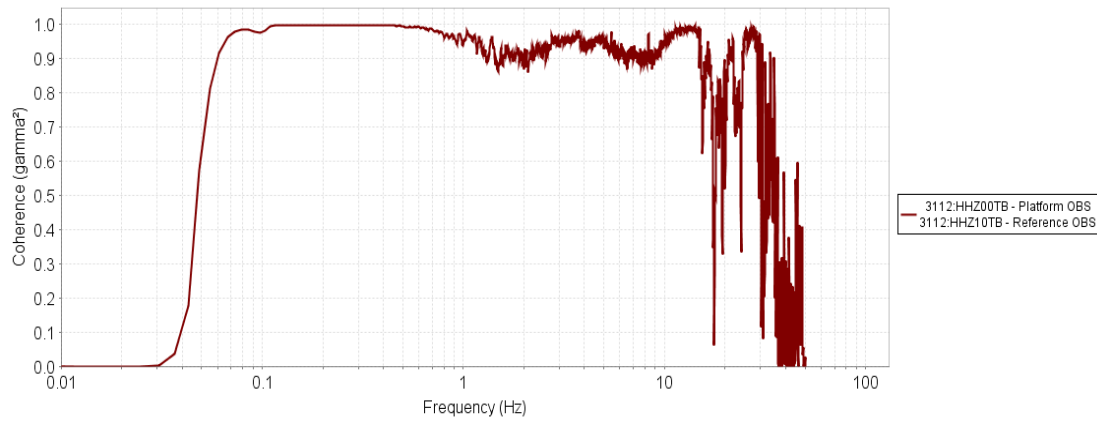


Figure 4 Background, Vertical Coherence

### 2.1.2 North

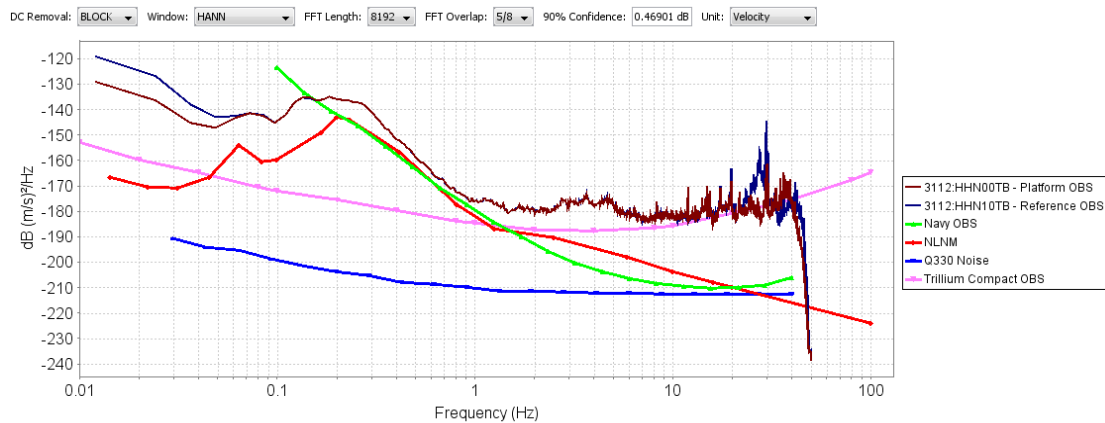
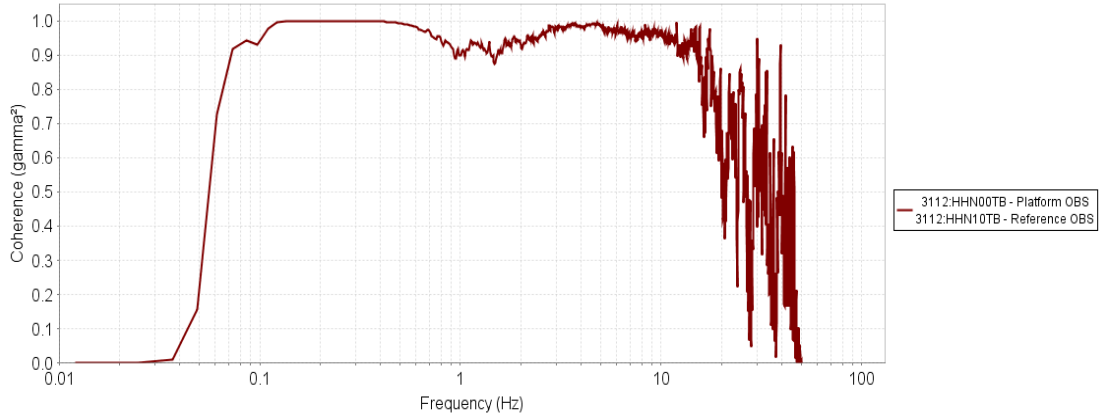
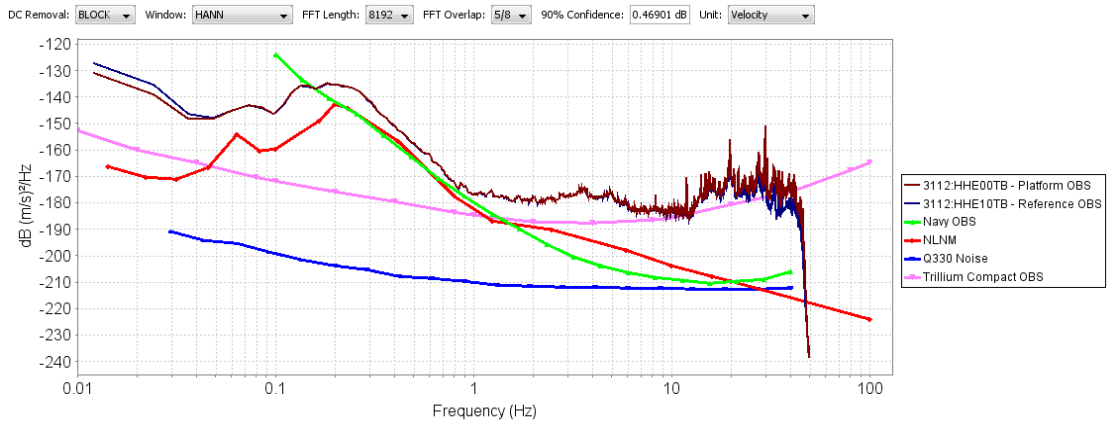


Figure 5 Background, North Power Spectra



**Figure 6 Background, North Coherence**

### 2.1.3 East



**Figure 7 Background, East Power Spectra**

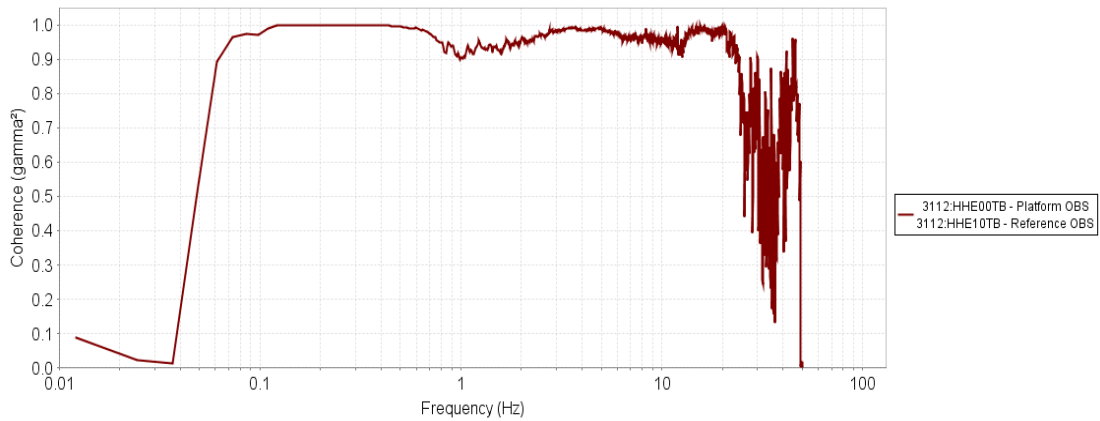


**Figure 8 Background, East Coherence**

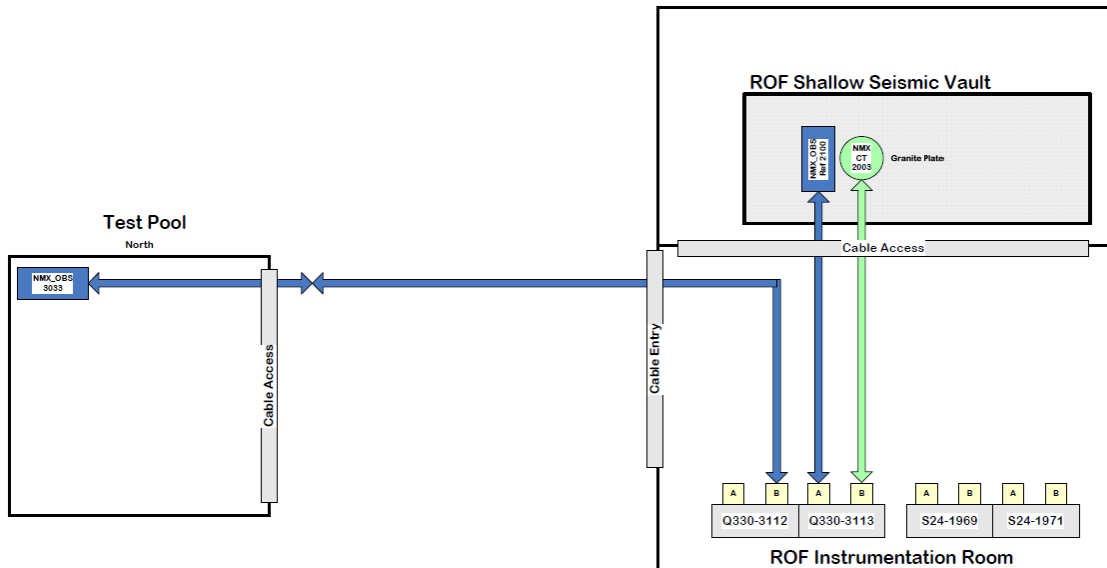


### 3 RESULTS

#### 3.1 Dry Testing

Dry Testing was performed with the reference Nanometrics Trillium OBS #3033 in direct contact with the bottom of the Test Pool. There was no water or seafloor material added to the Test Pool. The Underwater Platform was not placed in the Test Pool for this test. The purpose of this test was to determine the degree of coherence between the OBS in the Test Pool and an identical OBS #2100 placed within the ROF Shallow Vault some distance away. The results of this test will be used to determine the degree to which the reference sensors placed in the ROF Shallow Vault may be compared to the sensors in the Test Pool.

IV&V 5a Empty Pool Testing



PSRF SCE ML-2

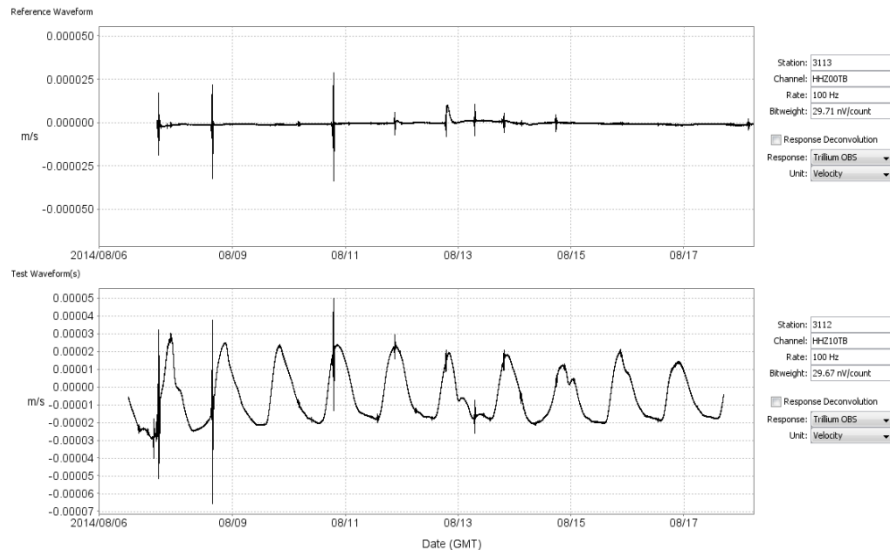
September 15, 2014

Figure 9 Dry Testing Diagram (RPKromer Consulting)

### 3.1.1 Transfer Function

Analysis of the test data will examine coherence between the two reference OBS sensors (#3033 and #2100) in their respective locations. The results of this testing will determine the suitability of utilizing the reference sensors within the ROF vault. Test data was collected for this test from August 7, 2014 to August 17, 2014.

The Nanometrics Trillium OBS in the Test Pool exhibited significant changes in output due to the day-night temperature swings as shown in the lower plot below:



**Figure 10 Dry Testing Waveforms**

A high-pass filter was applied to the data to remove frequencies below 0.01 Hz before further analysis.

A candidate event was identified with a duration of 1 hour and frequency content above the site noise at frequencies below 2 Hz on August 10, 2014 at approximately 18:50 UTC.

The waveform time series, power spectra, coherence, incoherent noise, relative magnitude, and relative phase for each of the Vertical, North, and East channels are shown below.

We observe that to the extent that there is sufficient signal above the background noise that there can be coherence between the ROF vault and the Test Pool between 0.05 and 1 Hz. However, we cannot observe coherence beyond those bounds. This limits the utility of the reference sensors in the ROF vault.

Note that for this event, there was minimal signal amplitude above background at frequencies greater than 1 Hz which limits the ability to comment on these higher frequencies. An event from the Wet Platform testing (5c) was also evaluated for coherence between the Test Pool and the ROF vault in the subsequent section.

### 3.1.1.1 Vertical

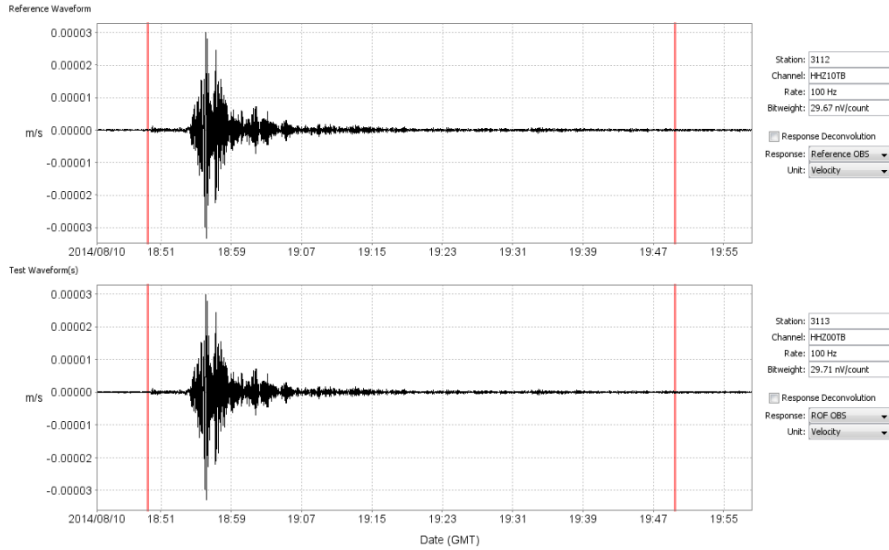


Figure 11 Dry Testing, Transfer Function, Vertical Waveforms

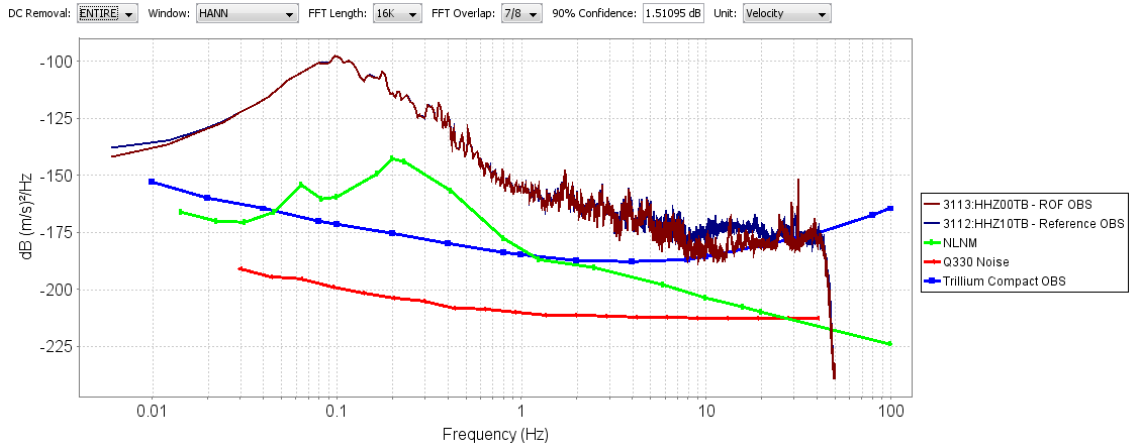


Figure 12 Dry Testing, Transfer Function, Vertical Power Spectra

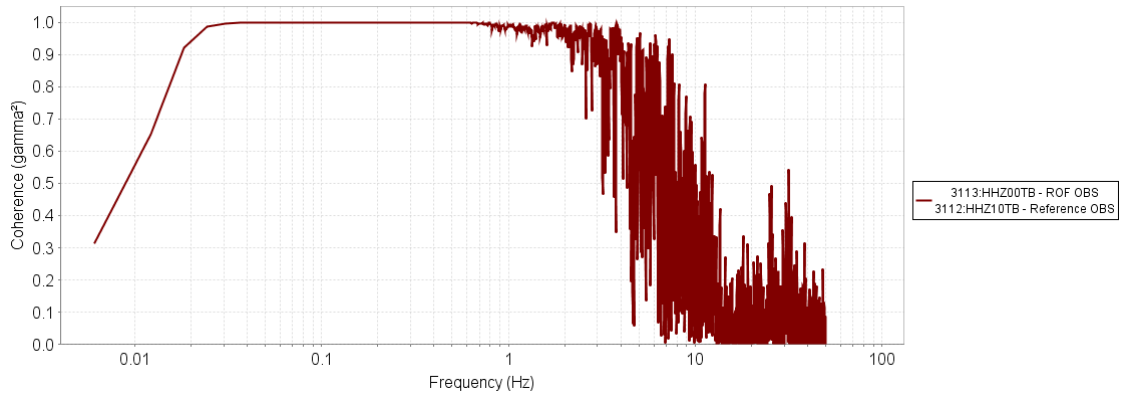
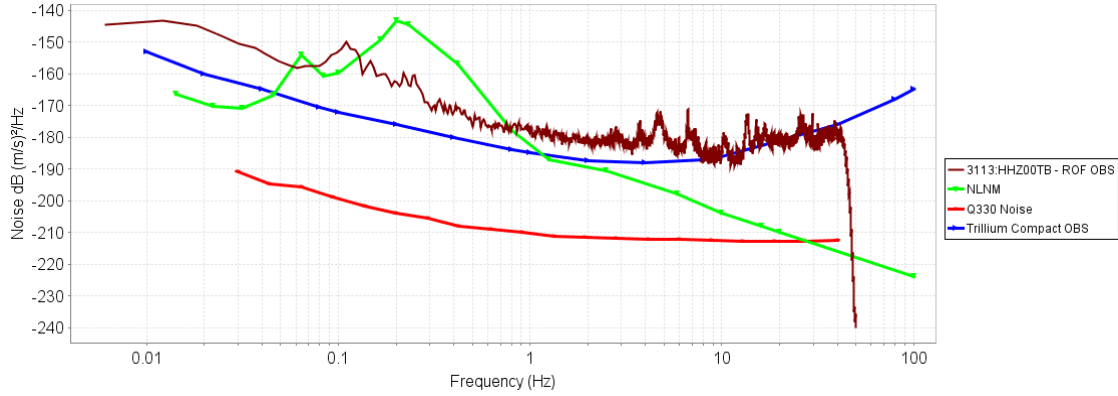
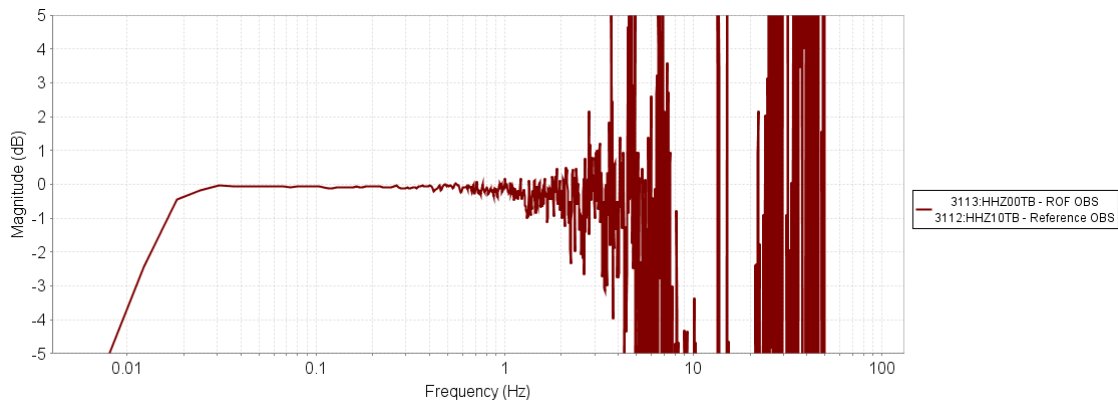


Figure 13 Dry Testing, Transfer Function, Vertical Coherence



**Figure 14 Dry Testing, Transfer Function, Vertical Incoherent Noise**



**Figure 15 Dry Testing, Transfer Function, Vertical Magnitude Response**

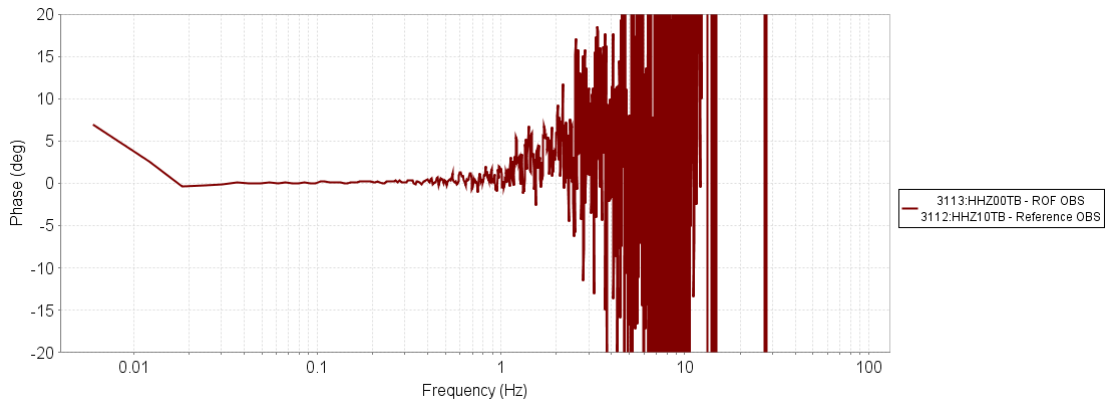


**Figure 16 Dry Testing, Transfer Function, Vertical Phase Response**

We see that the vertical channels have good coherence between approximately 0.03 and 1 Hz. Beyond those bounds, the coherence decreases rapidly. There is no appreciable difference in the amplitude and phase response over that passband to the limits of the available spectral resolution.

### 3.1.1.2 North

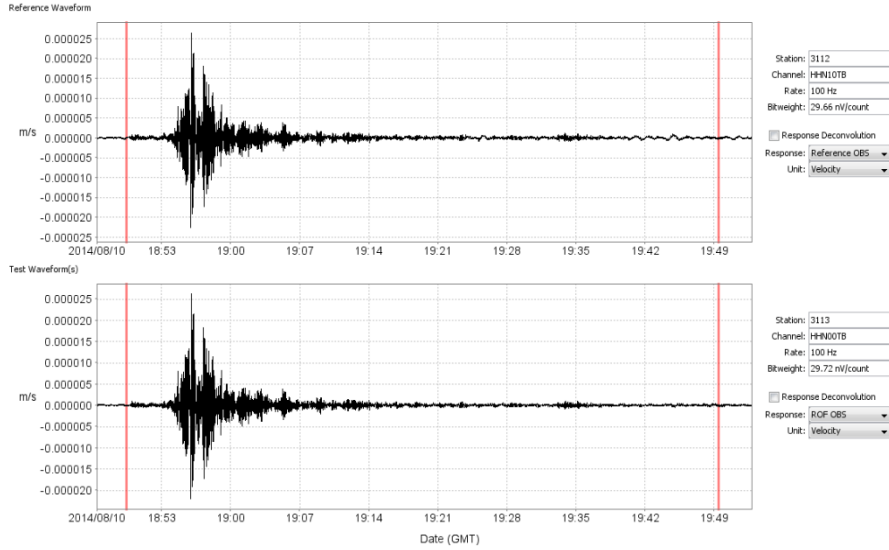


Figure 17 Dry Testing, Transfer Function, North Waveforms

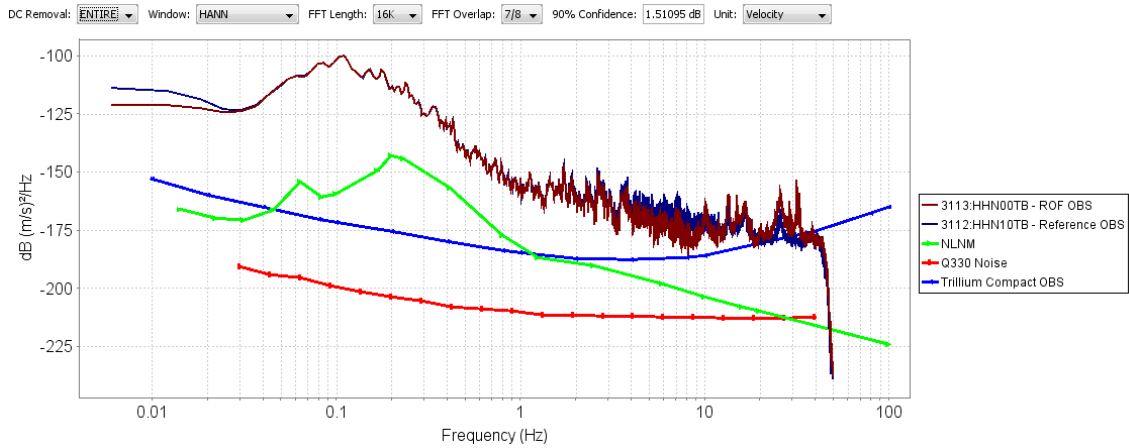


Figure 18 Dry Testing, Transfer Function, North Power Spectra

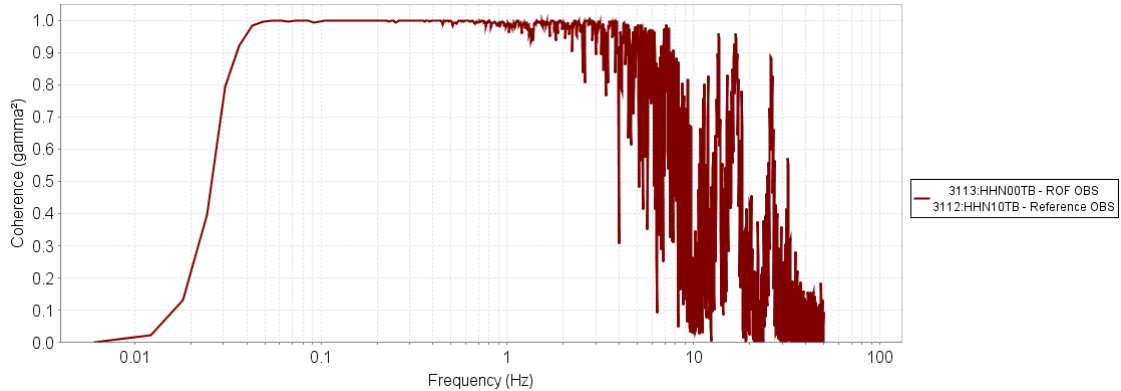
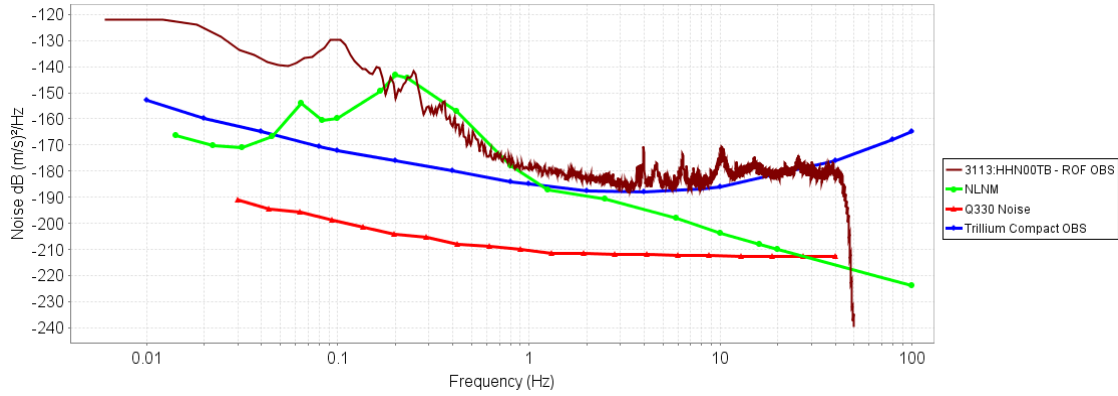
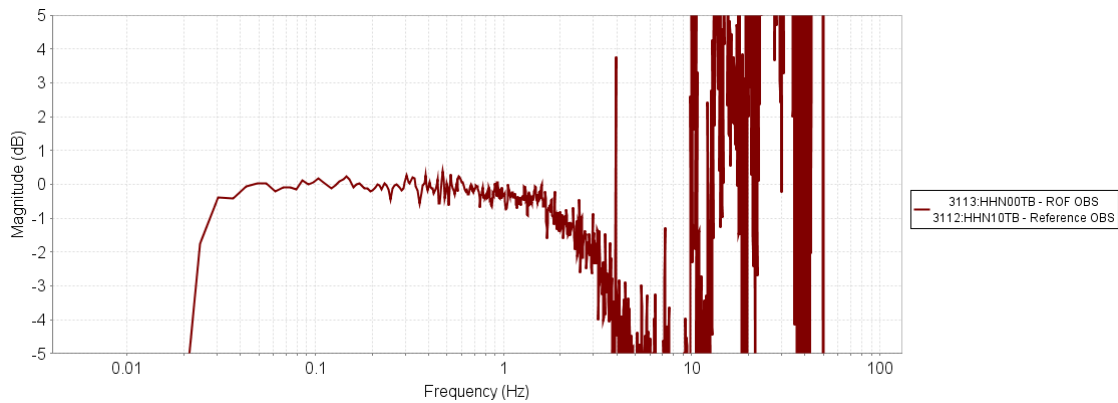


Figure 19 Dry Testing, Transfer Function, North Coherence



**Figure 20 Dry Testing, Transfer Function, North Incoherent Noise**



**Figure 21 Dry Testing, Transfer Function, North Magnitude Response**

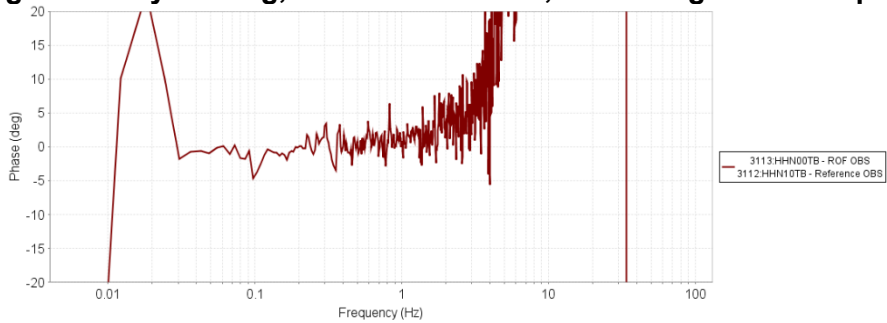


**Figure 22 Dry Testing, Transfer Function, North Phase Response**

We see that the north channels have good coherence between approximately 0.05 and 1 Hz. Beyond those bounds, the coherence decreases rapidly. There is no appreciable difference in the amplitude and phase response over that passband to the limits of the available spectral resolution.

### 3.1.1.3 East

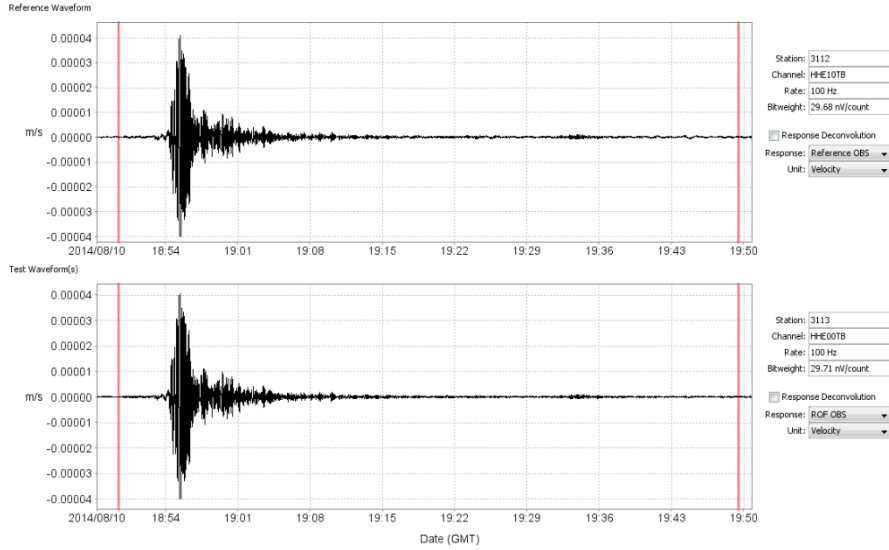


Figure 23 Dry Testing, Transfer Function, East Waveforms

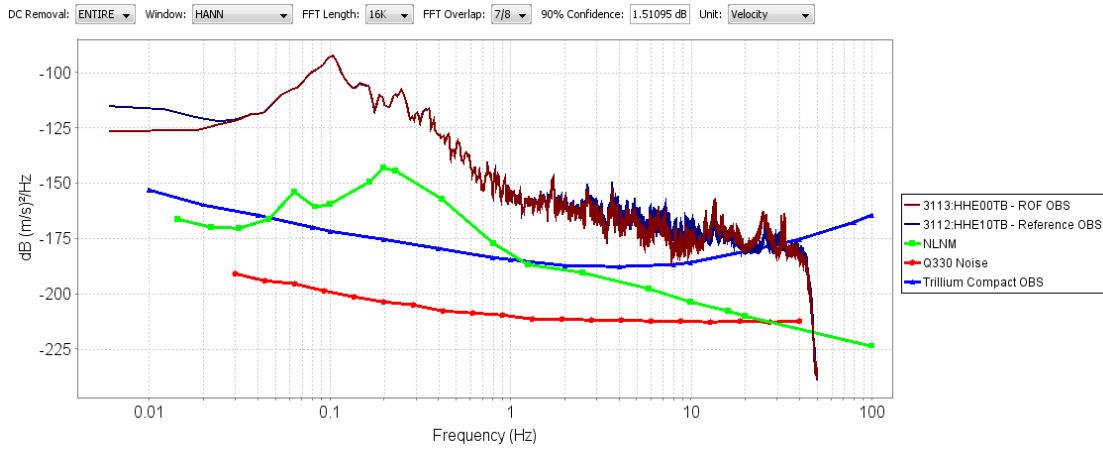


Figure 24 Dry Testing, Transfer Function, East Power Spectra

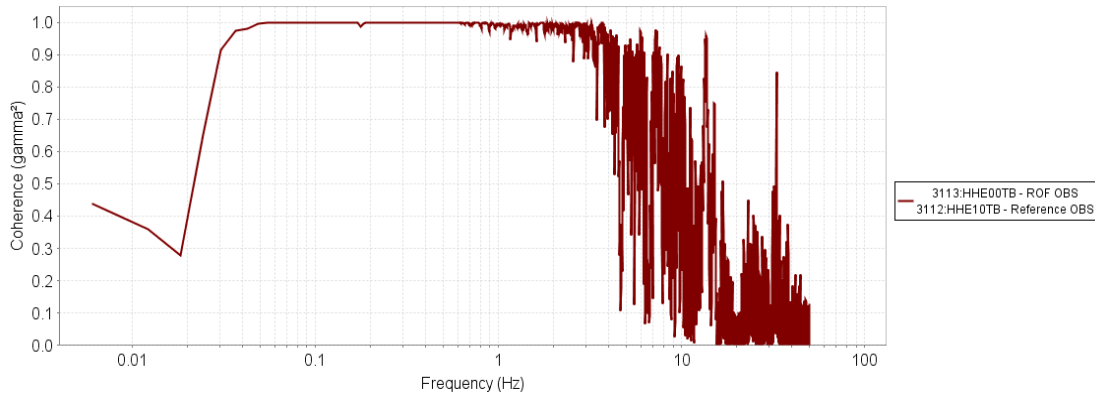
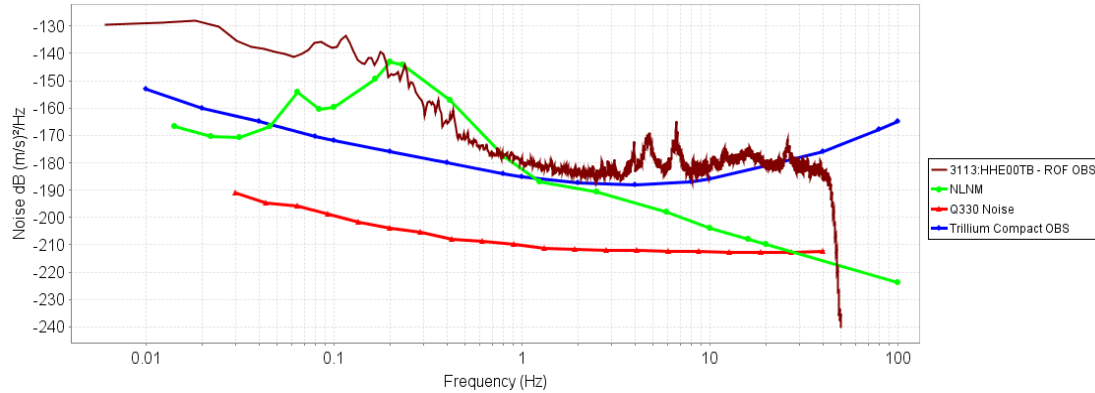
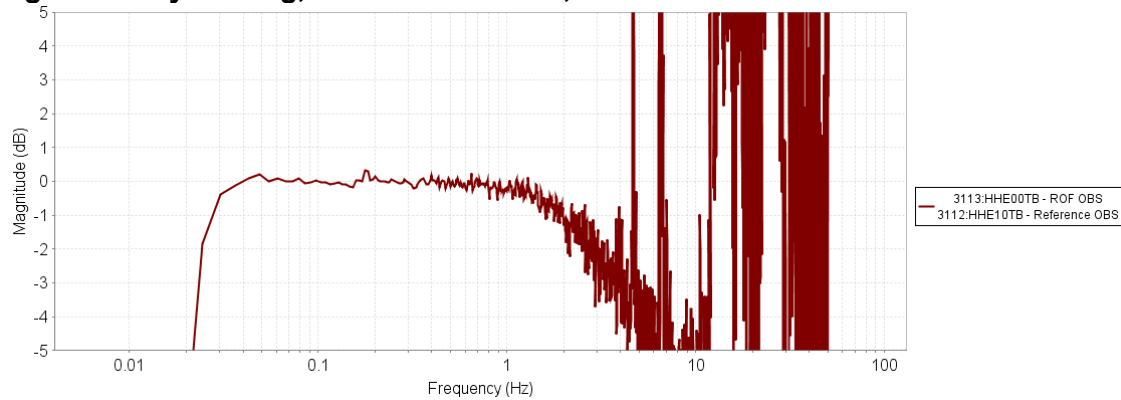


Figure 25 Dry Testing, Transfer Function, East Coherence



**Figure 26 Dry Testing, Transfer Function, East Incoherent Noise**



**Figure 27 Dry Testing, Transfer Function, East Magnitude Response**

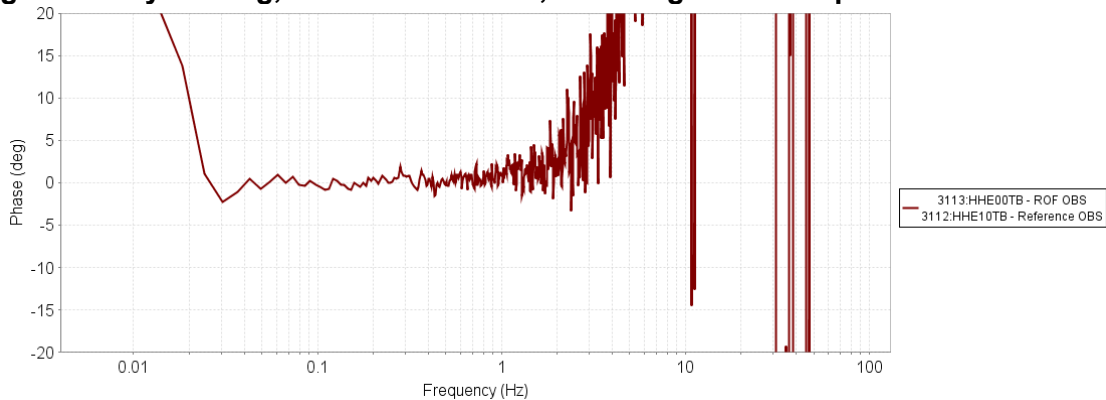


**Figure 28 Dry Testing, Transfer Function, East Phase Response**

We see that the east channels have good coherence between approximately 0.05 and 1 Hz. Beyond those bounds, the coherence decreases rapidly. There is no appreciable difference in the amplitude and phase response over that passband to the limits of the available spectral resolution.

### *3.1.2 Transfer Function – Wet Platform*

Analysis of the test data will examine coherence between the two reference OBS sensors (#3033 and #2100) in their respective locations. This evaluation examines data from the wet platform test to determine to a greater extent the degree of coherence between the Test Pool and the ROF Vault.

A candidate event was identified with duration of 2 minutes and frequency content above the site noise at frequencies above 0.2 Hz on August 30, 2014 at approximately 20:10 UTC.

The waveform time series, power spectra, and coherence for each of the Vertical, North, and East channels are shown below.

We observe that there is sufficient signal amplitude above the background and the sensor self-noise that we should be able to observe coherence between the Test Pool and the ROF vault out to approximately 20 Hz. However, the sensors only exhibit good coherence out to approximately 4 Hz and the coherence drops off considerably at frequencies above 10 Hz. These results indicate that there is a lack of sufficient coupling between the Test Pool and the ROF Vault to allow suitable coherence between the sensors for comparison at the frequencies of interest.

Evaluation of the test data will proceed with using the Trillium OBS (#3033) placed at the bottom of the Test Pool as a reference. The reference sensors within the ROF Vault will not be used due to the lack of coherence above 4 Hz.

### 3.1.2.1 Vertical

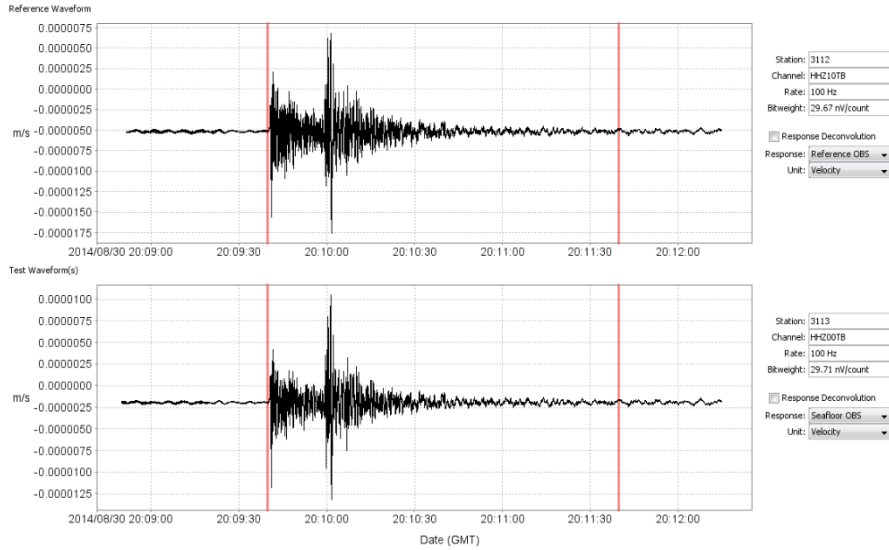


**Figure 29 Dry Testing, Transfer Function - Wet, Vertical Waveforms**

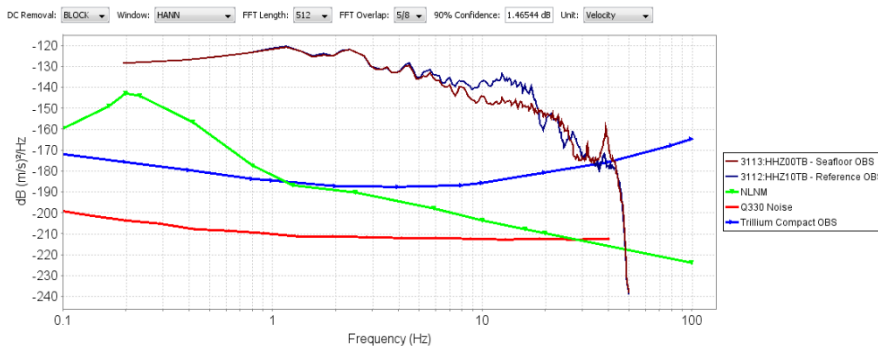


**Figure 30 Dry Testing, Transfer Function - Wet, Vertical Power Spectra**

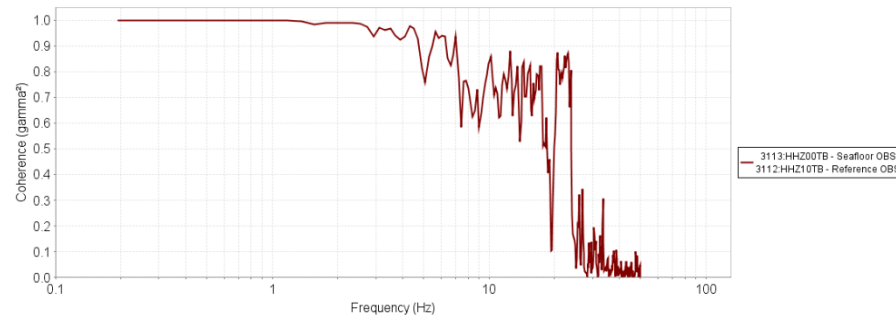


**Figure 31 Dry Testing, Transfer Function - Wet, Vertical Coherence**

We see that the vertical channels have good coherence below 3 Hz. Beyond those bounds, the coherence decreases rapidly. There are also considerable differences in the observed power spectra at frequencies above 3 Hz. Although the plots are not shown, there is no appreciable difference in the amplitude and phase response below 3 Hz to the limits of the available spectral resolution.

### 3.1.2.2 North

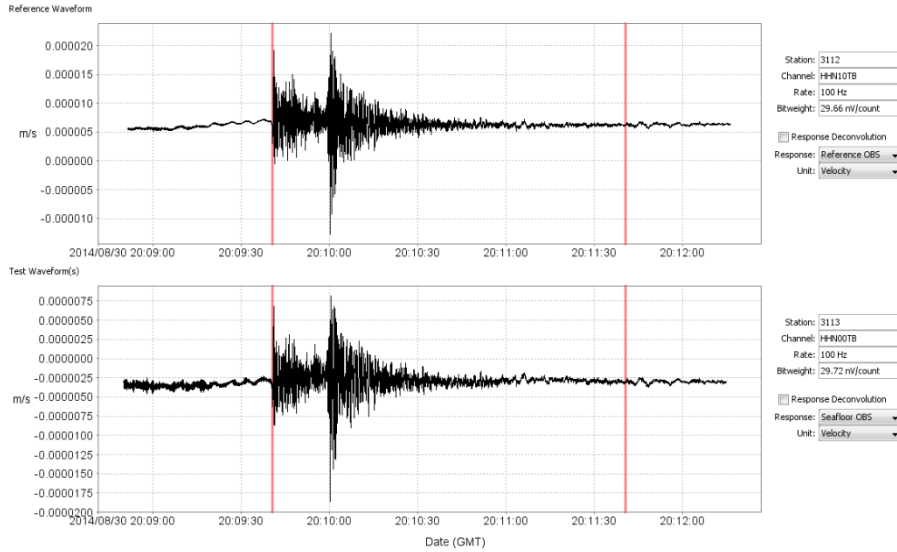


**Figure 32 Dry Testing, Transfer Function - Wet, North Waveforms**

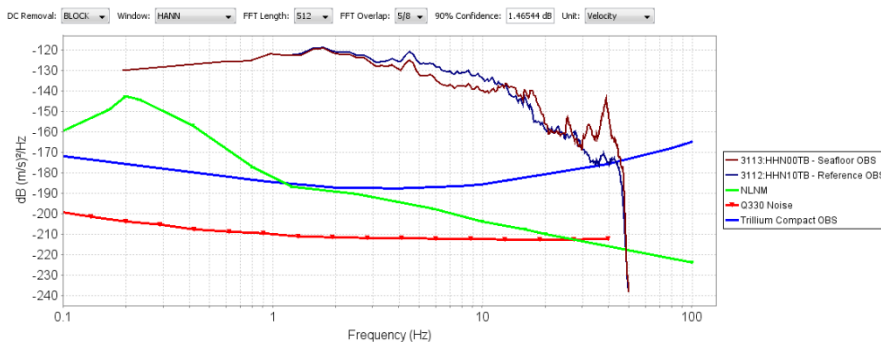


**Figure 33 Dry Testing, Transfer Function - Wet, North Power Spectra**

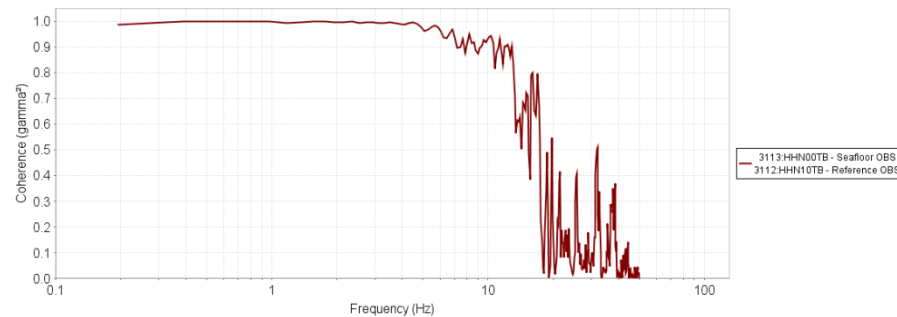


**Figure 34 Dry Testing, Transfer Function - Wet, North Coherence**

We see that the north channels have good coherence below 4 Hz. Beyond those bounds, the coherence decreases rapidly. There are also considerable differences in the observed power spectra at frequencies above 3 Hz. Although the plots are not shown, there is no appreciable difference in the amplitude and phase response below 3 Hz to the limits of the available spectral resolution.

### 3.1.2.3 East

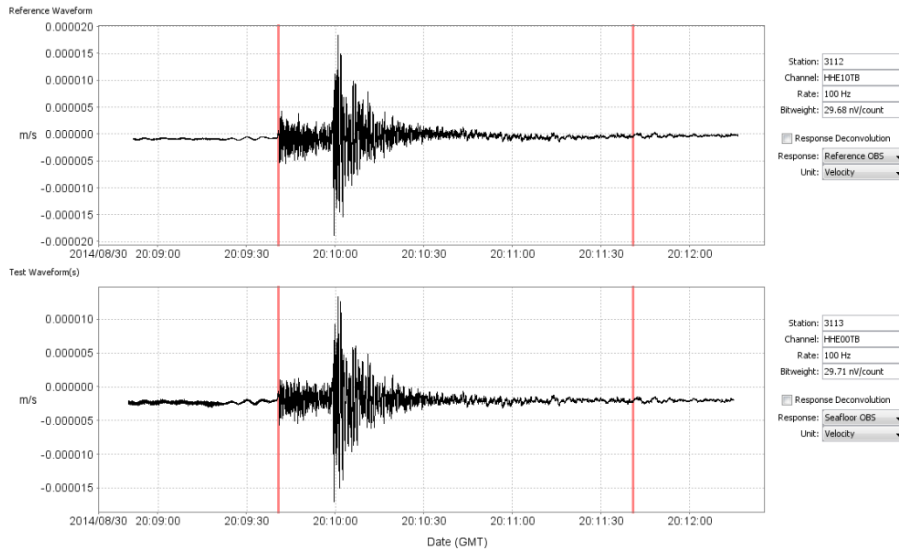


Figure 35 Dry Testing, Transfer Function - Wet, East Waveforms

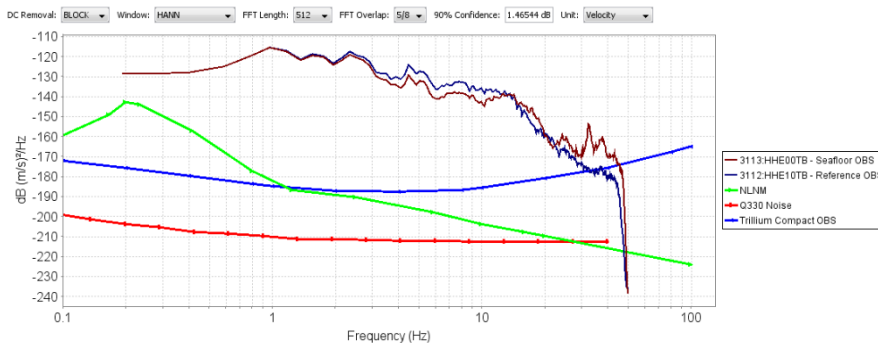


Figure 36 Dry Testing, Transfer Function - Wet, East Power Spectra

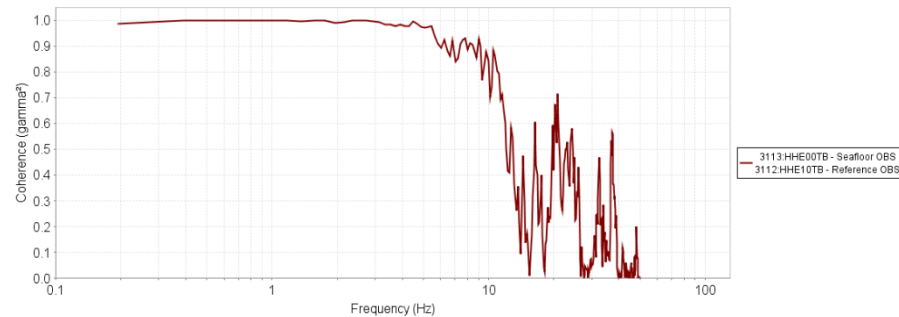


Figure 37 Dry Testing, Transfer Function - Wet, East Coherence

We see that the east channels have good coherence below 4 Hz. Beyond those bounds, the coherence decreases rapidly. There are also considerable differences in the observed power spectra at frequencies above 3 Hz. Although the plots are not shown, there is no appreciable difference in the amplitude and phase response below 3 Hz to the limits of the available spectral resolution.

### 3.2 Dry Platform Testing

Dry platform testing was performed with both the reference Nanometrics Trillium OBS and the Underwater Platform in direct contact with the bottom of the Test Pool. There was no water or seafloor material added to the Test Pool. The results of this test will be used to comment on any affect that the Underwater Platform has on the transfer function between the Nanometrics OBS reference sensor (#3033) and the Nanometrics OBS on the underwater platform (#3034). In addition, a comparison will be made between the performance of the Nanometrics OBS (#3034) and the Navy OBS, both of which are on the Underwater Platform.



Figure 38 Dry Platform Photo

IV&V 5b Dry Underwater Platform Testing

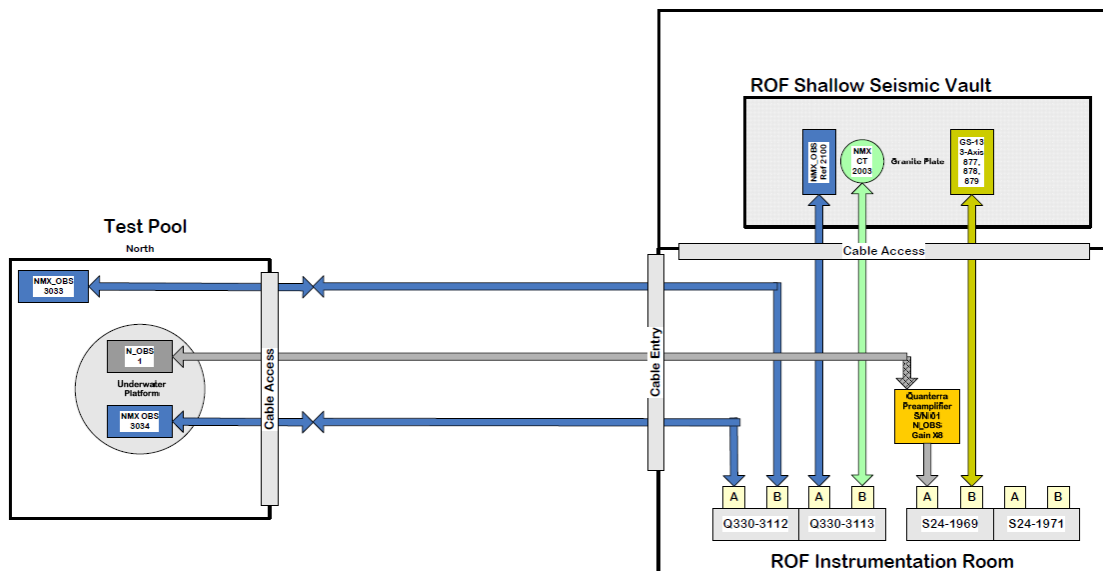


Figure 39 Dry Platform Testing Diagram (RP Kromer Consulting)

### 3.2.1 *Transfer Function*

Analysis of the test data will examine coherence between the reference OBS and the OBS on the Underwater Platform in order to establish the transfer function between the two sensors. Incoherent noise is “lumped” on to the Platform OBS. Test data was collected for this test on August 21, 2014 from 00:10 to 18:28 (GMT).

A single candidate event was identified on August 21, 2014 at 09:25 with duration of 3 minutes and frequency content above the site noise at frequencies above 0.5 Hz.

Note that on all of the channels, the OBS on the Underwater Platform exhibited significantly more noise below 0.05 Hz than the OBS directly on the bottom of the Test Pool. The source of this noise is unknown.

The waveform time series, power spectra, coherence, incoherent noise, relative magnitude, and relative phase for each of the Vertical, North, and East channels are shown below for each of the Vertical, North, and East channels.

### 3.2.1.1 Vertical

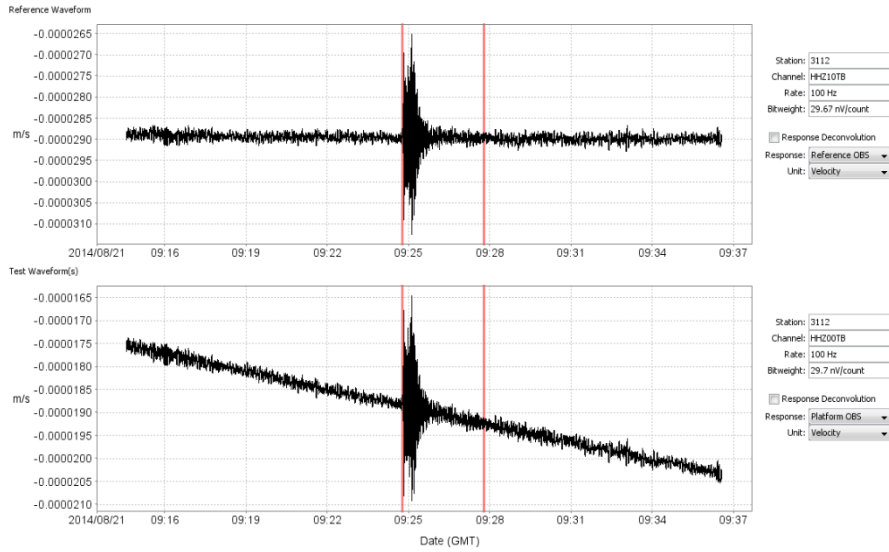


Figure 40 Dry Platform Testing, Transfer Function, Vertical Waveforms

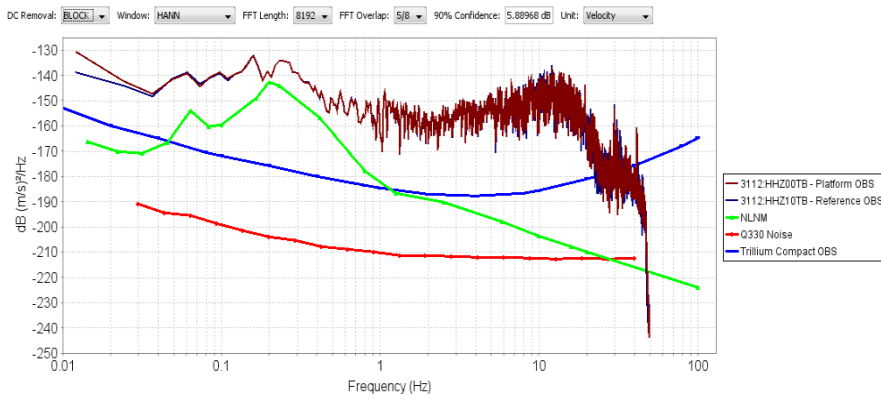


Figure 41 Dry Platform Testing, Transfer Function, Vertical Power Spectra

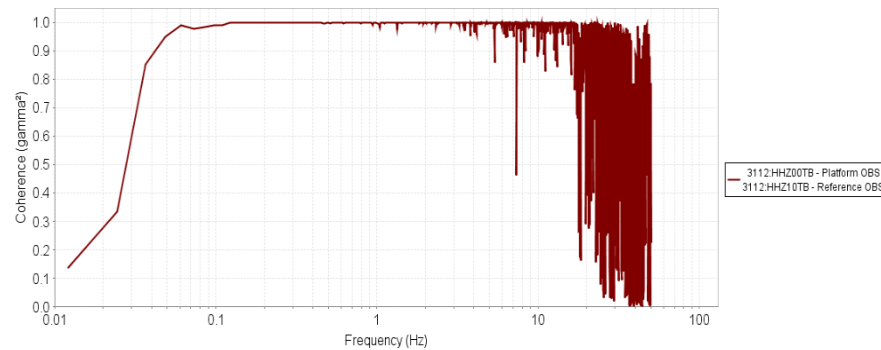
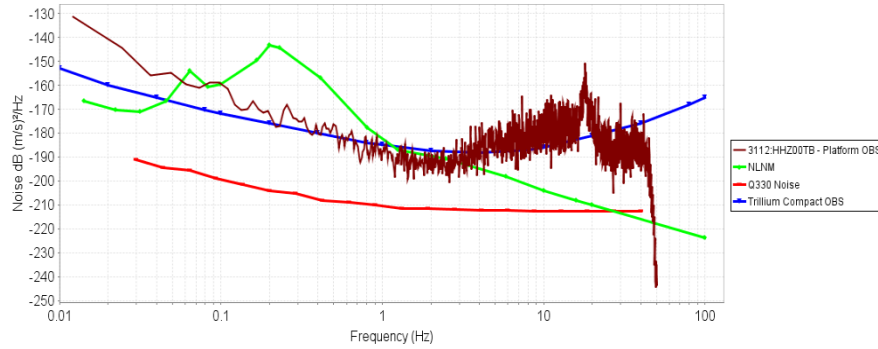
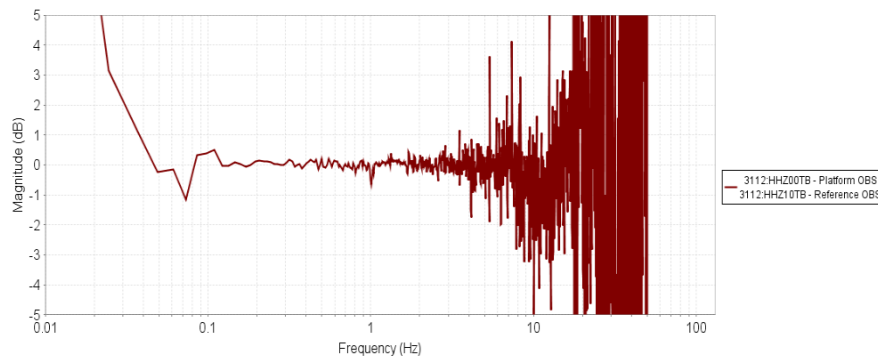


Figure 42 Dry Platform Testing, Transfer Function, Vertical Coherence



**Figure 43 Dry Platform Testing, Transfer Function, Vertical Incoherent Noise**



**Figure 44 Dry Platform Testing, Transfer Function, Vertical Magnitude Response**

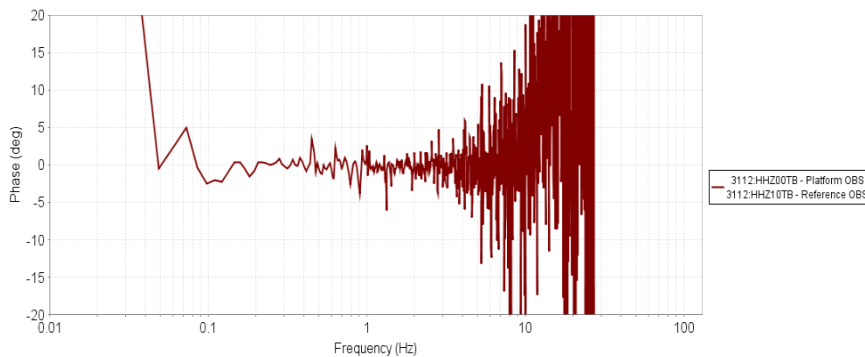


**Figure 45 Dry Platform Testing, Transfer Function, Vertical Phase Response**

We see that the vertical channels have good coherence between approximately 0.06 and 5 Hz for this event. Beyond those bounds, the coherence degrades rapidly. There is minimal difference in the amplitude and phase response over that passband to the limits of the available spectral resolution.

### 3.2.1.2 North

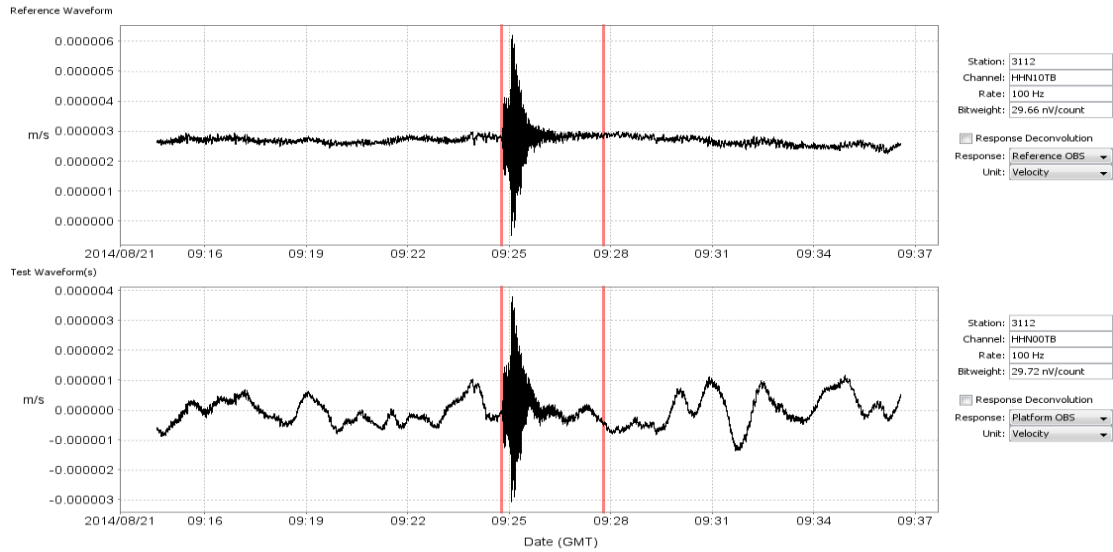


Figure 46 Dry Platform Testing, Transfer Function, North Waveforms

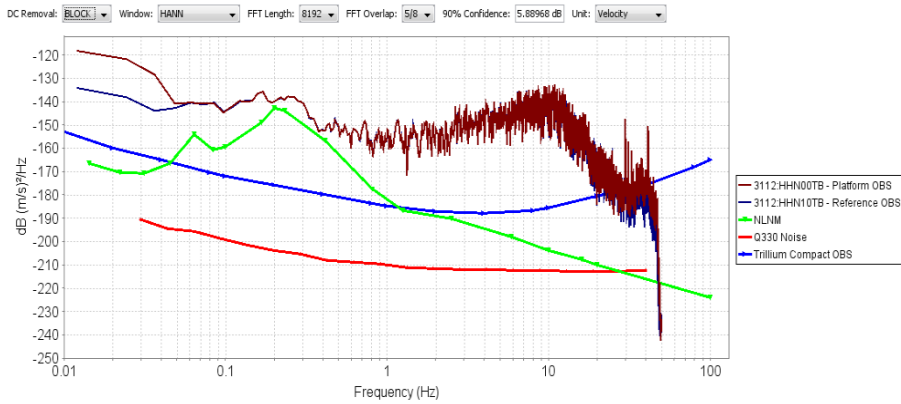


Figure 47 Dry Platform Testing, Transfer Function, North Power Spectra

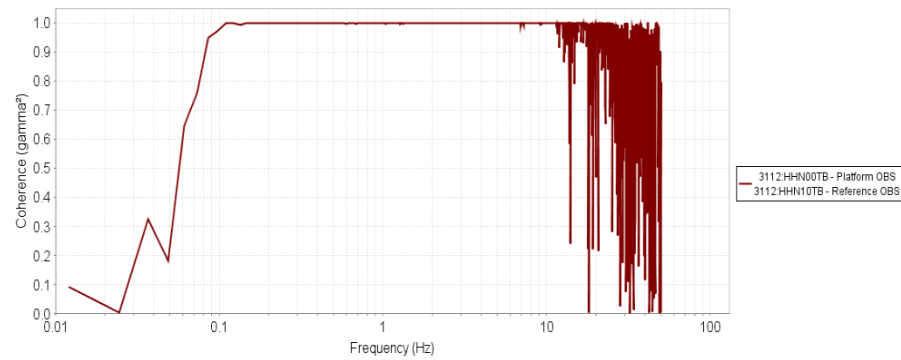
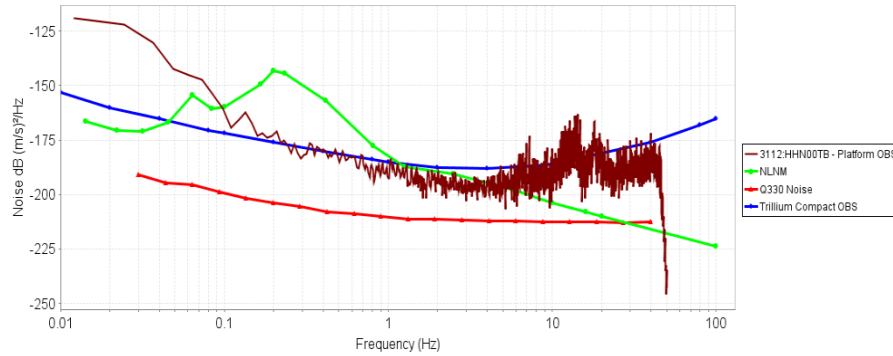
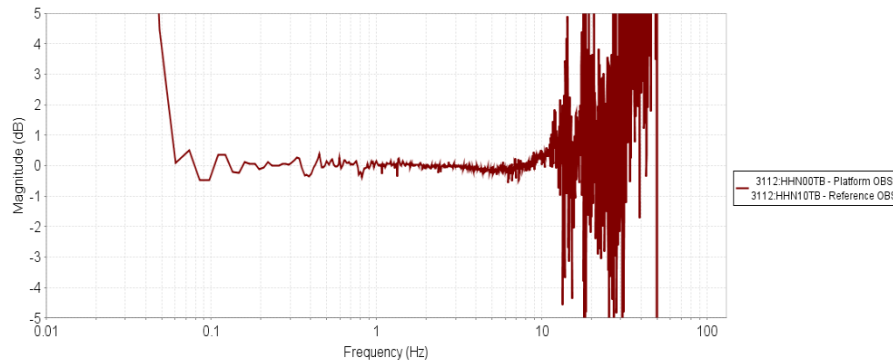


Figure 48 Dry Platform Testing, Transfer Function, North Coherence



**Figure 49 Dry Platform Testing, Transfer Function, North Incoherent Noise**



**Figure 50 Dry Platform Testing, Transfer Function, North Magnitude Response**

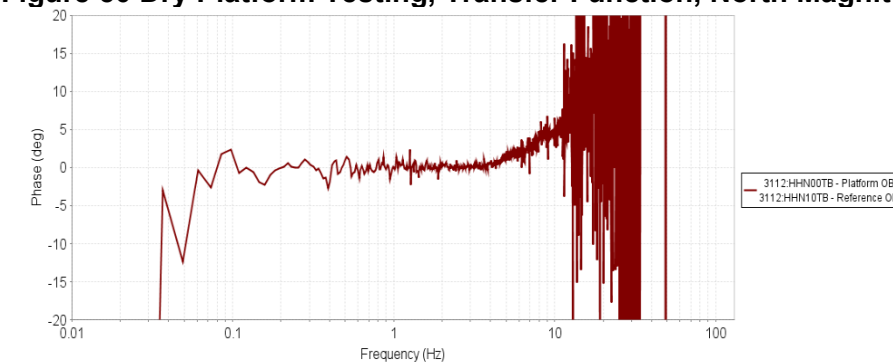


**Figure 51 Dry Platform Testing, Transfer Function, North Phase Response**

We see that the north channels have good coherence between approximately 0.1 and 10 Hz for this event. Beyond those bounds, the coherence decreases rapidly. There is no appreciable difference in the amplitude and phase response over that passband to the limits of the available spectral resolution.

### 3.2.1.3 East

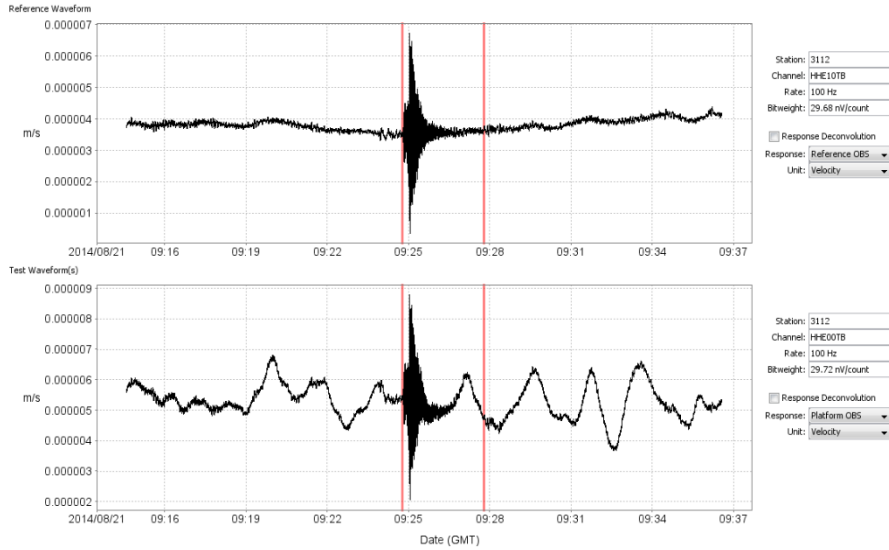


Figure 52 Dry Platform Testing, Transfer Function, East Waveforms

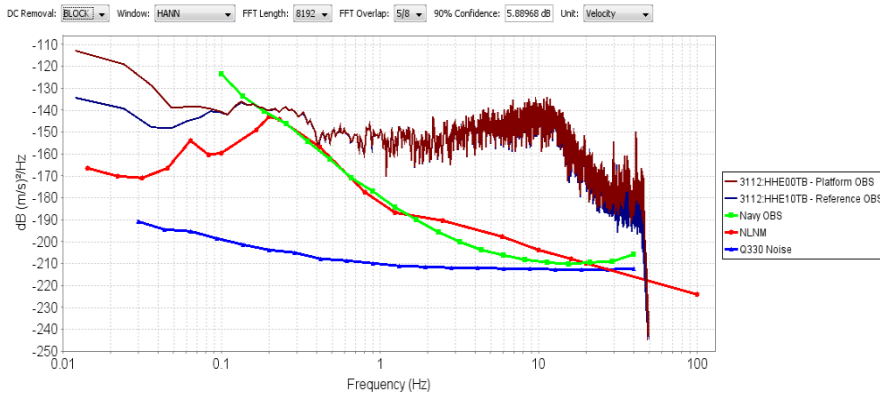


Figure 53 Dry Platform Testing, Transfer Function, East Power Spectra

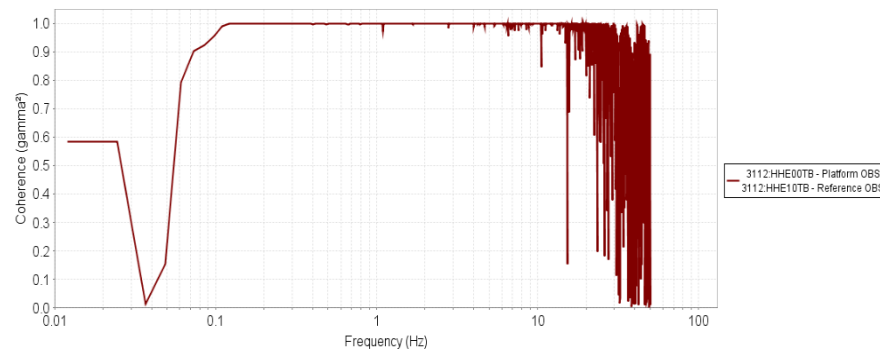
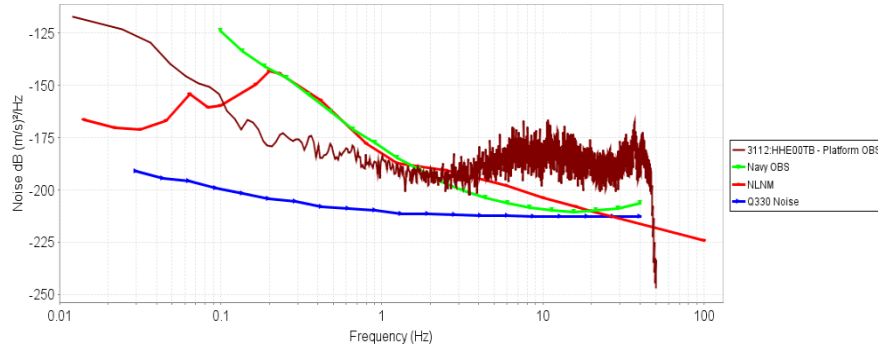
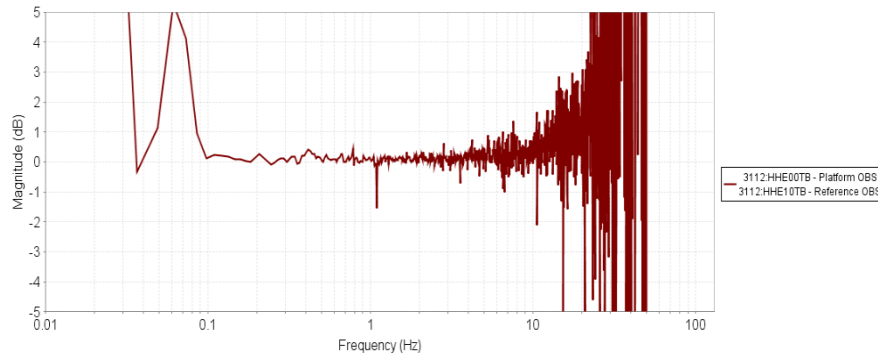


Figure 54 Dry Platform Testing, Transfer Function, East Coherence



**Figure 55 Dry Platform Testing, Transfer Function, East Incoherent Noise**



**Figure 56 Dry Platform Testing, Transfer Function, East Magnitude Response**

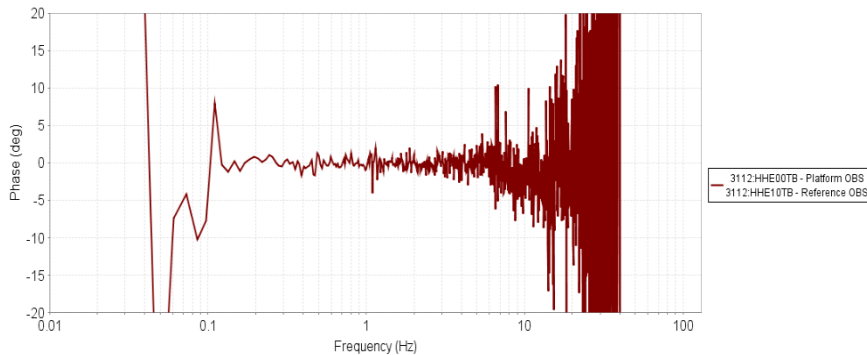


**Figure 57 Dry Platform Testing, Transfer Function, East Phase Response**

We see that the east channels have good coherence between approximately 0.12 and 10 Hz. Beyond those bounds, the coherence decreases rapidly. There is no appreciable difference in the amplitude and phase response over that passband to the limits of the available spectral resolution.

### 3.2.2 *Geophone*

Analysis of the test data will examine coherence between the Trillium Compact OBS and the Navy Geophone OBS on the Underwater Platform. Incoherent noise is “lumped” on to the Navy OBS. Test data was collected for this test on August 21, 2014 from 00:10 to 18:28 (GMT).

A single candidate event was identified at approximately 09:25 with duration of 3 minutes and frequency content above the site noise at frequencies above 0.5 Hz.

The waveform time series, power spectra, coherence, incoherent noise, relative magnitude, and relative phase for each of the Vertical, North, and East channels are shown below.

### 3.2.2.1 Vertical

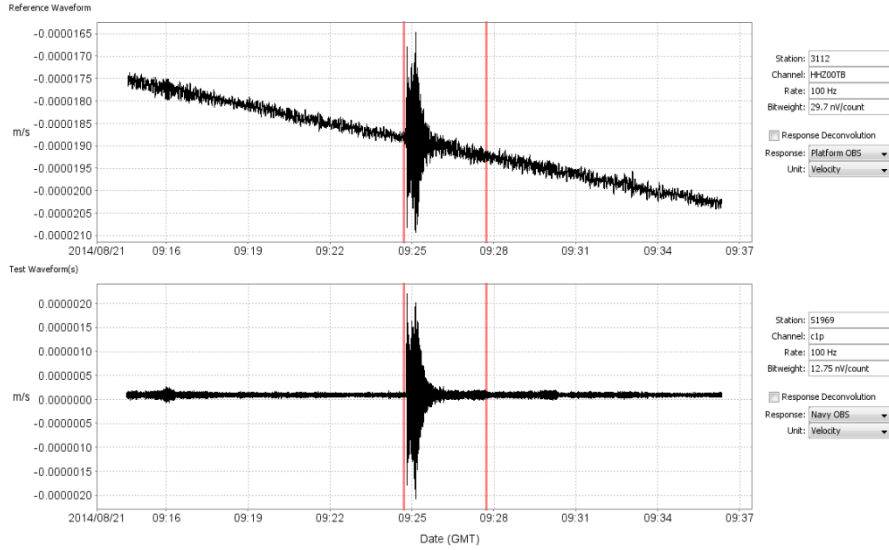


**Figure 58 Dry Platform Testing, Geophone, Vertical Waveforms**

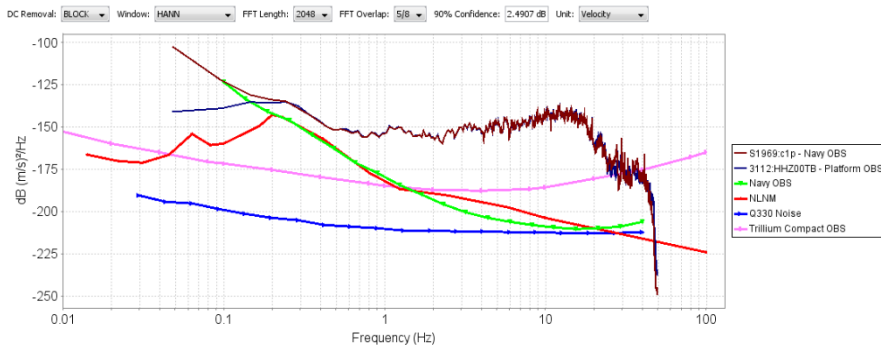


**Figure 59 Dry Platform Testing, Geophone, Vertical Power Spectra**

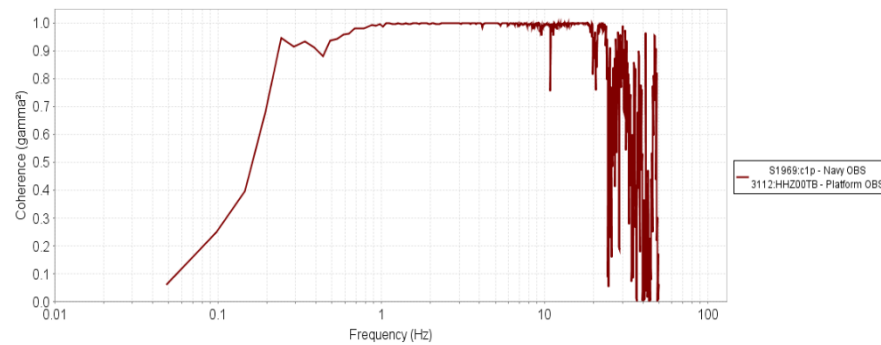


**Figure 60 Dry Platform Testing, Geophone, Vertical Coherence**

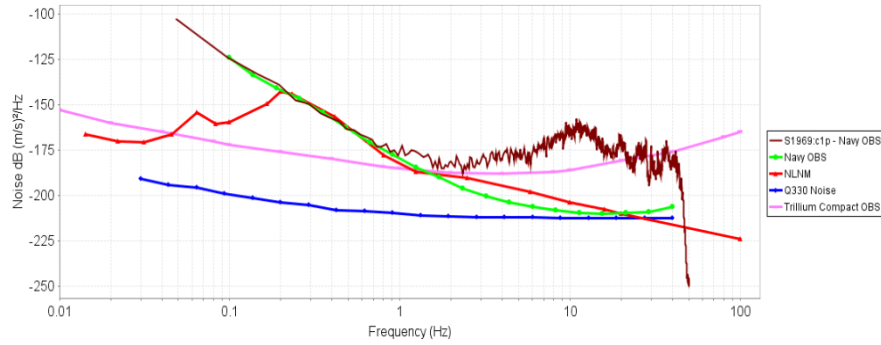


**Figure 61 Dry Platform Testing, Geophone, Vertical Incoherent Noise**

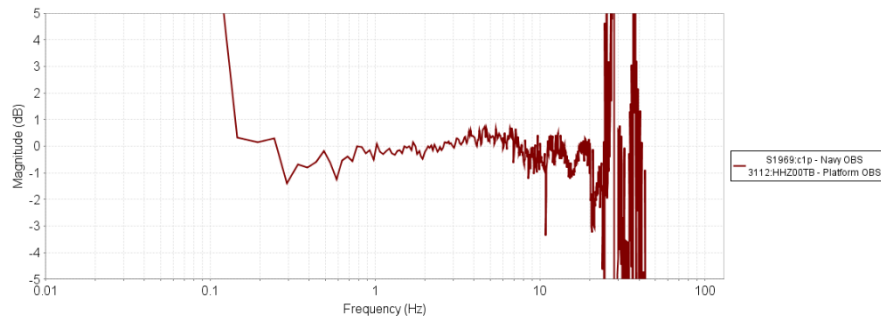


**Figure 62 Dry Platform Testing, Geophone, Vertical Magnitude Response**

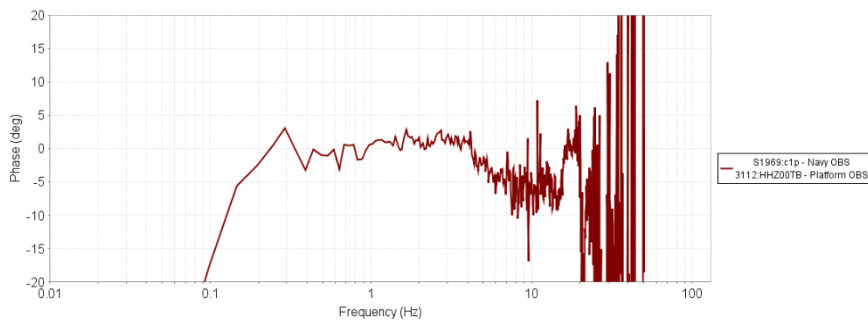


**Figure 63 Dry Platform Testing, Geophone, Vertical Phase Response**

We see that the vertical channels have good coherence between approximately 1.0 and 20 Hz for this event. Beyond those bounds, the coherence degrades rapidly. The magnitude and phase response are observed to deviate between +1/-1 dB and +5/-10 degrees, respectively, over that passband to the limits of the available spectral resolution.

### 3.2.2.2 North

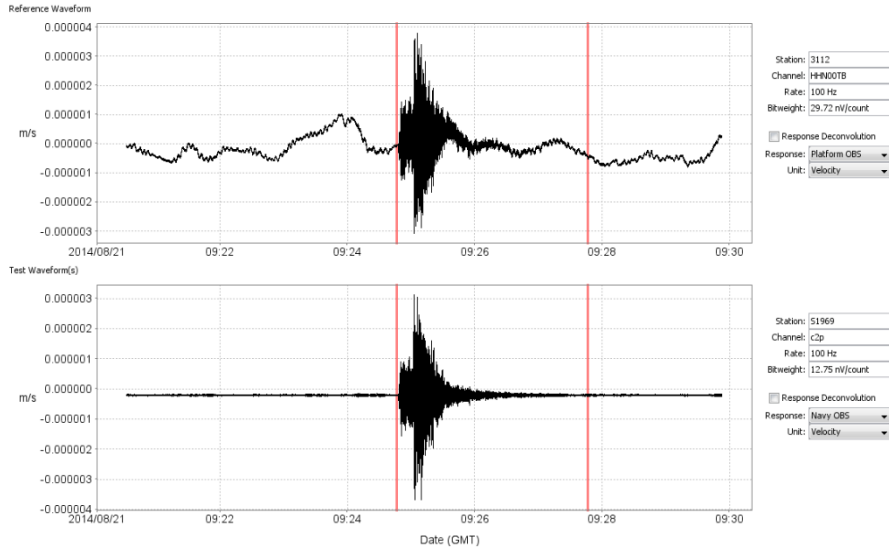


Figure 64 Dry Platform Testing, Geophone, North Waveforms

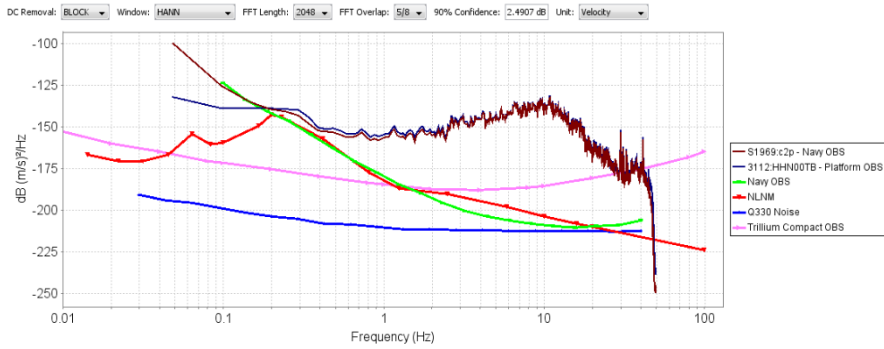


Figure 65 Dry Platform Testing, Geophone, North Power Spectra

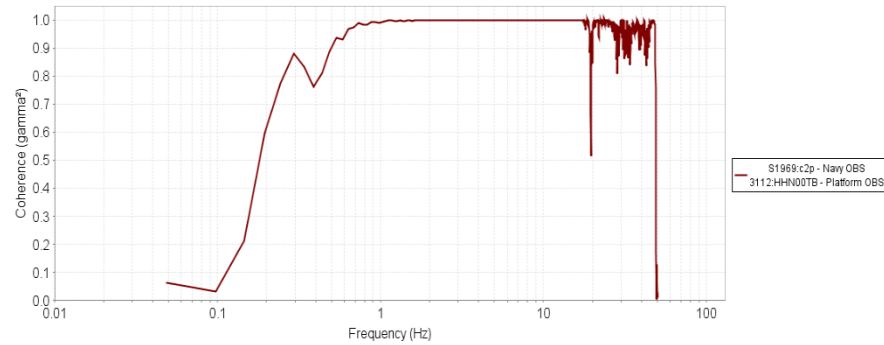
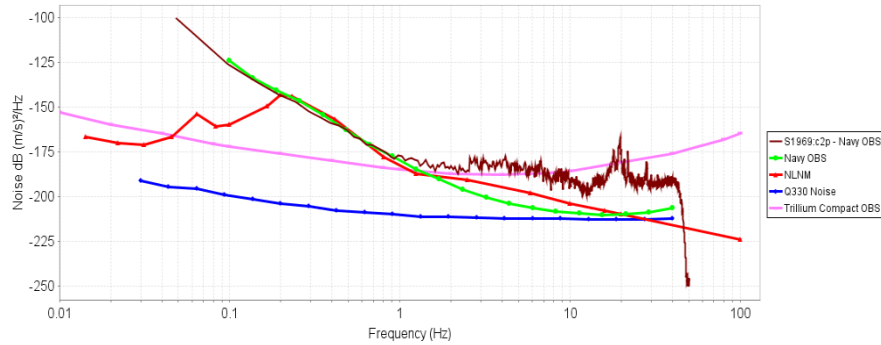
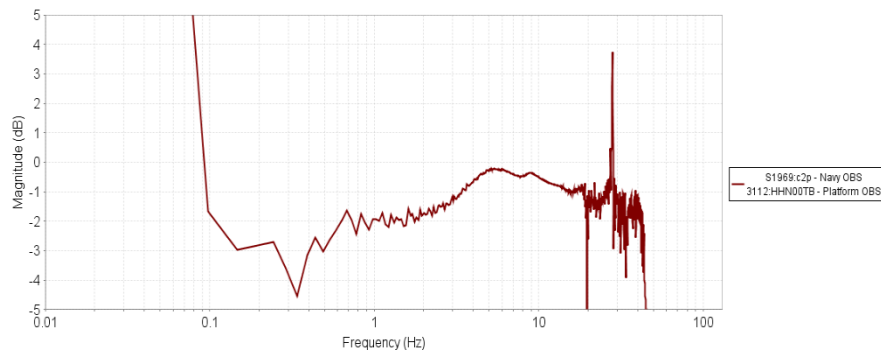


Figure 66 Dry Platform Testing, Geophone, North Coherence



**Figure 67 Dry Platform Testing, Geophone, North Incoherent Noise**



**Figure 68 Dry Platform Testing, Geophone, North Magnitude Response**

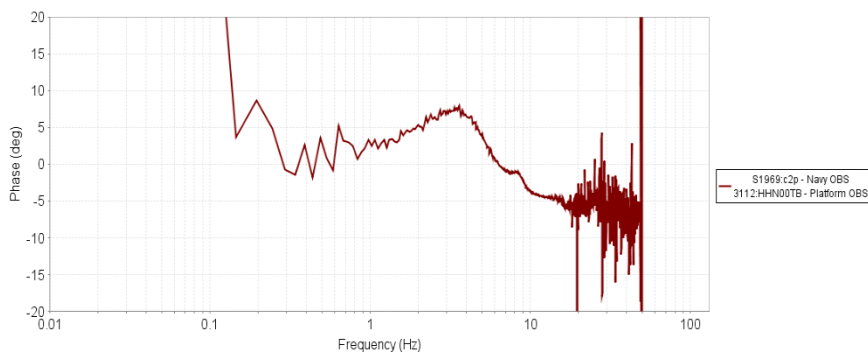


**Figure 69 Dry Platform Testing, Geophone, North Phase Response**

We see that the north channels have good coherence between approximately 0.7 and 18 Hz for this event. Beyond those bounds, the coherence decreases rapidly. The magnitude and phase response are observed to deviate between  $+0/-2.5$  dB and  $+8/-5$  degrees, respectively, over that passband to the limits of the available spectral resolution. The magnitude and phase response both have an observed transition at approximately 3 – 5 Hz, likely due to the complicated response function of the Navy OBS having multiple geophones connected in series.

### 3.2.2.3 East

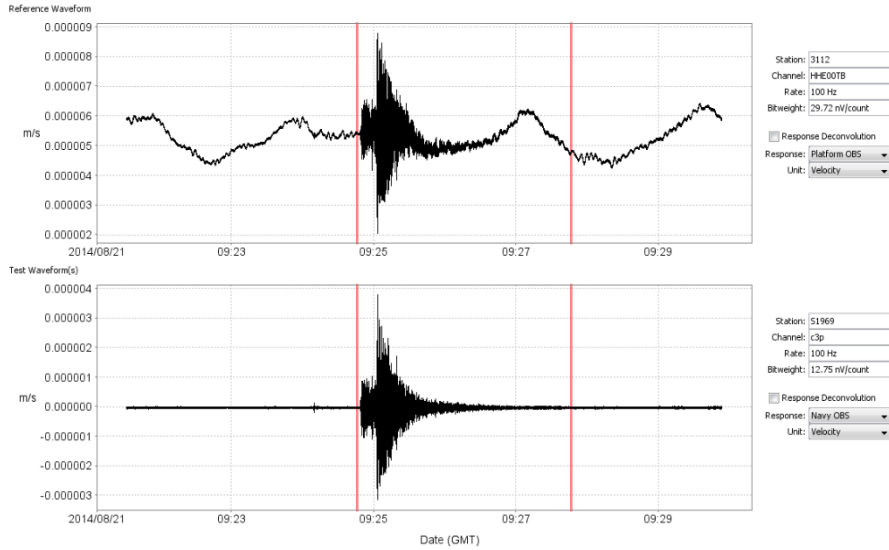


Figure 70 Dry Platform Testing, Geophone, East Waveforms

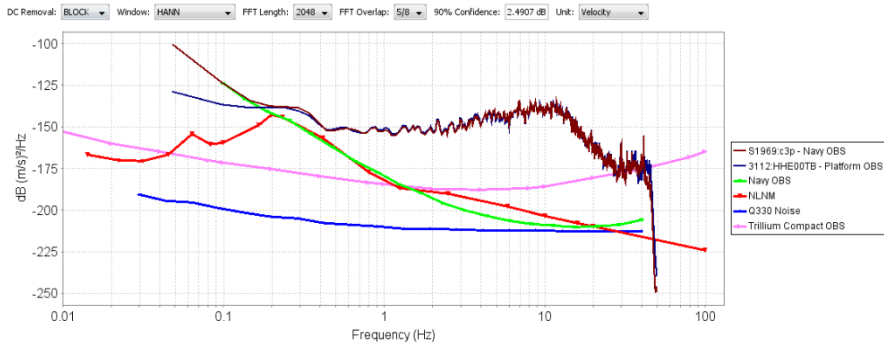


Figure 71 Dry Platform Testing, Geophone, East Power Spectra

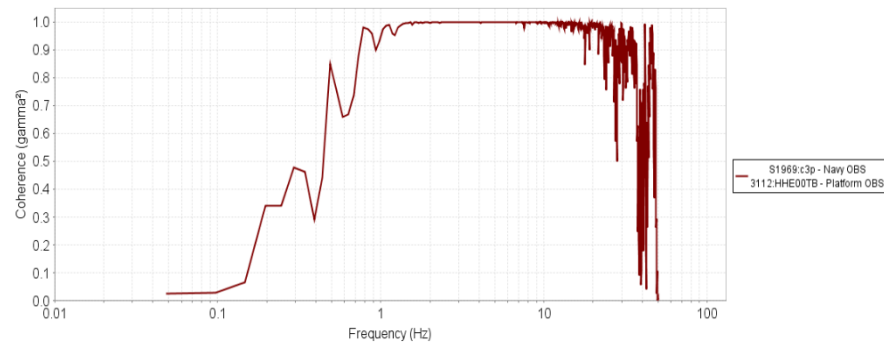
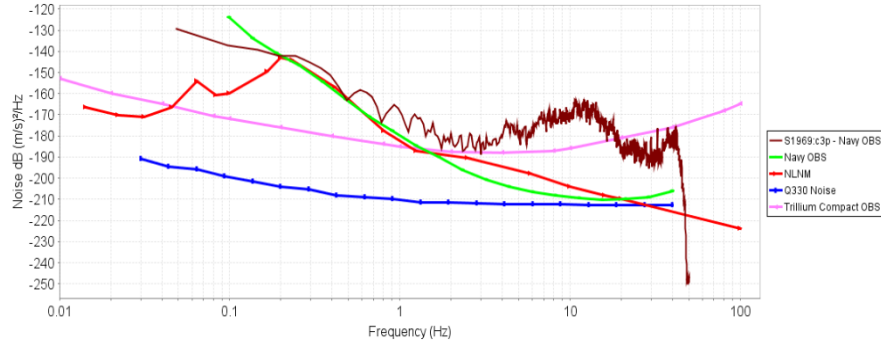
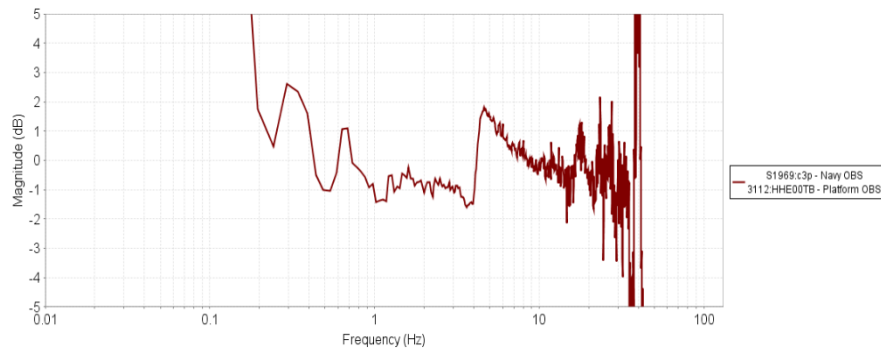


Figure 72 Dry Platform Testing, Geophone, East Coherence



**Figure 73 Dry Platform Testing, Geophone, East Incoherent Noise**



**Figure 74 Dry Platform Testing, Geophone, East Magnitude Response**

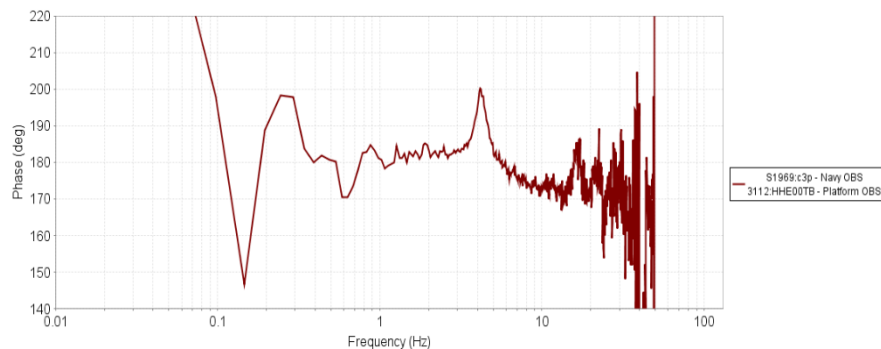


**Figure 75 Dry Platform Testing, Geophone, East Phase Response**

We see that the east channels have good coherence between approximately 1.5 and 15 Hz. Beyond those bounds, the coherence decreases rapidly. The magnitude and phase response are observed to deviate between  $\pm 2$  dB and  $\pm 20$  degrees, respectively, over that passband to the limits of the available spectral resolution. The magnitude and phase response both have an abrupt transition at approximately 4 Hz, likely due to the complicated response function of the Navy OBS having multiple geophones connected in series. Note from the phase response plot it appears that the east channel of the Navy OBS is connected with reverse polarity.

### 3.2.3 *Cross-Axis Coupling*

The cross-axis coupling will be evaluated by examining the coherence between the pairs of axis on each of the sensors in the test using the Sleemen 3-channel coherence technique. Changes in the cross-axis coupling across the varying test conditions will be compared. For this analysis 2 hours of background on August 21, 2014 from 07:00 – 09:00 GMT was used.

The power spectra and coherence are shown below for each of reference, Trillium OBS platform, and Navy OBS platform channels. Two plots were generated for each of the sensors: The first with a long window length for low frequencies below 0.1 Hz and the second with a short window length for high frequencies above 0.1 Hz.

The reference Trillium OBS directly coupled to the bottom of the Test Pool appears to have a slight increase in coupling between the horizontal channels at frequencies below 0.02 Hz. Otherwise, the axes do not appear to have any significant coherence.

The platform Trillium OBS also has a slight increase in horizontal axes coupling at frequencies below 0.01 Hz. Otherwise, the axes do not appear to have any significant coherence.

The platform Navy OBS does not have a similar increase in horizontal axes coupling. However, the observed frequency band in which coupling is occurring is so far outside of the Navy OBS low frequency corner at 4 Hz that it would not be expected to.

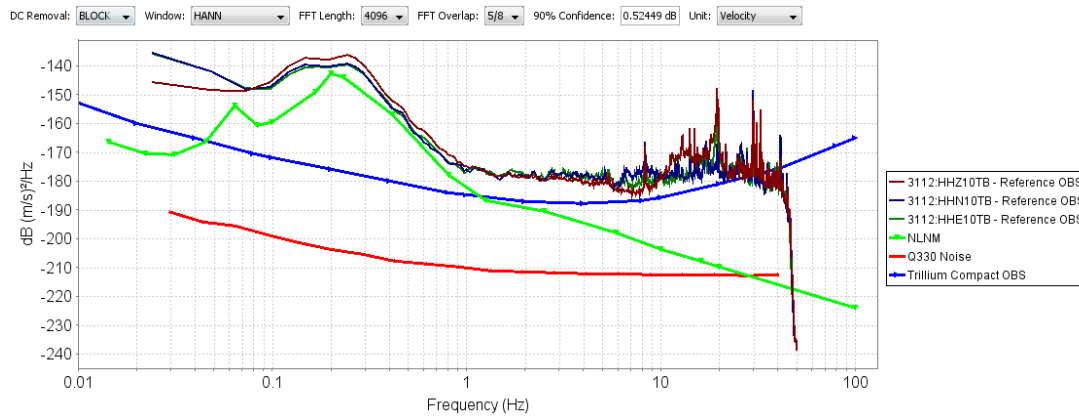
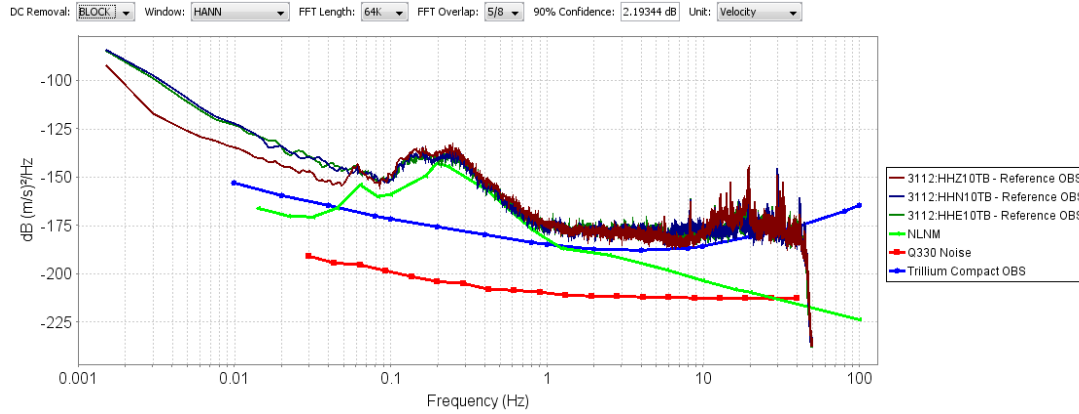


**Figure 76 Dry Platform, Cross-Axis Coupling, Reference Power Spectra**

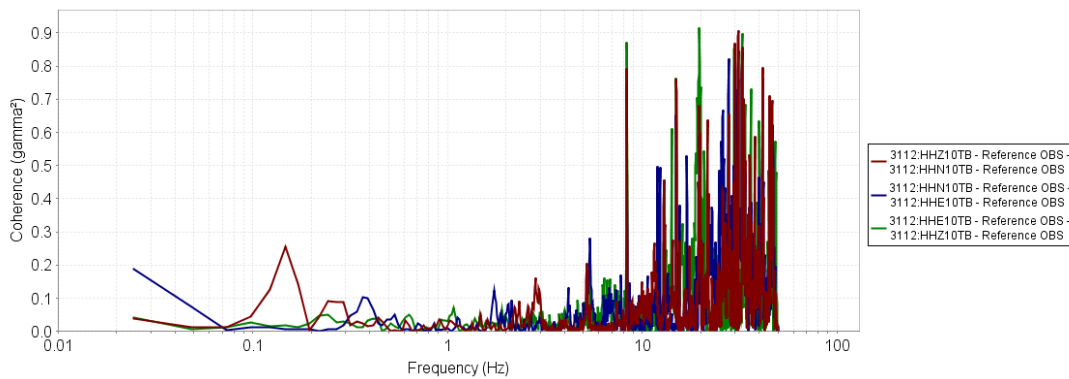
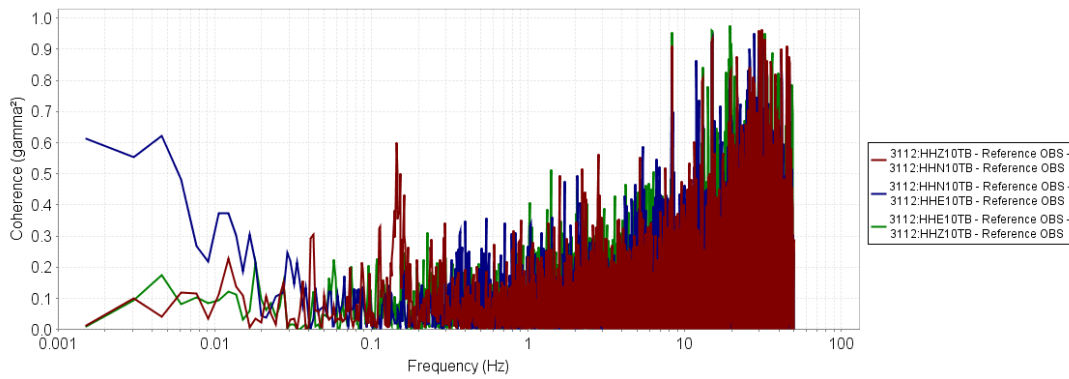


**Figure 77 Dry Platform, Cross-Axis Coupling, Reference Coherence**

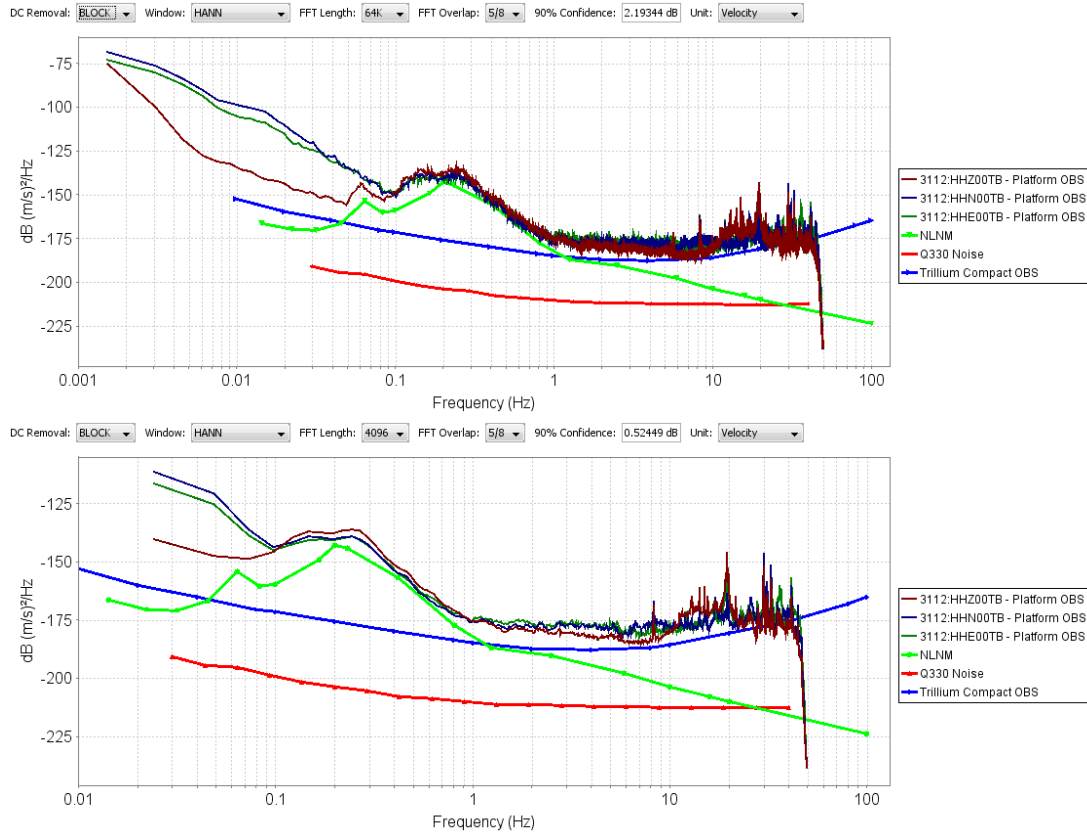


**Figure 78 Dry Platform, Cross-Axis Coupling, Trillium OBS Platform Power Spectra**

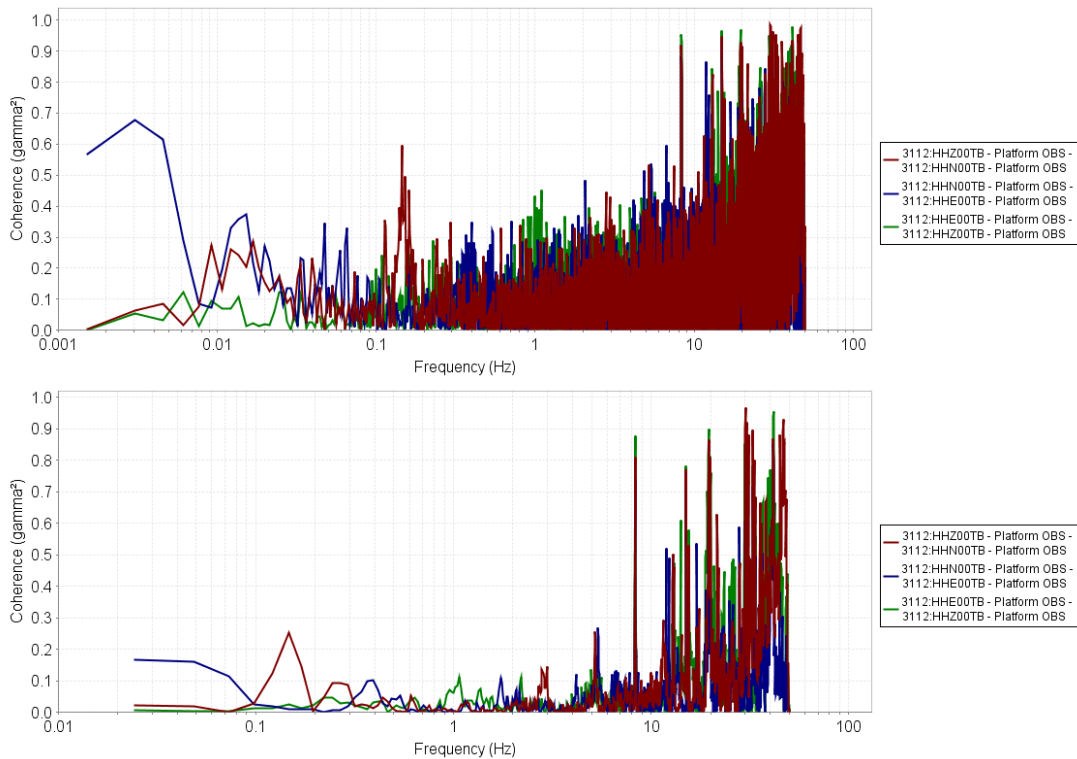


**Figure 79 Dry Platform, Cross-Axis Coupling, Trillium OBS Platform Coherence**

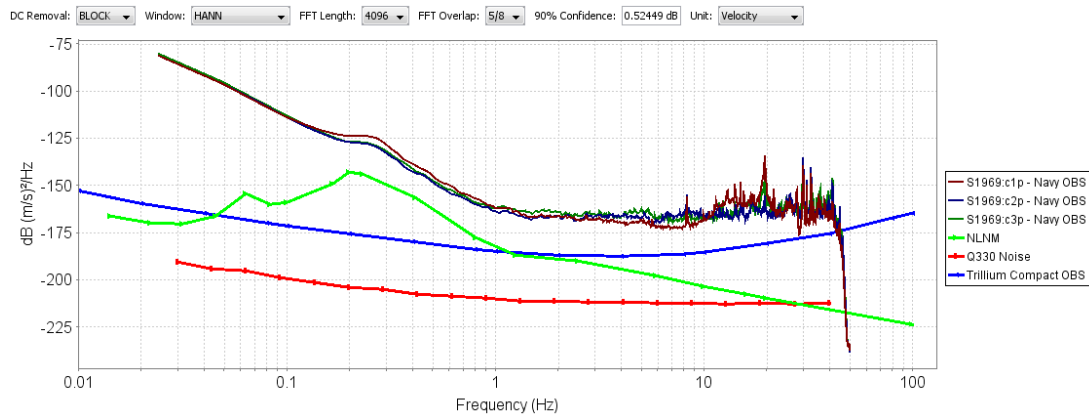
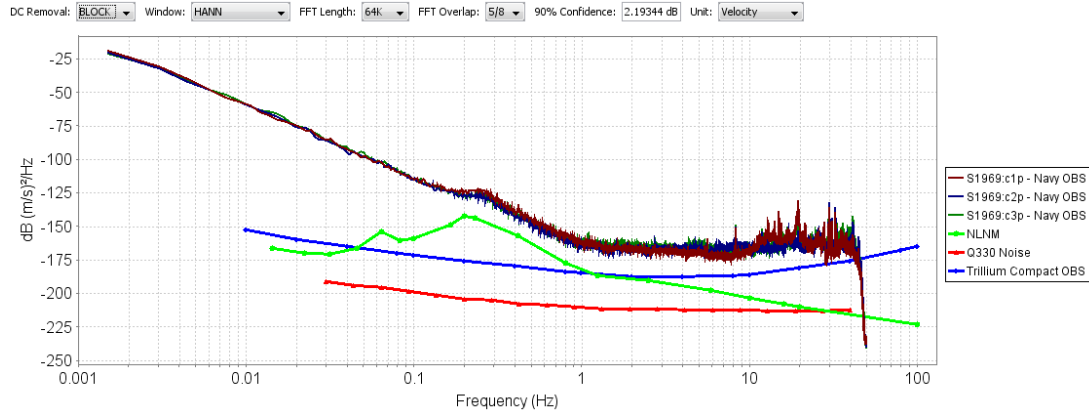


**Figure 80 Dry Platform, Cross-Axis Coupling, Navy OBS Platform Power Spectra**

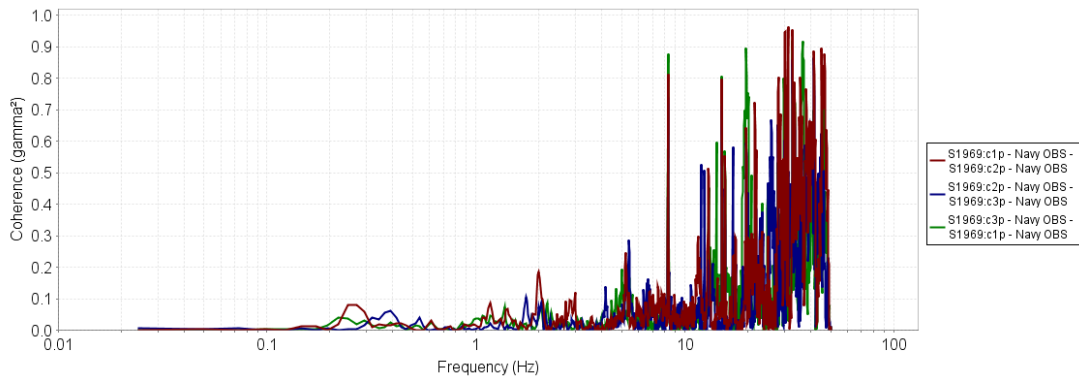
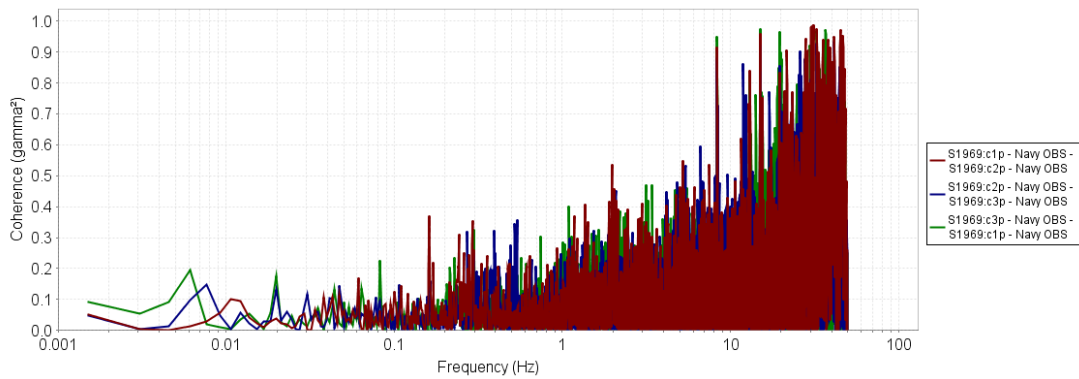


**Figure 81 Dry Platform, Cross-Axis Coupling, Navy OBS Platform Coherence**

### 3.3 Wet Platform Testing

The wet platform test was performed with both the reference Nanometrics Trillium OBS (#3033) and the Underwater Platform in direct contact with the bottom of the Test Pool. The Test Pool is filled with water; however, there is no seafloor material added to the Test Pool. The results of this test will be used to comment on any affect that the Underwater Platform in the presence of water has on the transfer function between the Nanometrics OBS reference sensor (#3033) and the Nanometrics OBS on the underwater platform (#3034). In addition, a comparison will be made between the performance of the Nanometrics OBS (#3034) and the Navy OBS, both of which are on the Underwater Platform.

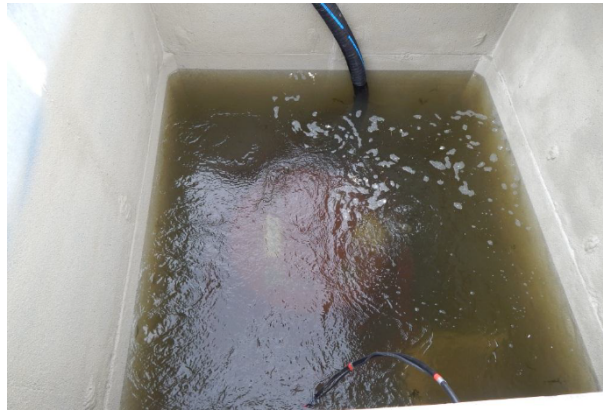


Figure 82 Wet Platform Photo

IV&V 5c Wet Underwater Platform Testing  
(no simulated seafloor)

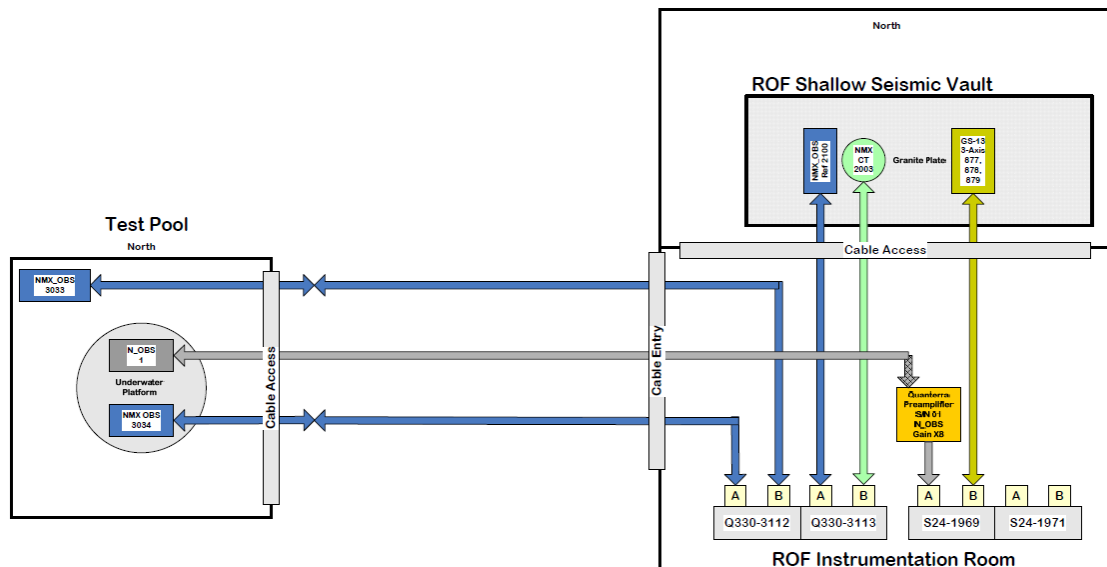


Figure 83 Wet Platform Testing Diagram (RPKromer Consulting)

### 3.3.1 Transfer Function

Analysis of the test data will examine coherence between the reference OBS and the OBS on the Underwater Platform in order to establish the transfer function between the two sensors. Incoherent noise is “lumped” on to the Platform OBS. Test data was collected for this test from August 24, 2014 to September 2, 2014.

Two candidate events were identified for this analysis: One for low frequencies and one for high frequencies.

#### 3.3.1.1 Low Frequency

The low frequency event has duration of approximately 1 hour and frequency content above the site noise at frequencies below 2 Hz at approximately 10:25 GMT on August 25, 2014.

Coherence analysis for this event was performed for each of the Vertical, North, and East channels of the reference OBS and the OBS on the Underwater Platform.

##### 3.3.1.1.1 Vertical

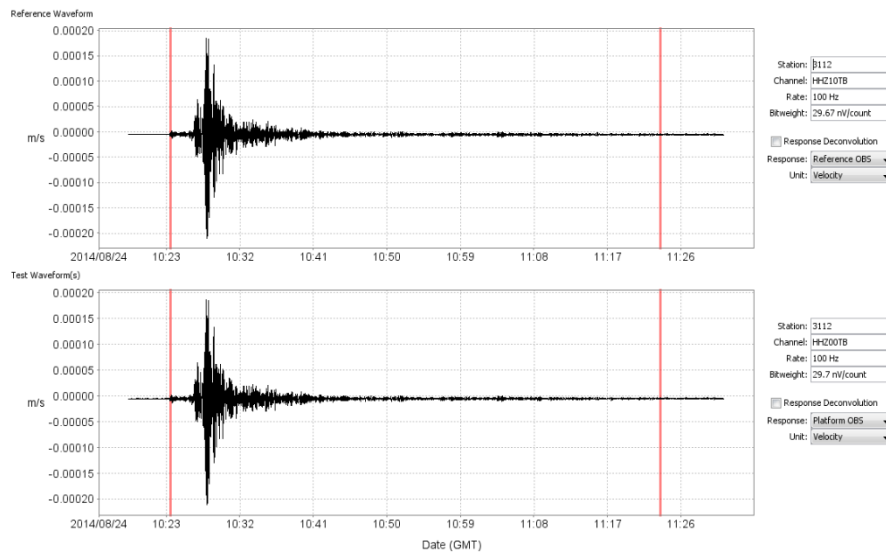


Figure 84 Wet Platform, Transfer Function, Low Frequency, Vertical Waveforms

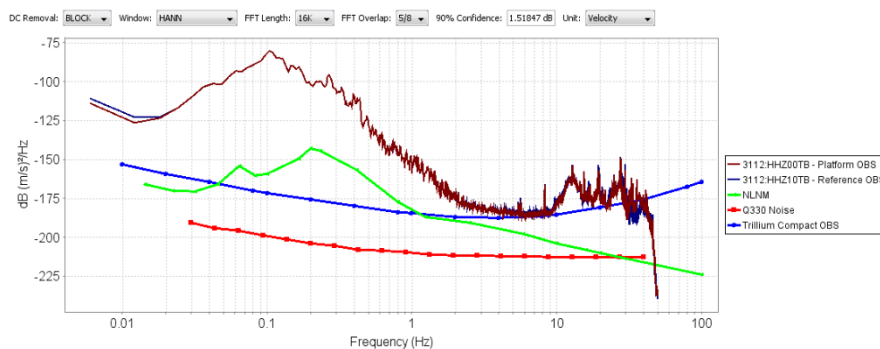
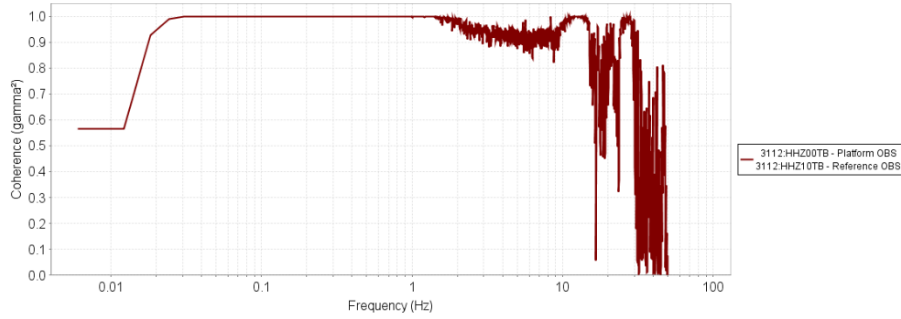
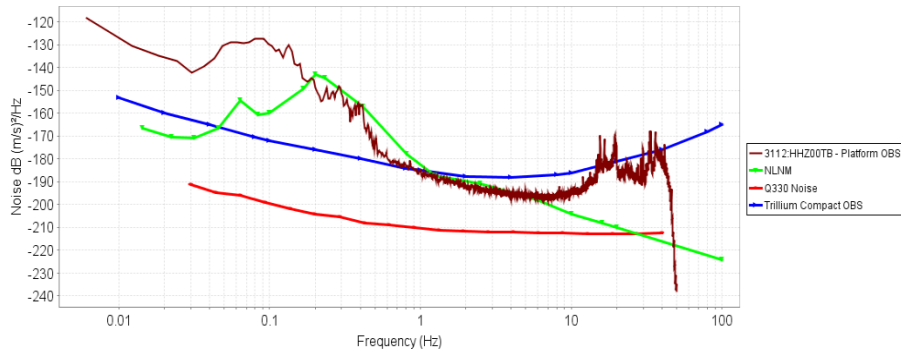


Figure 85 Wet Platform, Transfer Function, Low Frequency, Vertical Power Spectra



**Figure 86 Wet Platform, Transfer Function, Low Frequency, Vertical Coherence**



**Figure 87 Wet Platform, Transfer Function, Low Frequency, Vertical Incoherent Noise**

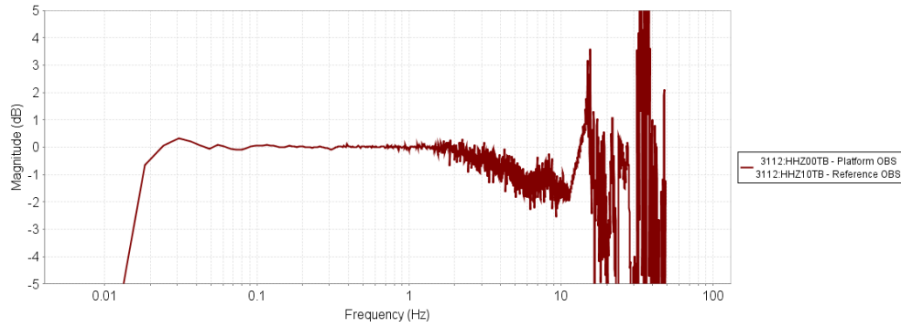


**Figure 88 Wet Platform, Transfer Function, Low Frequency, Vertical Magnitude Response**

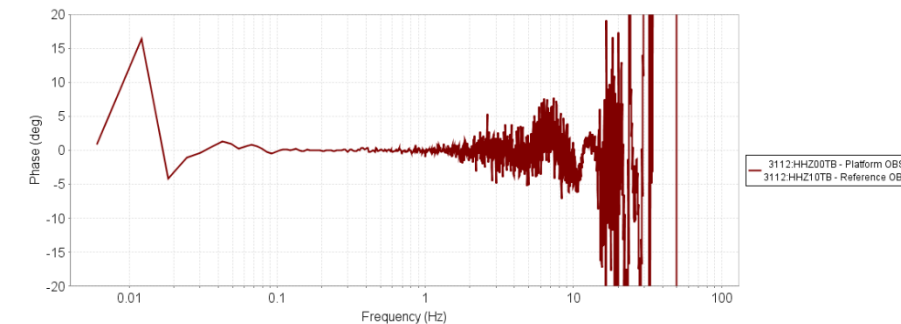


**Figure 89 Wet Platform, Transfer Function, Low Frequency, Vertical Phase Response**

We see that the vertical channels have good coherence between approximately 0.03 and 1.5 Hz for this event. Beyond those bounds, the coherence degrades rapidly as the observed signal amplitudes drop to near the sensor self-noise. There is minimal difference in the amplitude and phase response over that passband to the limits of the available spectral resolution.

### 3.3.1.1.2 North

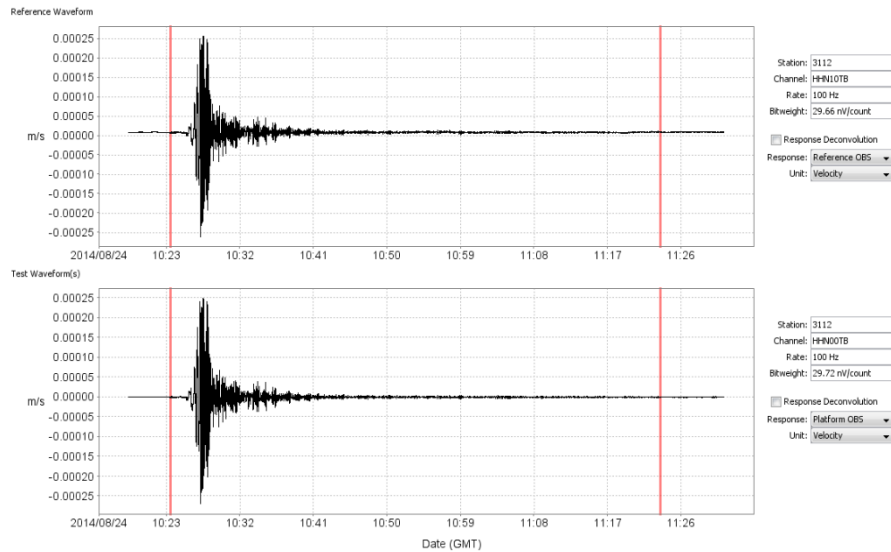


**Figure 90 Wet Platform, Transfer Function, Low Frequency, North Waveforms**

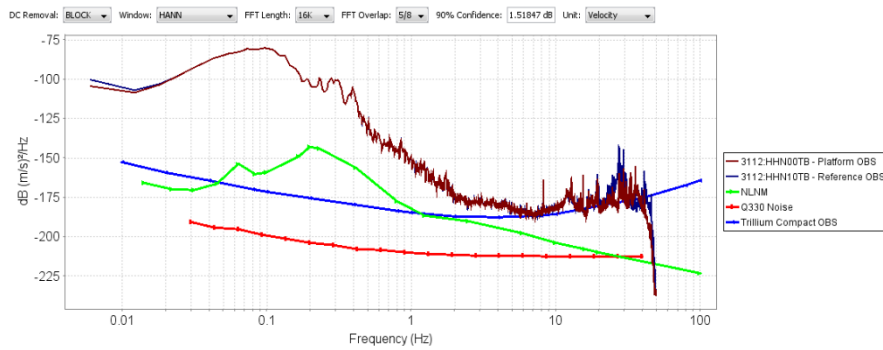


**Figure 91 Wet Platform, Transfer Function, Low Frequency, North Power Spectra**

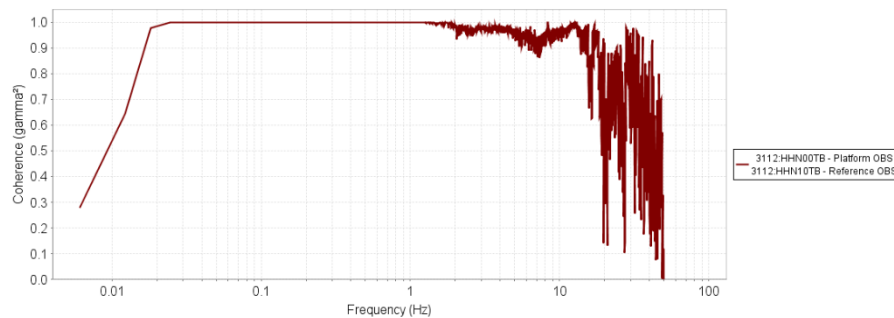


**Figure 92 Wet Platform, Transfer Function, Low Frequency, North Coherence**

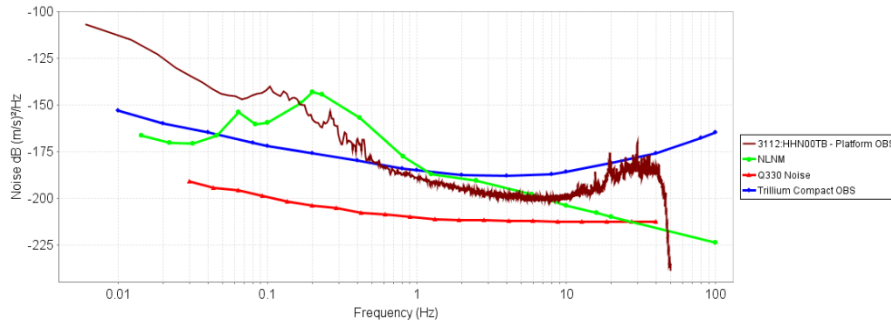


**Figure 93 Wet Platform, Transfer Function, Low Frequency, North Incoherent Noise**

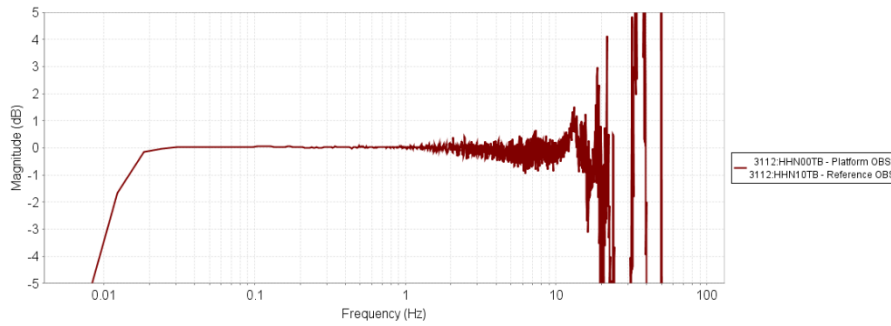


**Figure 94 Wet Platform, Transfer Function, Low Frequency, North Magnitude Response**

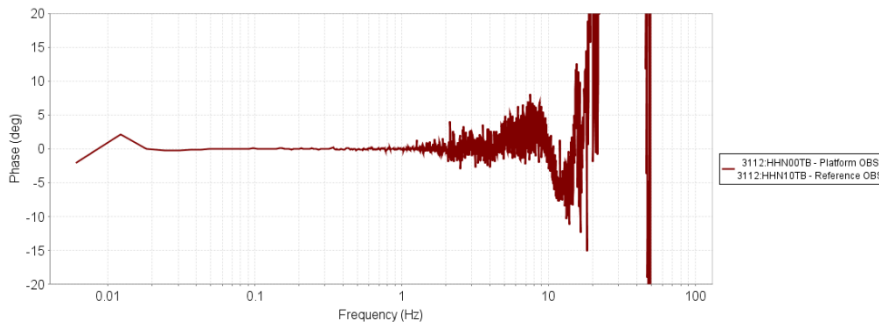


**Figure 95 Wet Platform, Transfer Function, Low Frequency, North Phase Response**

We see that the north channels have good coherence between approximately 0.02 and 1.5 Hz for this event. Beyond those bounds, the coherence decreases rapidly as the observed signal amplitudes drop to near the sensor self-noise. There is no appreciable difference in the amplitude and phase response over that passband to the limits of the available spectral resolution.

### 3.3.1.1.3 East

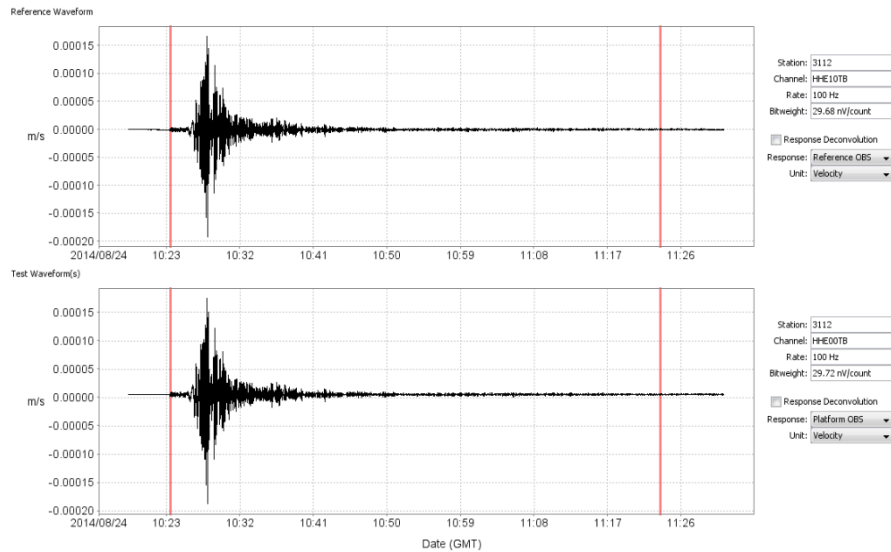


**Figure 96 Wet Platform, Transfer Function, Low Frequency, East Waveforms**

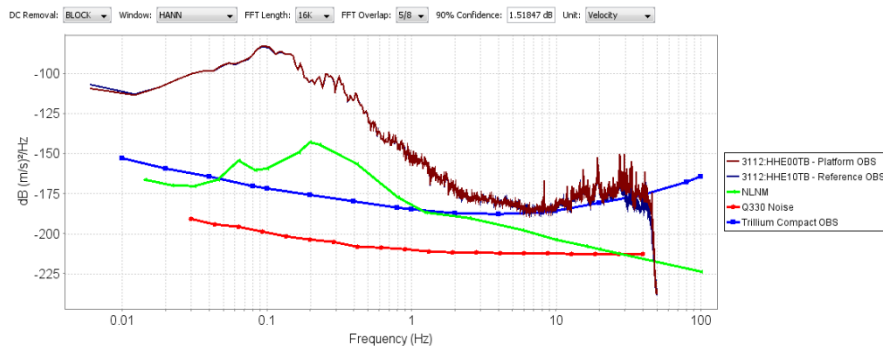


**Figure 97 Wet Platform, Transfer Function, Low Frequency, East Power Spectra**

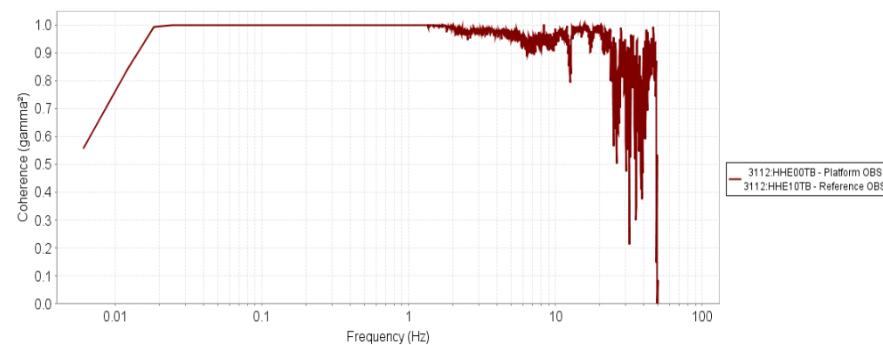


**Figure 98 Wet Platform, Transfer Function, Low Frequency, East Coherence**

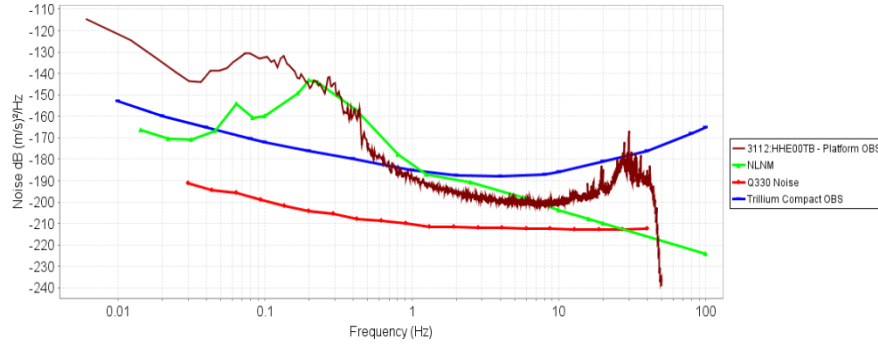


**Figure 99 Wet Platform, Transfer Function, Low Frequency, East Incoherent Noise**

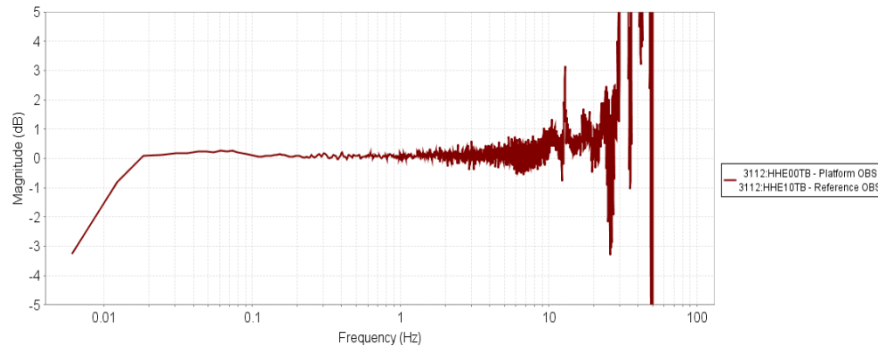


**Figure 100 Wet Platform, Transfer Function, Low Frequency, East Magnitude Response**

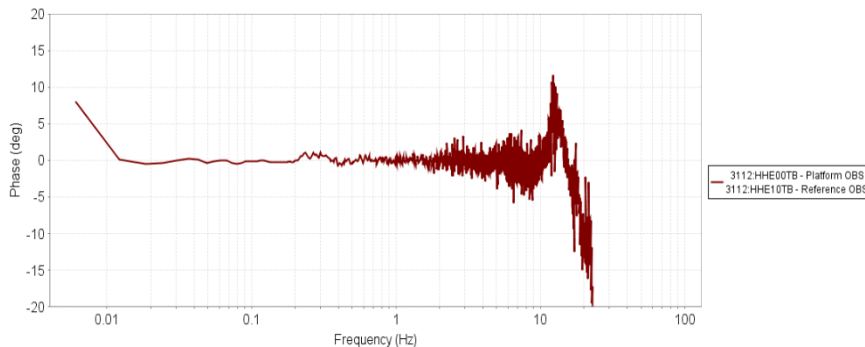


**Figure 101 Wet Platform, Transfer Function, Low Frequency, East Phase Response**

We see that the east channels have good coherence between approximately 0.02 and 1.5 Hz. Beyond those bounds, the coherence decreases rapidly as the observed signal amplitudes drop to near the sensor self-noise. There is no appreciable difference in the amplitude and phase response over that passband to the limits of the available spectral resolution.

### 3.3.1.2 High Frequency

The high frequency event has duration of approximately 2 minutes and frequency content above the site noise at frequencies above 0.2 Hz at approximately 20:10 GMT on August 30, 2014.

Coherence analysis for this event was performed for each of the Vertical, North, and East channels of the reference OBS and the OBS on the Underwater Platform.

#### 3.3.1.2.1 Vertical

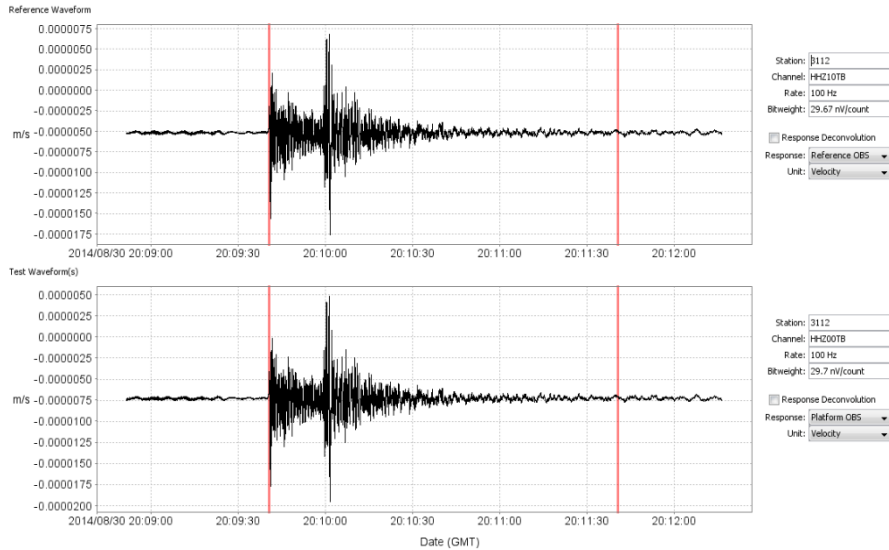


Figure 102 Wet Platform, Transfer Function, High Frequency, Vertical Waveforms

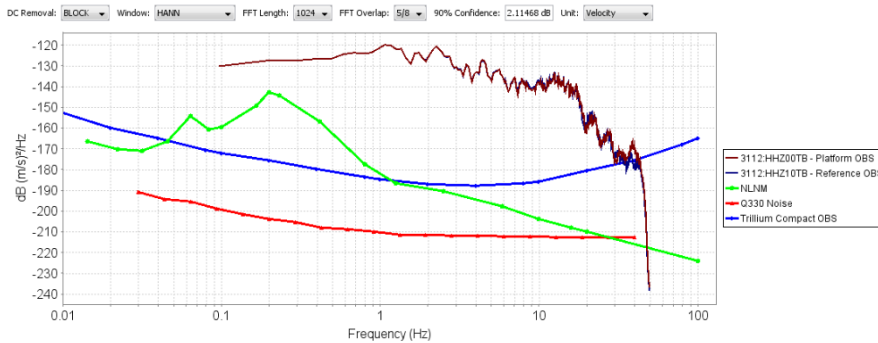


Figure 103 Wet Platform, Transfer Function, High Frequency, Vertical Power Spectra

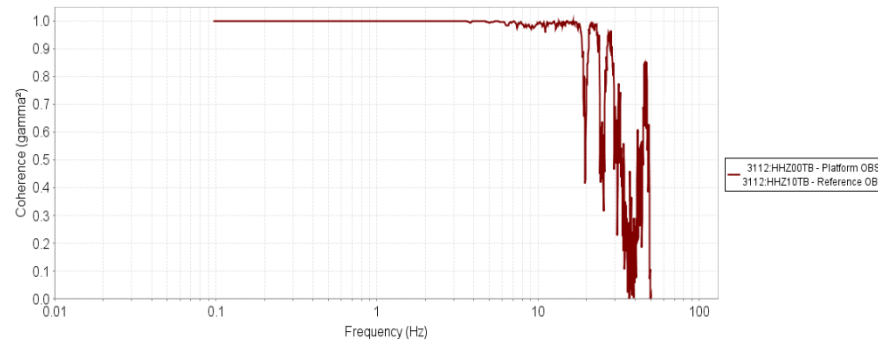
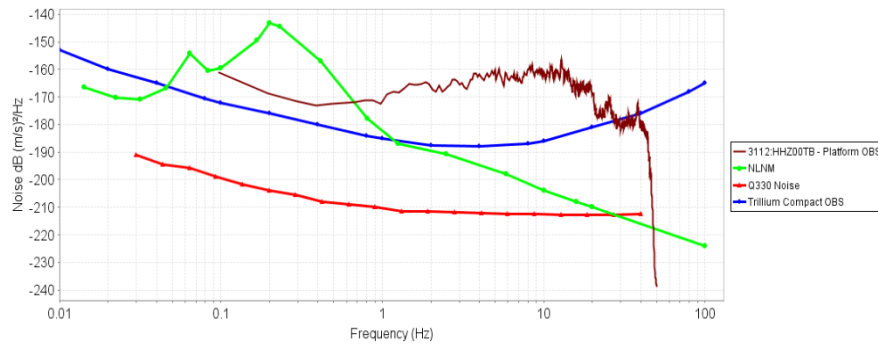
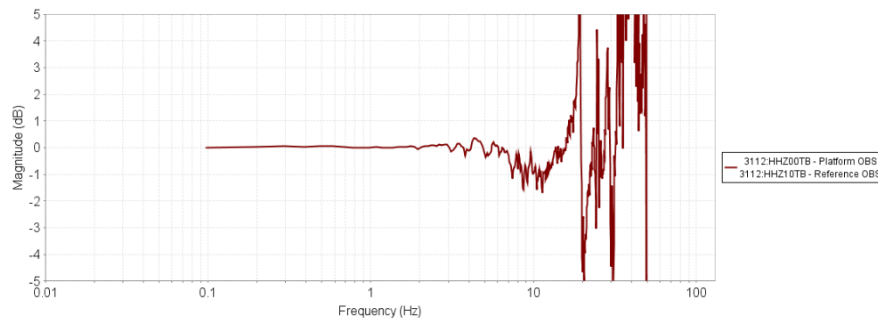


Figure 104 Wet Platform, Transfer Function, High Frequency, Vertical Coherence



**Figure 105 Wet Platform, Transfer Function, High Frequency, Vertical Incoherent Noise**



**Figure 106 Wet Platform, Transfer Function, High Frequency, Vertical Magnitude Response**

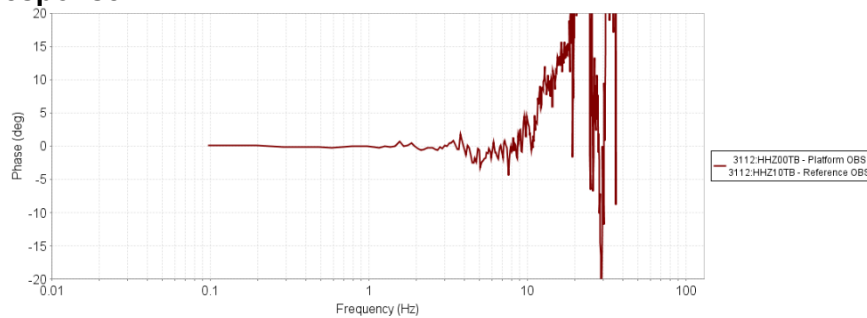


**Figure 107 Wet Platform, Transfer Function, High Frequency, Vertical Phase Response**

We see that the vertical channels have good coherence between approximately 0.2 and 15 Hz for this event. Beyond those bounds, the coherence degrades rapidly. There is minimal difference in the amplitude and phase response over that passband to the limits of the available spectral resolution.

### 3.3.1.2.2 North

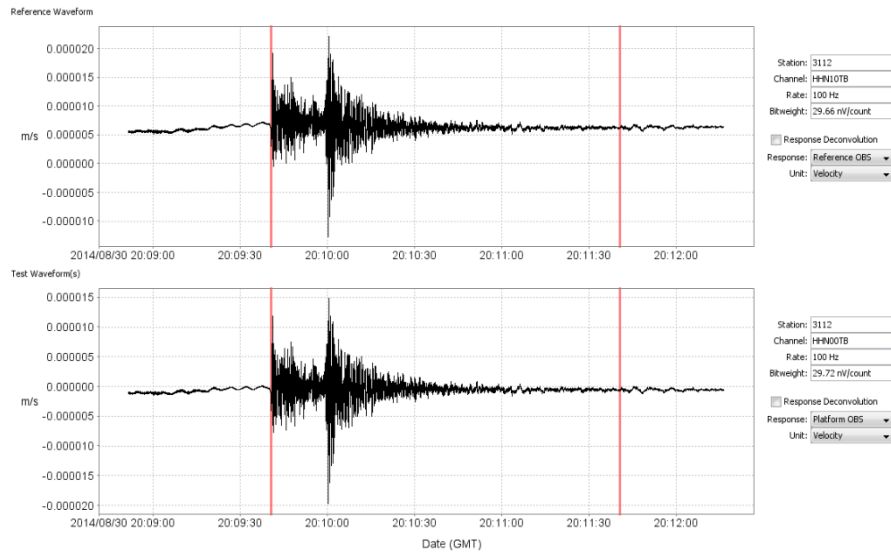


**Figure 108 Wet Platform, Transfer Function, High Frequency, North Waveforms**

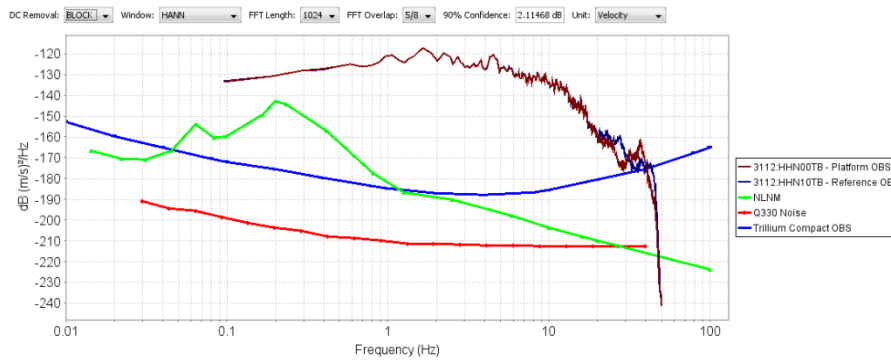


**Figure 109 Wet Platform, Transfer Function, High Frequency, North Power Spectra**

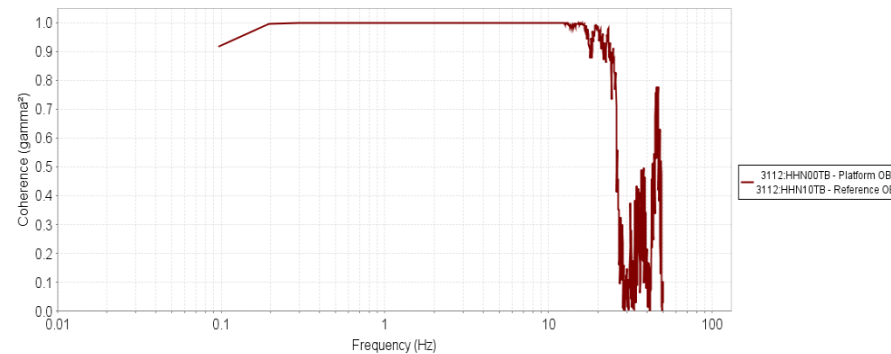


**Figure 110 Wet Platform, Transfer Function, High Frequency, North Coherence**

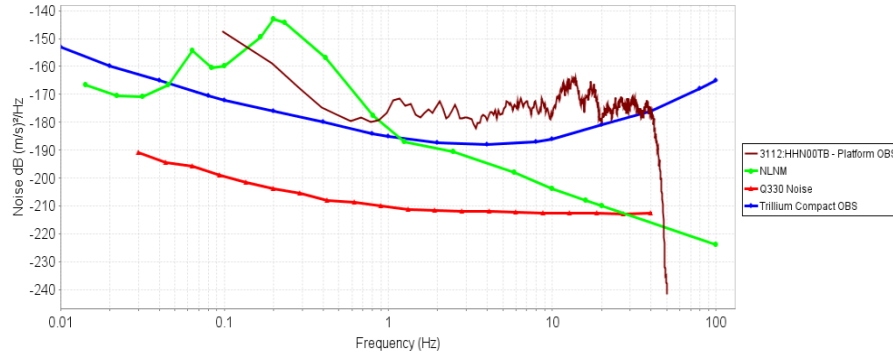


**Figure 111 Wet Platform, Transfer Function, High Frequency, North Incoherent Noise**

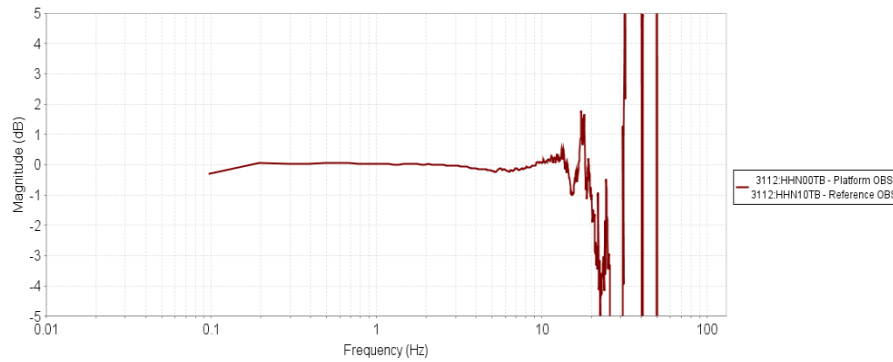


**Figure 112 Wet Platform, Transfer Function, High Frequency, North Magnitude Response**

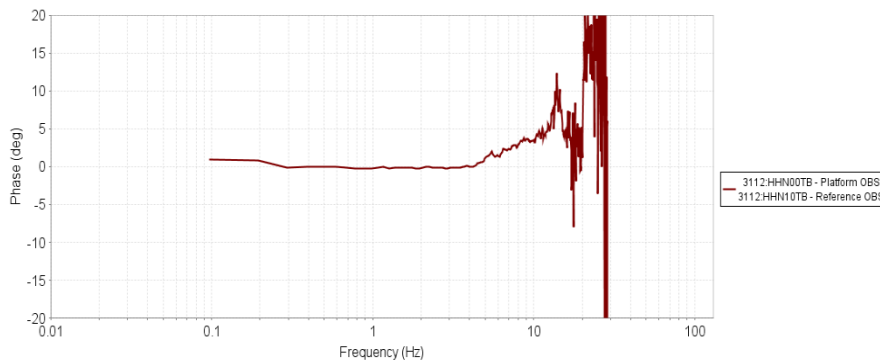


**Figure 113 Wet Platform, Transfer Function, High Frequency, North Phase Response**

We see that the north channels have good coherence between approximately 0.2 and 15 Hz for this event. Beyond those bounds, the coherence decreases rapidly. There is no appreciable difference in the amplitude and phase response over that passband to the limits of the available spectral resolution.

### 3.3.1.2.3 East

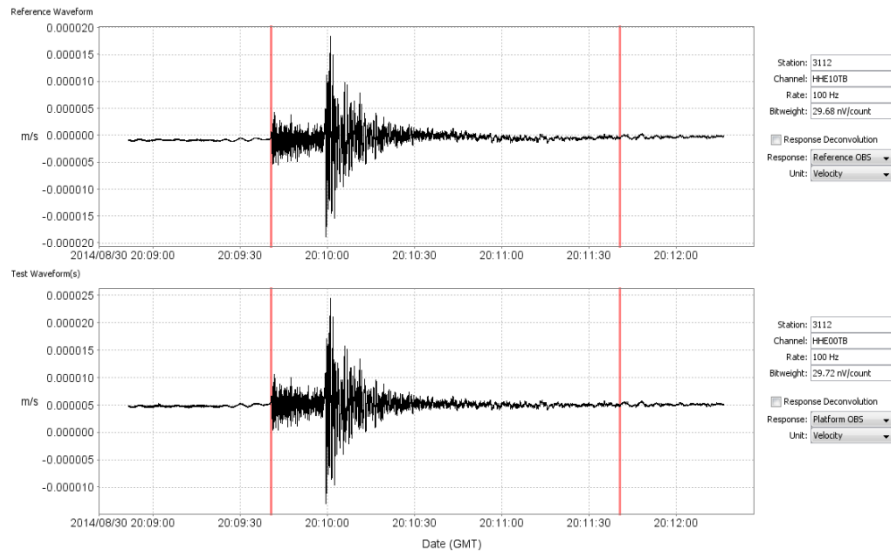


Figure 114 Wet Platform, Transfer Function, High Frequency, East Waveforms

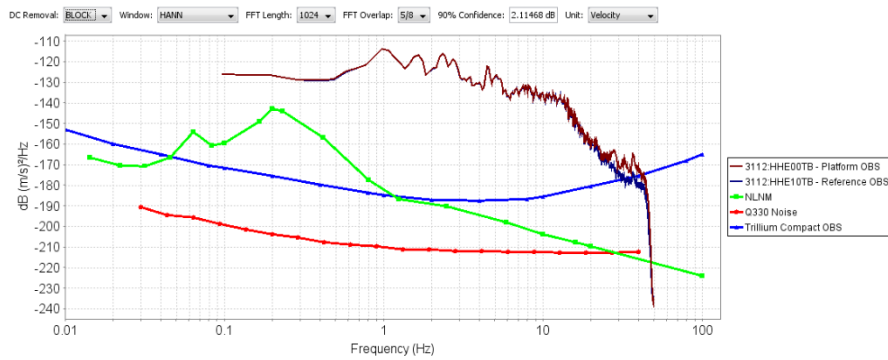


Figure 115 Wet Platform, Transfer Function, High Frequency, East Power Spectra

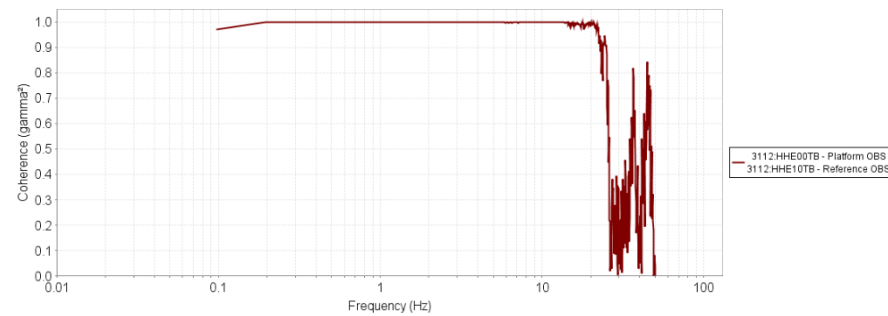
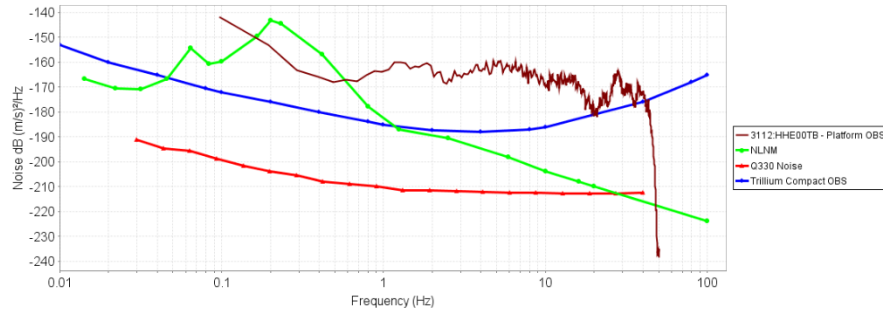
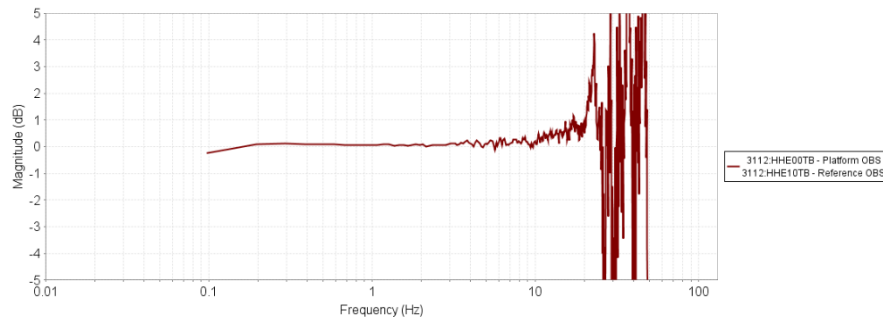


Figure 116 Wet Platform, Transfer Function, High Frequency, East Coherence



**Figure 117 Wet Platform, Transfer Function, High Frequency, East Incoherent Noise**



**Figure 118 Wet Platform, Transfer Function, High Frequency, East Magnitude Response**

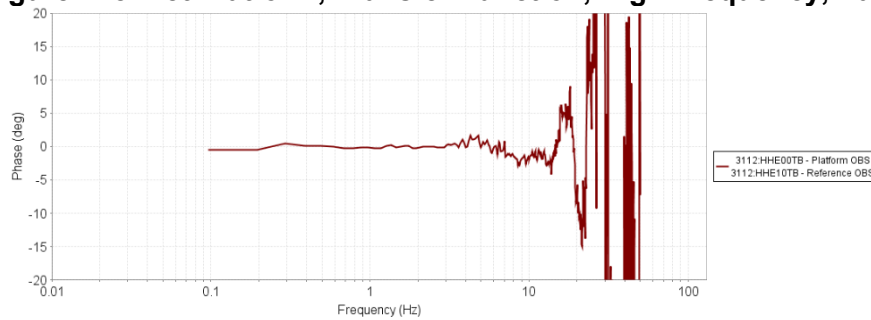


**Figure 119 Wet Platform, Transfer Function, High Frequency, East Phase Response**

We see that the east channels have good coherence between approximately 0.2 and 20 Hz. Beyond those bounds, the coherence decreases rapidly. There is no appreciable difference in the amplitude and phase response over that passband to the limits of the available spectral resolution.

### 3.3.2 Geophone

Analysis of the test data will examine coherence between the Trillium Compact OBS and the Navy Geophone OBS on the Underwater Platform. Incoherent noise is “lumped” on to the Navy OBS.

The event has duration of approximately 2 minutes and frequency content above the site noise at frequencies above 0.2 Hz on August 30, 2014 at approximately 20:10 GMT. Examining an event with low frequency content is unnecessary since the noise in the geophone is relatively high at these frequencies.

The waveform time series, power spectra, coherence, incoherent noise, relative magnitude, and relative phase for each of the Vertical, North, and East channels are shown below.

#### 3.3.2.1 Vertical

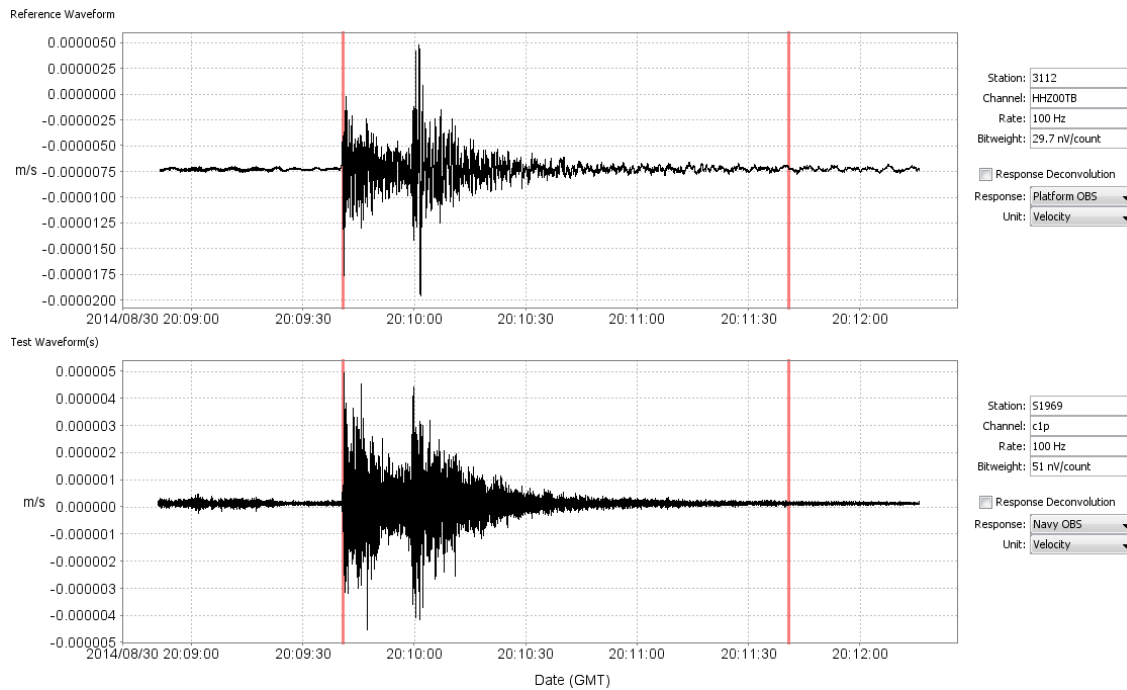


Figure 120 Wet Platform Testing, Geophone, Vertical Waveforms

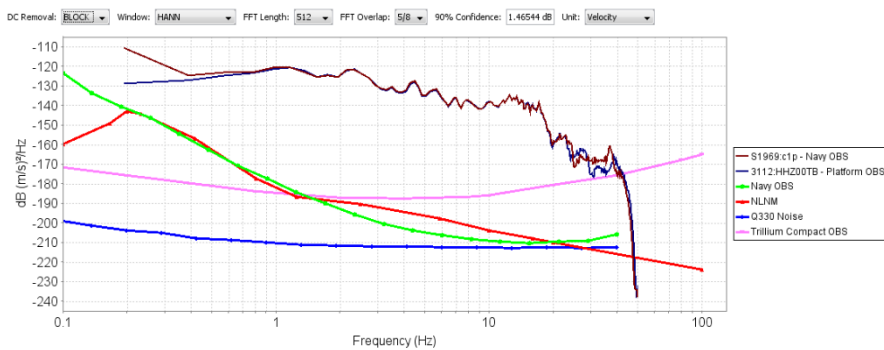
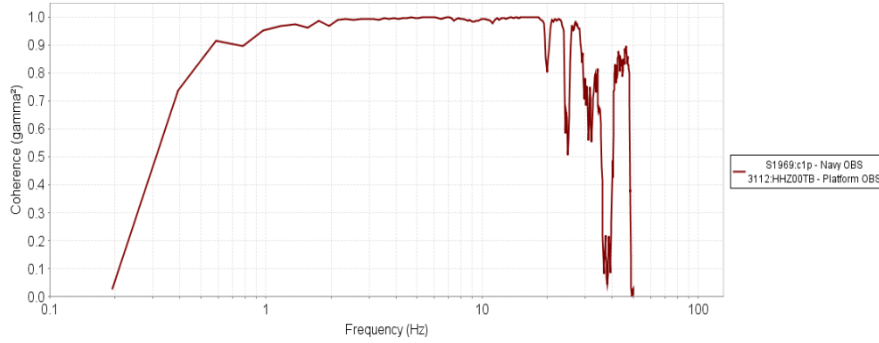
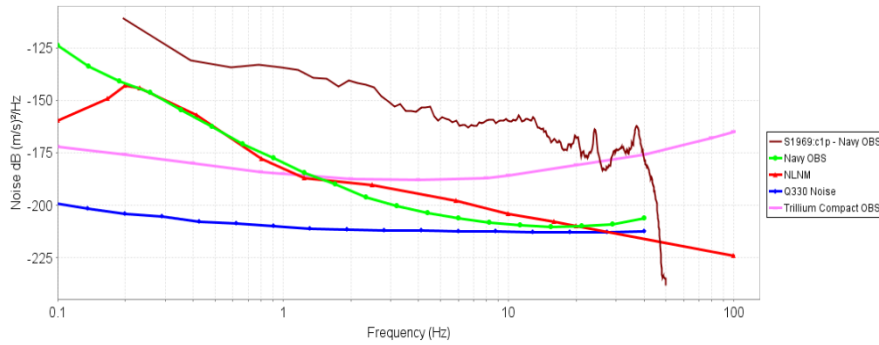


Figure 121 Wet Platform Testing, Geophone, Vertical Power Spectra



**Figure 122 Wet Platform Testing, Geophone, Vertical Coherence**



**Figure 123 Wet Platform Testing, Geophone, Vertical Incoherent Noise**

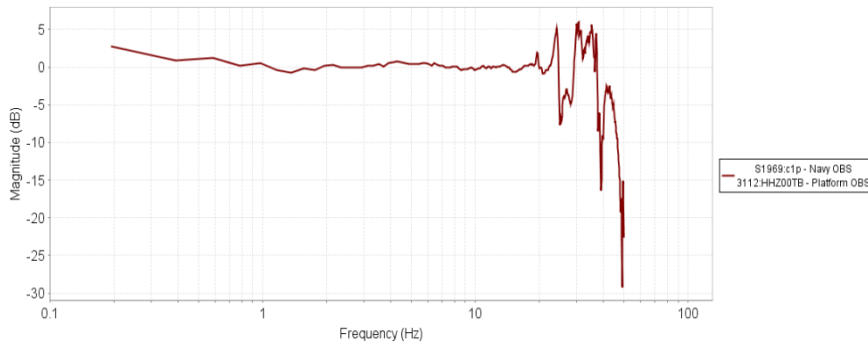


**Figure 124 Wet Platform Testing, Geophone, Vertical Magnitude Response**

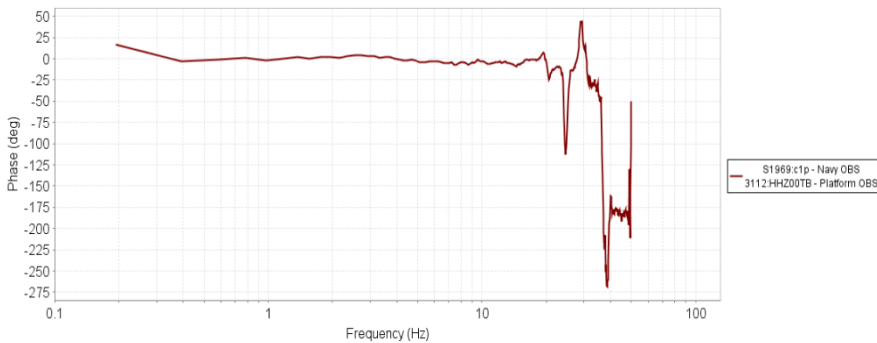


**Figure 125 Wet Platform Testing, Geophone, Vertical Phase Response**

We see that the vertical channels have good coherence between approximately 1.0 and 20 Hz for this event. Beyond those bounds, the coherence degrades rapidly. The magnitude and phase response are observed to deviate between +1/-1 dB and +5/-10 degrees, respectively, over that passband to the limits of the available spectral resolution.

### 3.3.2.2 North

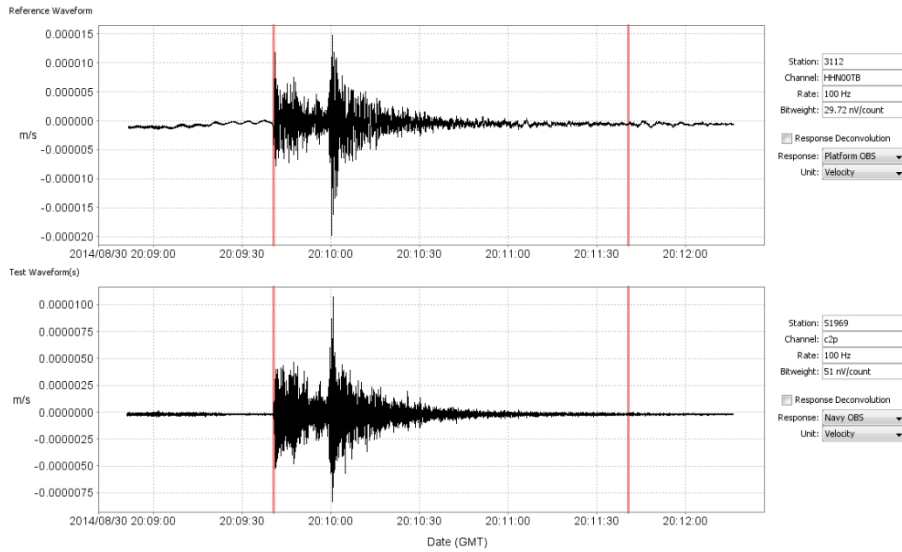


Figure 126 Wet Platform Testing, Geophone, North Waveforms

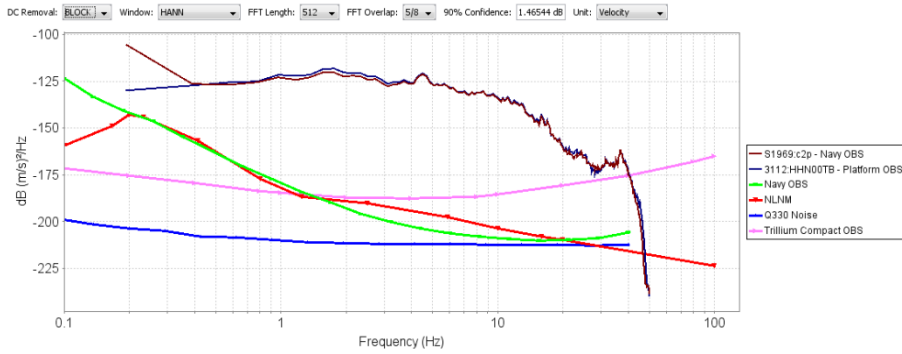


Figure 127 Wet Platform Testing, Geophone, North Power Spectra

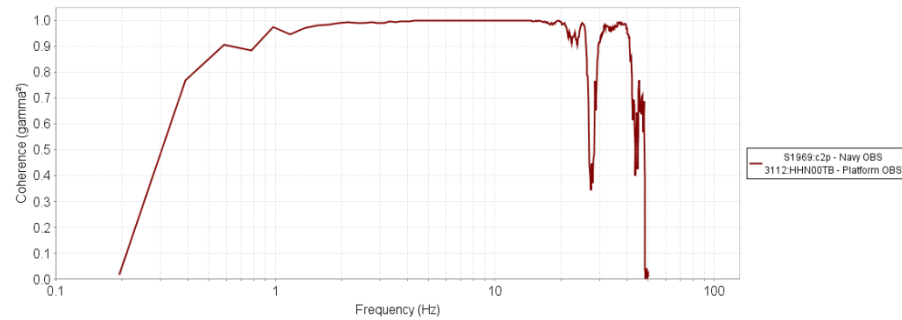
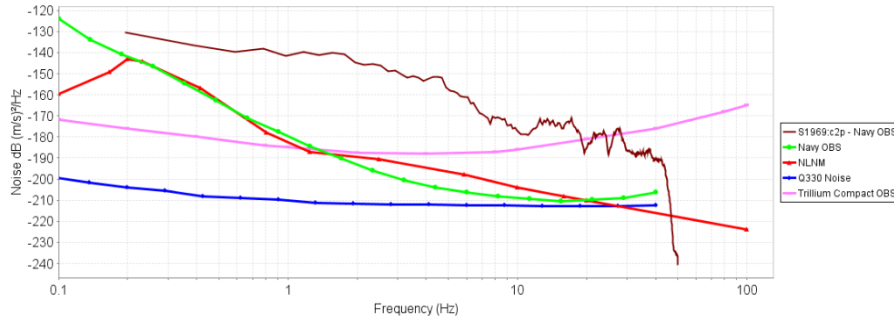
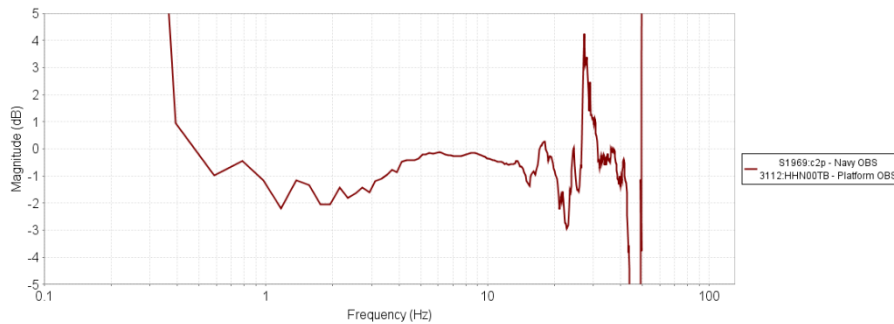


Figure 128 Wet Platform Testing, Geophone, North Coherence



**Figure 129 Wet Platform Testing, Geophone, North Incoherent Noise**



**Figure 130 Wet Platform Testing, Geophone, North Magnitude Response**

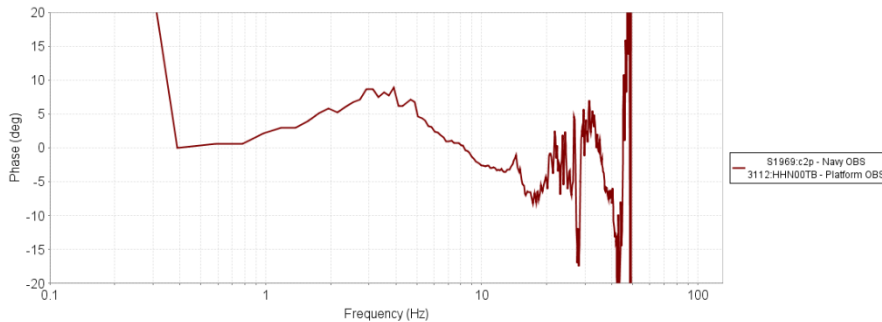


**Figure 131 Wet Platform Testing, Geophone, North Phase Response**

We see that the north channels have good coherence between approximately 0.7 and 18 Hz for this event. Beyond those bounds, the coherence decreases rapidly. The magnitude and phase response are observed to deviate between  $+0/-2.5$  dB and  $+8/-5$  degrees, respectively, over that passband to the limits of the available spectral resolution. The magnitude and phase response both have an observed transition at approximately 3 – 4 Hz, likely due to the complicated response function of the Navy OBS having multiple geophones connected in series.

### 3.3.2.3 East

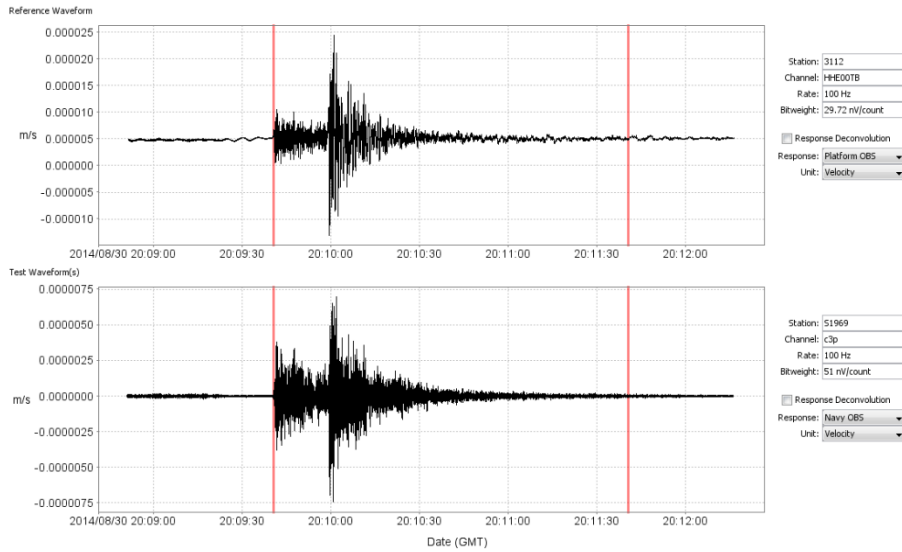


Figure 132 Wet Platform Testing, Geophone, East Waveforms

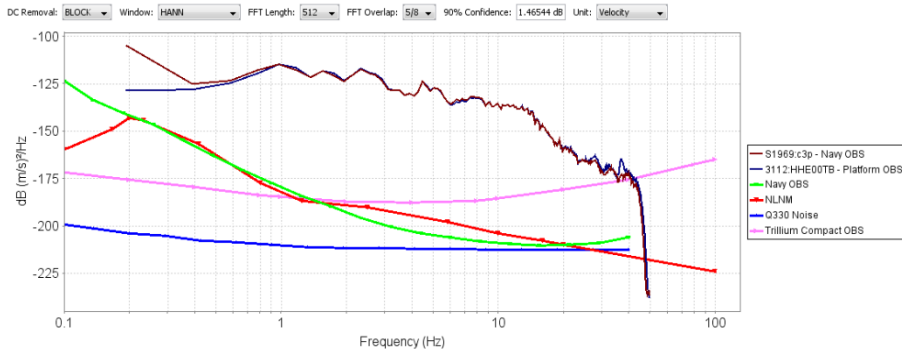


Figure 133 Wet Platform Testing, Geophone, East Power Spectra

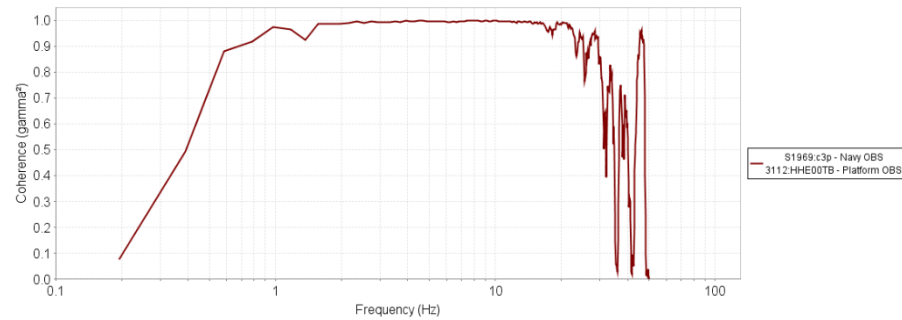
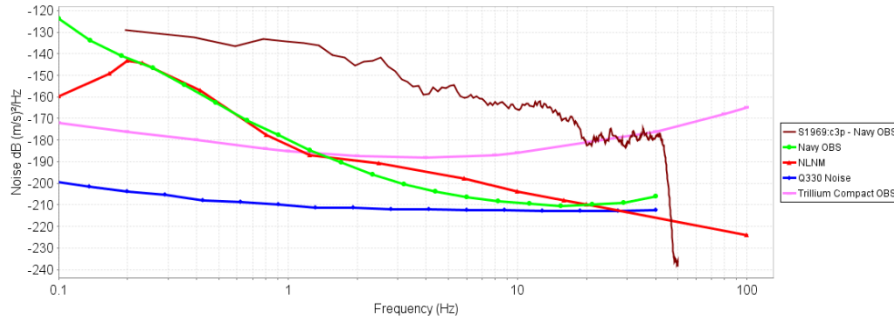
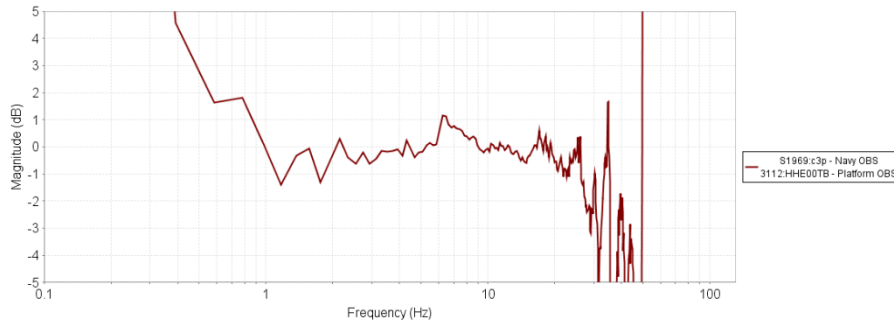


Figure 134 Wet Platform Testing, Geophone, East Coherence



**Figure 135 Wet Platform Testing, Geophone, East Incoherent Noise**



**Figure 136 Wet Platform Testing, Geophone, East Magnitude Response**

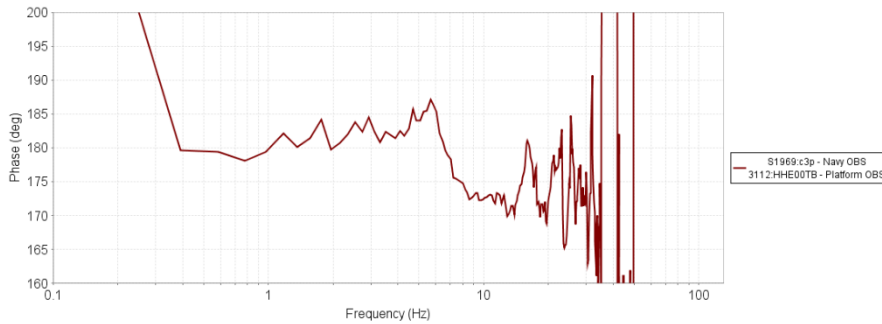


**Figure 137 Wet Platform Testing, Geophone, East Phase Response**

We see that the east channels have good coherence between approximately 1.5 and 15 Hz. Beyond those bounds, the coherence decreases rapidly. The magnitude and phase response are observed to deviate between +1/-1 dB and +17/-10 degrees, respectively, over that passband to the limits of the available spectral resolution. The magnitude and phase response both have an observed transition at approximately 6 Hz, likely due to the complicated response function of the Navy OBS having multiple geophones connected in series. Note from the phase response plot it appears that the east channel of the Navy OBS is connected with reverse polarity.

### 3.3.3 *Cross-Axis Coupling*

The cross-axis coupling will be evaluated by examining the coherence between the pairs of axis on each of the sensors in the test using the Sleemen 3-channel coherence technique. Changes in the cross-axis coupling across the varying test conditions will be compared. For this analysis 10 hours of background on August 30, 2014 from 02:00 – 12:00 GMT was used.

The power spectra and coherence are shown below for each of reference, seafloor, and Trillium OBS platform, and Navy OBS platform channels. Two plots were generated for each of the sensors: The first with a long window length for low frequencies below 0.1 Hz and the second with a short window length for high frequencies above 0.1 Hz.

The reference and platform Trillium OBSs appear to have a slight increase in coupling between the horizontal channels at frequencies below 0.01 Hz. The vertical channel has a very slight increase in coherence between each of the horizontal channels at around 0.1 Hz. Otherwise, the axes do not appear to have any significant coherence.

The platform Navy OBS does not have a similar increase in horizontal axes coupling. However, the observed frequency band in which coupling is occurring is so far outside of the Navy OBS low frequency corner at 4 Hz that it would not be expected to.

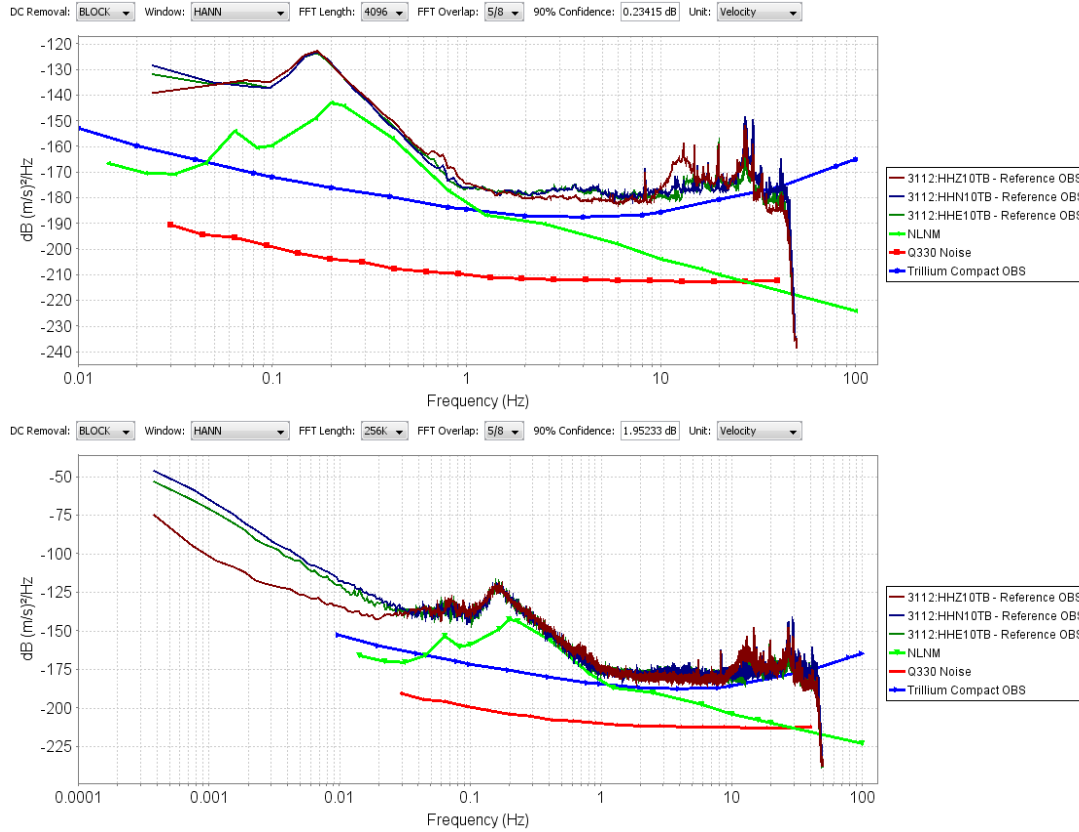


**Figure 138 Wet Platform, Cross-Axis Coupling, Reference Power Spectra**

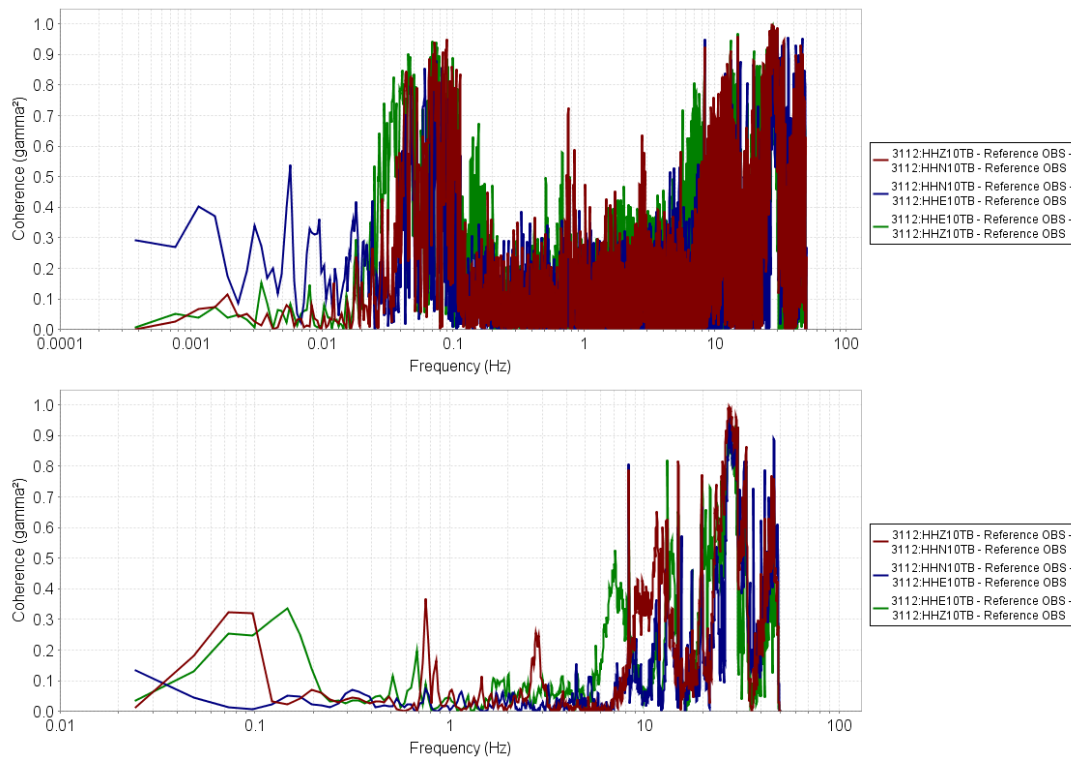


**Figure 139 Wet Platform, Cross-Axis Coupling, Reference Coherence**

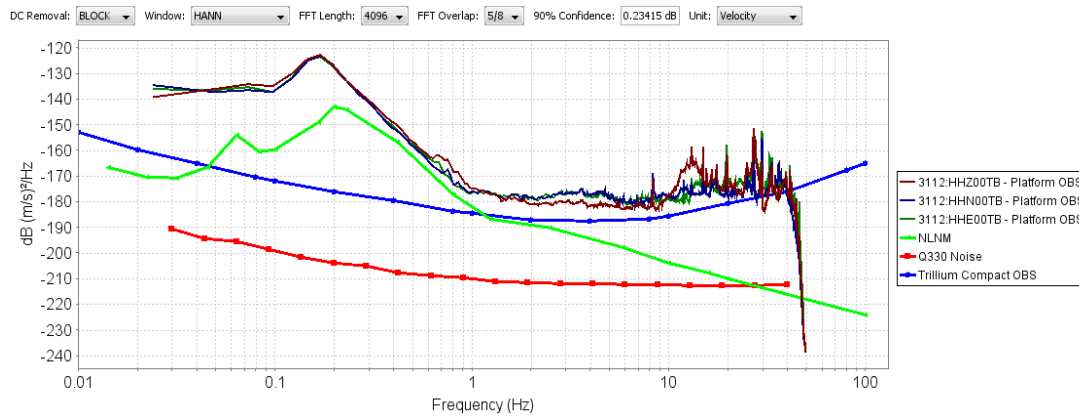
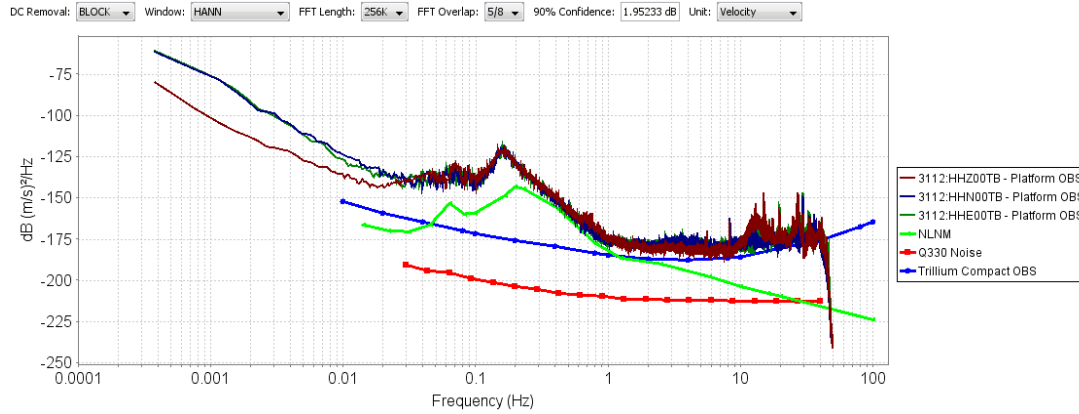


**Figure 140 Wet Platform, Cross-Axis Coupling, Trillium OBS Platform Power Spectra**

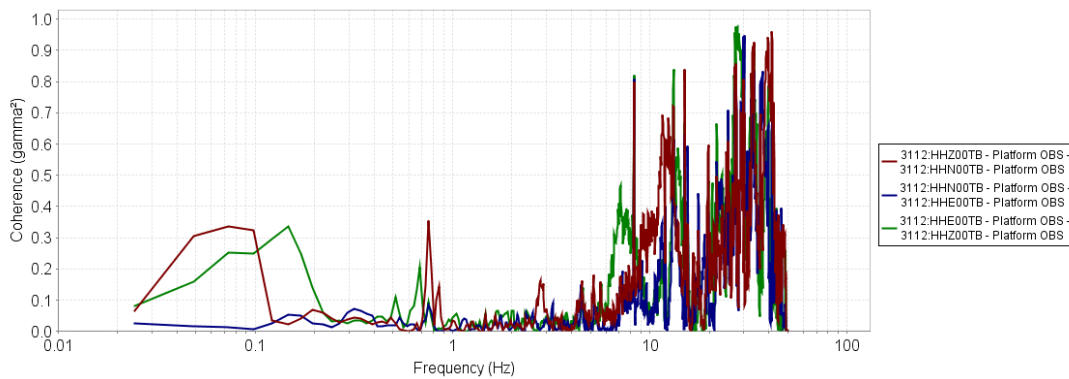
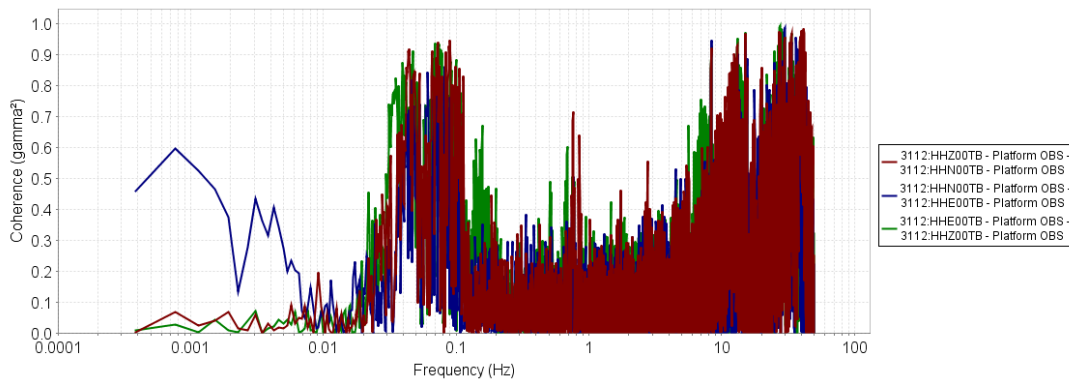


**Figure 141 Wet Platform, Cross-Axis Coupling, Trillium OBS Platform Coherence**

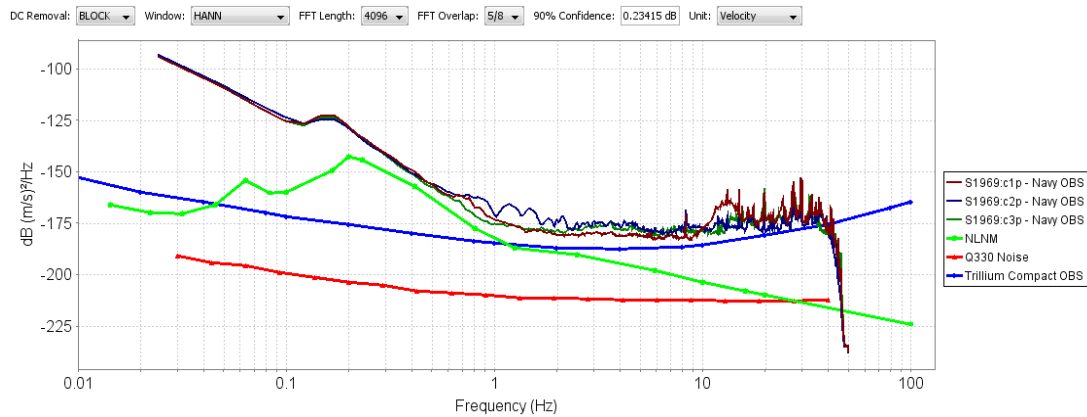
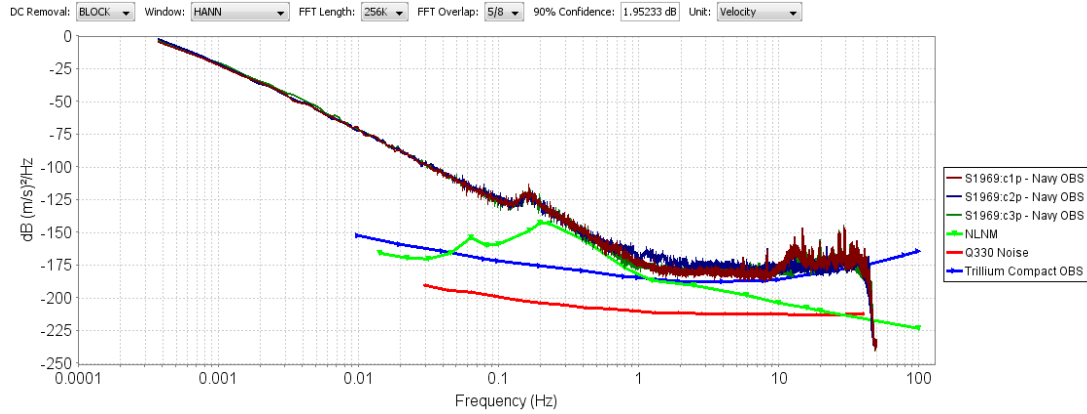


Figure 142 Wet Platform, Cross-Axis Coupling, Navy OBS Platform Power Spectra

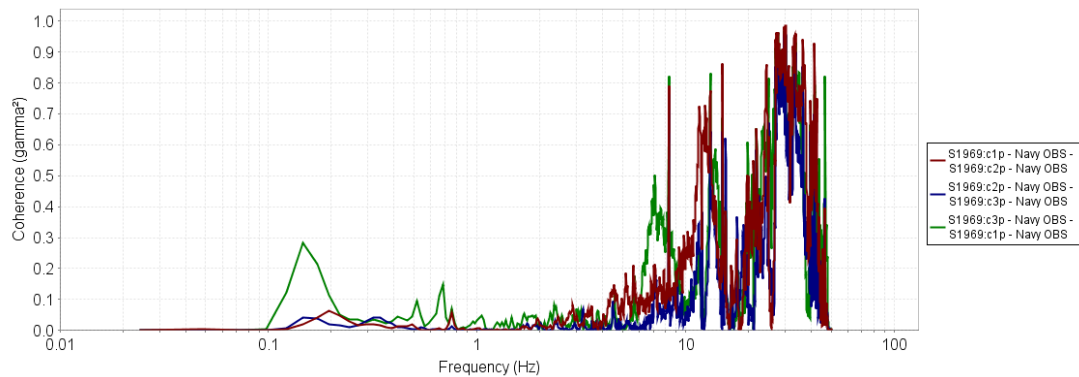
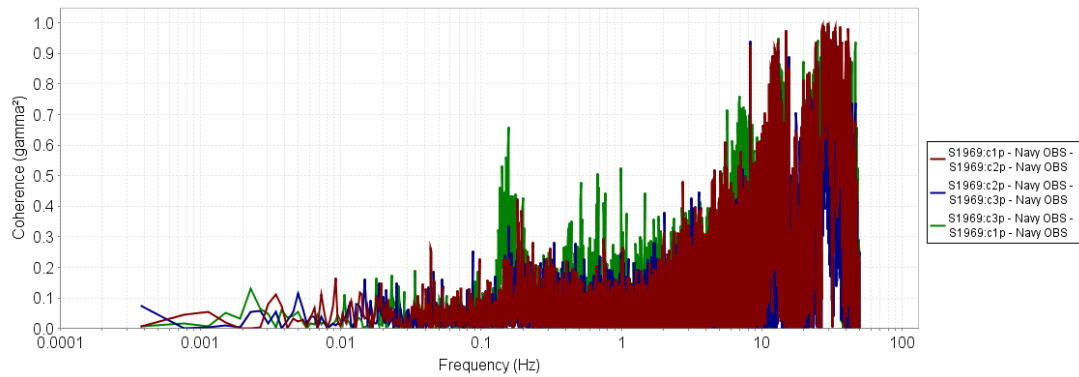


Figure 143 Wet Platform, Cross-Axis Coupling, Navy OBS Platform Coherence

### 3.4 Wet Seafloor Platform Testing

The Wet Seafloor Platform Test is a test with the reference Nanometrics Trillium OBS in direct contact with the bottom of the Test Pool. The bottom of the Test Pool was covered with Seafloor Material and the Underwater Platform was then placed on the Seafloor Material. The Test Pool was filled with water. The results of this test will be used to comment on any affect that the Underwater Platform and seafloor material have on the transfer function between the Nanometrics OBS reference sensor (#3033) and the Nanometrics OBS on the underwater platform (#3034). In addition, a comparison will be made between the performance of the Nanometrics OBS (#3034) and the geophone, both of which are on the Underwater Platform. Test data was collected for this test from September 8, 2014 to September 19, 2014.



Figure 144 Wet Seafloor Photo

IV&V 5d Wet Underwater Platform Testing  
(simulated seafloor)

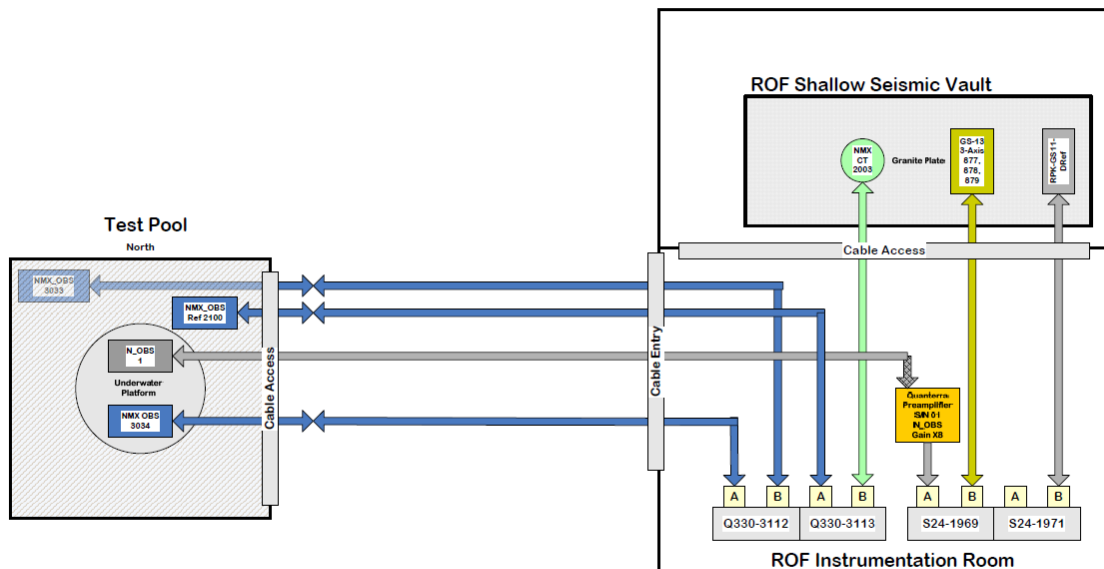


Figure 145 Wet Seafloor Platform Testing Diagram (RPKromer Consulting)

### 3.4.1 Transfer Function

Analysis of the test data will examine coherence between the reference OBS and the OBS on the Underwater Platform in order to establish the transfer function between the two sensors. Incoherent noise is “lumped” on to the Platform OBS. Two candidate events were identified for this analysis: One for low frequencies and one for high frequencies.

Coherence analysis for these events was performed for each of the Vertical, North, and East channels of the reference OBS, the OBS directly on the Seafloor Material, and the OBS on the Underwater Platform.

#### 3.4.1.1 Low Frequency

The low frequency event was identified September 15, 2014 at approximately 12:30 (GMT) with duration of 20 minutes and frequency content above the site noise at frequencies below 2 Hz

##### 3.4.1.1.1 Vertical

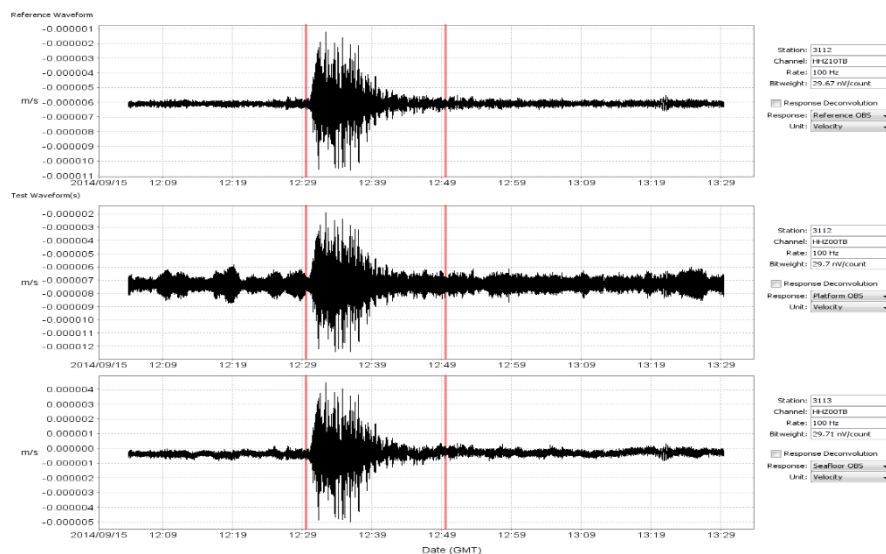
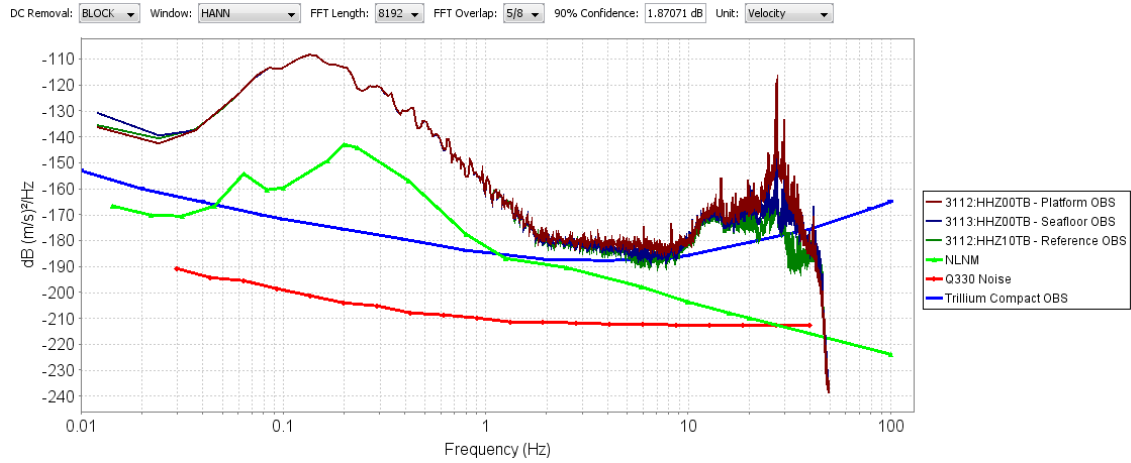
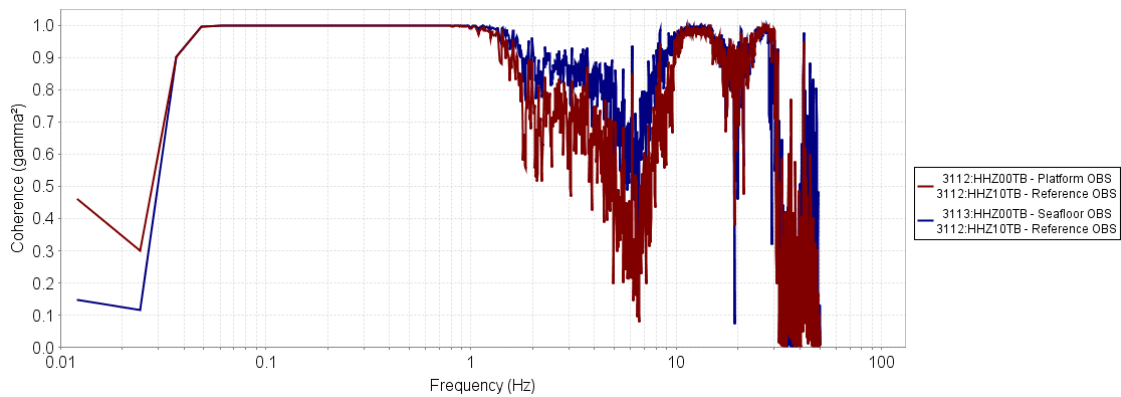


Figure 146 Seafloor, Transfer Function, Low Frequency, Vertical Waveforms



**Figure 147 Seafloor, Transfer Function, Low Frequency, Vertical Power Spectra**

We see from the time series and the power spectra that the Platform OBS exhibits more signal at high frequencies, above 10 Hz, than the Seafloor OBS. In turn, the Seafloor OBS exhibits more signal at high frequencies, above 10 Hz, than the Reference OBS on the bottom of the Test Pool.



**Figure 148 Seafloor, Transfer Function, Low Frequency, Vertical Coherence**

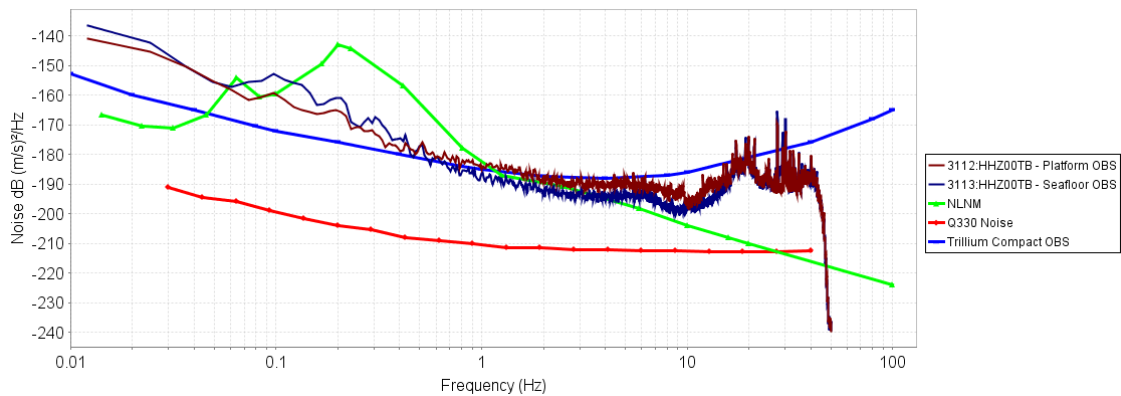


**Figure 149 Seafloor, Transfer Function, Low Frequency, Vertical Incoherent Noise**

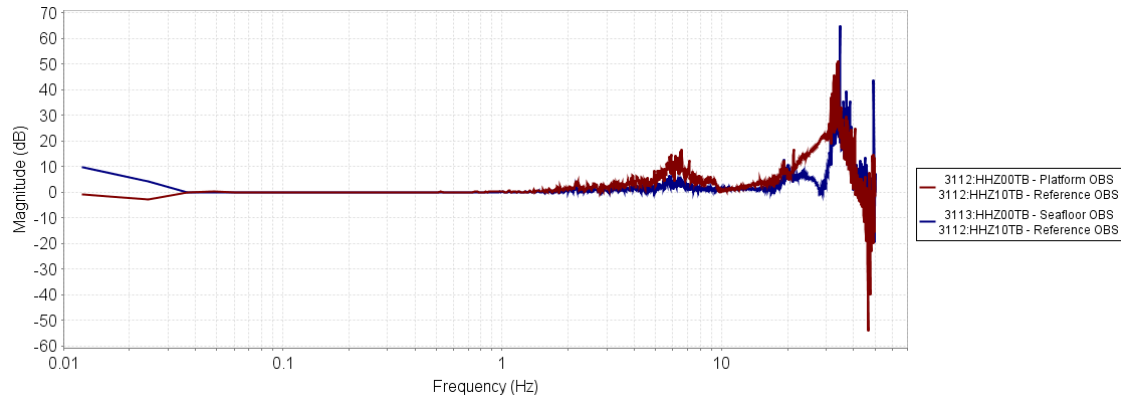


**Figure 150 Seafloor, Transfer Function, Low Frequency, Vertical Magnitude Response**

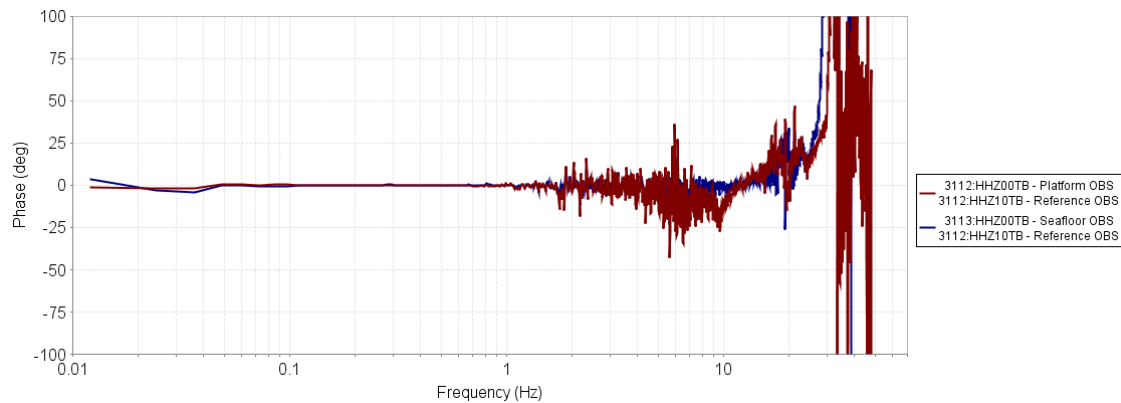


**Figure 151 Seafloor, Transfer Function, Low Frequency, Vertical Phase Response**

We see that the vertical channels have good coherence between approximately 0.05 and 1 Hz, 10 and 15 Hz, and 25 and 30 Hz for both the Platform OBS and Seafloor OBS. Outside those bounds, the coherence degrades rapidly as the observed signal amplitudes drop to near the sensor self-noise. There is minimal difference in the amplitude and phase response over that passband to the limits of the available spectral resolution.

Looking slightly into some of the frequencies in which there is decreased coherence, it appears from the increased amplitudes and the magnitude response that there may be some amount of a resonant mode visible between 20 and 40 Hz in both the Seafloor OBS and Platform OBS. However, it is difficult to make a definitive determination with reduced coherence.

### 3.4.1.1.2 North

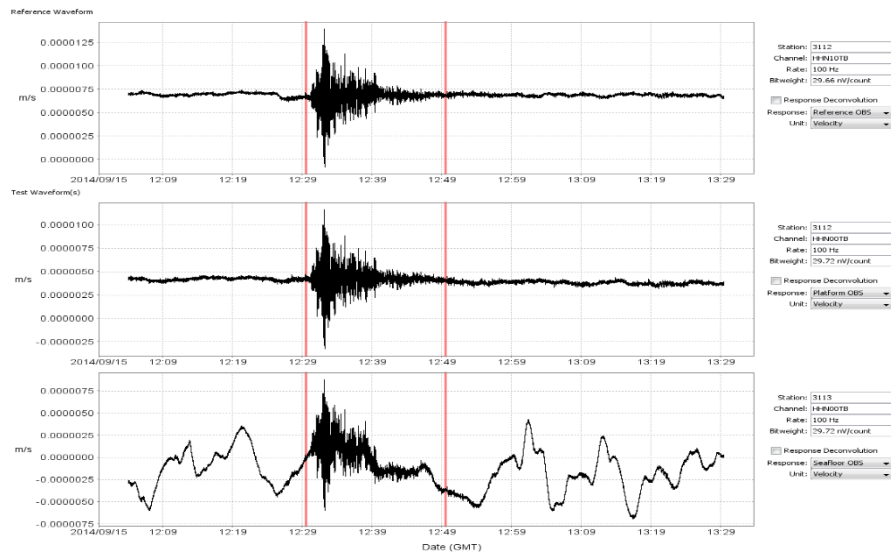


**Figure 152 Seafloor, Transfer Function, Low Frequency, North Waveforms**

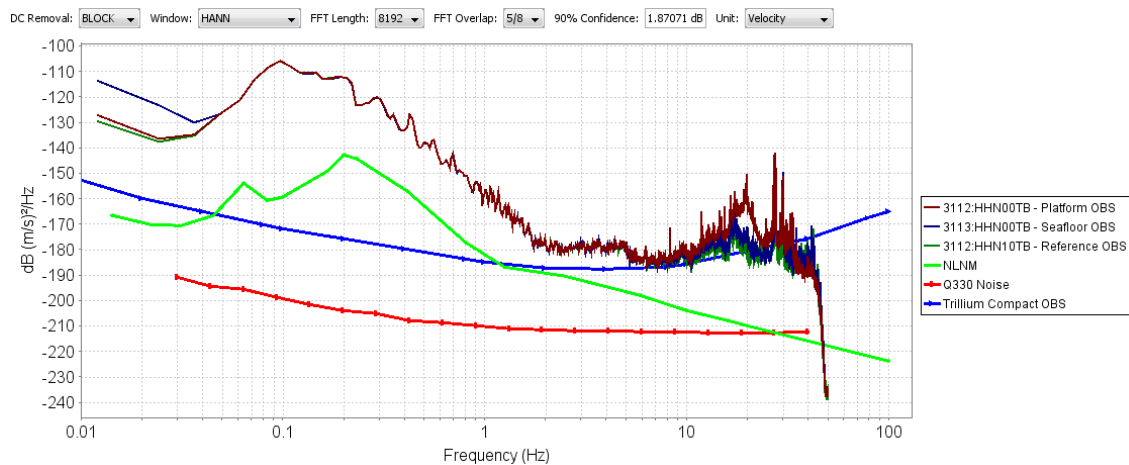


**Figure 153 Seafloor, Transfer Function, Low Frequency, North Power Spectra**

We see from the time series and the power spectra that the Seafloor OBS exhibits more noise at low frequencies, below 0.05 Hz, than the Reference or Platform OBS. The Platform OBS exhibits more signal at high frequencies, above 10 Hz, than the Seafloor OBS. In turn, the Seafloor OBS exhibits more signal at high frequencies, above 10 Hz, than the Reference OBS on the bottom of the Test Pool.

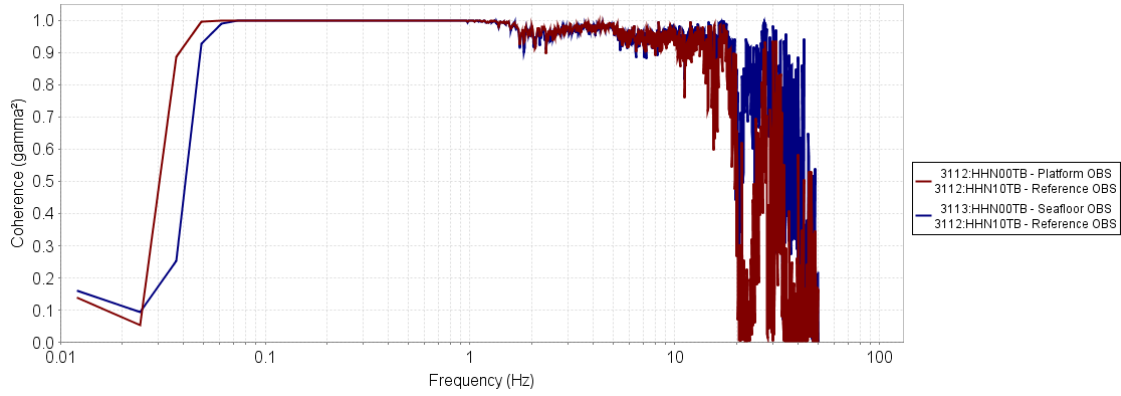


**Figure 154 Seafloor, Transfer Function, Low Frequency, North Coherence**

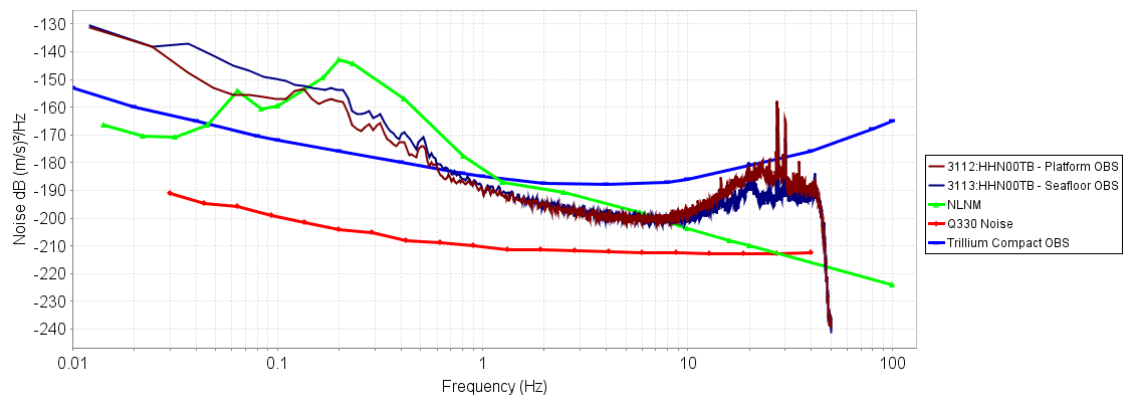


**Figure 155 Seafloor, Transfer Function, Low Frequency, North Incoherent Noise**

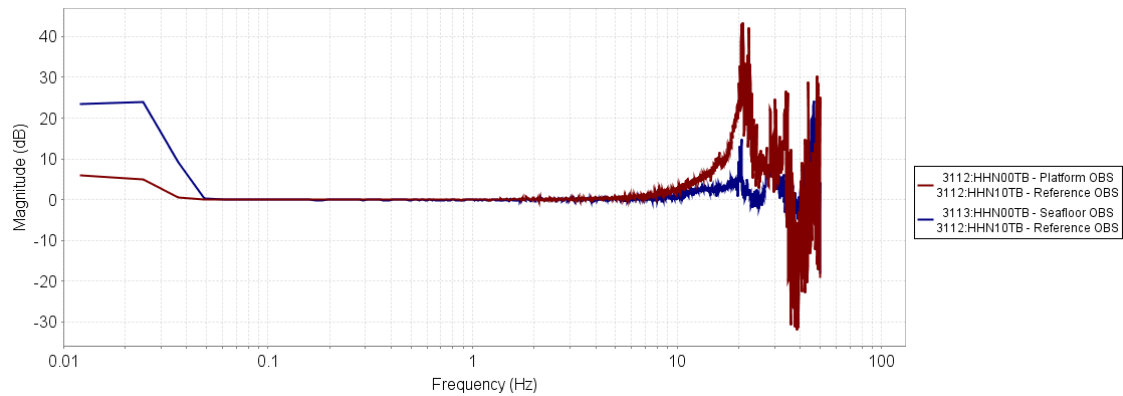


**Figure 156 Seafloor, Transfer Function, Low Frequency, North Magnitude Response**

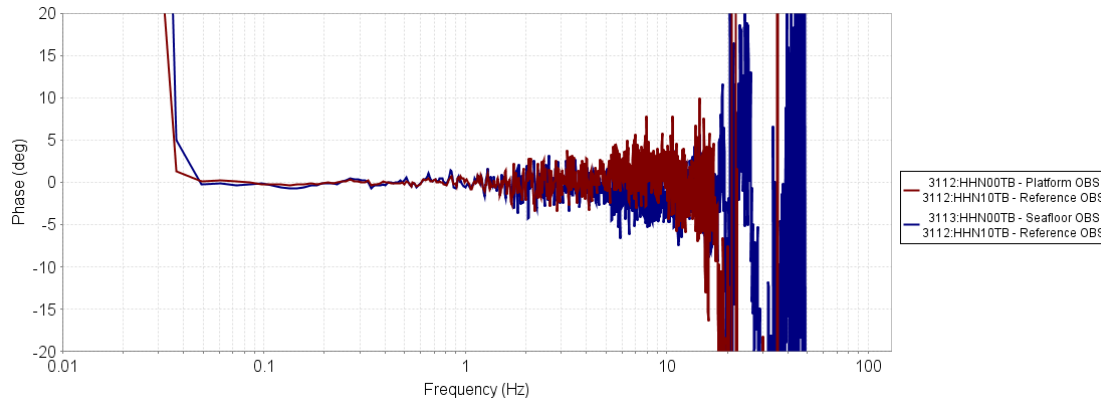


**Figure 157 Seafloor, Transfer Function, Low Frequency, North Phase Response**

We see that the north channels have good coherence between 0.05 and 1.5 Hz for the Platform OBS and between 0.06 and 1.5 Hz for the Seafloor OBS. Coherence is marginal on both the Platform OBS and the Seafloor OBS between 1.5 and 20 Hz. Beyond those bounds, the coherence decreases rapidly as the observed signal amplitudes drop to near the sensor self-noise. There is no appreciable difference in the magnitude and phase response over that passband to the limits of the available spectral resolution.

Looking slightly into some of the frequencies in which there is decreased coherence, it appears from the increased amplitudes and magnitude response that there is some amount of a resonant mode visible around 20 Hz in both the Seafloor OBS and Platform OBS. However, it is difficult to make a definitive determination with reduced coherence.

### 3.4.1.1.3 East

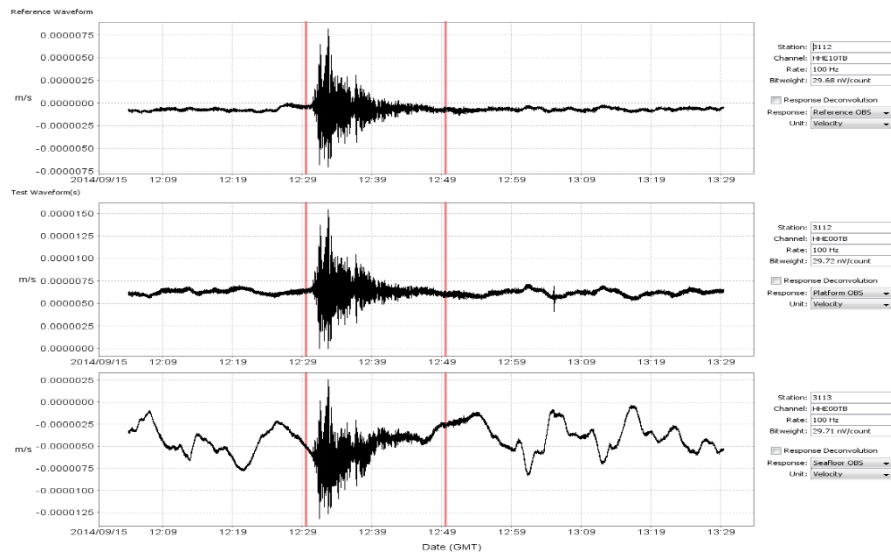


**Figure 158 Seafloor, Transfer Function, Low Frequency, East Waveforms**

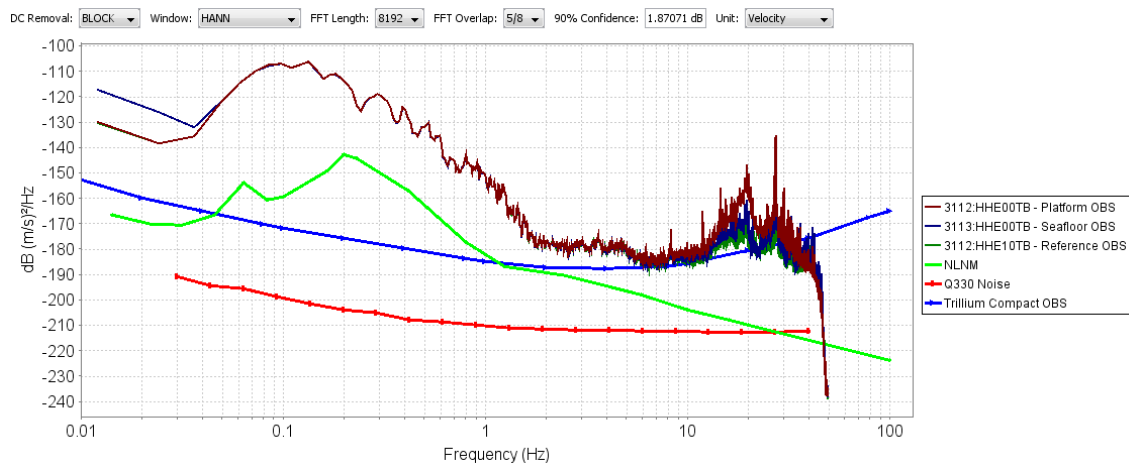


**Figure 159 Seafloor, Transfer Function, Low Frequency, East Power Spectra**

We see from the time series and the power spectra that the Seafloor OBS exhibits more noise at low frequencies, below 0.05 Hz, than the Reference or Platform OBS. The Platform OBS exhibits more signal at high frequencies, above 10 Hz, than the Seafloor OBS. In turn, the Seafloor OBS exhibits more signal at high frequencies, above 10 Hz, than the Reference OBS on the bottom of the Test Pool.

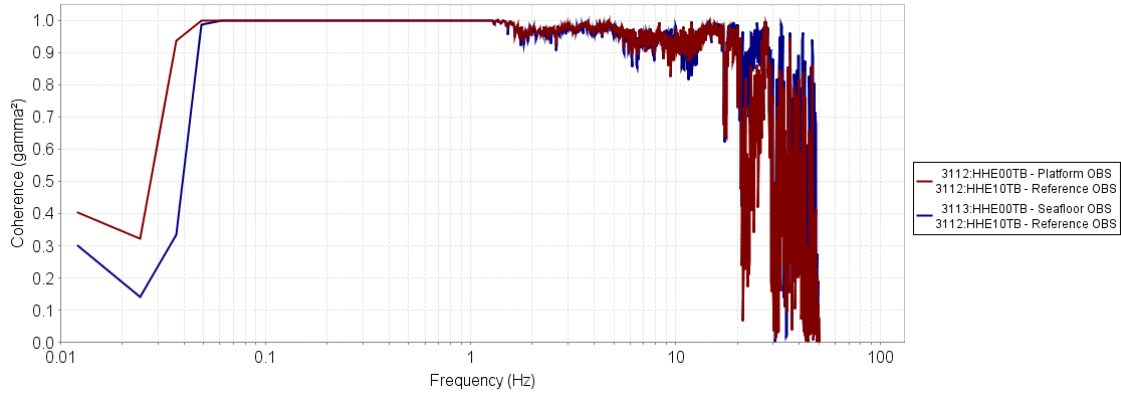


**Figure 160 Seafloor, Transfer Function, Low Frequency, East Coherence**

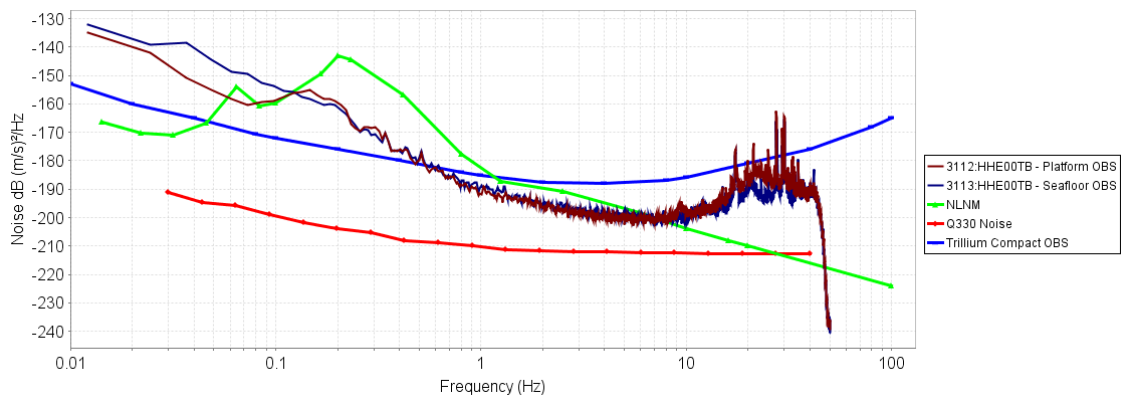


**Figure 161 Seafloor, Transfer Function, Low Frequency, East Incoherent Noise**

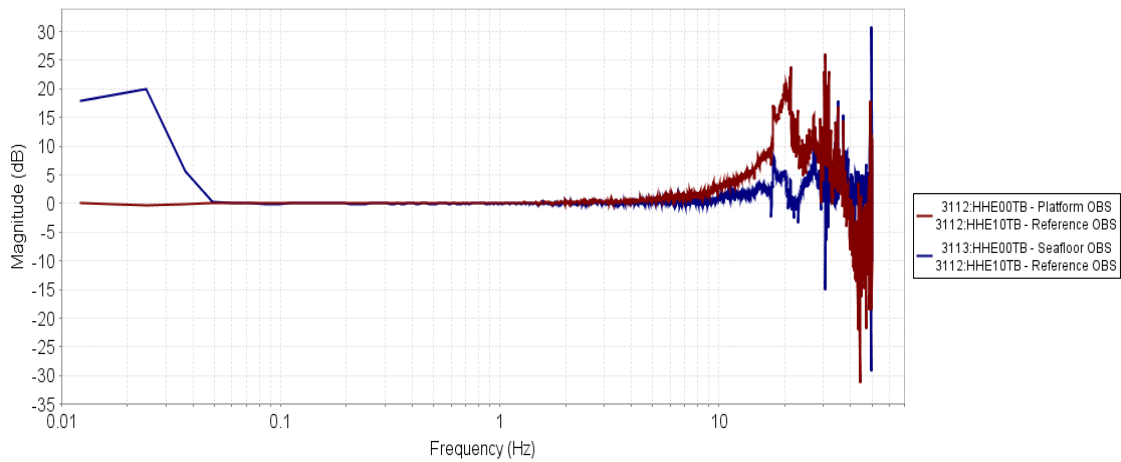


**Figure 162 Seafloor, Transfer Function, Low Frequency, East Magnitude Response**

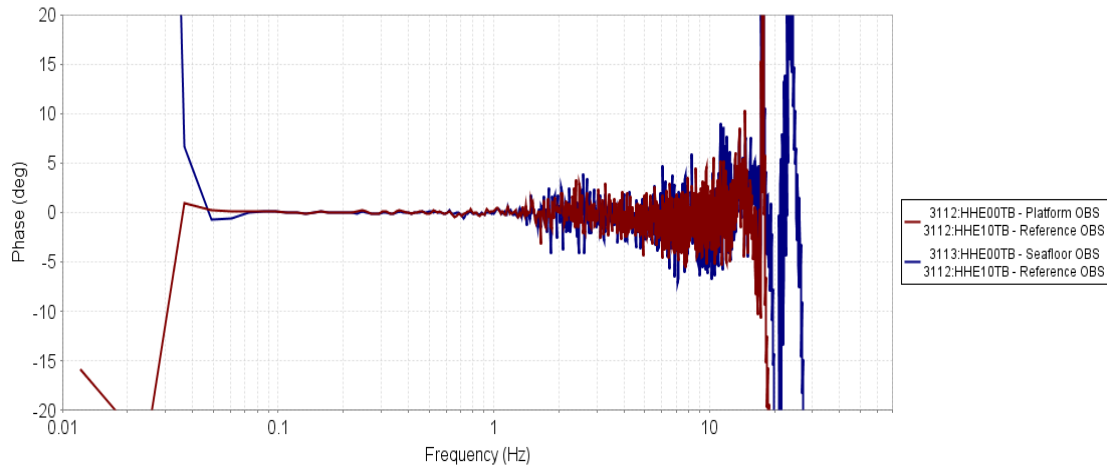


**Figure 163 Seafloor, Transfer Function, Low Frequency, East Phase Response**

We see that the east channels have good coherence between 0.05 and 1.5 Hz for the Platform OBS and between 0.06 and 1.5 Hz for the Seafloor OBS. Coherence is marginal on both the Platform OBS and the Seafloor OBS between 1.5 and 20 Hz. Beyond those bounds, the coherence decreases rapidly as the observed signal amplitudes drop to near the sensor self-noise. There is no appreciable difference in the amplitude and phase response over that passband to the limits of the available spectral resolution.

Looking slightly into some of the frequencies in which there is decreased coherence, it appears from the increased amplitudes and magnitude response that there is some amount of a resonant mode visible around 20 Hz in both the Seafloor OBS and Platform OBS. However, it is difficult to make a definitive determination with reduced coherence.

### 3.4.1.2 High Frequency

The high frequency event was identified September 12, 2014 at approximately 19:06 (GMT) with duration of 2 minutes and frequency content above the site noise at frequencies above 1 Hz

#### 3.4.1.2.1 Vertical

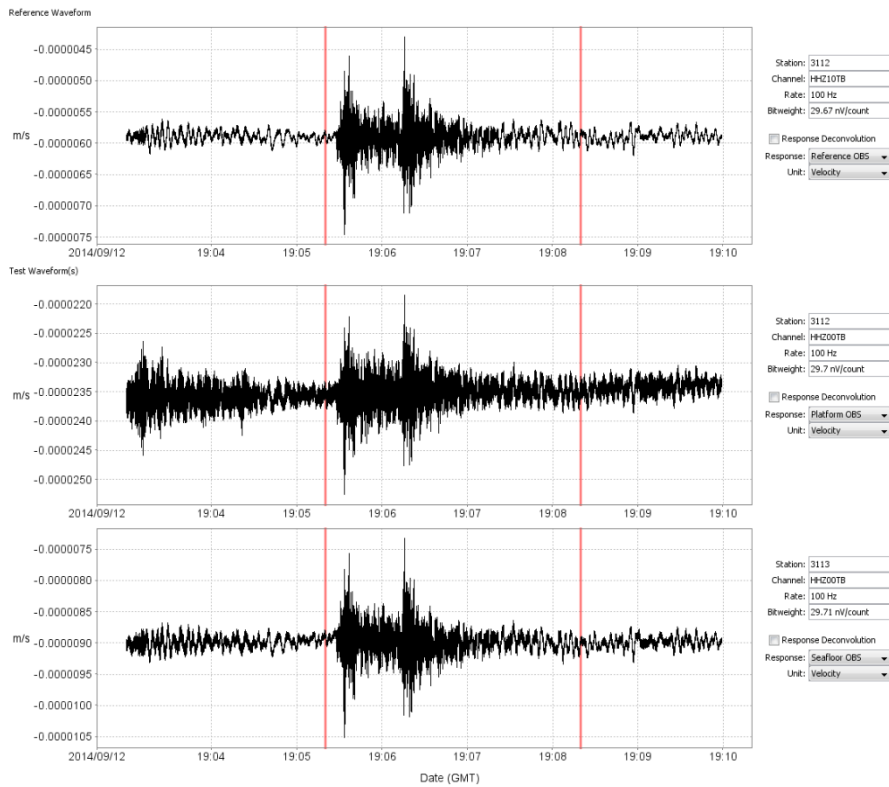


**Figure 164 Seafloor, Transfer Function, High Frequency, Vertical Waveforms**

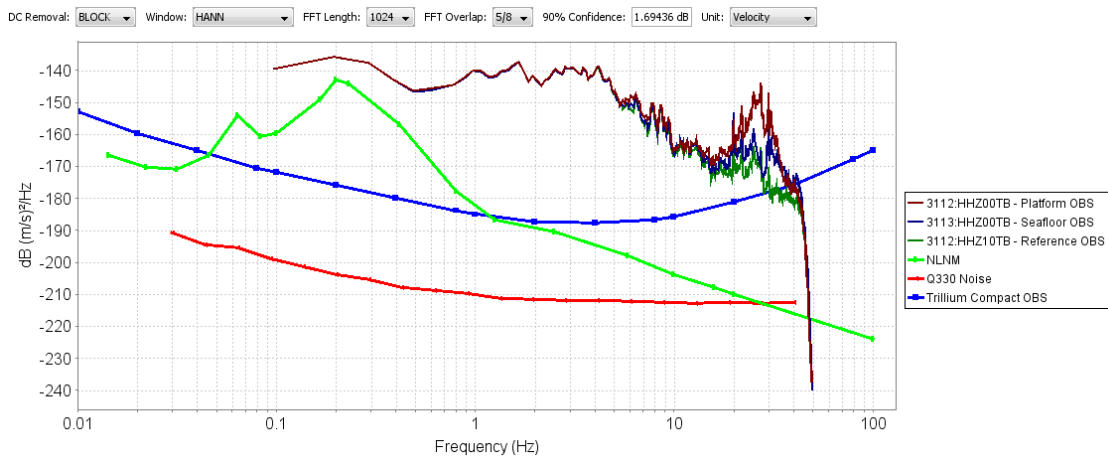


**Figure 165 Seafloor, Transfer Function, High Frequency, Vertical Power Spectra**

We see from the time series and the power spectra that the Platform OBS exhibits more signal at high frequencies, above 10 Hz, than the Seafloor OBS. In turn, the Seafloor OBS exhibits more signal at high frequencies, above 10 Hz, than the Reference OBS on the bottom of the Test Pool.

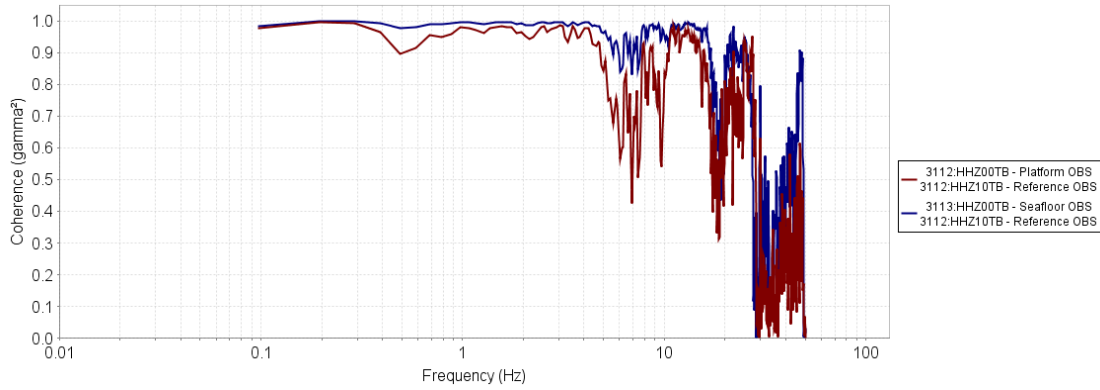


**Figure 166 Seafloor, Transfer Function, High Frequency, Vertical Coherence**

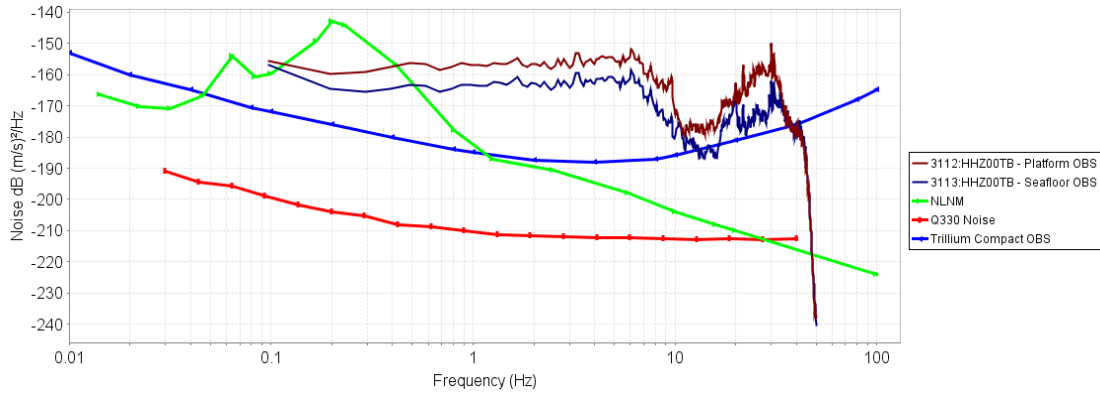


**Figure 167 Seafloor, Transfer Function, High Frequency, Vertical Incoherent Noise**

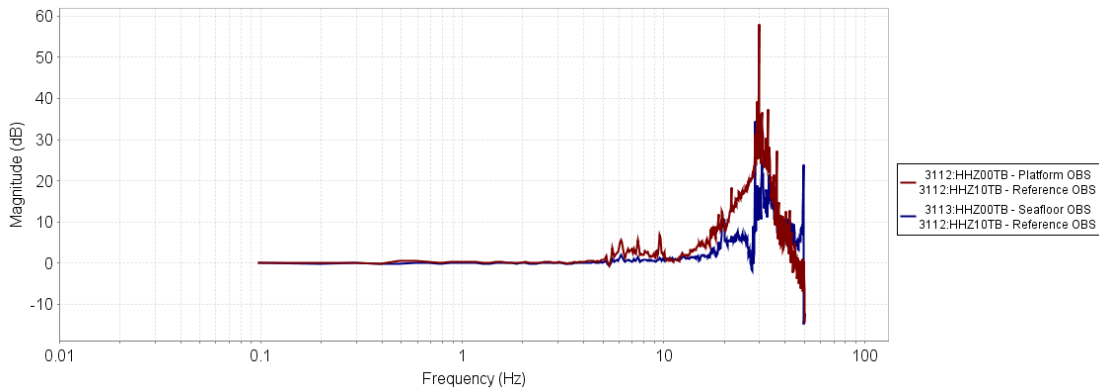


**Figure 168 Seafloor, Transfer Function, High Frequency, Vertical Magnitude Response**

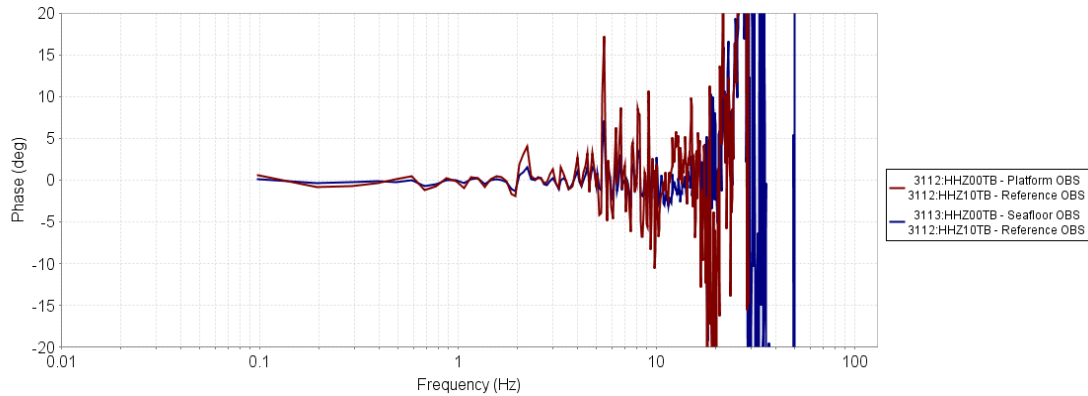


**Figure 169 Seafloor, Transfer Function, High Frequency, Vertical Phase Response**

We see that the vertical channels have good coherence between approximately 0.1 and 4 Hz for the Seafloor OBS. Coherence between the Reference OBS and the Underwater Platform OBS is noticeably degraded at frequencies above 0.3 Hz. There is minimal difference in the amplitude and phase response over that passband to the limits of the available spectral resolution.

Looking slightly into some of the frequencies in which there is decreased coherence, it appears from the increased amplitudes and magnitude response that there is some amount of a resonant mode visible around 27 Hz in both the Seafloor OBS and Platform OBS with a greater effect visible on the Platform OBS. However, it is difficult to make a definitive determination with reduced coherence.

The Seafloor and Platform OBS also exhibit significantly more incoherent noise relative to the Reference OBS than would be expected from the sensor noise model. Of the two, the Platform OBS is exhibiting more noise than the Seafloor OBS.

### 3.4.1.2.2 North

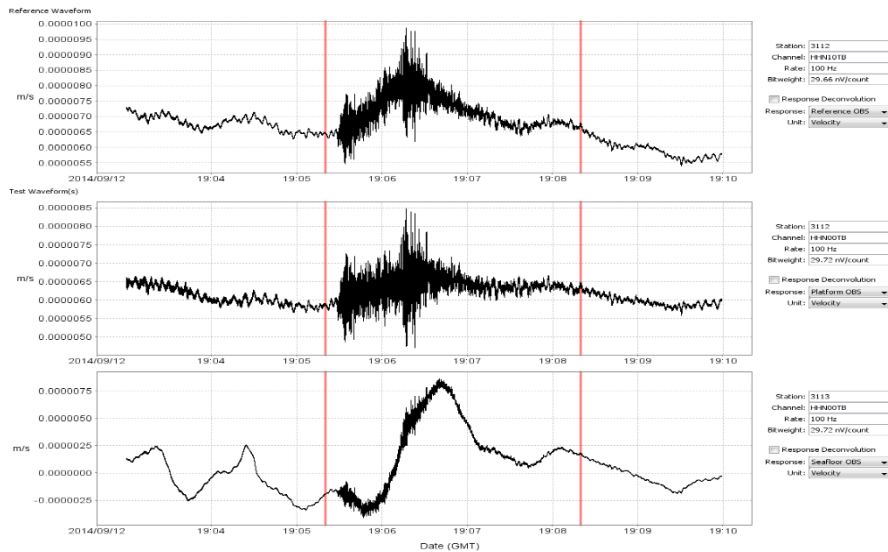


**Figure 170 Seafloor, Transfer Function, High Frequency, North Waveforms**

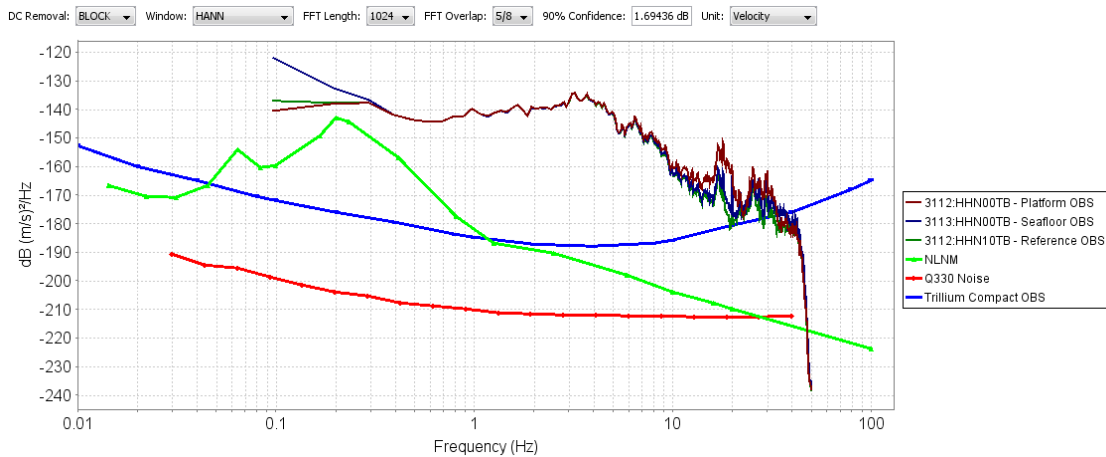


**Figure 171 Seafloor, Transfer Function, High Frequency, North Power Spectra**

We see from the time series and the power spectra that the Seafloor OBS exhibits more noise at low frequencies, below 0.05 Hz, than the Reference or Platform OBS. The Platform OBS exhibits more signal at high frequencies, above 10 Hz, than the Seafloor OBS. In turn, the Seafloor OBS exhibits more signal at high frequencies, above 10 Hz, than the Reference OBS on the bottom of the Test Pool.

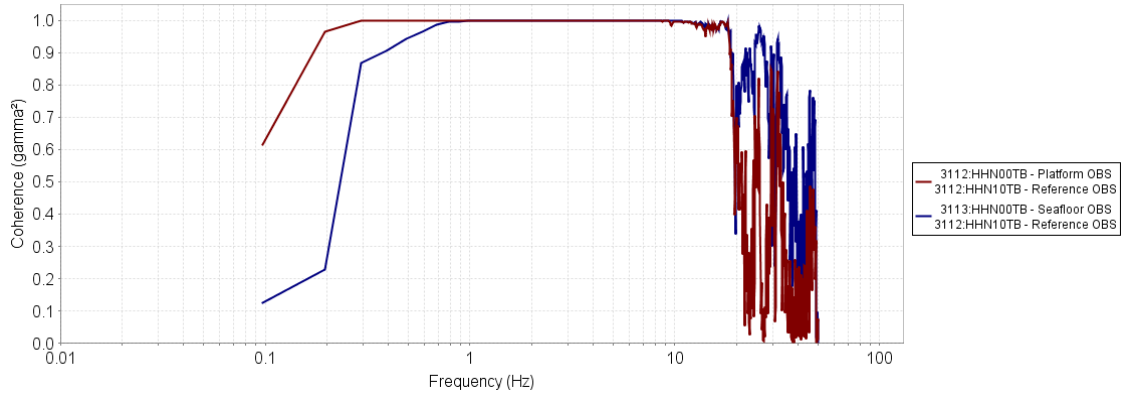


**Figure 172 Seafloor, Transfer Function, High Frequency, North Coherence**

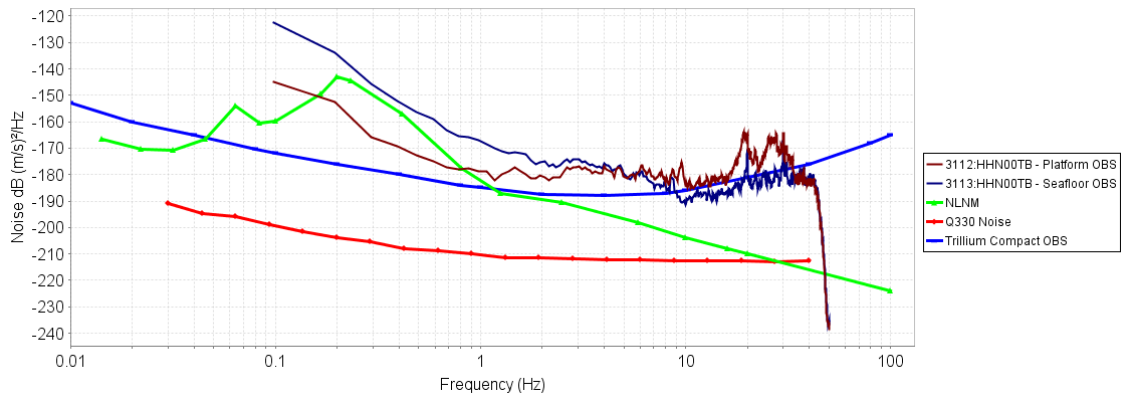


**Figure 173 Seafloor, Transfer Function, High Frequency, North Incoherent Noise**

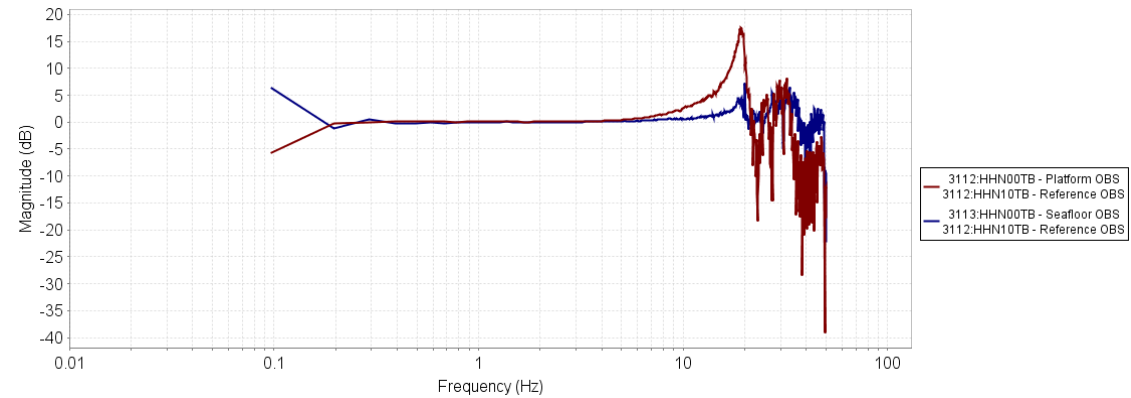


**Figure 174 Seafloor, Transfer Function, High Frequency, North Magnitude Response**

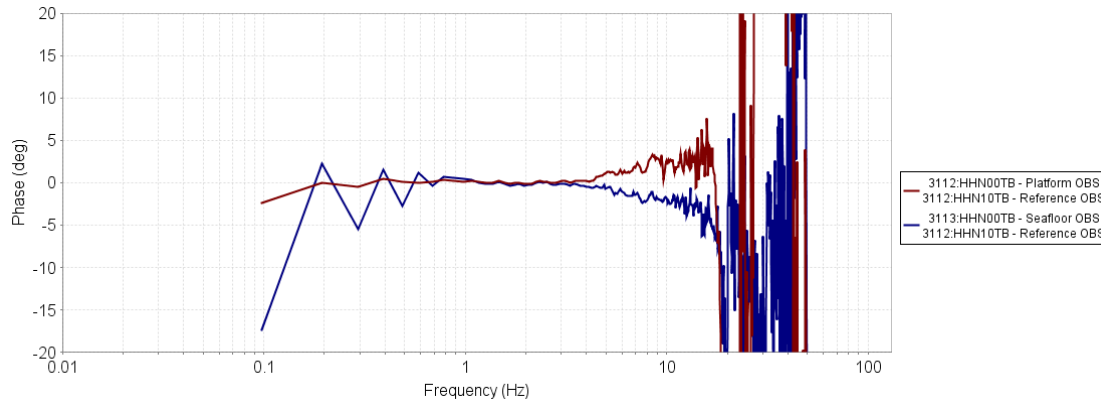


**Figure 175 Seafloor, Transfer Function, High Frequency, North Phase Response**

We see that the north channels have good coherence between 0.3 and 15 Hz for the Platform OBS and between 0.8 and 15 Hz for the Seafloor OBS. Beyond those bounds, the coherence decreases rapidly as the observed signal amplitudes drop to near the sensor self-noise. There is minimal difference in the amplitude and phase response over that passband to the limits of the available spectral resolution.

Looking slightly into some of the frequencies in which there is decreased coherence, it appears from the increased amplitude and magnitude response that there is some amount of a resonant mode visible at 19 Hz in both the Seafloor OBS and Platform OBS with a greater effect visible on the Platform OBS. However, it is difficult to make a definitive determination with reduced coherence.

### 3.4.1.2.3 East

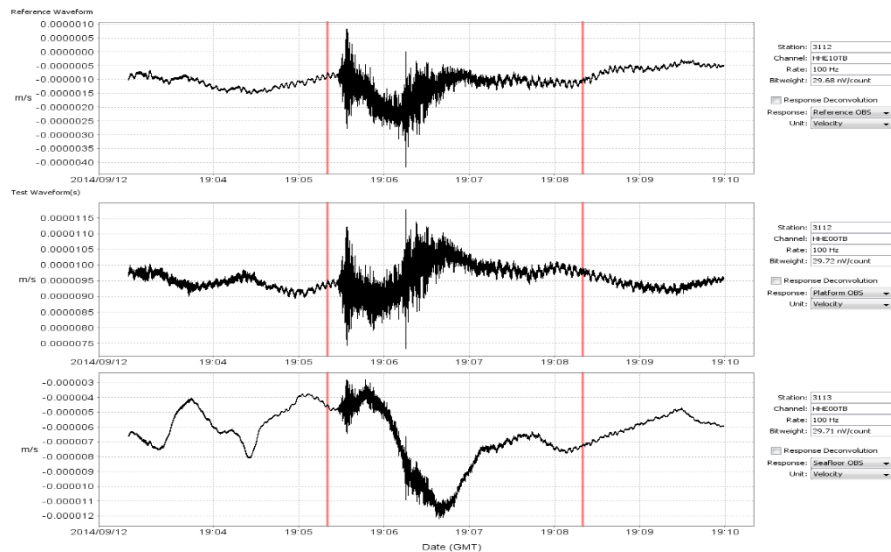


**Figure 176 Seafloor, Transfer Function, High Frequency, East Waveforms**

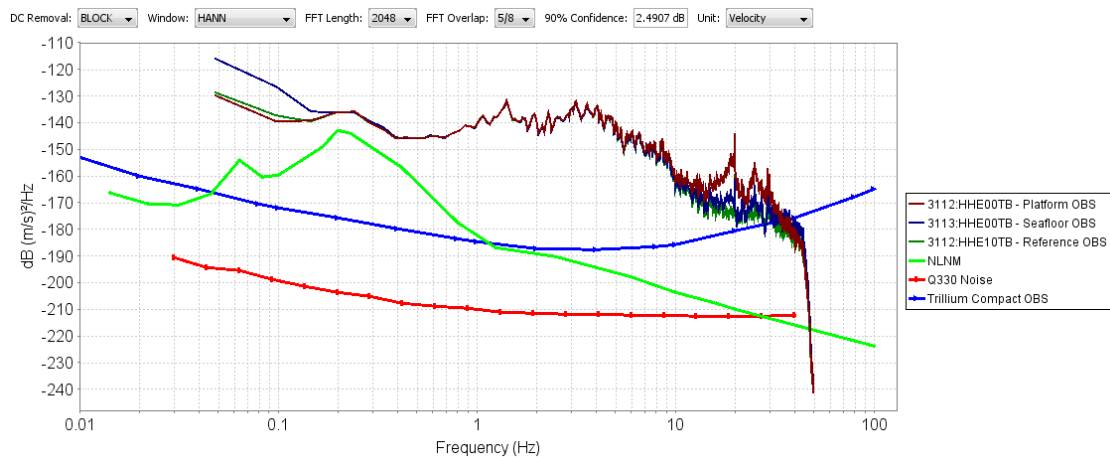


**Figure 177 Seafloor, Transfer Function, High Frequency, East Power Spectra**

We see from the time series and the power spectra that the Seafloor OBS exhibits more noise at low frequencies, below 0.2 Hz, than the Reference or Platform OBS. The Platform OBS exhibits more signal at high frequencies, above 10 Hz, than the Seafloor OBS. In turn, the Seafloor OBS exhibits more signal at high frequencies, above 10 Hz, than the Reference OBS on the bottom of the Test Pool.

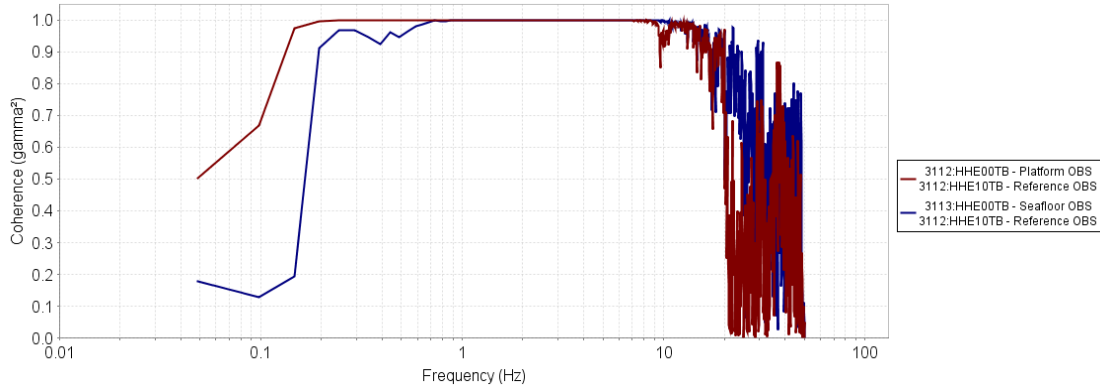


**Figure 178 Seafloor, Transfer Function, High Frequency, East Coherence**

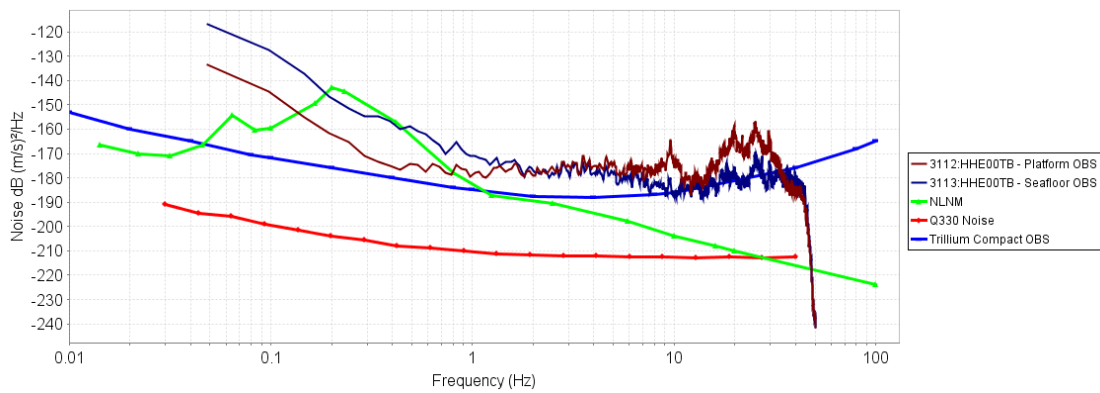


**Figure 179 Seafloor, Transfer Function, High Frequency, East Incoherent Noise**

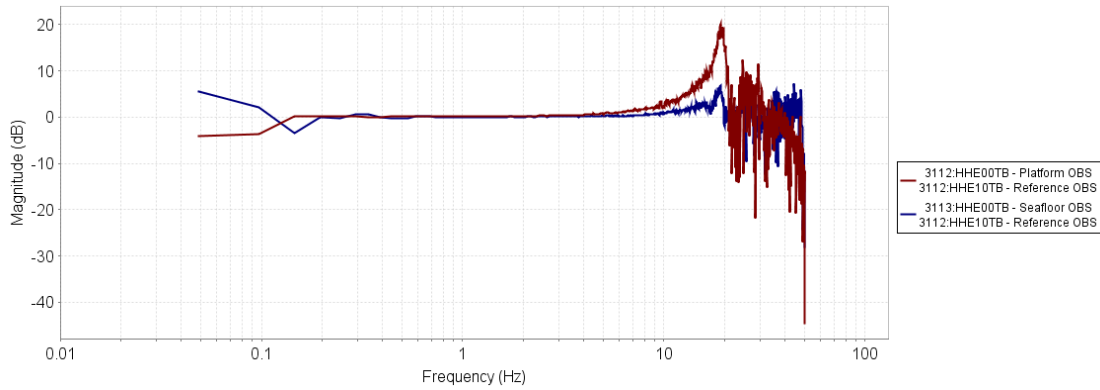


**Figure 180 Seafloor, Transfer Function, High Frequency, East Magnitude Response**

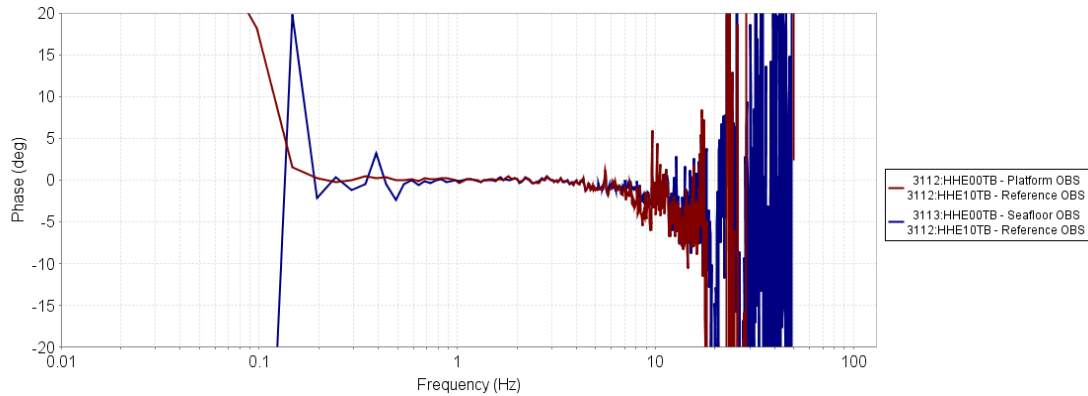


**Figure 181 Seafloor, Transfer Function, High Frequency, East Phase Response**

We see that the east channels have good coherence between 0.2 and 8 Hz for the Platform OBS and between 0.7 and 10 Hz for the Seafloor OBS. Beyond those bounds, the coherence decreases rapidly as the observed signal amplitudes drop to near the sensor self-noise. There is minimal difference in the amplitude and phase response over that passband to the limits of the available spectral resolution.

Looking slightly into some of the frequencies in which there is decreased coherence, it appears from the amplitude response that there is some amount of a resonant mode visible between 10 Hz and 30 Hz in both the Seafloor OBS and Platform OBS with a greater effect visible on the Platform OBS. However, it is difficult to make a definitive determination with reduced coherence.

### 3.4.2 Geophone

Analysis of the test data will examine coherence between the Trillium Compact OBS and the Navy Geophone OBS on the Underwater Platform. Incoherent noise is “lumped” on to the Platform Trillium OBS as it has higher noise than the Navy OBS at frequencies above 1 Hz.

The event has duration of approximately 3 minutes and frequency content above the site noise at frequencies above 0.4 Hz on September 12, 2014 at approximately 19:05 GMT. Examining an event with low frequency content is unnecessary since the noise in the geophone is relatively high at these frequencies.

The waveform time series, power spectra, coherence, incoherent noise, relative magnitude, and relative phase for each of the Vertical, North, and East channels are shown below.

#### 3.4.2.1 Vertical

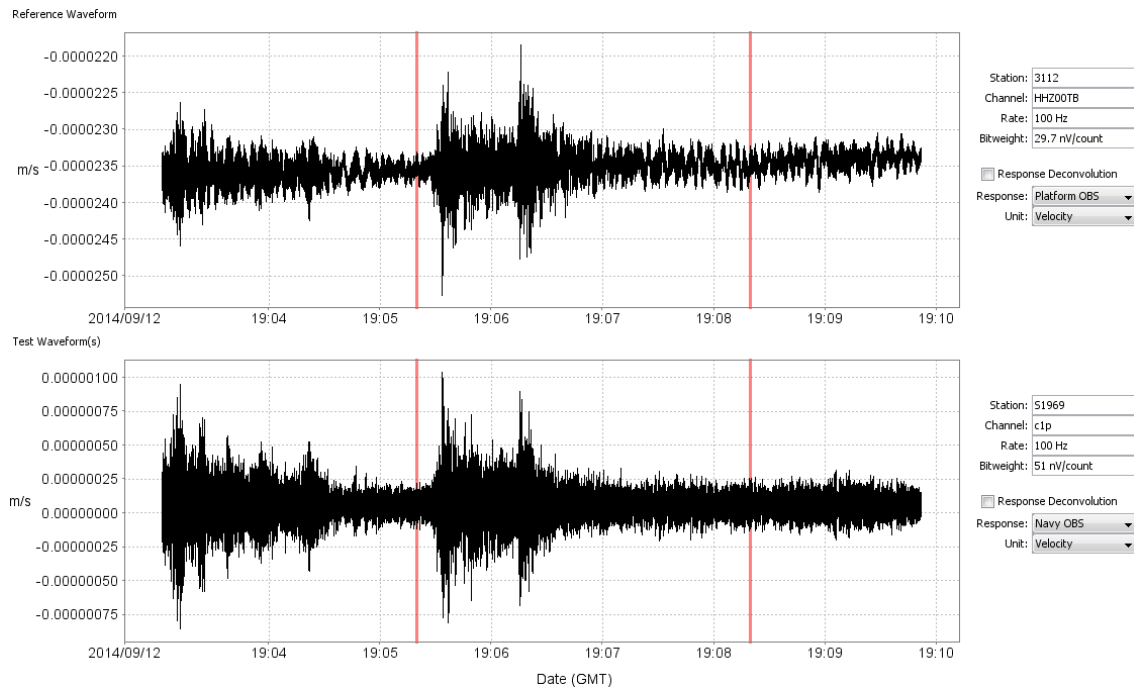


Figure 182 Seafloor, Geophone, Vertical Waveforms

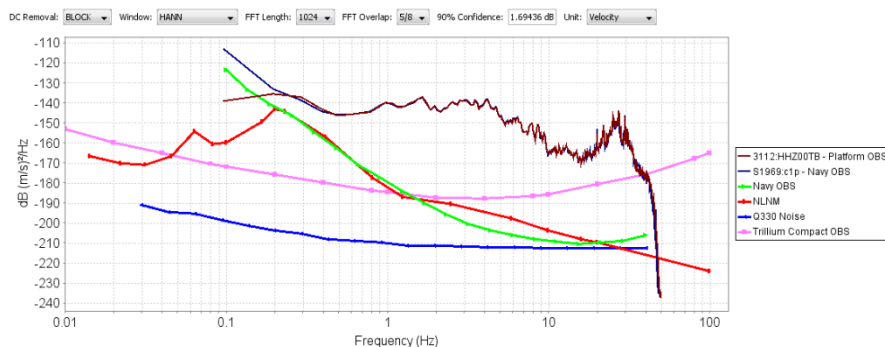
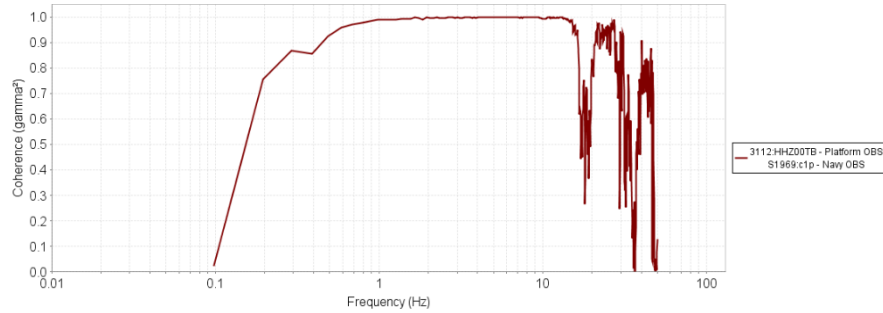
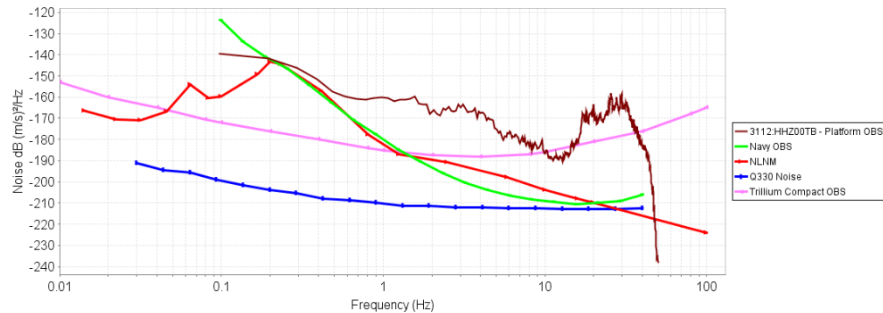


Figure 183 Seafloor, Geophone, Vertical Power Spectra



**Figure 184 Seafloor, Geophone, Vertical Coherence**



**Figure 185 Seafloor, Geophone, Vertical Incoherent Noise**

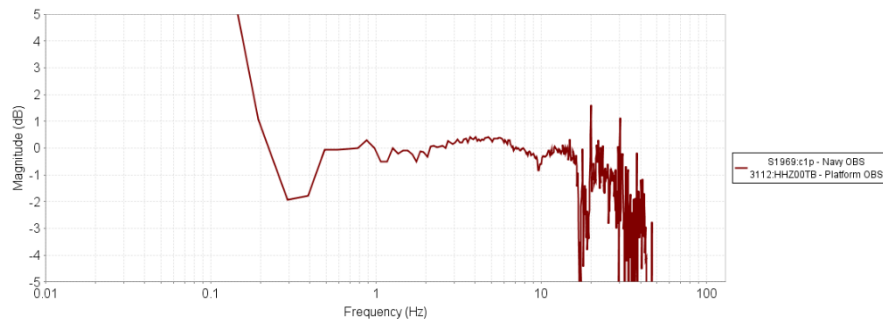


**Figure 186 Seafloor, Geophone, Vertical Magnitude Response**

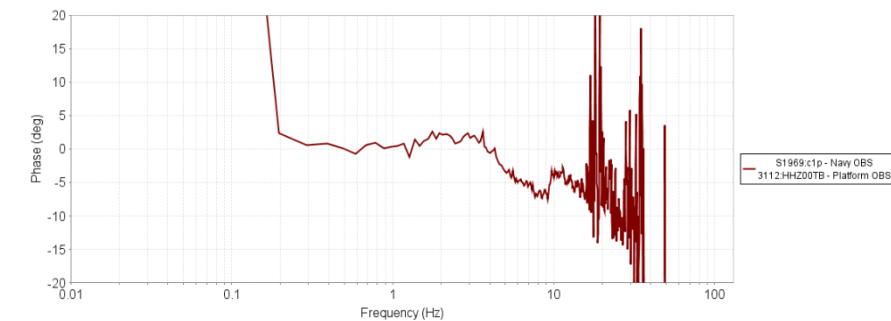


**Figure 187 Seafloor, Geophone, Vertical Phase Response**

We see that the vertical channels have good coherence between approximately 1.0 and 15 Hz for this event. Beyond those bounds, the coherence degrades rapidly as the observed signal amplitudes drop to near the sensor self-noise. The magnitude and phase response are observed to deviate between +1/-1 dB and +2.5/-7.5 degrees, respectively, over that passband to the limits of the available spectral resolution.

### 3.4.2.2 North

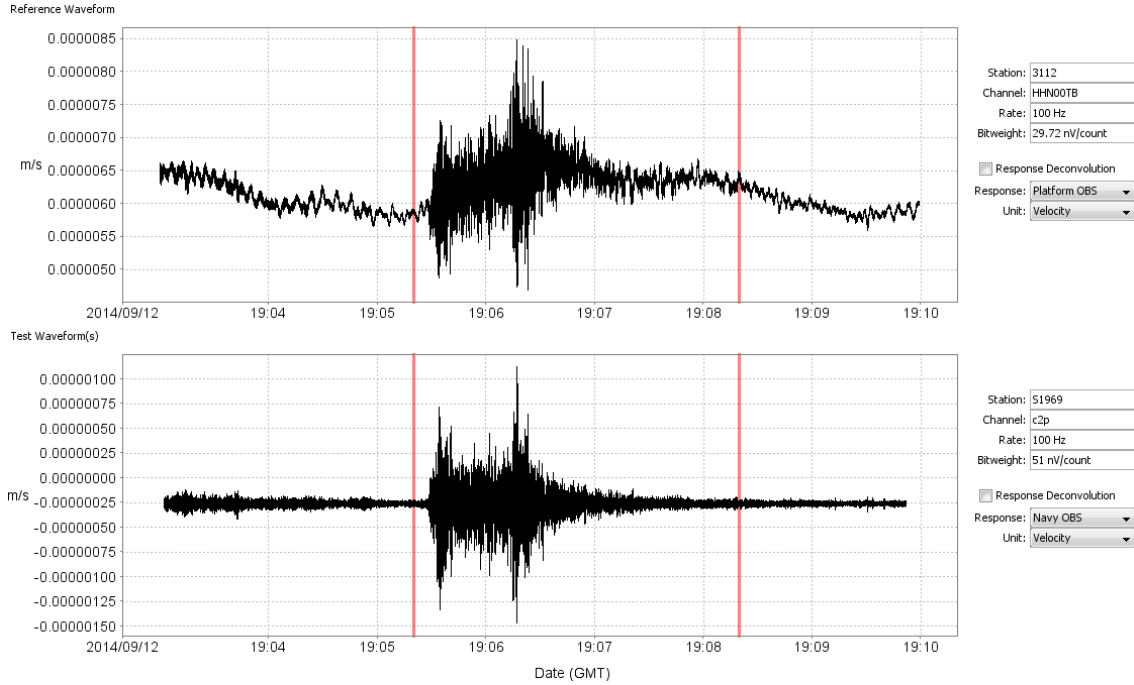


**Figure 188 Seafloor, Geophone, North Waveforms**

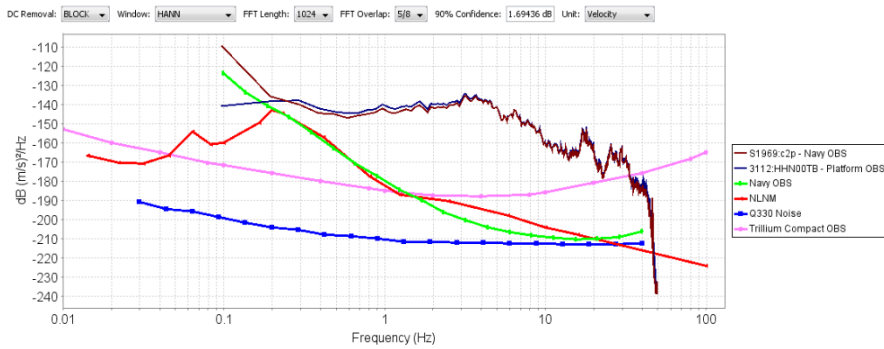


**Figure 189 Seafloor, Geophone, North Power Spectra**

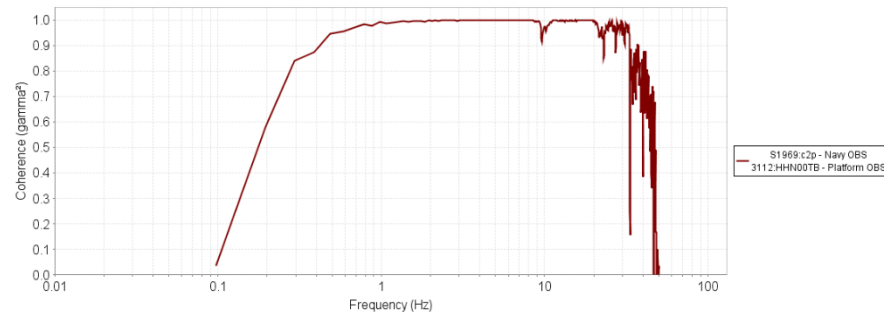


**Figure 190 Seafloor, Geophone, North Coherence**

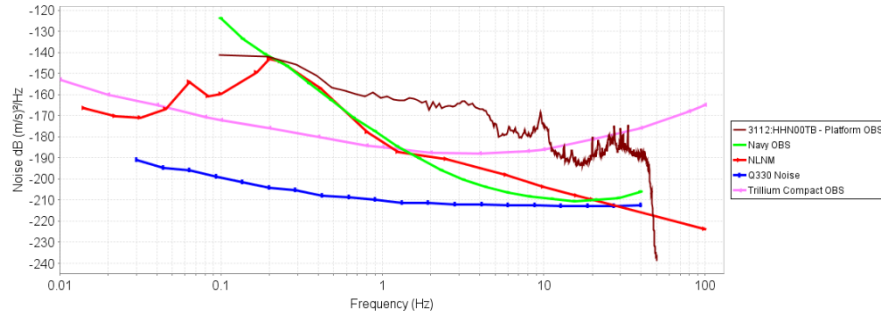


**Figure 191 Seafloor, Geophone, North Incoherent Noise**

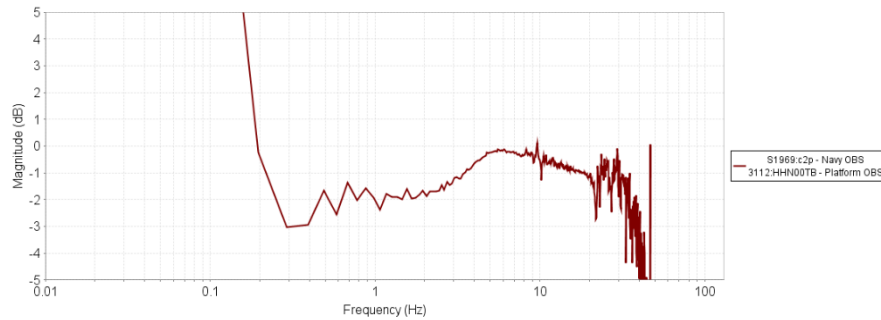


**Figure 192 Seafloor, Geophone, North Magnitude Response**

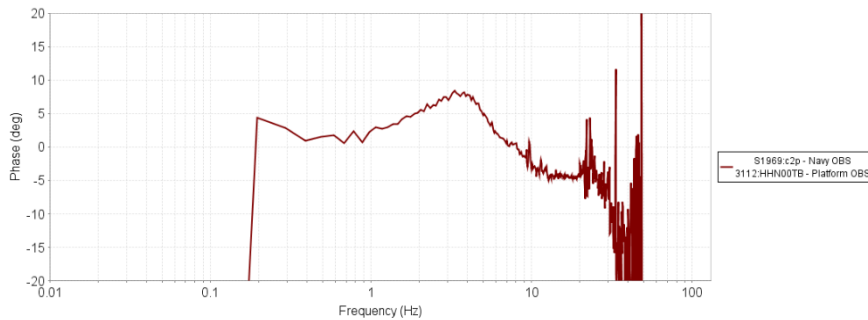


**Figure 193 Seafloor, Geophone, North Phase Response**

We see that the north channels have good coherence between approximately 1.0 and 20 Hz for this event. Beyond those bounds, the coherence decreases rapidly as the observed signal amplitudes drop to near the sensor self-noise. The magnitude and phase response are observed to deviate between  $+0/-2.5$  dB and  $+8/-5$  degrees, respectively, over that passband to the limits of the available spectral resolution. The magnitude and phase responses have an observed transition at approximately 3 – 4 Hz, likely due to the complicated response function of the Navy OBS having multiple geophones connected in series.

### 3.4.2.3 East

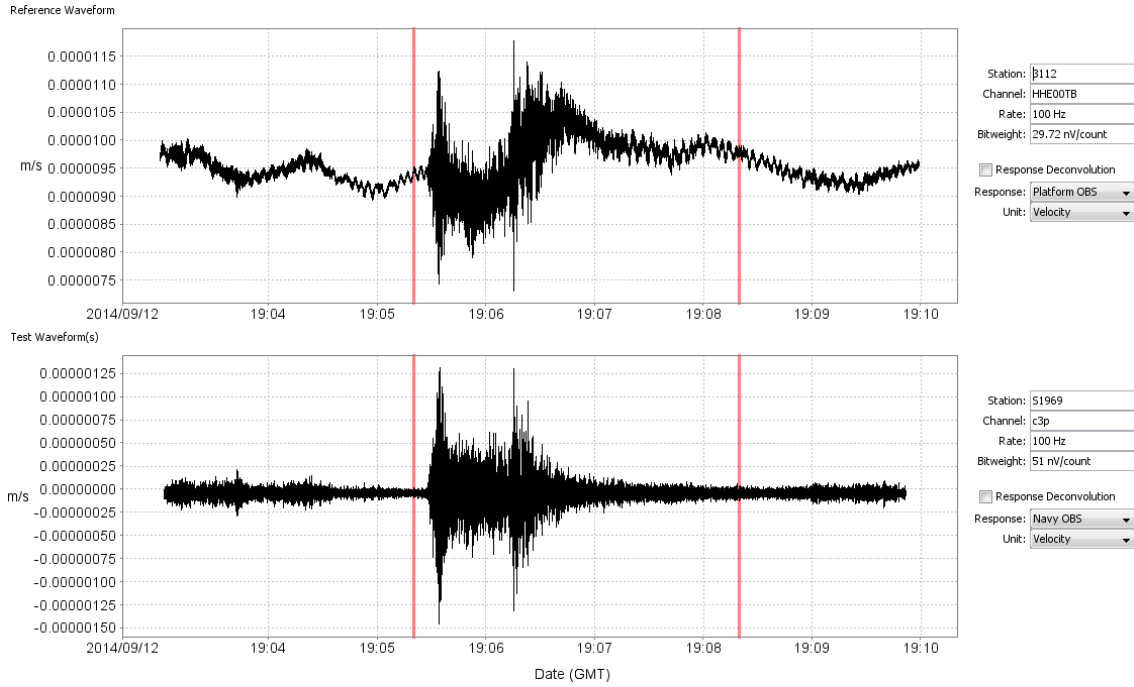


Figure 194 Seafloor, Geophone, East Waveforms

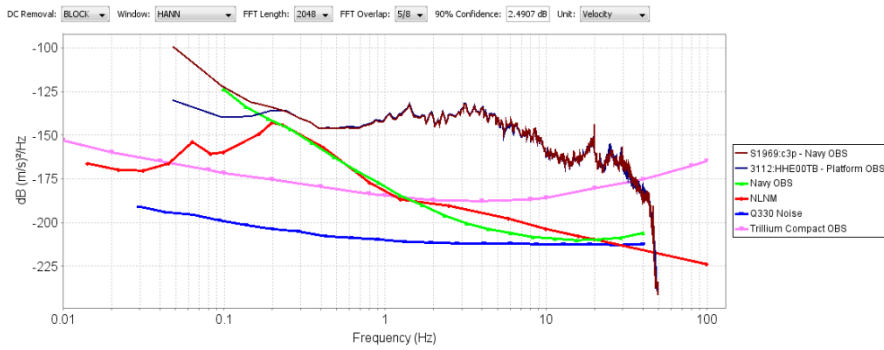


Figure 195 Seafloor, Geophone, East Power Spectra

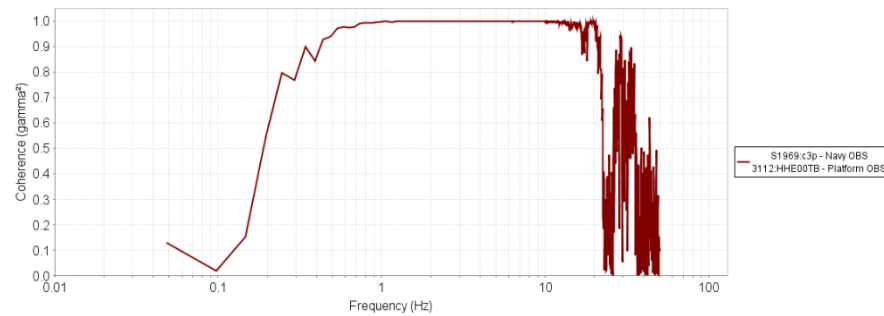
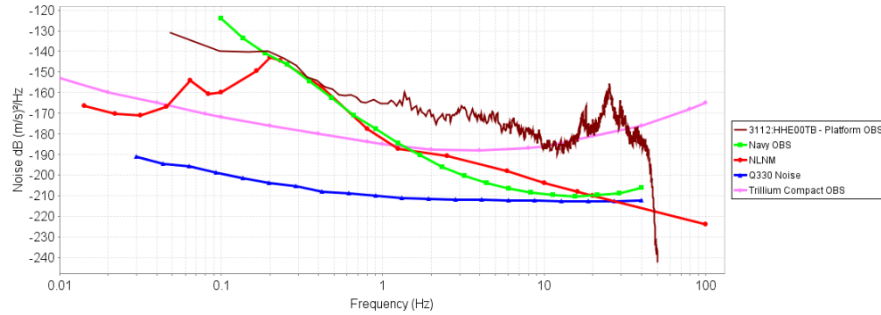
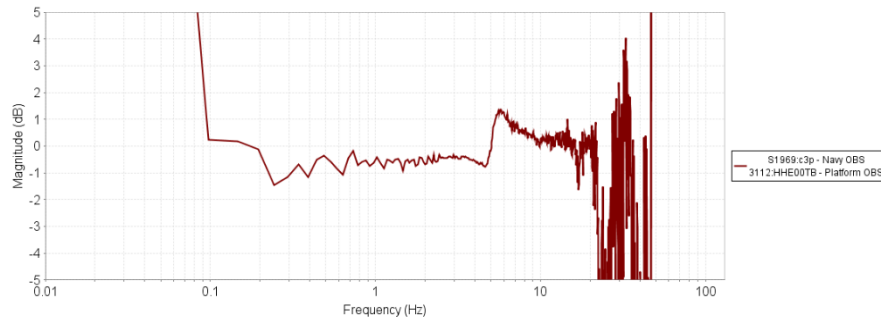


Figure 196 Seafloor, Geophone, East Coherence



**Figure 197 Seafloor, Geophone, East Incoherent Noise**



**Figure 198 Seafloor, Geophone, East Magnitude Response**

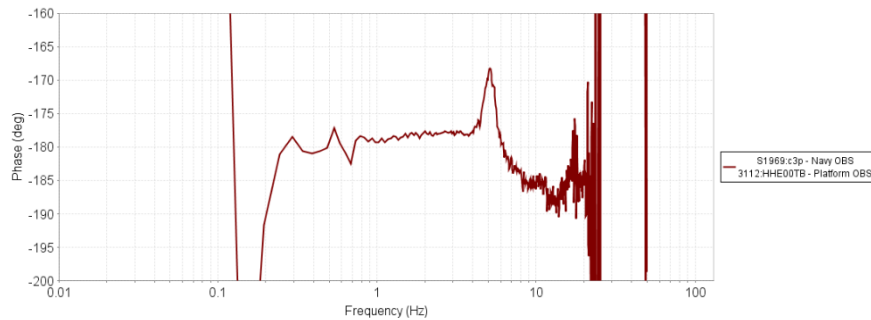


**Figure 199 Seafloor, Geophone, East Phase Response**

We see that the east channels have good coherence between approximately 0.8 and 15 Hz. Beyond those bounds, the coherence decreases rapidly. The magnitude and phase response are observed to deviate between +1/-1 dB and +12.5/-2.5 degrees, respectively, over that passband to the limits of the available spectral resolution. The magnitude and phase responses have an observed transition at approximately 5 Hz, likely due to the complicated response function of the Navy OBS having multiple geophones connected in series. Note from the phase response plot it appears that the east channel of the Navy OBS is connected with reverse polarity.

### 3.4.3 Cross-Axis Coupling

The cross-axis coupling will be evaluated by examining the coherence between the pairs of axis on each of the sensors in the test using the Sleemen 3-channel coherence technique. Changes in the cross-axis coupling across the varying test conditions will be compared. For this analysis 10 hours of background on September 13, 2014 from 04:00 – 14:00 GMT was used.

The power spectra and coherence are shown below for each of reference, seafloor, and Trillium OBS platform, and Navy OBS platform channels. Two plots were generated for each of the sensors: The first with a long window length for low frequencies below 0.1 Hz and the second with a short window length for high frequencies above 0.1 Hz.

The reference and seafloor Trillium OBSs appear to have a significant increase in coupling between the horizontal channels at frequencies below 0.1 Hz. However, the seafloor OBS has significantly more coupling. Otherwise, the axes do not appear to have any significant coherence. Both of these sensors are in direct contact with the seafloor material.

The platform Trillium OBS does not have an increase in horizontal axes coupling until below 0.03 Hz. It appears that the Underwater Platform is contributing in decreasing the horizontal axes coupling.

The platform Navy OBS does not have a similar increase in horizontal axes coupling. However, the observed frequency band in which coupling is occurring is so far outside of the Navy OBS low frequency corner at 4 Hz that it would not be expected to.

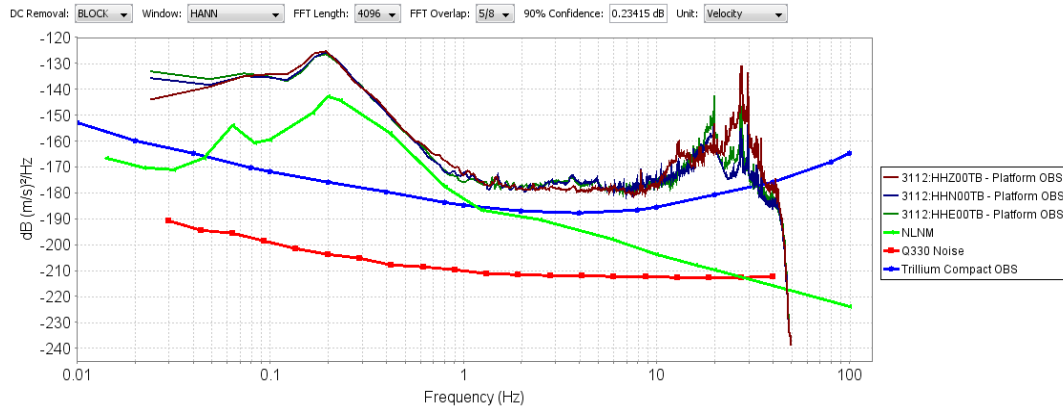
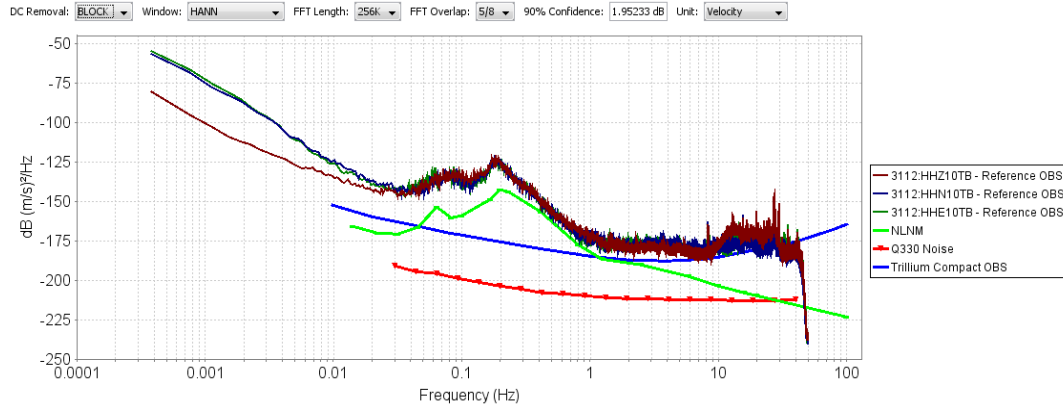


**Figure 200 Seafloor, Cross-Axis Coupling, Reference Power Spectra**

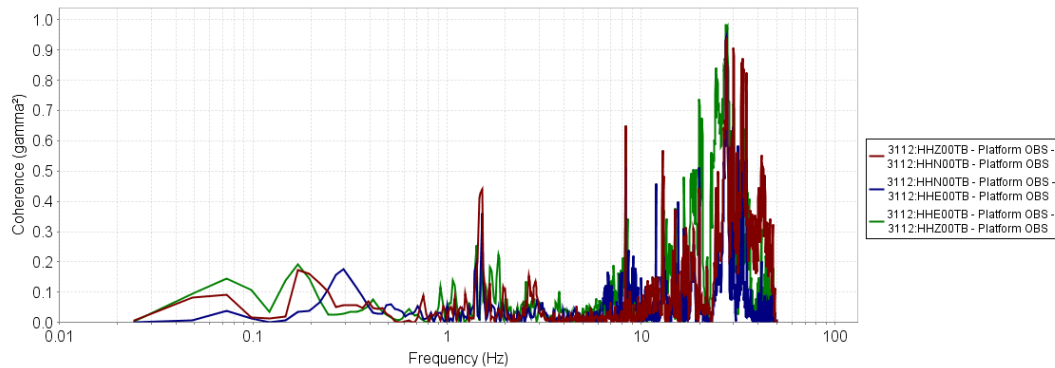
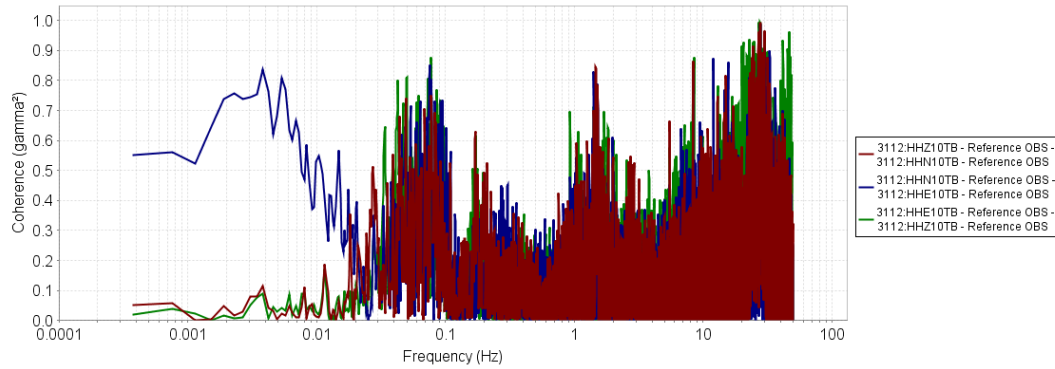


**Figure 201 Seafloor, Cross-Axis Coupling, Reference Coherence**

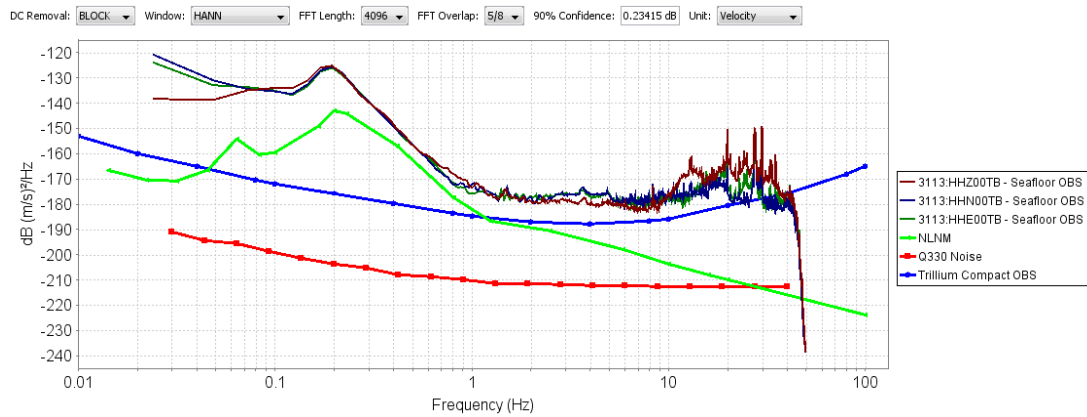
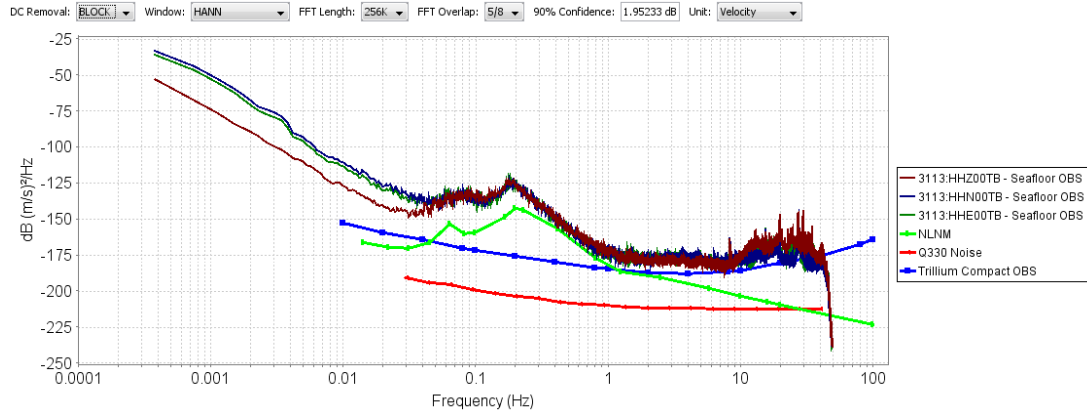


**Figure 202 Seafloor, Cross-Axis Coupling, Seafloor Power Spectra**

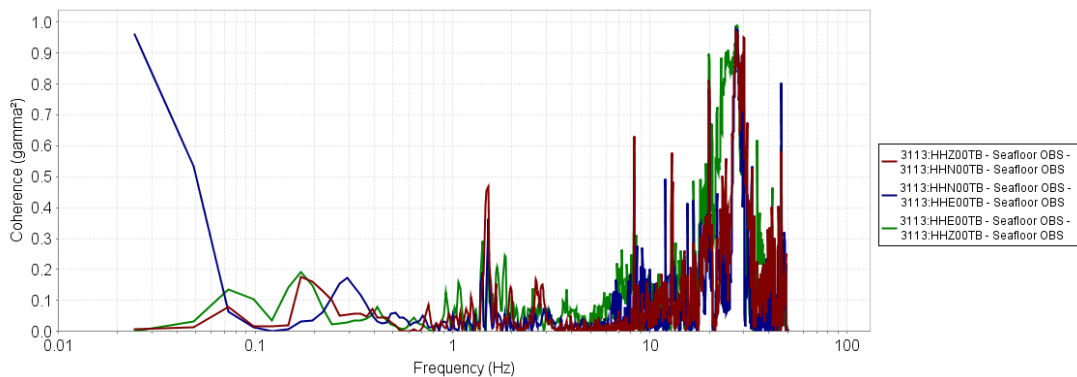
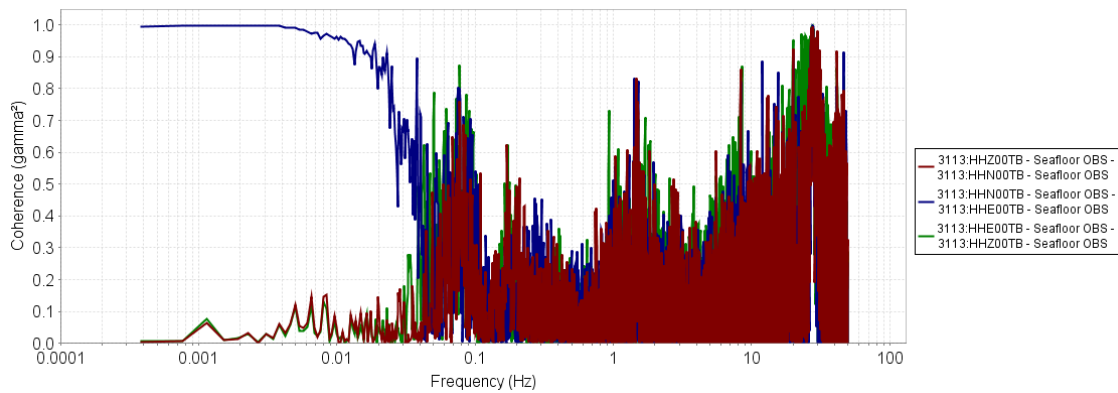


**Figure 203 Seafloor, Cross-Axis Coupling, Seafloor Coherence**

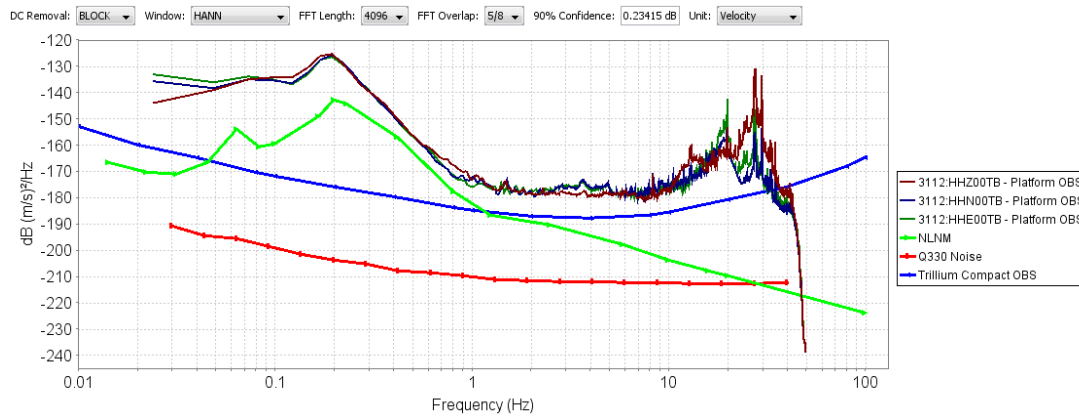
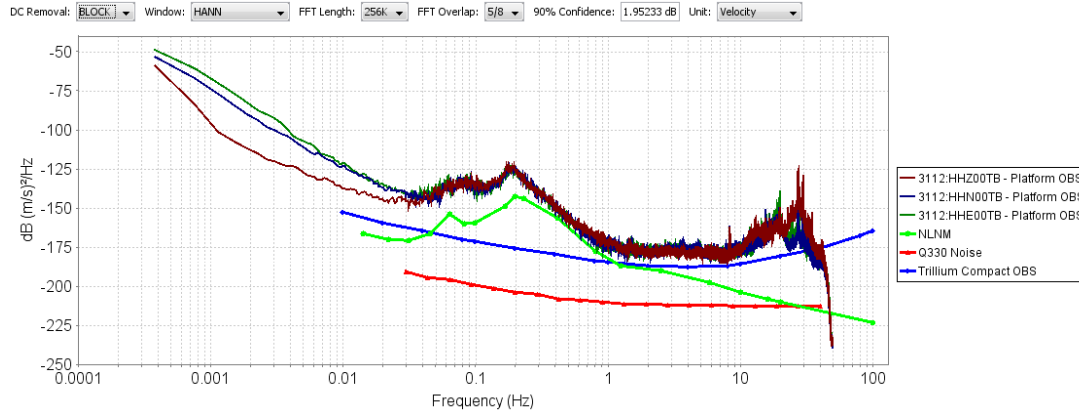


**Figure 204 Seafloor, Cross-Axis Coupling, Trillium OBS Platform Power Spectra**

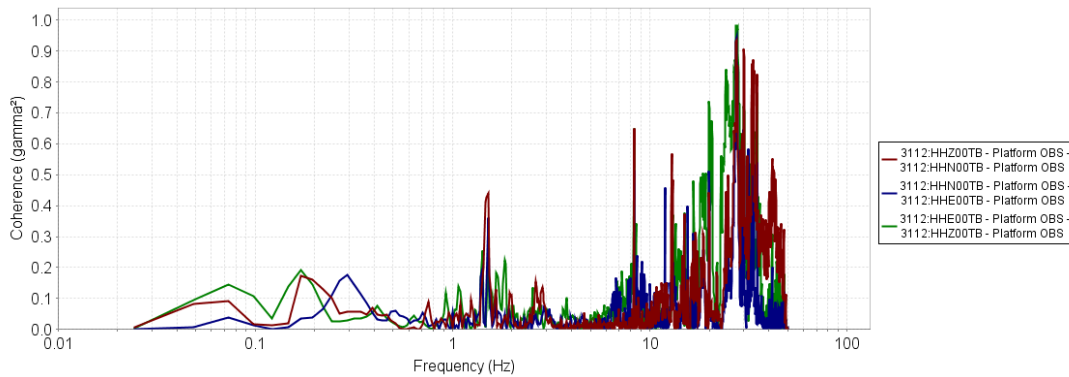
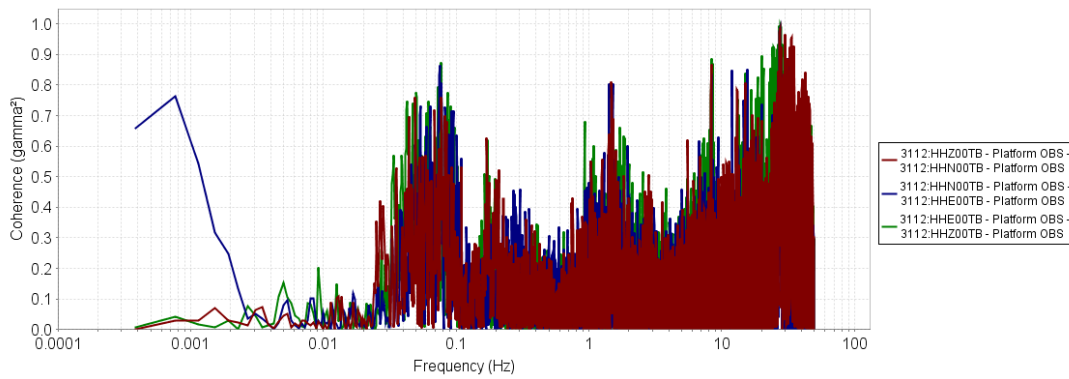


**Figure 205 Seafloor, Cross-Axis Coupling, Trillium OBS Platform Coherence**

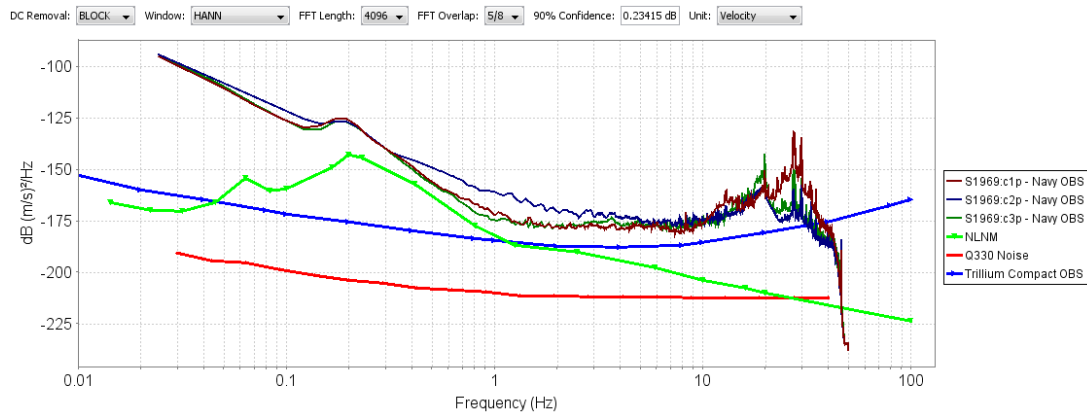
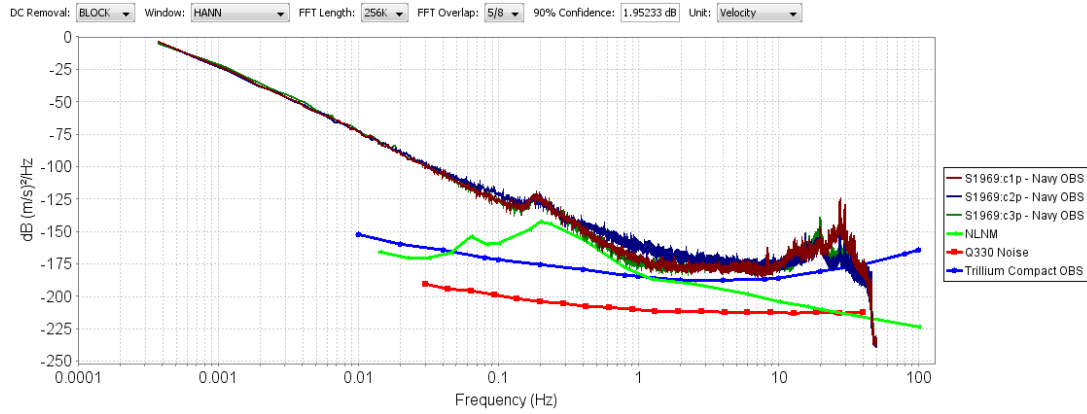


**Figure 206 Seafloor, Cross-Axis Coupling, Navy OBS Platform Power Spectra**

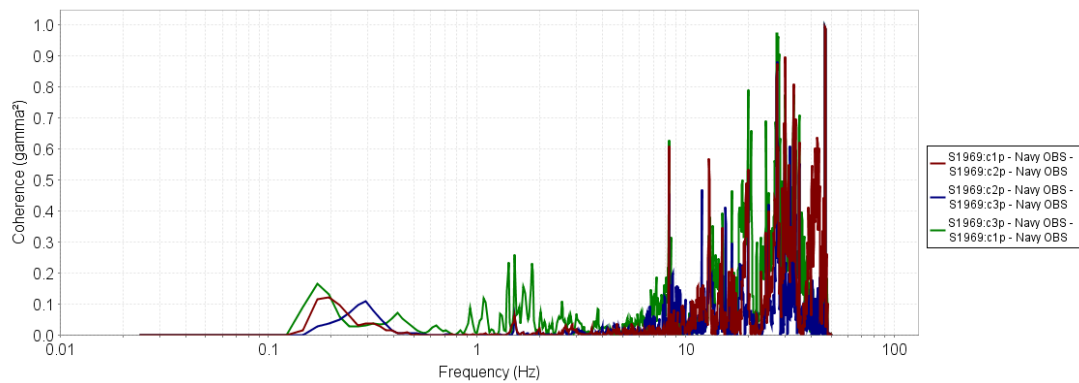
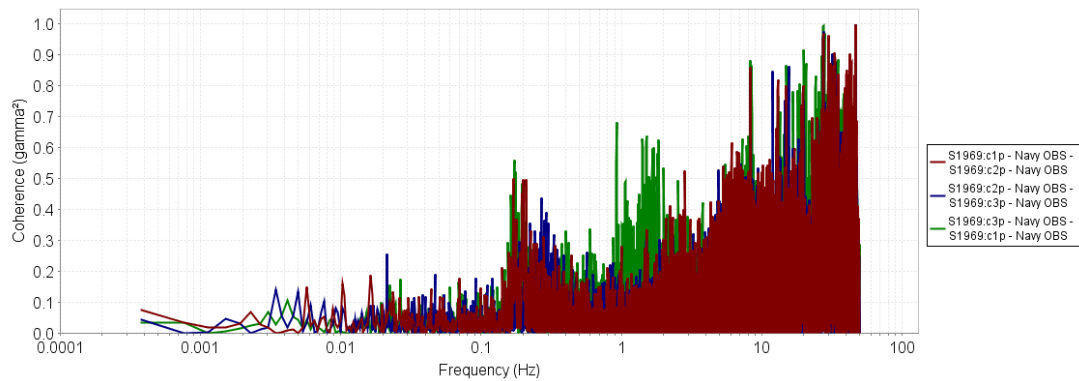


**Figure 207 Seafloor, Cross-Axis Coupling, Navy OBS Platform Coherence**

#### *3.4.4 Bubble Test*

A Bubble Test was performed on September 19, 2014 from approximately 15:52 – 16:00 (GMT) in which air was released from a hose within the water filled Test Pool. The purpose of the Bubble Test was to introduce “noise” in the water environment that was not due to ground motion and observe its effect on the sensors. Specifically, how susceptible the sensors on the platform are to water noise. Analysis of the test data will examine the power spectra and coherence between the Trillium Compact OBS on the Underwater Platform and the Seafloor Material.

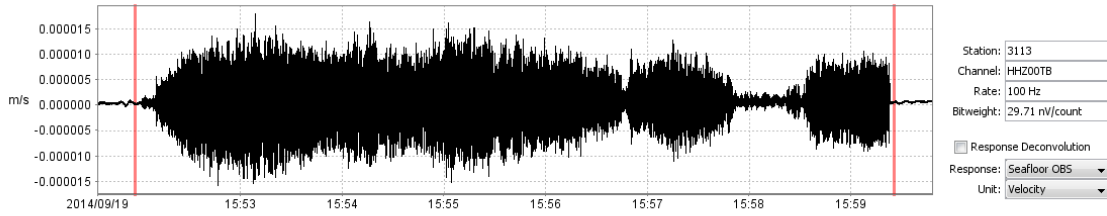
We observe that on all three axis of motion that on both the OBS on the Underwater Platform and the Seafloor Material there is increased signal above background at around 20 Hz and then between 35 and 45 Hz.

At 20 Hz, similar to what was observed in the transfer function analysis, there appears to be a resonant mode present in the horizontal axis of the Underwater Platform and Seafloor Material signals. The resonance is more significant on the Underwater Platform.

For the signal at 35 to 45 Hz, the Underwater Platform and Seafloor Material signals appear to be fairly consistent with good coherence between them.

### 3.4.4.1 Vertical

Reference Waveform



Test Waveform(s)

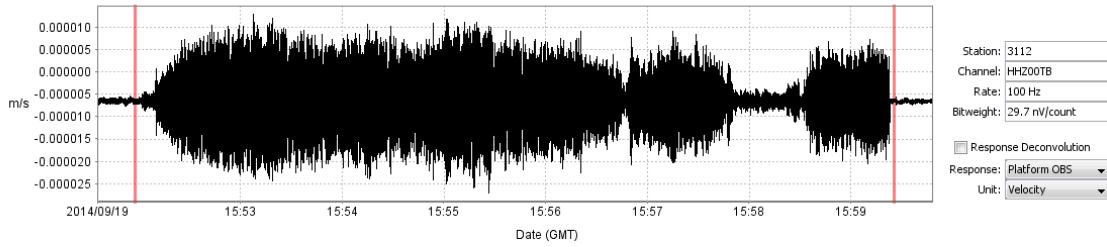


Figure 208 Seafloor, Bubble, Vertical Waveforms

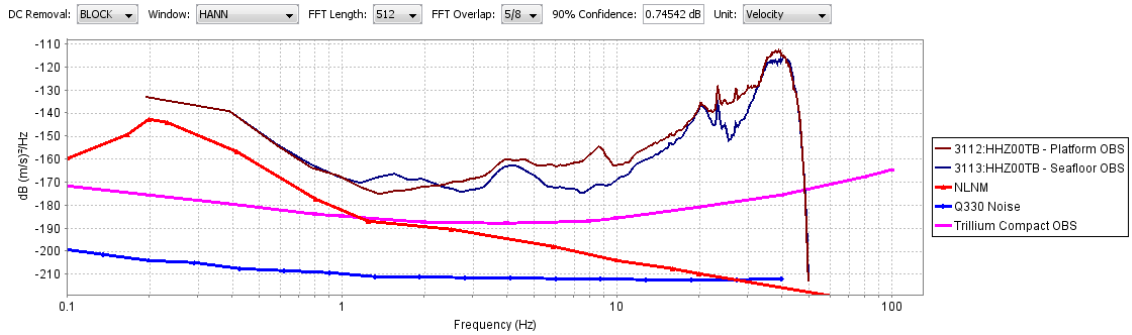


Figure 209 Seafloor, Bubble, Vertical Power Spectra

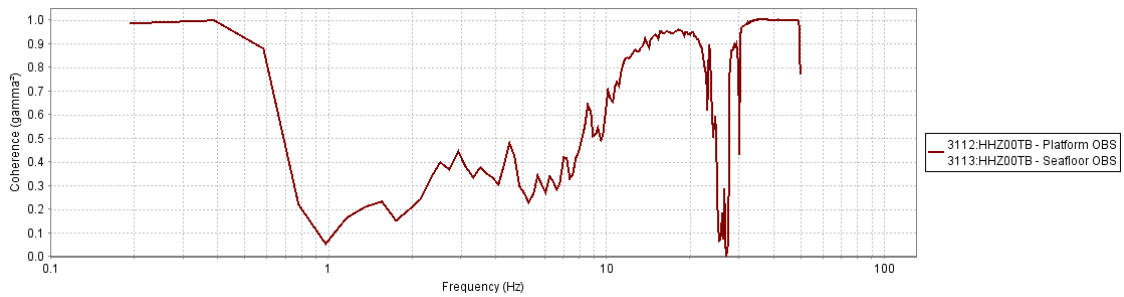


Figure 210 Seafloor, Bubble, Vertical Coherence

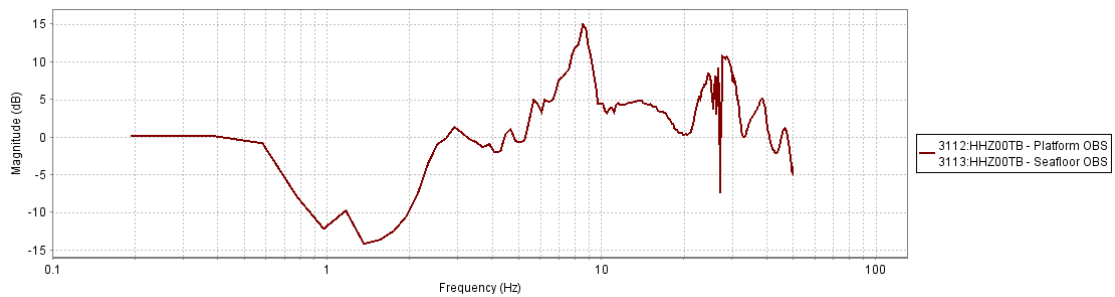


Figure 211 Seafloor, Bubble, Vertical Magnitude Response

### 3.4.4.2 North

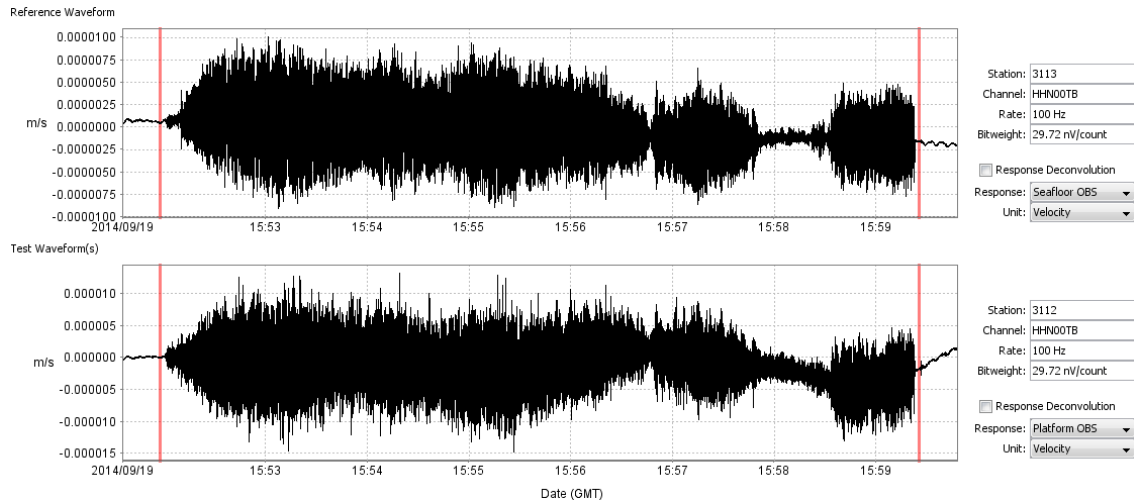


Figure 212 Seafloor, Bubble, North Waveforms

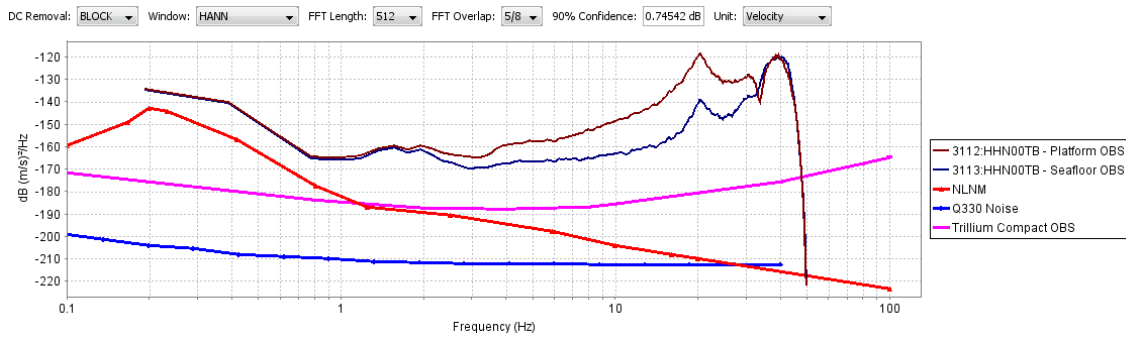


Figure 213 Seafloor, Bubble, North Power Spectra

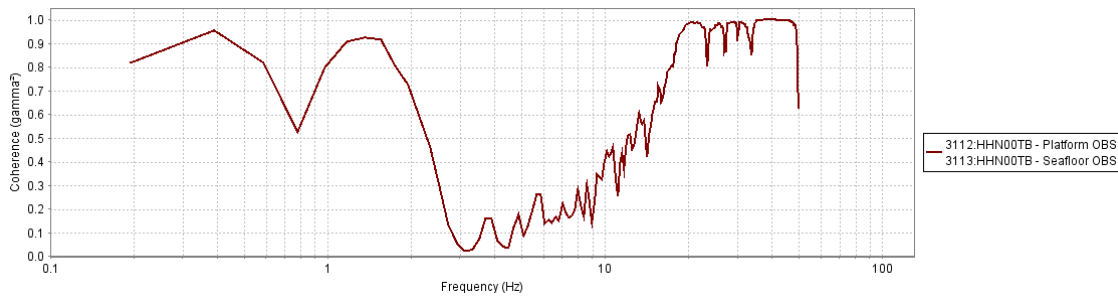


Figure 214 Seafloor, Bubble, North Coherence

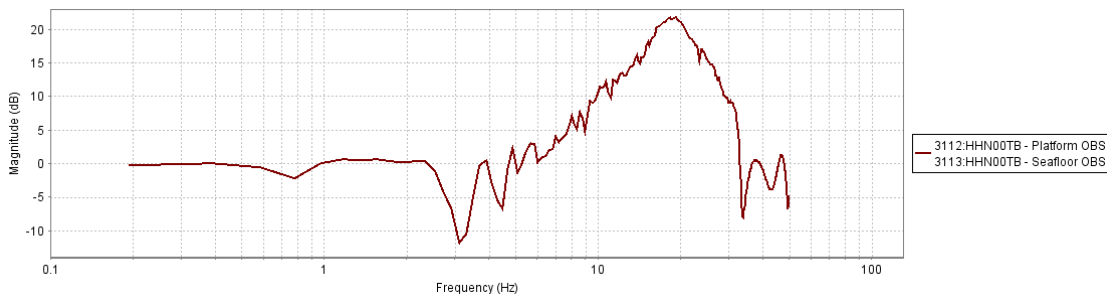
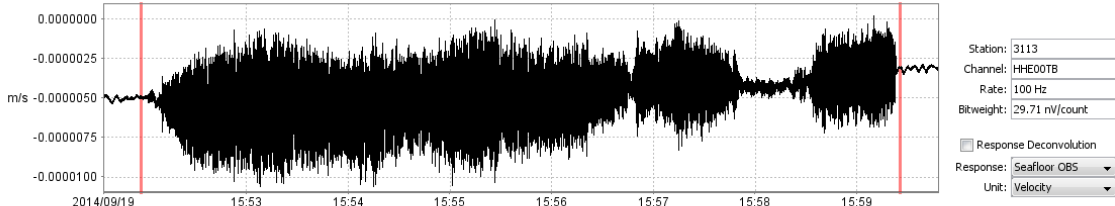


Figure 215 Seafloor, Bubble, North Magnitude Response

### 3.4.4.3 East

Reference Waveform



Test Waveform(s)

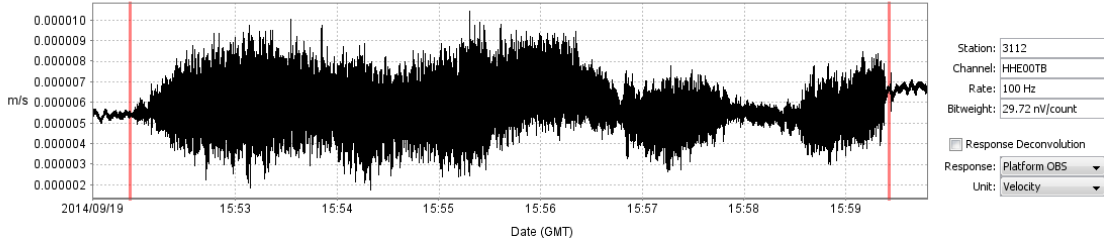


Figure 216 Seafloor, Bubble, East Waveforms

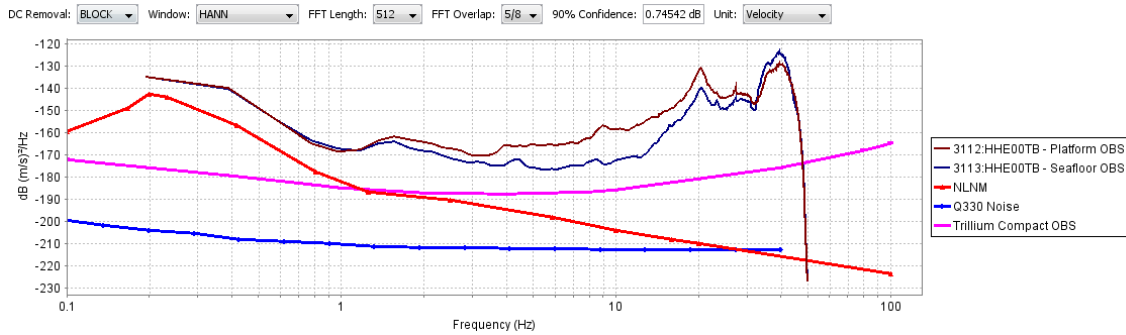


Figure 217 Seafloor, Bubble, East Power Spectra

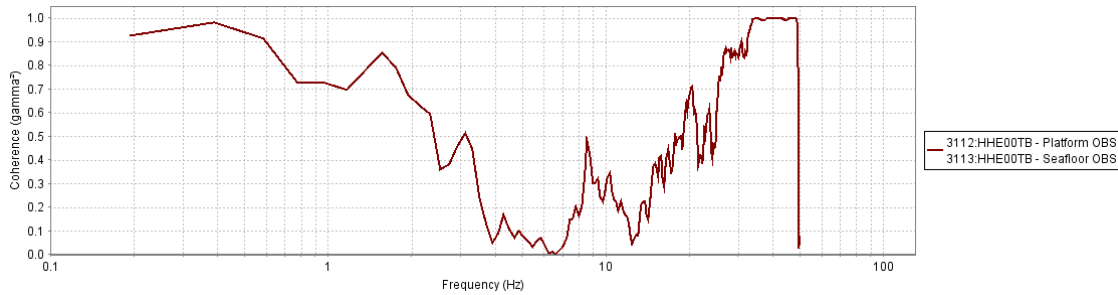


Figure 218 Seafloor, Bubble, East Coherence

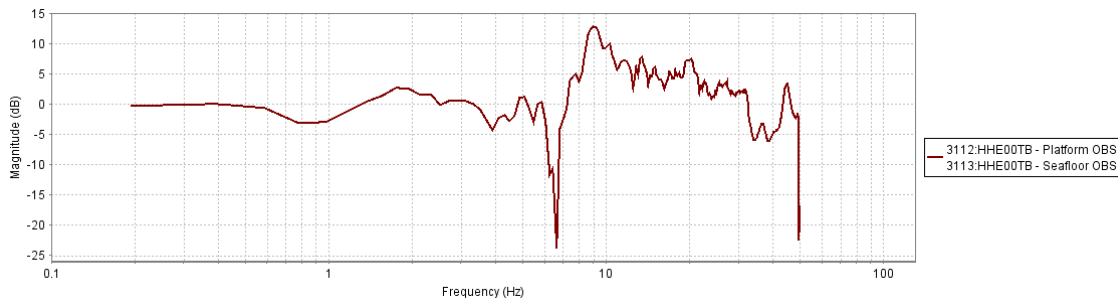


Figure 219 Seafloor, Bubble, East Magnitude Response

### 3.5 Wet Seafloor Platform with Backfill Testing

The wet seafloor test was performed with the reference Nanometrics Trillium OBS in direct contact with the bottom of the Test Pool. The bottom of the Test Pool was covered with Seafloor Material and the Underwater Platform was then placed on the Seafloor Material. The Test Pool was then filled with water. The Underwater Platform was backfilled with glass bead material.

The results of this test will be used to comment on any affect that the addition glass beads have on the sensor performance. The glass beads are intended to fill the volume surrounding the OBS and reduce the flow of water, and any resulting noise, around the sensor. Test data was collected for this test from September 20, 2014 to October 3, 2014.



Figure 220 Wet Seafloor with Backfill Photo

IV&V 5e Wet Platform Testing (simulated seafloor)  
Glass beads installed in Underwater Platform

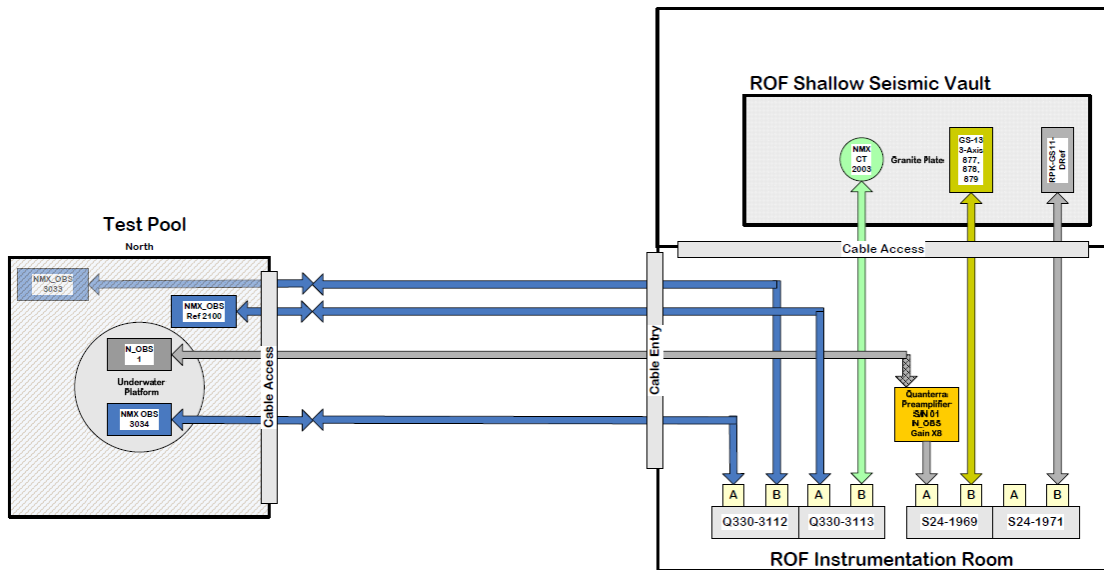


Figure 221 Wet Seafloor Platform with Backfill Testing Diagram (RPKromer Consulting)

### 3.5.1 Transfer Function

Analysis of the test data will examine coherence between the reference OBS and the OBS on the Underwater Platform. A single event was identified for this analysis on September 25, 2014 at 18:00 (GMT) with duration of 20 minutes and frequency content above the site noise at frequencies below 3 Hz. There were no other signals of significance for analysis within this time period.

Coherence analysis for these events was performed for each of the Vertical, North, and East channels of the reference OBS, the OBS directly on the Seafloor Material, and the OBS on the Underwater Platform.

#### 3.5.1.1 Vertical

Note that data from the Seafloor OBS vertical channel was not available for this time period.

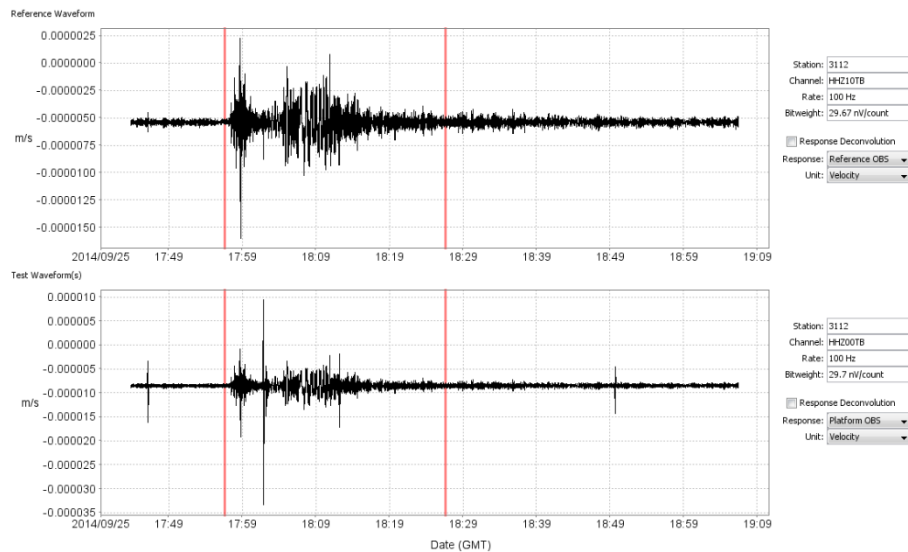


Figure 222 Backfill, Transfer Function, Vertical Waveforms

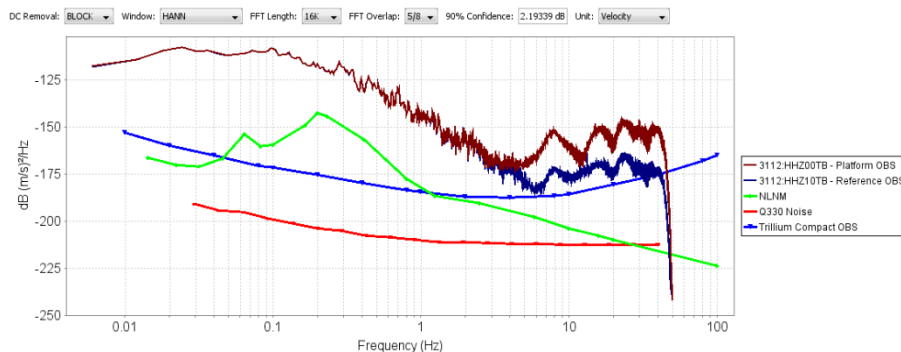
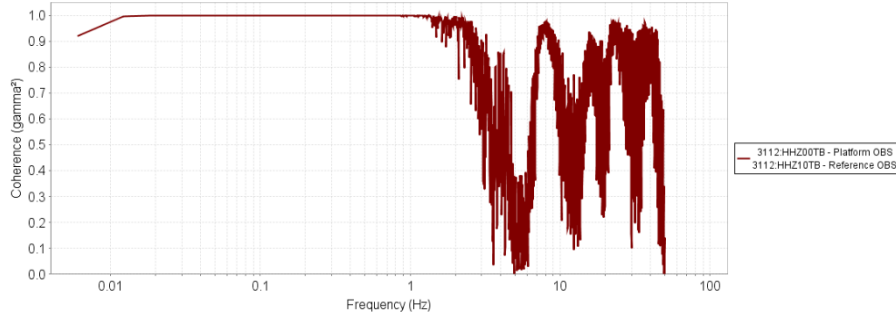
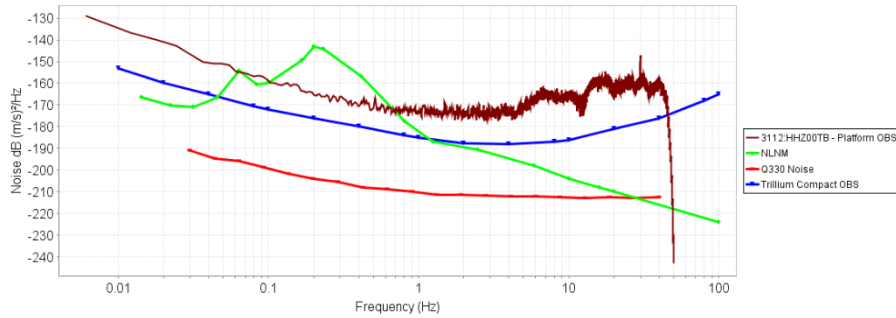


Figure 223 Backfill, Transfer Function, Vertical Power Spectra



**Figure 224 Backfill, Transfer Function, Vertical Coherence**



**Figure 225 Backfill, Transfer Function, Vertical Incoherent Noise**

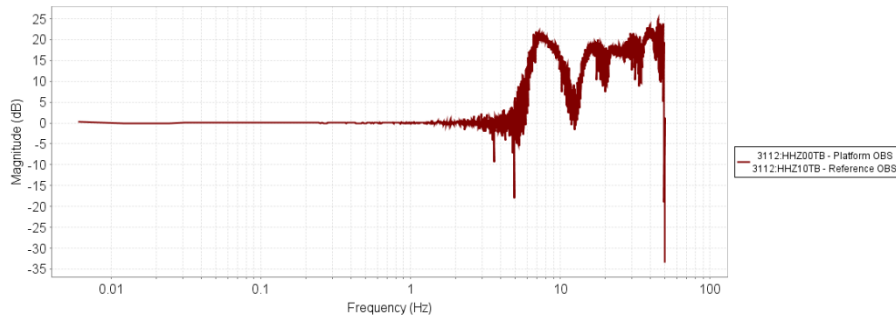


**Figure 226 Backfill, Transfer Function, Vertical Magnitude Response**

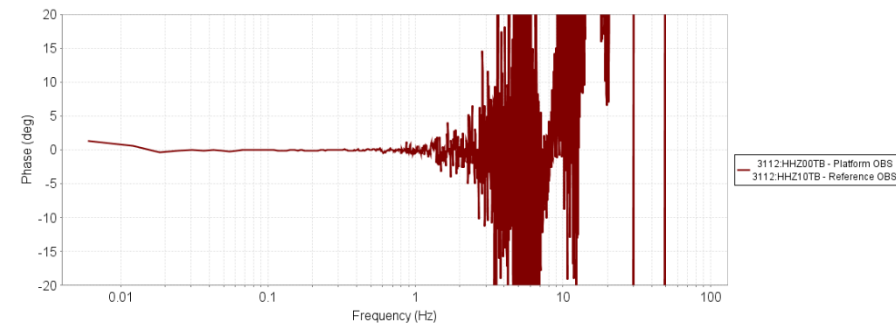


**Figure 227 Backfill, Transfer Function, Vertical Phase Response**

We see that the vertical channels have good coherence between approximately 0.012 and 1.2 Hz for this event. Beyond those bounds, the coherence degrades rapidly. There is minimal difference in the amplitude and phase response over that passband to the limits of the available spectral resolution.

The power spectra indicates that the Platform OBS is recording signals well above the Reference OBS above 4 Hz. However, the poor coherence between the two sensors at frequencies above 1.2 Hz makes it difficult to make any determination of resonance. There are some peaks in the spectral coherence, most notably at 8 Hz, 16 Hz, 24 Hz and 40 Hz, where the coherence levels are reasonably high (above 0.9). At these frequencies, the magnitude response indicates that the platform OBS is measuring signals approximately 20 dB greater than the reference OBS. The amplified magnitude response with high level of coherence demonstrates evidence of resonance at these higher frequencies. In addition, much of the elevated signal levels above 5 Hz are incoherent with the Reference OBS, indicating that there may be noise introduced by the platform or backfill material.

### 3.5.1.2 North

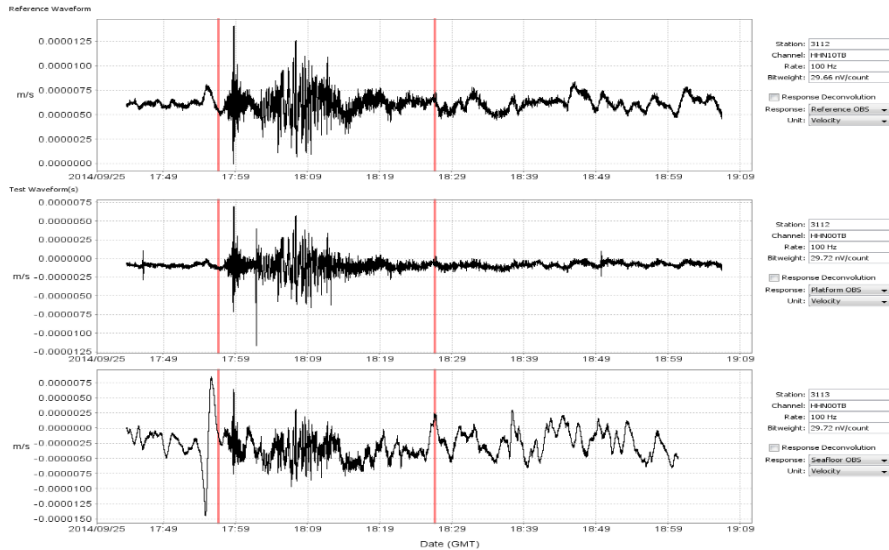


**Figure 228 Backfill, Transfer Function, North Waveforms**

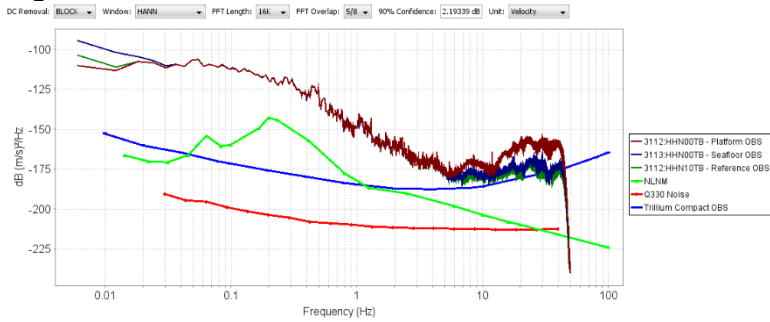


**Figure 229 Backfill, Transfer Function, North Power Spectra**

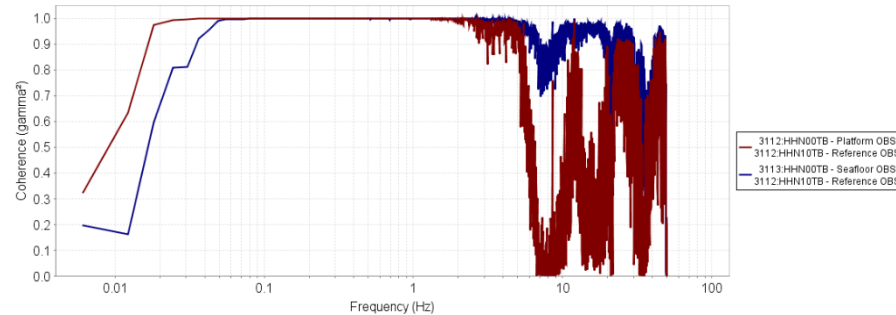


**Figure 230 Backfill, Transfer Function, North Coherence**

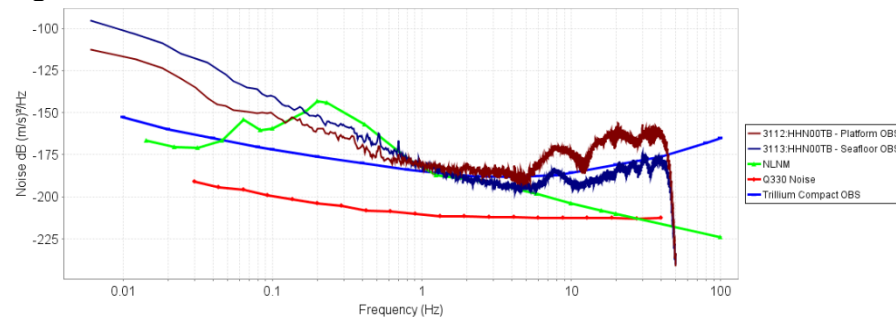


**Figure 231 Backfill, Transfer Function, North Incoherent Noise**

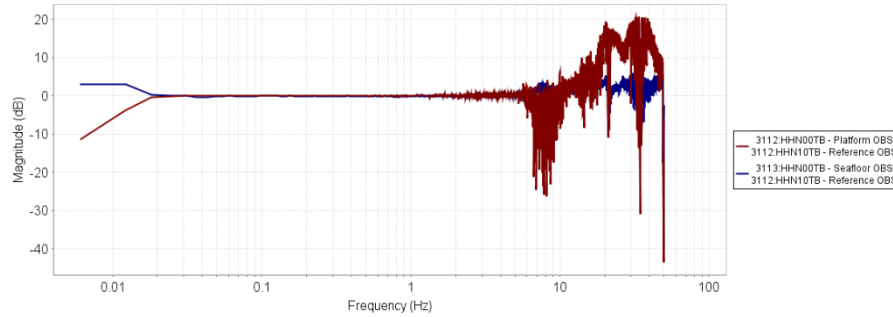


**Figure 232 Backfill, Transfer Function, North Magnitude Response**

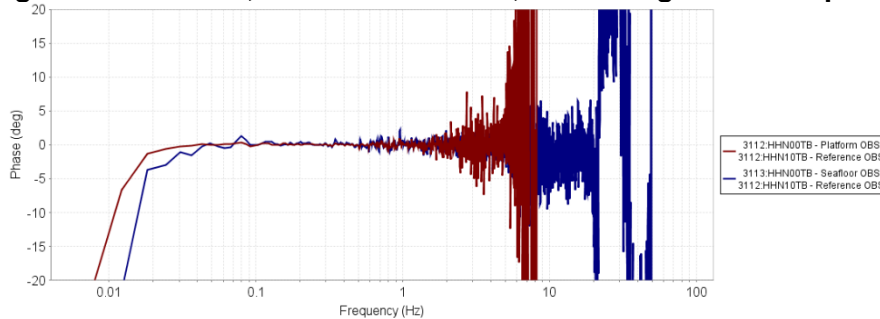


**Figure 233 Backfill, Transfer Function, North Phase Response**

We see that the north channels have good coherence between 0.03 and 2.5 Hz for the Platform OBS and between 0.07 and 4 Hz for the Seafloor OBS. Beyond those bounds, the coherence decreases rapidly. There is minimal difference in the amplitude and phase response over that passband to the limits of the available spectral resolution. The platform does appear to be improving coupling at frequencies below 0.07 Hz.

The power spectra indicates that the Platform OBS is recording signals well above the Reference OBS above 5 Hz. However, the poor coherence between the two sensors at frequencies above 2.5 Hz makes it difficult to make any determination of resonance. There are some peaks in the spectral coherence, most notably at 12 Hz, 24-30 Hz, and 45 Hz, where the coherence levels are reasonably high (above 0.9). At these frequencies, the magnitude response indicates that the platform OBS is measuring signals at least 20 dB greater than the reference OBS. The amplified magnitude response with high level of coherence demonstrates evidence of resonance at these higher frequencies. In addition, much of the elevated signal levels above 5 Hz are incoherent with the Reference OBS, indicating that there may be noise introduced by the platform or backfill material.

The Seafloor OBS is much closer in comparison to the Reference OBS than the Platform OBS and does not exhibit nearly the same level of decreases in coherence or increases in the relative magnitude above 5 Hz. These differences indicate that the Platform OBS performance is due to the platform or the backfill material and not the seafloor material.

### 3.5.1.3 East

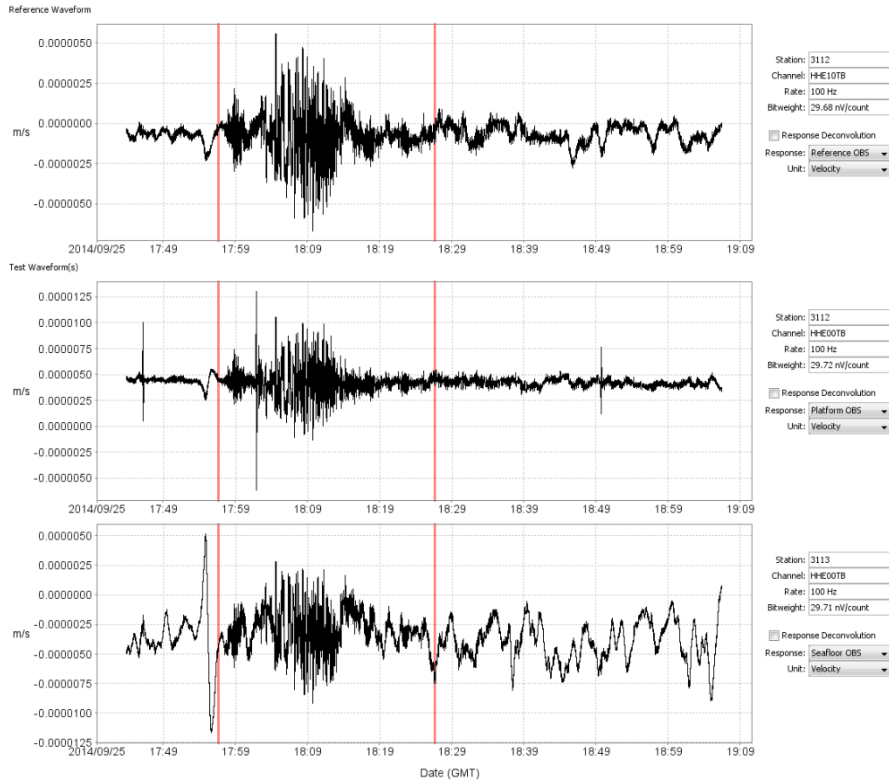


Figure 234 Backfill, Transfer Function, East Waveforms

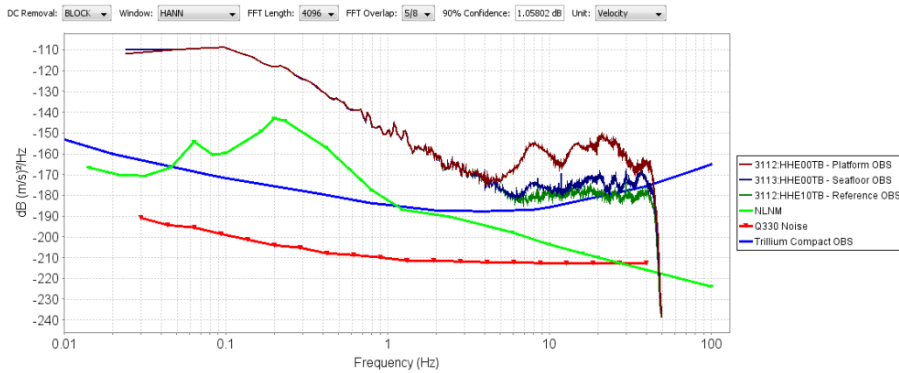


Figure 235 Backfill, Transfer Function, East Power Spectra

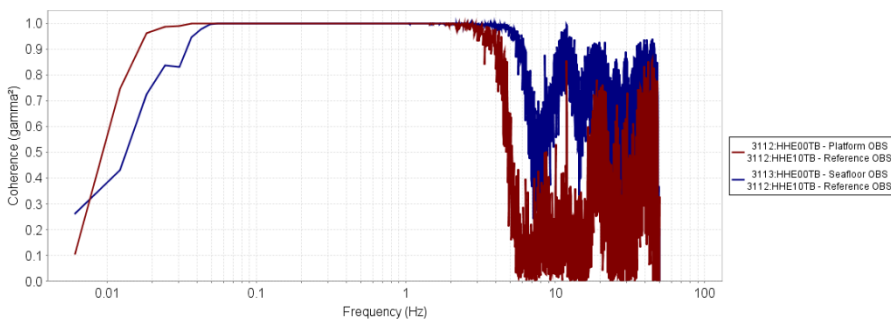
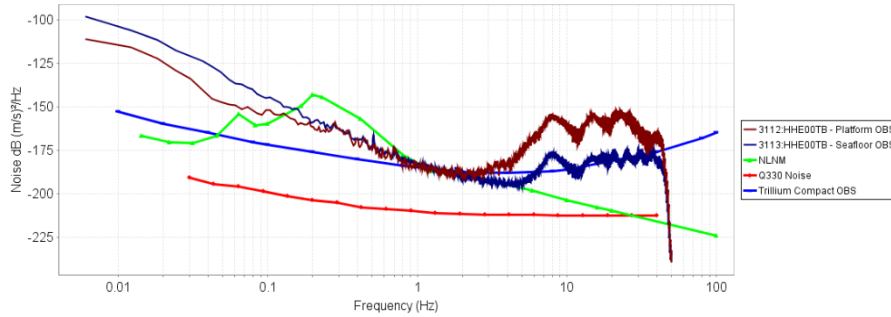
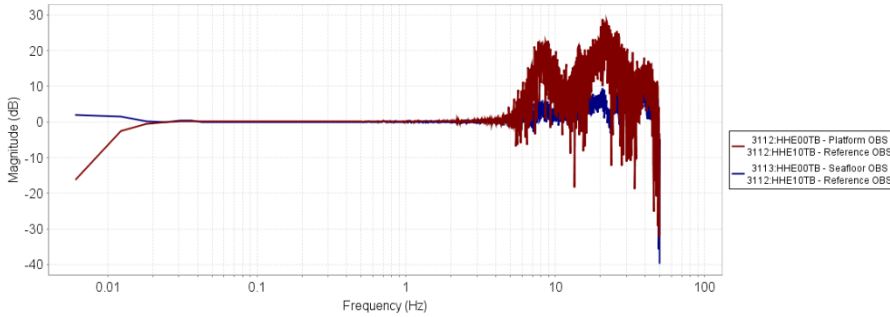


Figure 236 Backfill, Transfer Function, East Coherence



**Figure 237 Backfill, Transfer Function, East Incoherent Noise**



**Figure 238 Backfill, Transfer Function, East Magnitude Response**

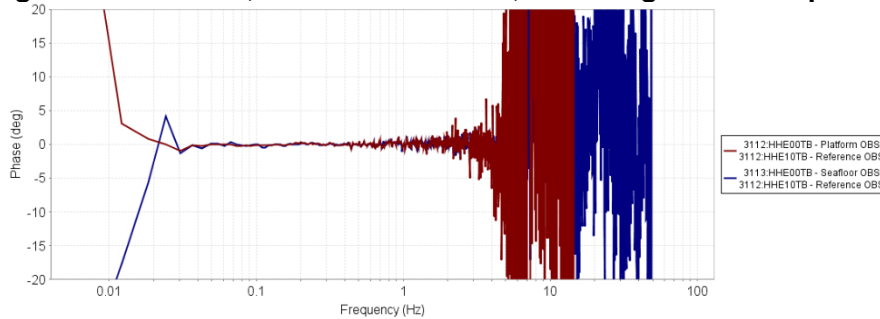


**Figure 239 Backfill, Transfer Function, East Phase Response**

We see that the east channels have good coherence between 0.03 and 2 Hz for the Platform OBS and between 0.05 and 4 Hz for the Seafloor OBS. Beyond those bounds, the coherence decreases rapidly. There is minimal difference in the amplitude and phase response over that passband to the limits of the available spectral resolution. The platform does appear to be improving coupling at frequencies below 0.05 Hz.

The power spectra indicates that the Platform OBS is recording signals well above the Reference OBS above 5 Hz. However, the poor coherence between the two sensors at frequencies above 2 Hz makes it difficult to make any determination of resonance. In addition, much of the elevated signal levels above 5 Hz are incoherent with the Reference OBS, indicating that it is noise introduced by the platform or backfill material.

The Seafloor OBS is much closer in comparison to the Reference OBS than the Platform OBS and does not exhibit nearly the same level of decreases in coherence or increases in the relative magnitude above 5 Hz. These differences indicate that the Platform OBS performance is due to the platform or the backfill material and not the seafloor material.

### 3.5.2 Cross-Axis Coupling

The cross-axis coupling will be evaluated by examining the coherence between the pairs of axis on each of the sensors in the test using the Sleemen 3-channel coherence technique. Changes in the cross-axis coupling across the varying test conditions will be compared. For this analysis 10 hours of background on September 23, 2014 from 01:00 – 11:00 GMT was used.

The power spectra and coherence are shown below for each of reference, seafloor, Trillium OBS platform, and Navy OBS platform channels. Two plots were generated for each of the sensors: The first with a long window length for low frequencies below 0.1 Hz and the second with a short window length for high frequencies above 0.1 Hz.

There appears to be a high level of cross-axis coupling between the horizontal axes below 0.1 Hz on the reference Trillium OBS that is directly coupled to the bottom of the Test Pool and the Trillium OBS directly on the seafloor material. Both of these sensors are in direct contact with Seafloor Material. Neither the Trillium OBS nor the Navy OBS on the Underwater Platform exhibit this coupling at low frequencies. The Underwater Platform appears to be reducing the degree of horizontal axis coupling at low frequencies.

Both the Trillium OBS and Navy OBS on the Underwater Platform have a significant amount of coupling between all three axes across 5 to 12 Hz. This coupling was not present in any of the prior tests; suggesting that the presence of the backfill material is responsible.

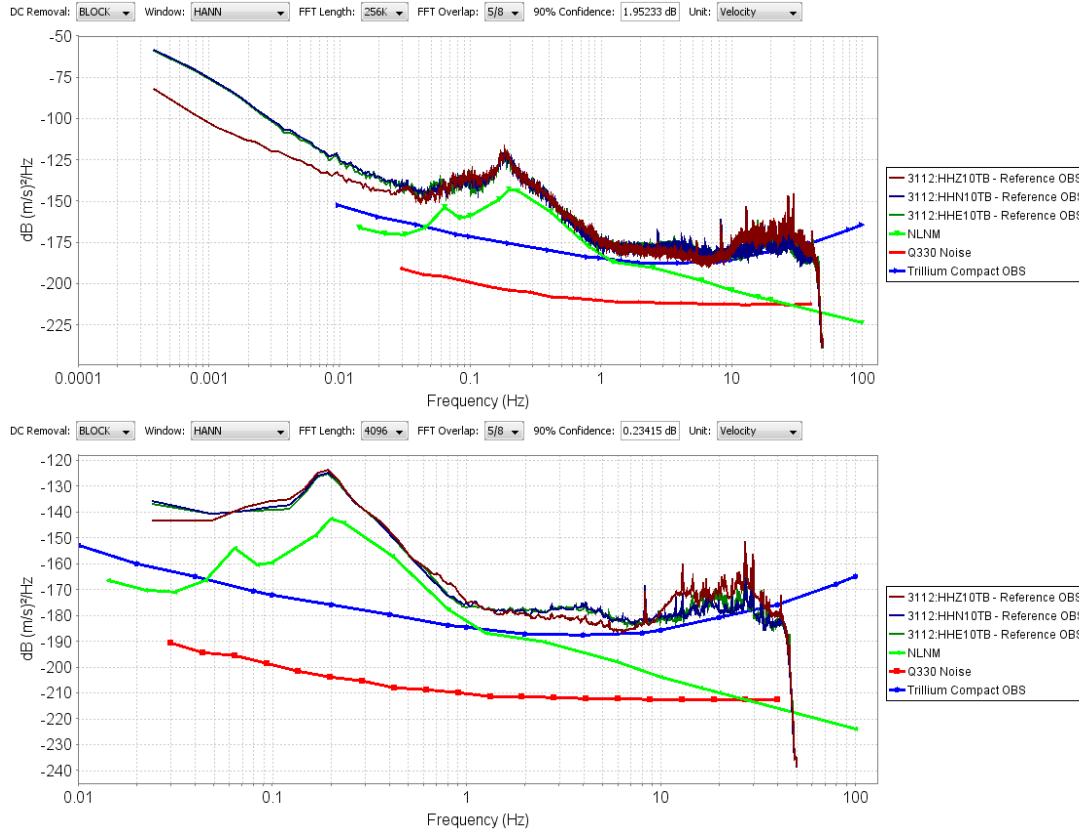


**Figure 240 Backfill Testing, Cross-Axis Coupling, Reference Power Spectra**

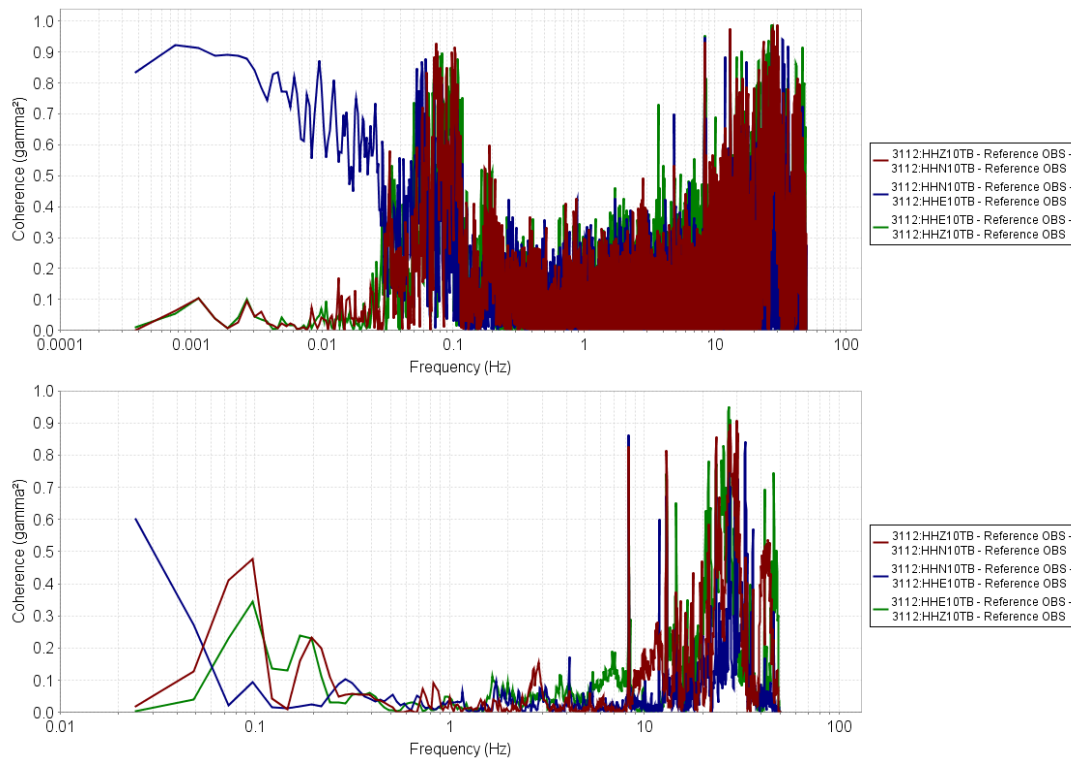


**Figure 241 Backfill Testing, Cross-Axis Coupling, Reference Coherence**

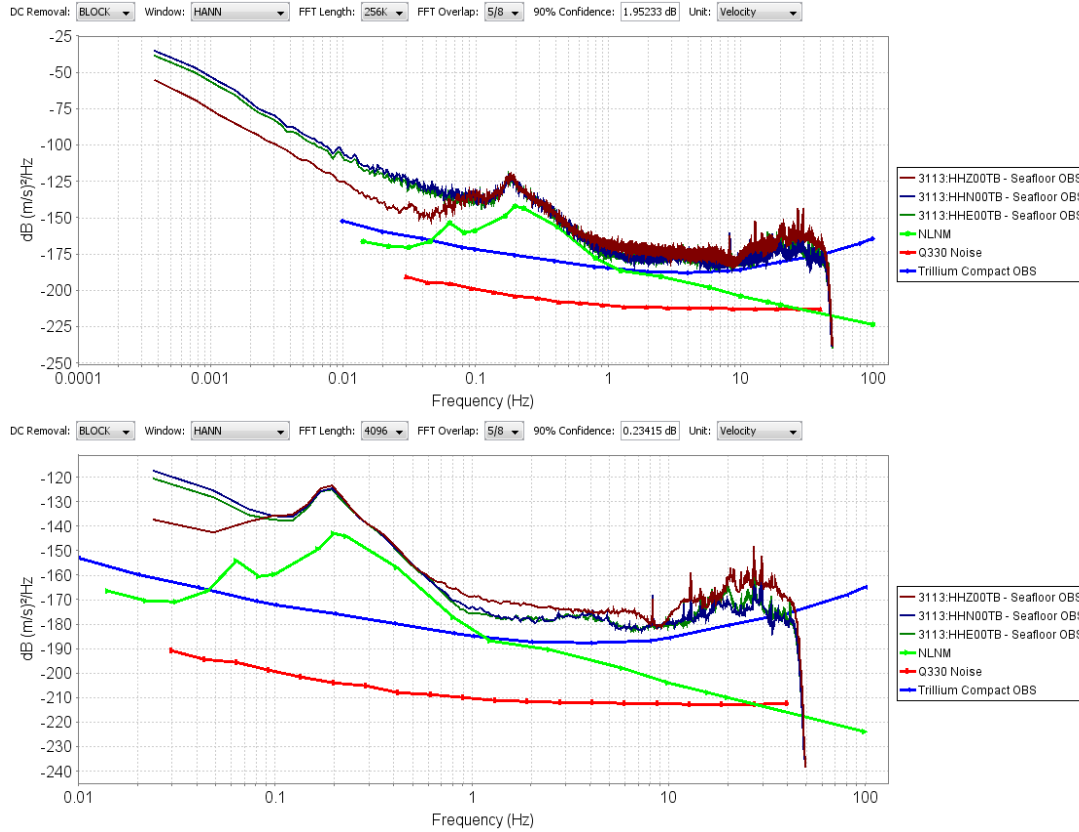


**Figure 242 Backfill Testing, Cross-Axis Coupling, Seafloor Power Spectra**

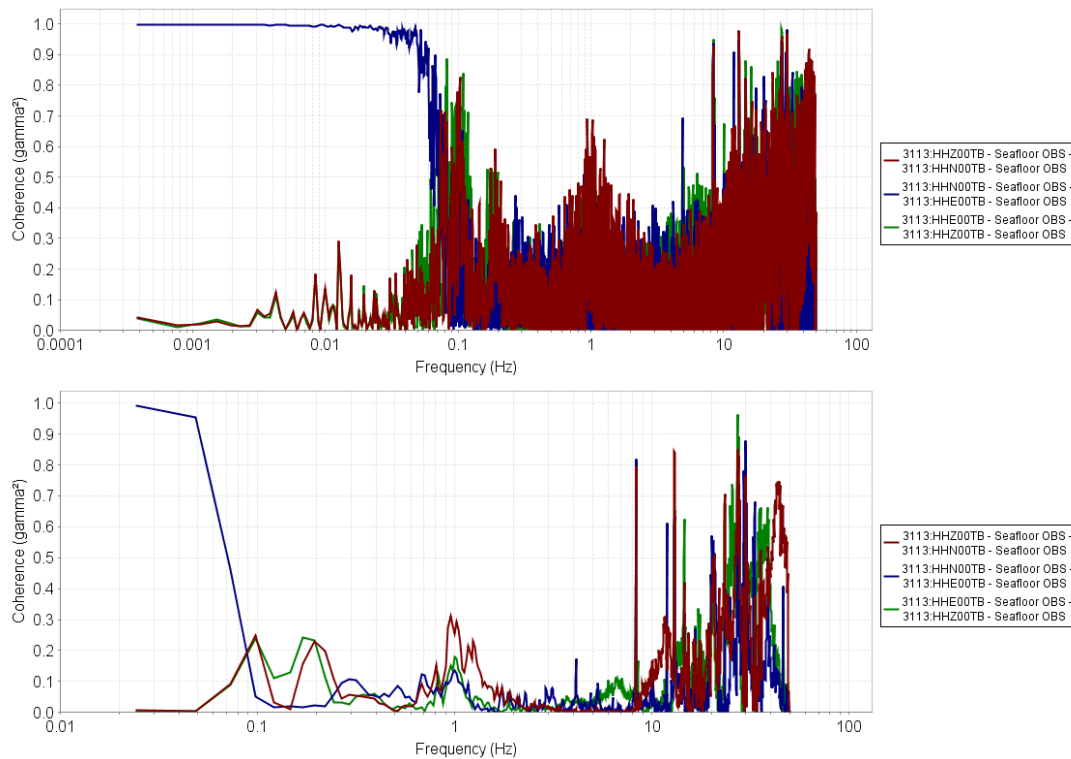


**Figure 243 Backfill Testing, Cross-Axis Coupling, Seafloor Coherence**

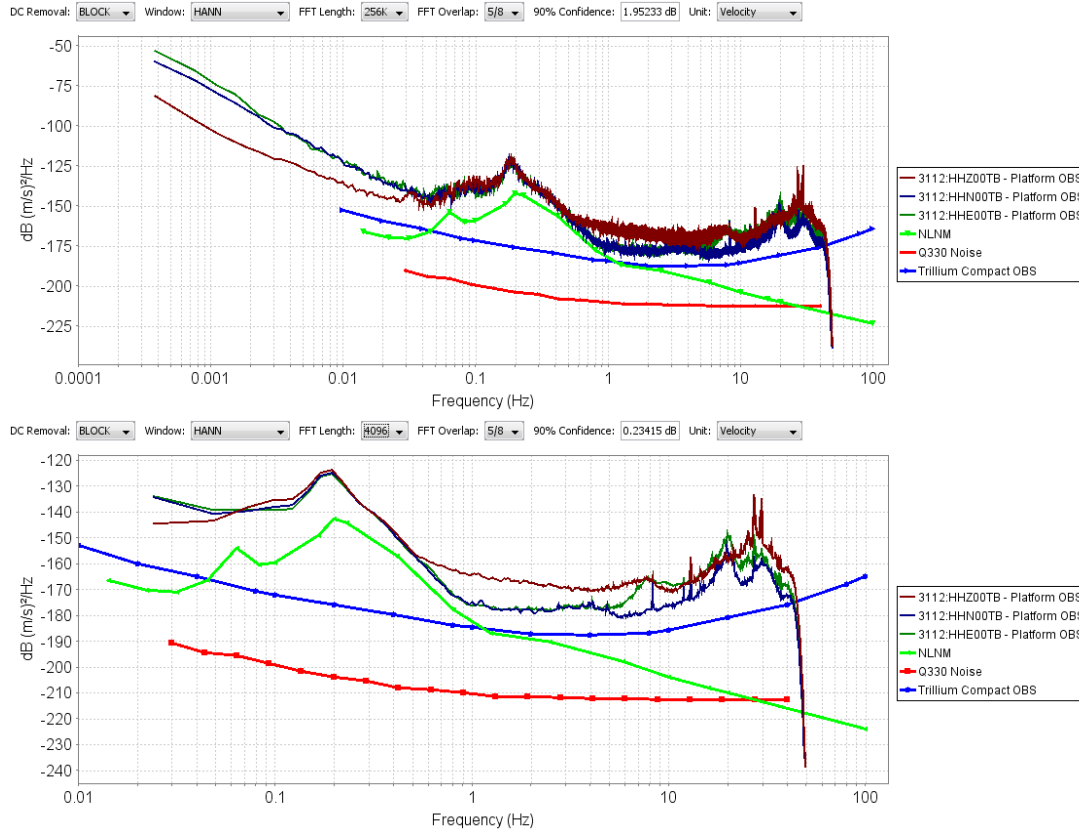


**Figure 244 Backfill Testing, Cross-Axis Coupling, Trillium OBS Platform Power Spectra**

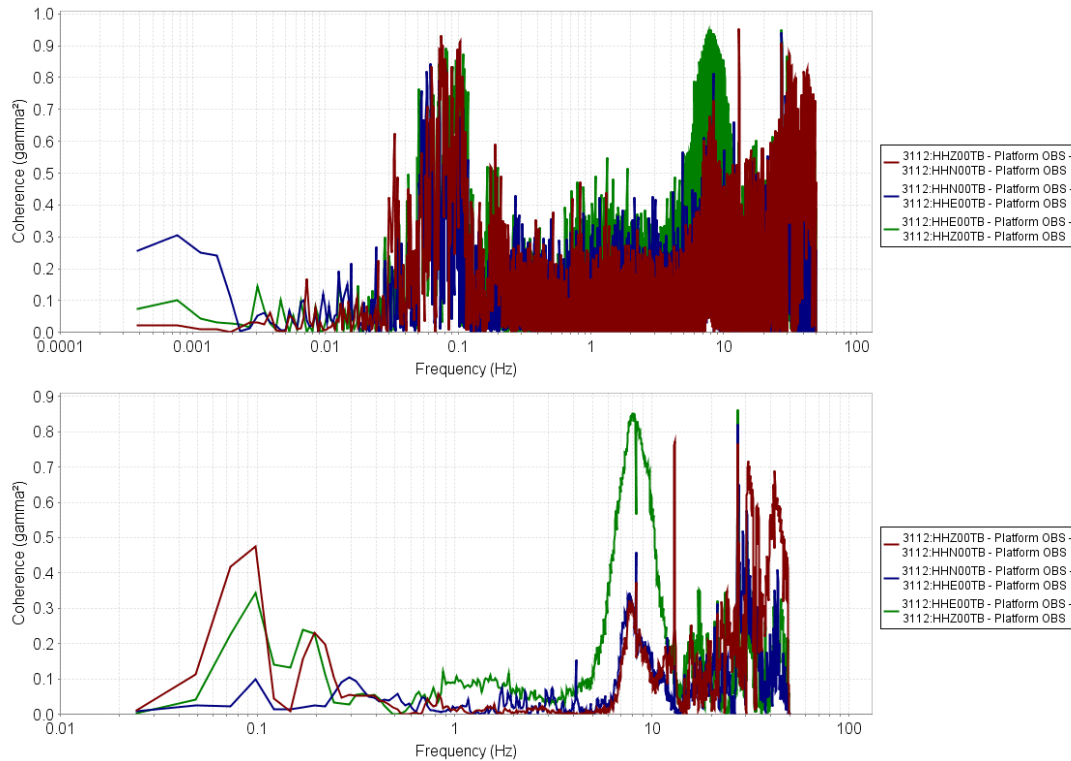


**Figure 245 Backfill Testing, Cross-Axis Coupling, Trillium OBS Platform Coherence**

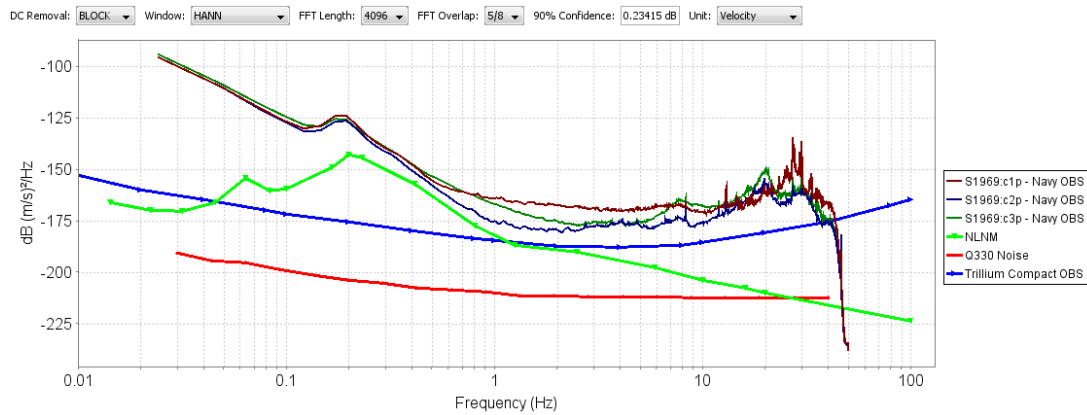
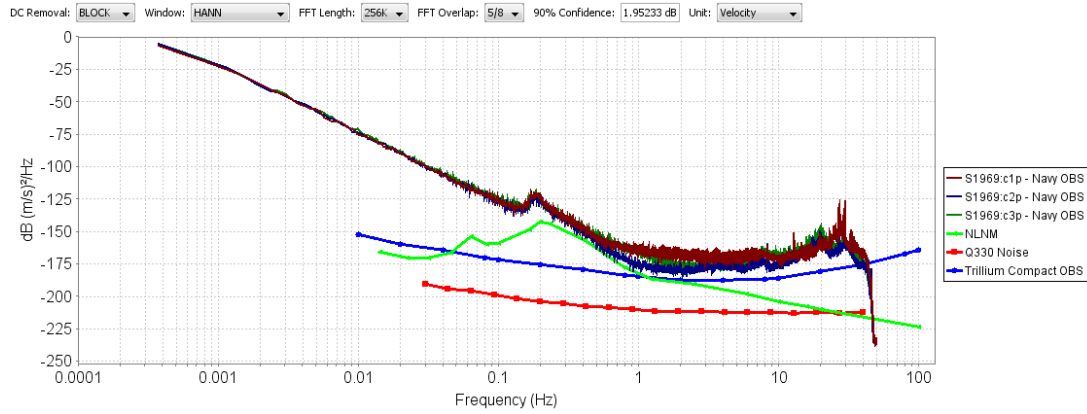


**Figure 246 Backfill Testing, Cross-Axis Coupling, Navy OBS Power Spectra**

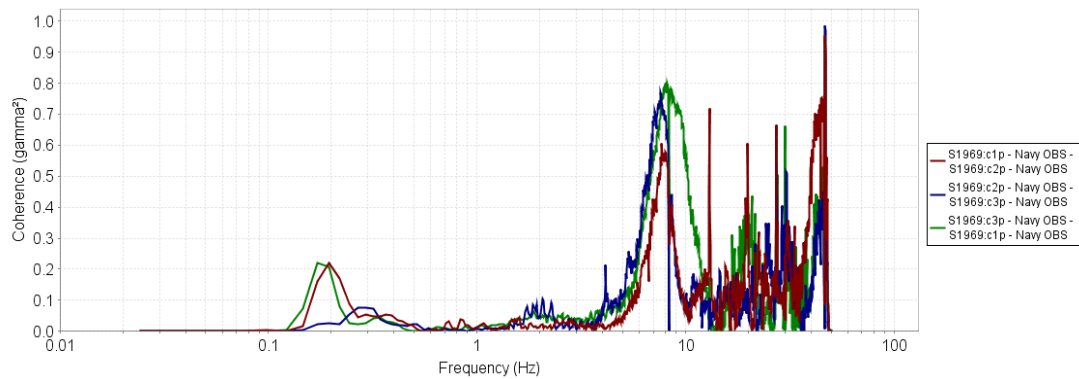
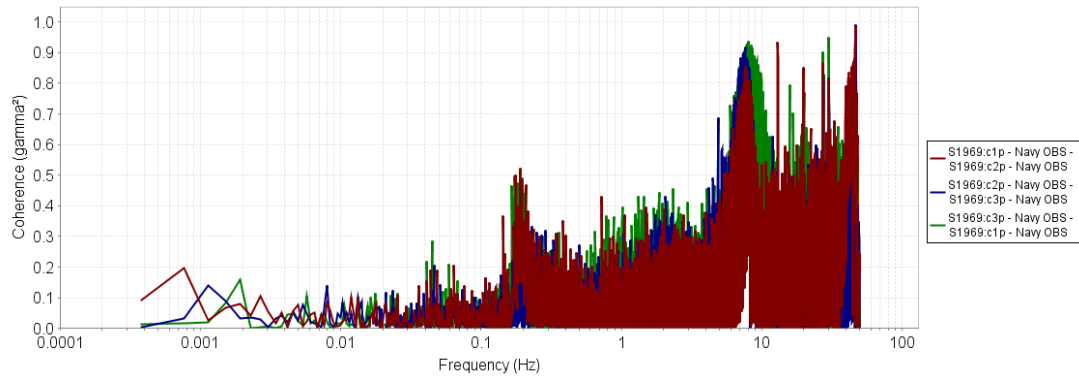


**Figure 247 Backfill Testing, Cross-Axis Coupling, Navy OBS Coherence**

### 3.5.3 *Bubble Test*

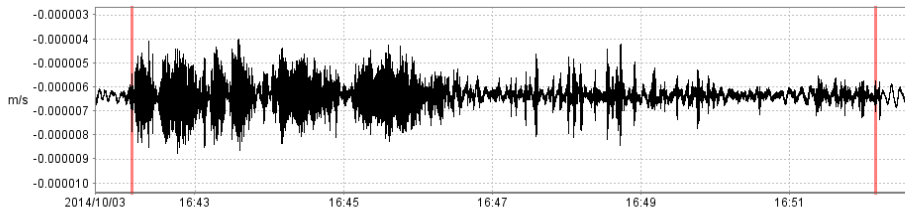
A Bubble Test was performed on October 3, 2014 from approximately 16:42 – 16:52 (GMT) in which air was released from a hose within the water filled Test Pool. The purpose of the Bubble Test was to introduce “noise” in the water environment that was not due to ground motion and observe its effect on the sensors. Specifically, how susceptible the sensors on the platform are to water noise. Analysis of the test data will examine the power spectra and coherence between the Trillium Compact OBS on the Underwater Platform and the reference on the bottom of the Test Pool. Data was not available during this time period for the OBS on the Seafloor Material; therefore analysis will be performed relative to the OBS on the bottom of the Test Pool.

We observe that on all three axis of motion that the OBS on the Underwater Platform exhibits increased signal and a greater magnitude response across the entire passband relative to the reference OBS on the bottom of the Test Pool.

It appears from this test that the presence of the Seafloor Material and Underwater Platform are resulting in increased signal levels over much of the frequency pass-band that is incoherent with the reference sensor.

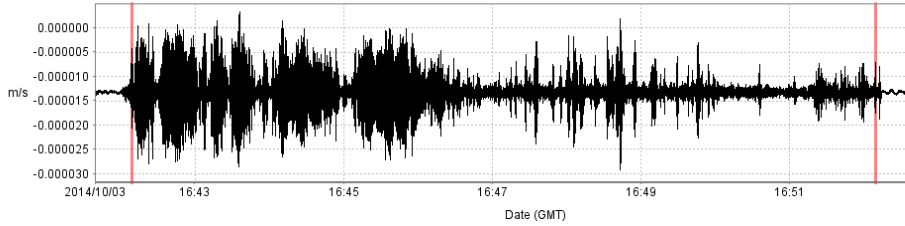
### 3.5.3.1 Vertical

Reference Waveform



Station: 3112  
 Channel: HHZ10TB  
 Rate: 100 Hz  
 Bitweight: 29.67 nV/count  
 Response Deconvolution  
 Response: Reference OBS  
 Unit: Velocity

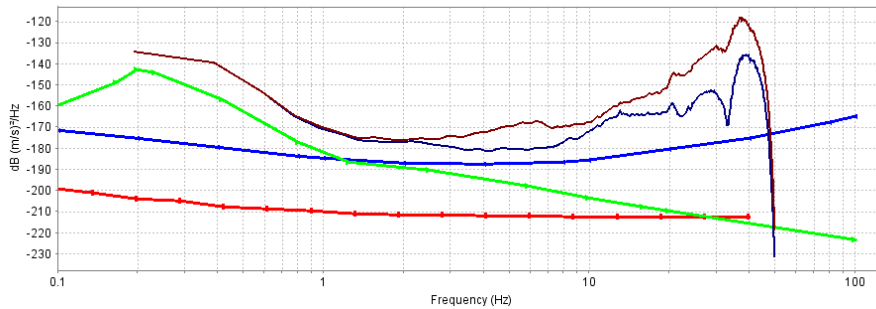
Test Waveform(s)



Station: 3112  
 Channel: HHZ00TB  
 Rate: 100 Hz  
 Bitweight: 29.7 nV/count  
 Response Deconvolution  
 Response: Platform OBS  
 Unit: Velocity

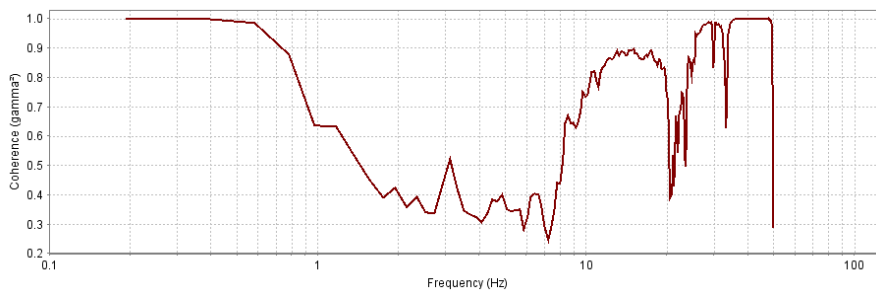
Figure 248 Backfill, Bubble, Vertical Waveforms

DC Removal: BLOCK Window: HANN FFT Length: 512 FFT Overlap: 5/8 90% Confidence: 0.64335 dB Unit: Velocity



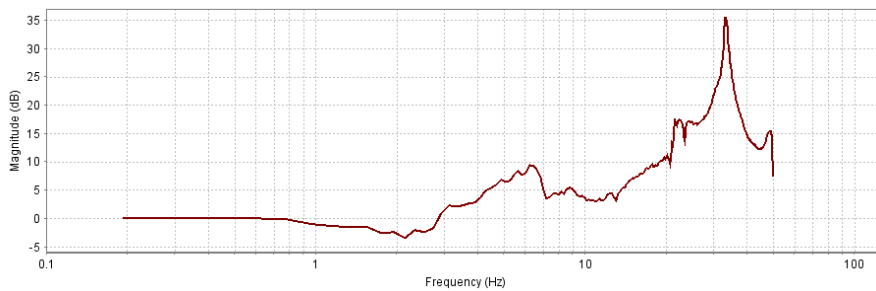
3112:HHZ00TB - Platform OBS  
 3112:HHZ10TB - Reference OBS  
 NLNM  
 Q330 Noise  
 Trillium Compact OBS

Figure 249 Backfill, Bubble, Vertical Power Spectra



3112:HHZ00TB - Platform OBS  
 3112:HHZ10TB - Reference OBS

Figure 250 Backfill, Bubble, Vertical Coherence

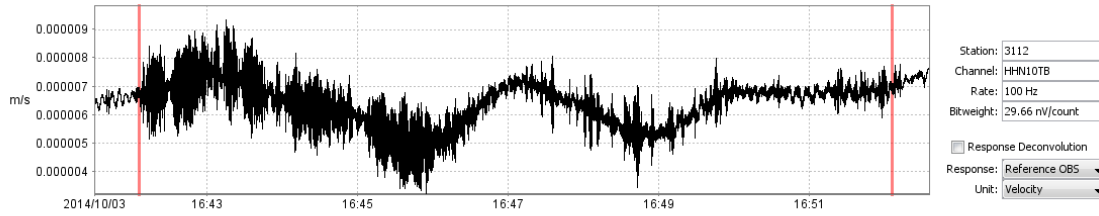


3112:HHZ00TB - Platform OBS  
 3112:HHZ10TB - Reference OBS

Figure 251 Backfill, Bubble, Vertical Magnitude Response

### 3.5.3.2 North

Reference Waveform



Test Waveform(s)

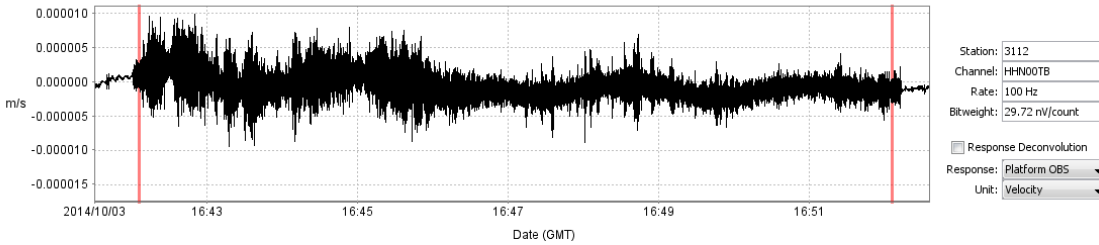


Figure 252 Backfill, Bubble, North Waveforms

DC Removal: BLOCK Window: HANN FFT Length: 512 FFT Overlap: 5/8 90% Confidence: 0.64335 dB Unit: Velocity

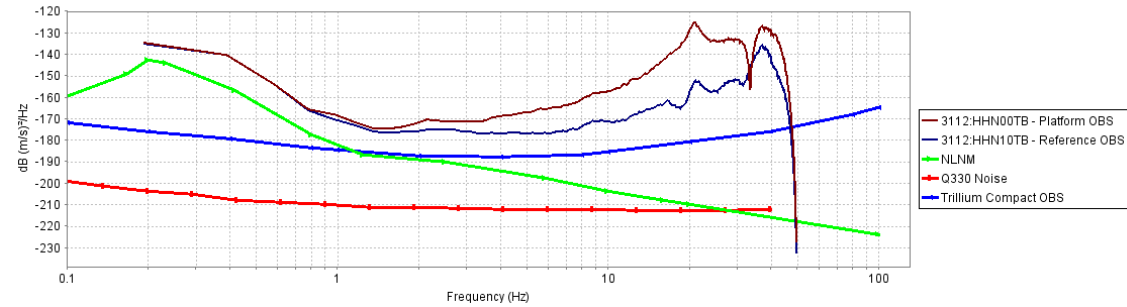


Figure 253 Backfill, Bubble, North Power Spectra

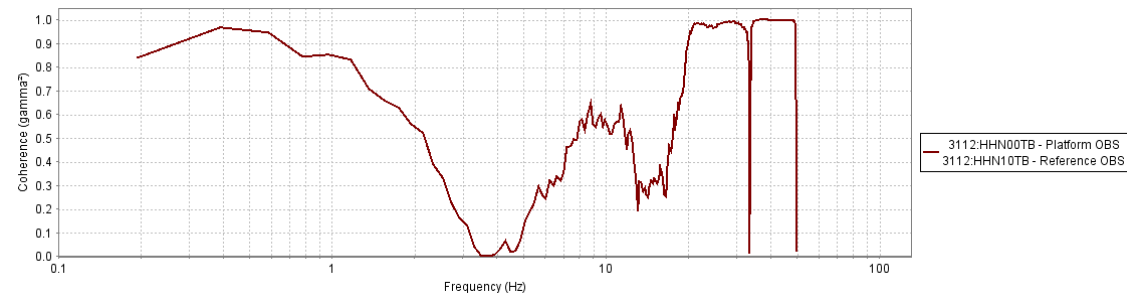


Figure 254 Backfill, Bubble, North Coherence

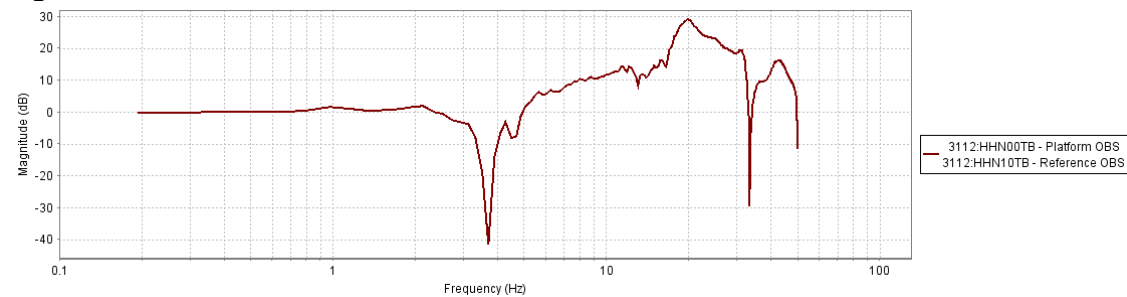


Figure 255 Backfill, Bubble, North Magnitude Response

### 3.5.3.3 East

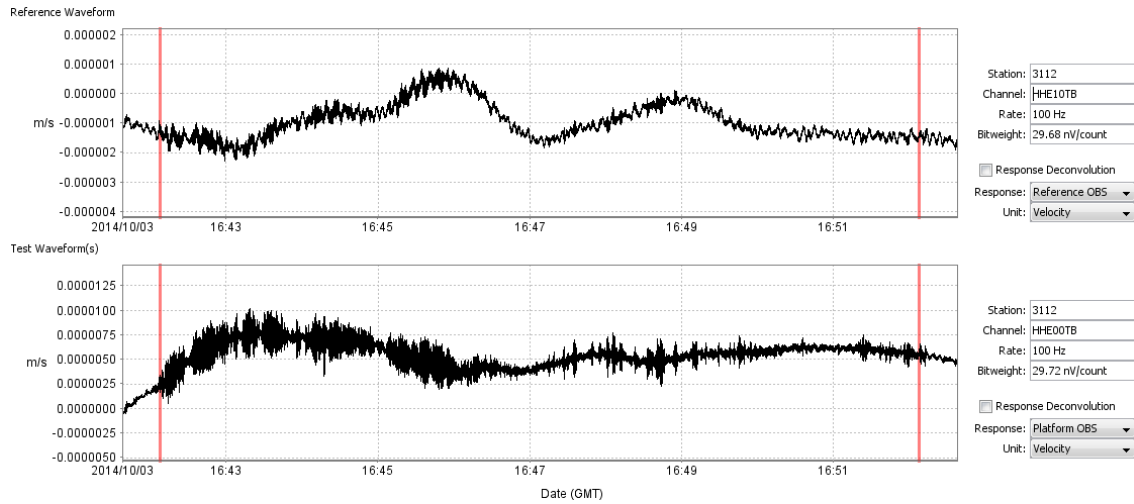


Figure 256 Backfill, Bubble, East Waveforms

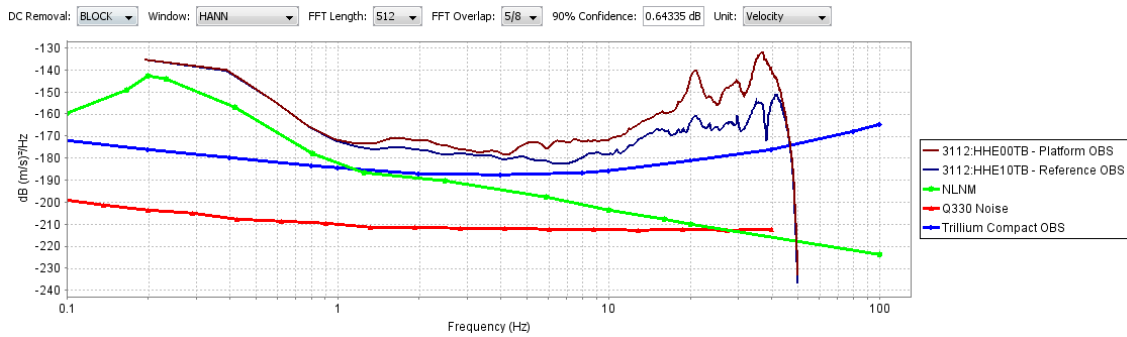


Figure 257 Backfill, Bubble, East Power Spectra

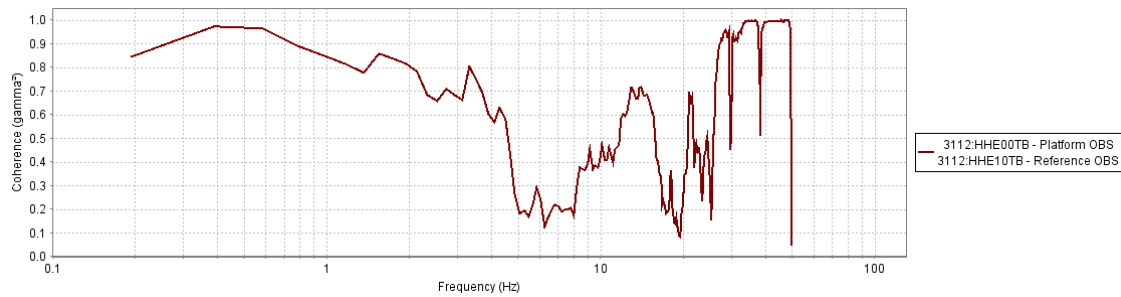


Figure 258 Backfill, Bubble, East Coherence

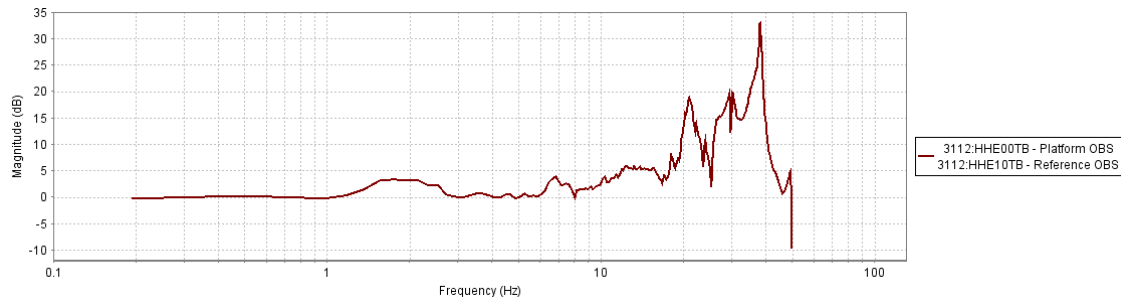


Figure 259 Backfill, Bubble, East Magnitude Response

### 3.5.4 Thumper Test

A Thumper Test was performed on October 3, 2014 from approximately 15:00 – 16:15 (GMT) in which a repeated ground impact was performed using a mobile piston shear generator. The impacts from this test were too small and short in duration to perform any reliable spectral or coherence measurements. Instead, the measurements from the Underwater Platform OBS was compared to the Test Pool floor OBS to determine whether the amplitudes were consistent and verify that there were no time-domain artifacts present. Data from the Seafloor Material OBS was not available for this test.



**Figure 260 Thumper Generator**

The waveform data was filtered with a band-pass Butterworth filter with a cut-off frequencies of 0.01 Hz and 40 Hz were performed to remove any noise present in the sensor or digitizer response roll-off. Plots of the waveforms for a single “thump” are shown for each of the Vertical, North, and East axes.

There are significant differences in the time-series between the OBS on the Underwater Platform and on the Test Pool floor. The Underwater Platform OBS has significantly higher amplitudes and greater frequency content. This is consistent with the prior results showing increased noise and resonant modes on the Underwater Platform and Seafloor Material.

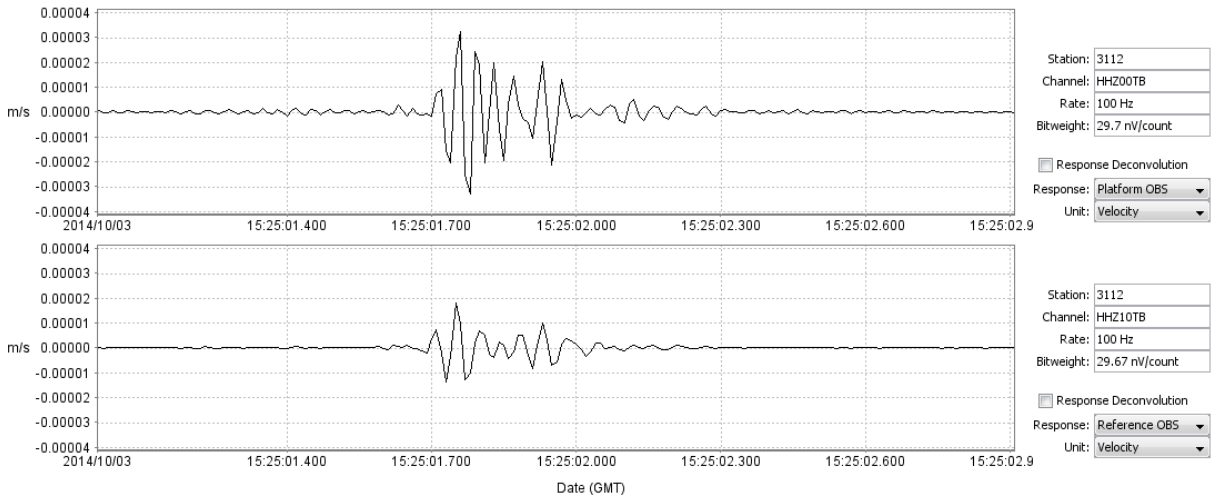


**Figure 261 Backfill, Thumper, Vertical Waveforms**

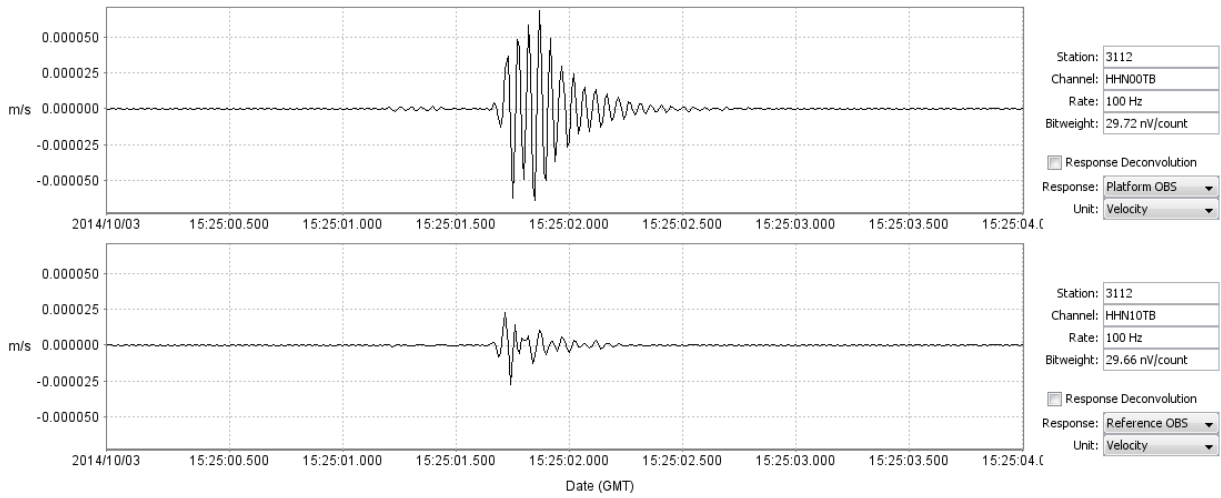


**Figure 262 Backfill, Thumper, North Waveforms**

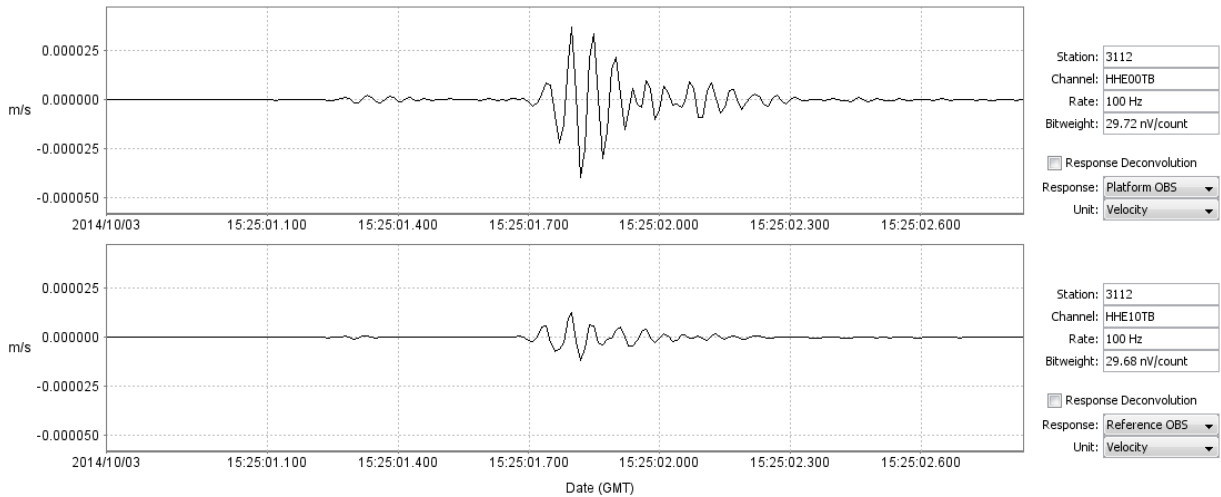


**Figure 263 Backfill, Thumper, Single Thump East Waveforms**



## 4 SUMMARY

The following observations are made from the evaluation of the test data. Note that in all cases, the conditions observed in the test environment may not represent the conditions present in the deployment environment.

In addition, it is important to note that the tests were conducted over relatively short time periods. The time periods do not necessarily encompass seismic sources with sufficiently high amplitude levels to evaluate the entire frequency passband. It is also possible that the Underwater Platform may not have had sufficient time to stabilize to the test conditions, such as settling within the seafloor material or allowing the backfill material to fully compact and air to escape.

### 4.1 Transfer Function

The evaluation of the Underwater Platform's transfer function was performed across a series of test conditions: dry platform, wet platform, wet seafloor, and wet seafloor with backfill. The following observations may be made across these conditions by comparing the output of the OBS seismometers placed on the bottom of the Test Pool, on the Seafloor Material, and on the Underwater Platform.

In the dry platform testing, there was no discernable difference in the amplitude and phase response over the frequency passbands (generally 0.1 to 10 Hz) over which the reference and platform sensors were coherent. Coherence was limited due to the lack of sufficient signal content above the sensor self-noise outside this passband.

In the wet platform testing, there was no discernable difference in the amplitude and phase response over the frequency passbands (generally 0.02 to 15 Hz) over which the reference and platform sensors were coherent. Coherence was limited due to the lack of sufficient signal content above the sensor self-noise outside this passband. The improved coherent frequency passband over the dry platform testing is due to the availability of larger amplitude signals above the sensor self-noise.

In the wet seafloor platform testing, there was no discernable difference in the amplitude and phase response across approximately 0.02 to 10 Hz. The seafloor OBS exhibited what appear to be increased noise levels below 0.02 Hz and above 10 Hz. Above 10 Hz the seafloor OBS also appeared to have a slight increase in its amplitude response relative to the reference, indicating a possible resonance. The platform OBS exhibited lower noise levels than the seafloor OBS below 0.02 Hz and was consistent with the reference OBS at these frequencies. Above 10 Hz the platform OBS exhibited significantly more noise and resonance than the reference. This would seem to indicate that the Underwater Platform improves performance at low frequencies but introduces noise and resonance above 10 Hz.

In the wet seafloor with backfill platform testing, there was no discernable difference in the amplitude and phase response at frequencies below 1.2 Hz where the reference and platform sensors were coherent. Coherence was limited due to the lack of sufficient signal content above

the sensor self-noise outside these passbands. At frequencies above 4-5 Hz the platform OBS exhibited significantly more noise and resonance than the reference and seafloor sensors. This would seem to indicate that the Underwater Platform with backfill introduces noise and resonance above 4-5 Hz.

## **4.2 Geophone**

The Trillium OBS and the Navy Geophone OBS on the underwater platform were compared to each other in order to evaluate the relative performance between the two sensors and determine how well coupled the two sensors are on the Underwater Platform. In all phases of testing that were performed the two sensors had similar responses over the frequency passbands in which there was sufficient signal amplitude above each sensor's self-noise. This would tend to indicate that the two seismometers are sufficient well coupled to the Underwater Platform such that they are able to measure the same signal.

The Navy Geophone OBS appears to have a complicated amplitude and phase response around 3 - 5 Hz that is unique to each axis. This is the approximate roll off region of the Navy Geophone OBS response. This may be due to the Navy OBS being made of multiple geophones, each with a unique corner frequency, connected in series. It is possible that better matching of the individual geophones could simplify the response characteristics around the corner frequency.

## **4.3 Cross-Axis Coupling**

The individual axes of each seismometer were compared to each other in order to determine the degree of coupling between each of the Z, N, and E axes. This comparison was performed for each Test Pool floor, Seafloor Material, and Underwater Platform OBS for each phase of platform testing involving the underwater platform. Several hours of relatively stable seismic background waveform data were used for each test in order to comment on the long period coupling.

In the dry platform testing, there appears to be a slight amount of coherence between the horizontal channels of the reference OBS on the Test Pool floor below 0.02 Hz. There is less coherence between the horizontal axes of the Underwater Platform OBS, indicating that the Underwater Platform may be reducing cross-axis coupling.

In the wet platform testing, there appears to be similar amounts of coherence between the horizontal channels of both the Test Pool floor and Underwater Platform OBS sensors at frequencies below 0.01 Hz. There is also a similar amount of coherence between the vertical and each of the horizontal axes at 0.1 Hz on both OBS sensors. There is no appreciable difference observed in the Test Pool floor and Underwater Platform OBS cross-axis coupling.

In the wet seafloor platform testing, both the Test Pool floor OBS and Seafloor Material OBS exhibit significantly more coherence between their horizontal channels below 0.1 Hz than in the prior tests. However, the Underwater Platform OBS does not exhibit increases in horizontal axis coupling until below 0.03 Hz and even then the horizontal coherence is greatly reduced relative

to the Test Pool reference OBS. It appears that the Underwater Platform is contributing in decreasing the horizontal axes coupling that is otherwise present on the seafloor material.

In the wet seafloor with backfill platform testing, both the Test Pool floor OBS and Seafloor Material OBS exhibit significantly more coherence between their horizontal channels below 0.1 Hz than in the prior tests. However, the Underwater Platform OBS has only slight amount of horizontal coupling and only at much lower frequencies. It appears that the Underwater Platform is contributing in decreasing the horizontal axes coupling. The sensors on the Underwater Platform do exhibit a significant amount of coherence between all axes at between 5 and 12 Hz. This coherence is not present on any other of the sensors in the test or in any prior tests. This suggests that the presence of the backfill material may be responsible.

#### **4.4 Bubble Tests**

Bubble tests were performed for both the wet seafloor and wet seafloor with backfill platform tests in which air bubbles were introduced into the water in the test pool in order to evaluate the impact of water noise on the seismometers. Comparisons were made between the Test Pool floor, Seafloor, and Underwater Platform OBS sensors.

In the wet seafloor platform testing, the observed signal levels are elevated on the OBS on the Underwater Platform relative to the OBS on the seafloor. This holds for all axes, however, it is more visible on the horizontal axes.

In the wet seafloor with backfill platform testing, the observed signal levels on the Underwater Platform OBS are even greater, relative to the other OBS, than in the wet seafloor without backfill testing.

Direct comparison of the Underwater Platform OBS time series data from the two tests is not possible because of the random and non-repeatable nature of the generated signal.

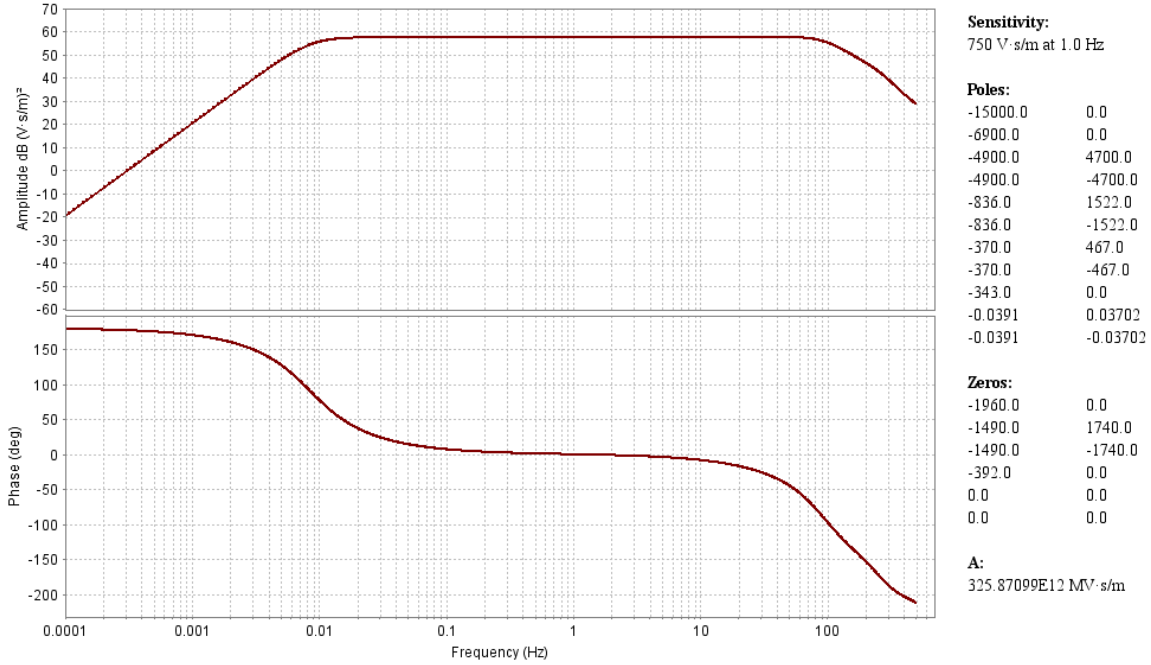
#### **4.5 Thumper Test**

A Thumper test was performed for the wet seafloor with backfill platform test. Time-domain comparisons were made between the Test Pool floor and Underwater Platform OBS sensors.

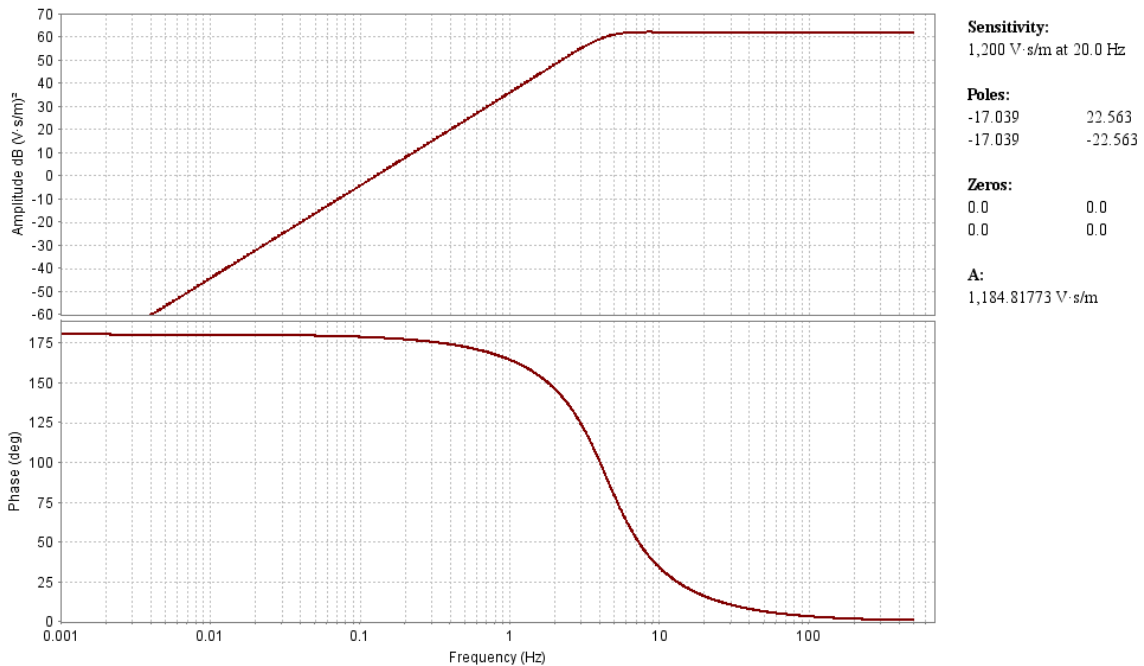
We observe that the OBS on the Underwater Platform has signals that are elevated relative to the Test Pool floor. In addition, the Underwater Platform signals contained greater high frequency content. This is consistent with the prior results showing increased noise and resonant modes on the Underwater Platform and Seafloor Material.

# APPENDIX

## Nanometrics Trillium OBS Response



## Navy Geophone OBS Response



## REFERENCES

1. Holcomb, Gary L. (1989), *A Direct Method for calculating Instrument Noise Levels in Side-by-Side Seismometer Evaluations*, DOI USGS Open-File Report 89-214.
2. IEEE Standard for Digitizing Waveform Recorders, IEEE Std. 1057-1994.
3. IEEE Standard for Analog to Digital Converters, IEEE Std. 1241-2001.
4. Kromer, Richard P., Hart, Darren M. and J. Mark Harris (2007), *Test Definitions for the Evaluation of Seismic Sensors Version 1.0*, SAND2007-5025.
5. Merchant, B. John, and Darren M. Hart (2011), *Component Evaluation Testing and Analysis Algorithms*, SAND2011-8265.
6. Sleeman, R., Wettum, A., Trampert, J. (2006), *Three-Channel Correlation Analysis: A New Technique to Measure Instrumental Noise of Digitizers and Seismic Sensors*, Bulletin of the Seismological Society of America, Vol. 96, No. 1, pp. 258-271, February 2006.

## **DISTRIBUTION**

1      MS0899      Technical Library      9536 (electronic copy)



**Sandia National Laboratories**